VO_2 ON-KINETICS IN ISOLATED CANINE MUSCLE *IN SITU* DURING SLOWED CONVECTIVE O_2 DELIVERY

Except where reference is made to the work of others, the work described in this dissertation is my own or was done in collaboration with my advisory committee. This dissertation does not include proprietary or classified information.

_____
Matthew Lawrence Goodwin

Certificate of Approval:

_____	_____
David D. Pascoe Professor Kinesiology	L. Bruce Gladden, Chair Professor Kinesiology
_____	_____
Lawrence C. Wit Professor Biological Sciences	Douglas C. Goodwin Associate Professor Chemistry and Biochemistry

_____
George T. Flowers
Dean
Graduate School

VO_2 ON-KINETICS IN ISOLATED CANINE MUSCLE *IN SITU* DURING SLOWED CONVECTIVE O_2 DELIVERY

Matthew Lawrence Goodwin

A Dissertation

Submitted to

the Graduate Faculty of

Auburn University

in Partial Fulfillment of the

Requirements for the

Degree of

Doctor of Philosophy

Auburn, Alabama
December 19, 2008

VO_2 ON-KINETICS IN ISOLATED CANINE MUSCLE *IN SITU* DURING SLOWED CONVECTIVE O_2 DELIVERY

Matthew Lawrence Goodwin

_____
Signature of Author

_____
Date of Graduation

VITA

Matthew Lawrence Goodwin, son of Stephen Hilton Goodwin and Deborah Frances Goodwin, was born on August 4, 1981 in Greenville, SC. He graduated from both Wade Hampton High School and The Greenville Fine Arts Center in 1999. He then attended Brevard College for one year before transferring to Furman University, where he earned his Bachelor's degree in Exercise Science and his Master's degree in Education (Emotional and Behavioral Disorders). While at Brevard and Furman, he ran both cross country and track. His interest in Exercise Physiology was born out of his athletic pursuits and interactions in the Molnar Human Performance Lab with Dr. Ray Moss at Furman University. Wishing to pursue study in the Physiology of Exercise in a top laboratory, in the fall of 2004 Matthew was accepted as a Ph.D. student in Bruce Gladden's muscle physiology laboratory. Upon completing his Ph.D., Matthew will be moving to Haiti for 6 months, where he will be conducting HIV/AIDS research with *le Groupe Haitien d'Étude du Sarcome de Kaposi et des infections Opportunistes* (the Haitian Group for the Study of Kaposi's Sarcoma and Opportunistic Infections; "GHESKIO"). His interest in medicine and physiology has led him to then continue his education in the fall of 2009 at Weill Cornell Medical College in New York City, where he will pursue his doctorate of medicine.

DISSERTATION ABSTRACT

VO_2 ON-KINETICS IN ISOLATED CANINE MUSCLE *IN SITU* DURING SLOWED CONVECTIVE O_2 DELIVERY

Matthew Lawrence Goodwin

Doctor of Philosophy, December 19, 2008
(M.A., Furman University, 2004)
(B.A., Furman University, 2003)

204 Typed Pages

Directed by L. Bruce Gladden

A substantial body of evidence now suggests that while increasing O_2 delivery to a working muscle during submaximal contractions onset may not speed VO_2 on-kinetics, slowing the rate of O_2 delivery may slow the VO_2 on-kinetics response. While many studies have used techniques that measure limb blood flow, central blood flow, pulmonary VO_2, and limb VO_2, relatively few studies have characterized blood flow on-kinetics and VO_2 on-kinetics directly across a working muscle *in situ*. Previous research has established that increasing O_2 delivery to the muscle prior to contractions onset (via increased blood flow delivery) does not speed the VO_2 on-kinetics response in transitions to submaximal contractions in isolated muscle *in situ*.

The purpose of this study was to determine the effect of slowing blood flow on-kinetics on VO_2 on-kinetics. The isolated canine gastrocnemius muscle complex *in situ* was used (n=11). After surgical isolation of the muscle, four trials were performed. A Control Trial (CT) was always the first trial, as it was a trial to establish resting blood flow and steady state blood flow. The remaining three trials were randomized: Control Trial 20 (CT20), in which pump perfusion of the muscle was set to follow a

monoexponential rise in which the tau (time to ~63.2% response) was set at 20 sec; Experimental Trial 45 (EX45), in which pump perfusion of the muscle was set to follow a monoexponential rise in which the tau was set at 45 sec; and Experimental Trial 70 (EX70), in which pump perfusion of the muscle was set to follow a monoexponential rise in which the tau was set at 70 sec.

VO_2 average mean response time (time delay + tau = MRT) values for CT20, EX45, and EX70 were 19.9±3.8, 26.3±5.9, and 31.7±4.1 sec, respectively. MRT values for EX70 and EX45 were significantly different from CT20 ($p=<0.0001$, $p=0.0031$) and each other ($p=0.0092$). Furthermore, when MRT values of the VO_2 on-response were plotted against the MRT values from the blood flow/O_2 delivery on-response, there was a linear relationship ($R=0.99997$). These results, combined with earlier work done with this same model, suggest that in this model the muscle contracts with a blood flow/O_2 delivery very closely matched to the O_2 utilization. The progressive, linear slowing of VO_2 on-kinetics with slower O_2 delivery suggests that either 1) the appropriate level of metabolites needed to stimulate the control VO_2 at any given time during the on-transition could not be reached, or 2) the appropriate levels of metabolites needed to stimulate the control VO_2 at any given time during the on-transition were reached, yet the O_2 was not available. These results show that muscle VO_2 and blood flow/O_2 delivery are very closely matched during contractions onset. Given the inherent weakness in studies that must estimate muscle VO_2 and muscle blood flow from other measures, we have carried out experiments that directly measure the variables of interest (blood flow, VO_2). To our knowledge, this is the first study of its kind to progressively slow the O_2 delivery rate by altering the time course of the normal monoexponetial blood flow on-response without altering the resting or steady state O_2 delivery rate. Because various disease states present with impaired O_2 delivery on-kinetics and/or impaired VO_2 on-kinetics, these results offer great insight into mechanisms of both healthy and diseased mammalian muscle.

ACKNOWLEDGEMENTS

I first must thank Dr. Bruce Gladden and the Department of Kinesiology, as they provided me with a flexible environment in which I could thrive. I thank the rest of my committee, Dr. David Pascoe, Dr. Lawrence Wit, and Dr. Douglas Goodwin for providing challenges, critiques, insights and support as teachers and committee members. I also thank Dr. Jim Sartin for contributing as an outside reader and teacher. Mr. Henry Cobb of Auburn's Research Electronics Support Facility (RESF) was an integral part of our project's success, as he designed a computer program we are using and would troubleshoot our equipment. Thank you to Dr. Pat Rynders and Ms. Andrea Brown for allowing us to use animals from previous studies so that the most can be learned from each animal. Drs. Marco Cabrera and Nicola Lai were critical in our kinetics analysis and I am grateful to them. I am indebted to my fellow graduate student, Mr. Andrés Hernández, for his long hours of work in the lab and the tremendous amount of help he put into this project. I must also thank my family; my parents Steve and Debbie, Tracey and Branham, FJ, Kevin Crosby, and Granny and Gainor for providing me with encouragement and laughter along the way, and of course, my love Mandy, for providing me with so much love and support during this long journey. Although I know I will leave many out, I want to thank a few teachers who greatly shaped my development earlier in life; they inspired me, provided guidance, and showed me a unique perspective I would not have gotten anywhere else: Rev. Gentry McColm, Coach Rick Zeller, Ms. Sue Wilson, Mr. Jim Campbell, Coach Gene Mullin, Dr. Scott Henderson, The Furman Exercise Science Dept. (especially Drs. Ray Moss and Bill Pierce), Coach Chris Fox, and my mother, who still finds time and energy to teach me. I also want to thank Dr. Gladden for his example as a mentor, teacher, scientist, citizen, man, and friend. More was gleaned from spending time in experimentation and discussion with Dr. Gladden than could ever be learned in a classroom. Finally, I thank you if you were one of the many that engaged me in debate or discussion and especially if you were one of my students who ever questioned me as a teacher and made me explain "why" by providing evidence; hopefully there are many more "problem" students like you out there.

Style manual or journal used Journal of Applied Physiology

Computer software used Microsoft Word 2007

TABLE OF CONTENTS

LIST OF TABLES AND FIGURES

I. INTRODUCTION

Despite the fact that the major metabolic pathways of skeletal muscle energetics were elucidated in the early part of the 20th century, major gaps exist in our understanding of the exact controls of many of those pathways. One prime example of this is the control of oxidative phosphorylation (OxPhos) during transitions from one metabolic rate to another ("VO_2 on-kinetics"). (Note that "VO_2" is used here to represent "oxygen uptake per minute"; traditionally this is represented as "$\dot{V}O_2$" with a dot over the V.) This transition is something most people experience numerous times during the day, coordinating the pulmonary, cardiovascular, and muscular systems in such a way as to rapidly increase OxPhos ATP production. The more rapidly this transition occurs, the less one must rely on the limited supply of "anaerobic" energy stores within the cell (phosphocreatine (PCr), glycogen) and the better chance one will have of tolerating the activity for longer periods of time (80). Trained endurance athletes tend to exhibit faster VO_2 on-kinetics than untrained controls, while patients with certain diseases present with slowed VO_2 on-kinetics (80).

After almost 100 years of investigation into the controls of OxPhos at contractions onset (68), the exact controls of the OxPhos response are still an area of debate (34, 59, 79). While many factors have been proposed to influence this response time of OxPhos in various situations, there are conflicting data when it comes to the exact role of convective O_2 delivery to working muscle. While many studies have estimated or measured cardiac output, limb blood flow, or lower body pressure as surrogates for muscle blood flow; and pulmonary VO_2 and limb VO_2 as surrogates for muscle VO_2, relatively few studies have directly measured VO_2 and blood flow directly across a working muscle *in situ*. In the canine gastrocnemius muscle complex *in situ*, it has been previously shown that providing an excess of O_2 to the working muscle before contractions start has no influence on the VO_2 on-kinetics response during transitions to submaximal work rates (36). However, the effect of slowing the rate of O_2 delivery (by slowing blood flow delivery rate) on the VO_2 on-kinetics response has not been determined. Data from

human subjects are mixed (21, 22, 42, 43, 50, 53, 56, 71, 77, 86, 92, 98), yet overall suggest that the blood flow response is faster than the VO_2 on-kinetics response or at least matches it (42, 58). Further, some data (43, 71, 98) suggest that slowing of the blood flow on-kinetics response does not lead to an obligatory slowing of the VO_2 on-kinetics response (i.e. blood flow may be in excess of what is needed and thus some slowing of blood flow could be done before slowing of VO_2 on-kinetics is seen). Thus, the purpose of this study was to examine the resultant VO_2 on-kinetics when the blood flow on-kinetics response (and thereby O_2 delivery on-kinetics response) was progressively slowed.

II. REVIEW OF LITERATURE

It is a well known phenomenon that as energy demand increases in a square-wave fashion (Figure 1) at the onset of steady-state contractions (or exercise) there is some delay in matching ATP supply from OxPhos to this ATP demand (Figure 2) (5, 9, 18, 33, 34, 59, 67, 83, 90). This "slow" response of O_2 uptake was described qualitatively by Krogh and Lindhard in 1913 (68). Years after this (1947-1955), Berg (10), Henry (44), and Henry and DeMoor (45) provided quantitative data that characterized this response (91). In 1966 Ceretelli et al. (17) referred to "early blood lactate" during these transitions, recognizing that aerobic metabolism was indeed insufficient to provide for the ATP demand during these on transients.

If whole-body exercise is in the form of a submaximal, below-lactate threshold (LT), or below-ventilatory threshold (VT) work rate, steady state energy provision by OxPhos is not fully reached until about three minutes (32). At that time, OxPhos by the mitochondria supplies enough ATP to meet the entire demand for the given work rate. In exercise of this type, VO_2 is constant from approximately three minutes onward (33, 59, 90). Due to the initial lag, the primary square wave increase in ATP demand must be met by ATP-synthesizing pathways in addition to the mitochondrial OxPhos. This ATP demand above that met by OxPhos is referred to as the "O_2 deficit" (12).

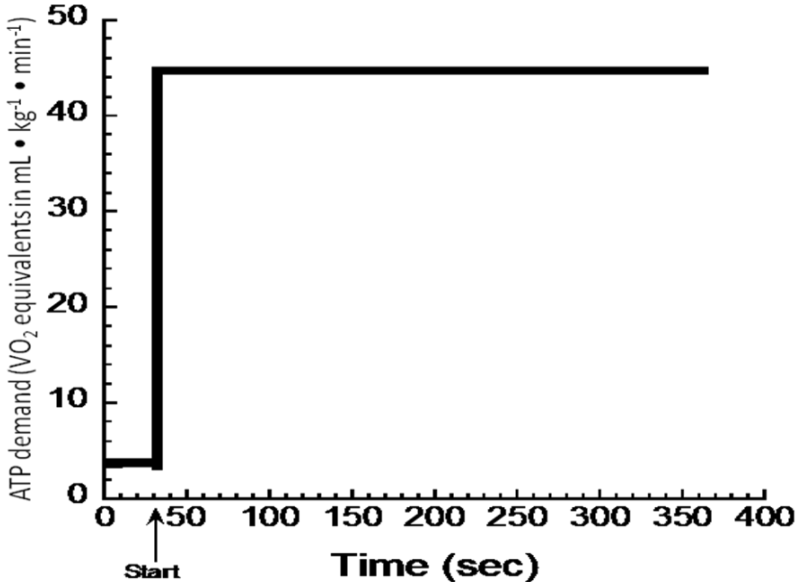

Figure 1: Schematic graph showing the immediate square-wave increase in ATP demand upon exercise/contractions onset. "Start" represents contractions onset.

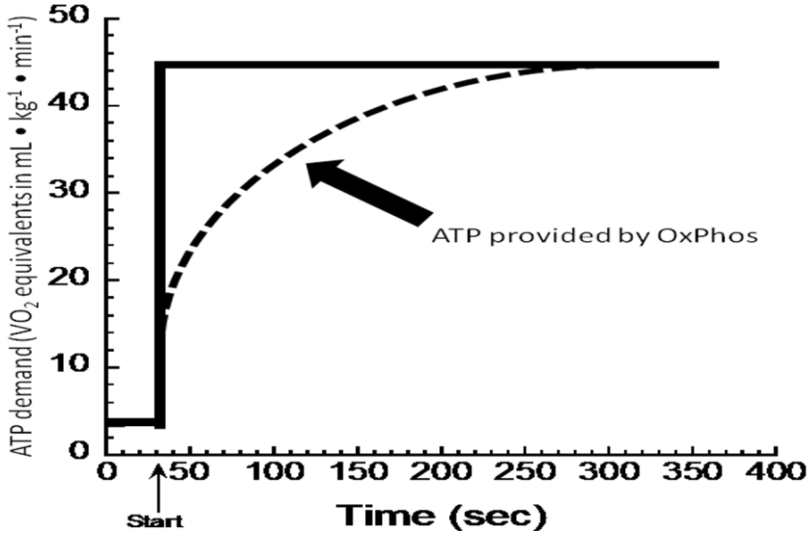

Figure 2: Schematic graph showing the exponential rise in ATP supply via OxPhos upon exercise/contractions onset. "Start" represents exercise/contractions onset. Note that full ATP provision via OxPhos is not met until ~3 min in whole body exercise.

More specifically, the VO_2 on-kinetics response seen during moderate exercise has been partitioned into three "phases", as shown in Figure 3 (83). "Phase one" represents the rapid entry of relatively deoxygenated venous blood into pulmonary circulation at the onset of exercise (also called the "cardiodynamic phase"). Because this is not representative of muscle O_2 usage *per se*, it is usually left out of curves fit to data *in vivo* (83). "Phase two" represents the fundamental monoexponential rise in VO_2, and "phase three" represents the steady state VO_2. It should be mentioned for completeness that a "slow component" (a slow upward drift of VO_2 without achievement of a steady state) is often seen in "heavy exercise" (above LT).

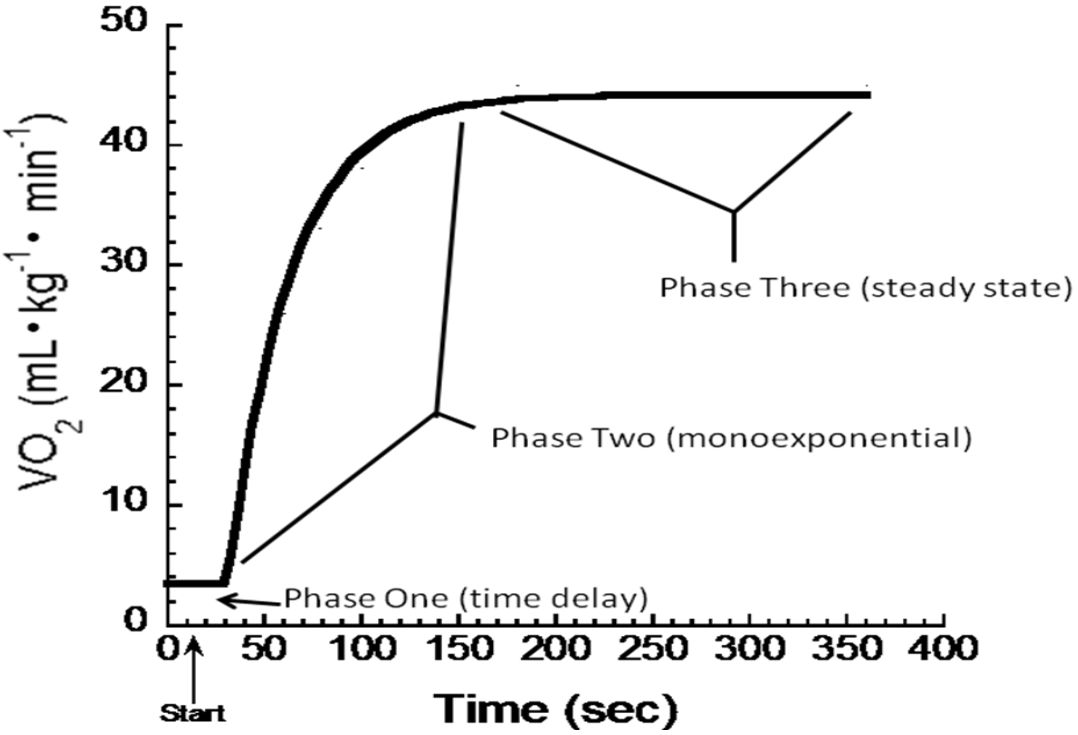

Figure 3: Idealized graph of the three phases of the VO_2 on-response to exercise/contractions onset (83).

The VO_2 as a function of time varies depending on the experimental model utilized (pulmonary VO_2 (at the mouth), VO_2 across an isolated muscle, ΔPO_2 in an isolated muscle fiber), but can be expressed with the following equation for isolated muscle preparations *in situ*:

$$\mathbf{VO_2(t)=VO_2(rest)+\Delta VO_2(ss)*(1-e^{-t/\tau})}$$

where $VO_2(t)$ is the VO_2 at any time t, $VO_2(rest)$ is VO_2 at rest, $\Delta VO_2(ss)$ is the difference between resting VO_2 and steady state VO_2, and $(1-e^{-t/\tau'})$ describes the monoexponential rise ("phase two", or "fundamental component") from resting VO_2 to steady state VO_2 (83). Tau (τ) is used here to represent the mean response time, or time from VO_2(rest) to ~63.2% of the final steady state value. This equation was further adapted by Rossiter et al. for whole body exercise where gases are measured at the mouth to include the appropriate time delay (δ) (83):

$$\mathbf{VO_2(t)=VO_2(rest)+\Delta VO_2(ss)*(1-e^{-(t-\delta)/\tau})}$$

This time delay is included to cover "phase one", which would include the "cardiodynamic phase" in whole-body models in which the first few points are ignored during fitting (when measuring VO_2 at the mouth, the first few points after exercise starts represent the relatively deoxygenated venous blood being rapidly brought to the lungs). In other models (isolated muscles, isolated fibers), "phase one" refers to the delay before the monoexponential rise in VO_2 (83). Even with the isolated dog gastrocnemius model *in situ* there is some time delay that is yet to be fully explained (38). This delay is in part due to the fact that even across an isolated muscle group there must be some delay due to the distance from the sampling site back to where the O_2 is actually being used (mitochondria).

Currently, models rooted in indicator dilution theory (93) are being developed by our group (based on the seminal work by the van Beek group) that aim to account for this delay. Indicator dilution theory can be used to determine and correct for the delay in VO_2 response caused by transport time ($t_{transport}$) from the mitochondria to the venous site of VO_2 measurement outside the muscle, in isolated muscle preparations (93). Using isolated rabbit hearts, van Beek and Westerhof (93) have adapted indicator dilution theory to develop a method of determining $t_{transport}$. This delay can then be subtracted from the venous VO_2 response time (t_{venous}) in order to determine the VO_2 response at the mitochondria (t_{mito}) as shown in equation 3 (93).

$$\mathbf{t_{mito} = t_{venous} - t_{transport}}$$

As shown in Table 1, "tau", "half-time" (time to ½ of the steady state response), and "mean response time" (MRT; time to ~63% of final response with any time delay included) are all used in the literature as ways of describing OxPhos response time (62).

Table 1: Terminology that can be applied to VO_2 on-kinetics, blood flow on-kinetics, PO_2 on-kinetics, or any other parameter kinetically analyzed in this manner. VO_2 on-kinetics is used here as an example.

Term	Definition
Time Delay (TD)	**Time from when contractions start to when O_2 uptake begins to increase. Note that a time delay may be included when fitting data to "ignore" the cardiodynamic phase because it does not reflect muscle VO_2.**
Tau (τ)	**Time to $^1/e$ % of full response remaining (~63.2% of response from baseline value to steady state value).**
Mean Response Time (MRT)	**Tau + Time delay**
Half-time ($t_{½}$)	**Time to 50% of full response (50% of response from baseline value to steady state value).**

IMPORTANCE OF VO_2 ON-KINETICS INQUIRIES

Many things must be considered in order to determine what controls or regulates this OxPhos response time in mammalian muscle cells. Two questions must first be addressed before pursuing this inquiry further: 1) Why is VO_2 on-kinetics an area worthy of extensive research? 2) What can be gained in health and/or science from the proposed line of study? The latter should help answer the former. Clinically, the applications of understanding what factors control the adjustment of oxidative metabolism are broad and far-reaching. Any patient who is prone to fatigue upon light exertion or has trouble carrying out daily tasks, whether due to a pathology or a normal physiological response (such as the loss of muscle mass and decline in VO_{2max} with age) would benefit from a greater ability to minimize the O_2 deficit; turning on oxidative metabolism faster would minimize this deficit, thus delaying the onset of fatigue (80). Furthermore, previous work has shown that the VO_2 on-kinetics response is slowed in diabetics (81), in peripheral vascular disease patients (6, 7), in heart failure patients (2, 87), with aging (3), in heart transplant patients (15, 39), in heart and lung recipients (35), in chronic respiratory disease patients (74), in those with

HIV (13), in McArdle's disease patients (40), and in those with mitochondrial myopathies (40, 80). *Why* each particular pathology presents a slowed oxidative response is an area of great concern and can only be elucidated once the controls of oxidative metabolism are fully understood. To that end, the matching of ATP demand to ATP supply by OxPhos must adjust at multiple steps in the O_2 transport cascade, allowing pathologies at any step along this cascade to cause a slowed VO_2 on-kinetics response (Figure 4) (80). By understanding the basic controls of oxidative metabolism during these transitions one can begin to understand how to better treat various pathologies as well as develop a deeper understanding of physiological controls. It should also be pointed out that much of the physical activity during a typical person's day consists of transitioning from one "below-LT work rate" to another different "below-LT work rate" (sitting to walking, walking to walking up stairs, etc). Thus, it is paramount that we understand these transition periods.

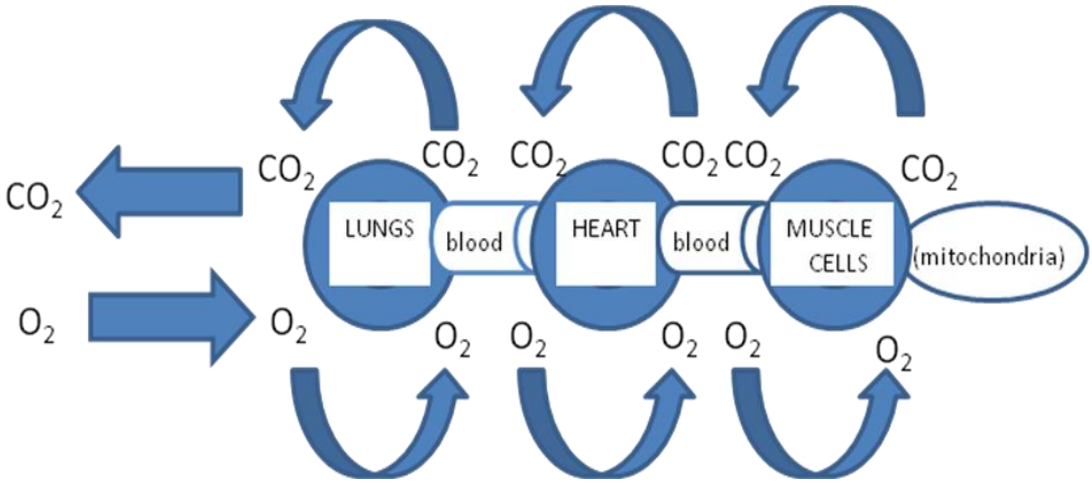

Figure 4: The simplified O_2/CO_2 transport cascade. Idealized from Wasserman et al.(94)

OXIDATIVE PHOSPHORYLATION OVERVIEW AND METABOLIC CONTROL

In order to harness the energy in reducing equivalents that are generated from the catabolism of substrates, eukaryotes utilize a process within their mitochondria that allows them to regenerate ATP oxidatively (i.e. OxPhos). Briefly, this is accomplished by electrons being donated from products of metabolism (e.g. NADH) and accepted by a protein complex within the inner membrane of the mitochondria. This protein complex then passes these electrons down to other molecules and complexes in

accordance with their increasingly higher reduction potentials (73). For NADH, the process follows the general outline of:

NADH → Complex I → Ubiquinone → Complex III → cytochrome c → Complex IV

Complexes I and III both cause a net efflux of 4 protons from the mitochondrial matrix into the intermembrane space (IMS) and Complex IV causes a net efflux of 2 protons from the mitochondrial matrix into the IMS. This "proton gradient" then drives the synthesis of ATP from ADP and Pi via Complex V (for a thorough review, the reader is directed elsewhere (73)).

Oxygen must be present in the mitochondrial matrix in order for OxPhos to continue at any given rate for any given period of time according to the overall OxPhos reaction that involves the reduction of O_2 to H_2O at complex IV (99):

3 ADP + 3Pi + NADH + H+ + ½O_2 → NAD^+ + H_2O + 3ATP

Although $FADH_2$ does contribute to this reduction series, inhibition data have shown that the bulk of electron passing in skeletal muscle oxidative metabolism occurs via the general NADH pathway as represented earlier (99). Without adequate oxygen, OxPhos can no longer continue due to the inability of reducing equivalents to pass electrons down the electron transport chain (ETC) to Complex IV. This is the result of oxygen not being available to function as the final electron acceptor at Complex IV.

Although studies of VO_2 on-kinetics in many different types of transitions date back to at least 1913 (68), the current concern is with controls of the transition from rest to a below-LT, below-VT, or submaximal work rate steady state. For the purpose of this review, these three intensity parameters will be used interchangeably to describe exercise in which no "slow component" is seen (the "slow component" is the slow upward drift of O_2 consumption without achievement of a steady state; this is common in exercise above the LT or VT). While numerous experiments have been done on transitions to work rates both above and below the LT or VT, those are beyond the scope of this review. In a 1990 review, Balaban (4) suggested that there are three major groups of control sites regulating OxPhos during steady state conditions: 1) delivery of reducing equivalents, NADH and $FADH_2$, to the cytochrome chain (dependent on substrate availability and status of intermediary metabolism (32)), 2) cytosolic levels of ADP and Pi, and 3) the reduction of O_2 to water at complex IV.

To date, two explanations for the OxPhos response time have been emphasized and hotly debated, although they are not mutually exclusive (79, 91): 1) OxPhos is stimulated by some or many metabolites (e.g. NADH, NAD^+, ADP, ATP, Pi) that must adequately change in concentration in order to stimulate an increase in OxPhos metabolism (this has often been termed "metabolic inertia"); and 2) O_2 delivery to the muscle limits the rate of OxPhos adjustment at contractions onset.

ROLE OF SUBSTRATE SUPPLY, REDOX STATE, ENERGY CHARGE, AND PO_2 IN VO_2 ON-KINETICS

In explaining the delay in OxPhos response, the "metabolic inertia" hypothesis states that OxPhos is stimulated by metabolites that must adequately change in concentration in order to stimulate an increase in OxPhos metabolism. Specifically, the "major players" that contribute to Balaban's (4) first two proposed metabolic regulators of OxPhos should be examined: 1) delivery of reducing equivalents and 2) cytosolic levels of ADP and Pi. Among the factors that would impact these two broad areas are: substrate supply in the TCA cycle, the role of Ca^{++} in turning on dehydrogenases, the role of ADP and Pi, and the role of mitochondrial capacity.

David Wilson (99) classified explanations for OxPhos rate as adhering to one of three hypotheses. While pointing out that respiration rate is ultimately determined by ATP demand and not by any change in substrate (46, 99), he posits that there are different ways (intracellularly) to achieve the same rate. The three main hypotheses are: 1) The ADP hypothesis, 2) The adenine nucleotide translocase (ANT) hypothesis, and 3) The near equilibrium hypothesis. While the first is fairly simple (the primary regulator of OxPhos is ADP), the second hypothesis espouses that ANT is the rate-limiting step to respiration. That is, ADP and ATP are exchanged between the mitochondria and cytosol such that the rate of exchange must be greater than or equal to ATP hydrolysis (99). Because extramitochondrial ATP competitively competes with extramitochondrial ADP for the ANT, the rate of translocation is dependent on the [ATP]/[ADP] ratio; thus respiration is dependent on the same ratio (99).

The central tenet of the "near equilibrium hypothesis" is that cytochrome c oxidase (complex IV) is the rate-determining step of OxPhos, while the other reactions of OxPhos function at near-equilibrium. This third hypothesis posits that respiration rate is interrelated to both the intracellular [ATP]/[ADP]X[Pi]

("energy charge") and the intramitchondrial [NAD^+]/[NADH]("redox state"). That is, the same respiration rate for any given PO_2 can be obtained by either a relatively low [NAD^+]/[NADH] and high [ATP]/[ADP]X[Pi] or the opposite (99, 102, 103). Figure 5 shows how energy charge and redox state may interact with PO_2 to achieve various respiration rates. That is, mitochondrial respiration rates in Figure 5A with a low energy charge remain O_2 independent down to a very low PO_2. However, when energy charge is higher and PO_2 drops below ~30 Torr, mitochondrial respiration will drop, requiring a lowering of energy charge to achieve the given respiration. Figure 5B shows the same scenario, but instead of changing energy charge, redox state is altered to achieve the needed VO_2 at any given PO_2.

Russ Richardson and colleagues (82) have provided compelling evidence using ^1H NMR that during transitions to moderate exercise, intracellular PO_2 declines to values less than 5 Torr, well into the range that would require significant intracellular adjustment of metabolites to achieve the desired OxPhos rate (see Figures 5A and 5B). To that end, Hughson (52) presented the interaction of enzyme and substrates supply (effectively redox state), energy charge, and PO_2 on respiration rate (see Figure 5C). The flat portion of the three dimensional "wave" represents the same mitochondrial respiration rate achieved in different ways. Thus, in transitions to exercise, when PO_2 presumably undergoes a transient drop, energy charge and/or redox state must change to produce the needed ATP. This idea has recently been adapted from the steady state model by Wilson et al. (99, 102, 103) and applied to VO_2 on-kinetics (62, 79). It should be noted that in conditions that appear to be relatively O_2-independent (on the right part of 5C), disease states can alter O_2 delivery such that these conditions become O_2-dependent, as shown in Figure 5D. For a complete review of 5A and 5B, the reader is directed to Wilson's 1994 review (99) and the 1979 paper by Wilson et al. (102). Although the original idea was that OxPhos was controlled by either O_2 delivery or "metabolic inertia", it now appears that during transitions to submaximal work rates the "metabolic inertia" is dependent in many situations on the intracellular PO_2 (PO_2 less than ~30 Torr). It appears that these ideas are not mutually exclusive, but rather interrelated.

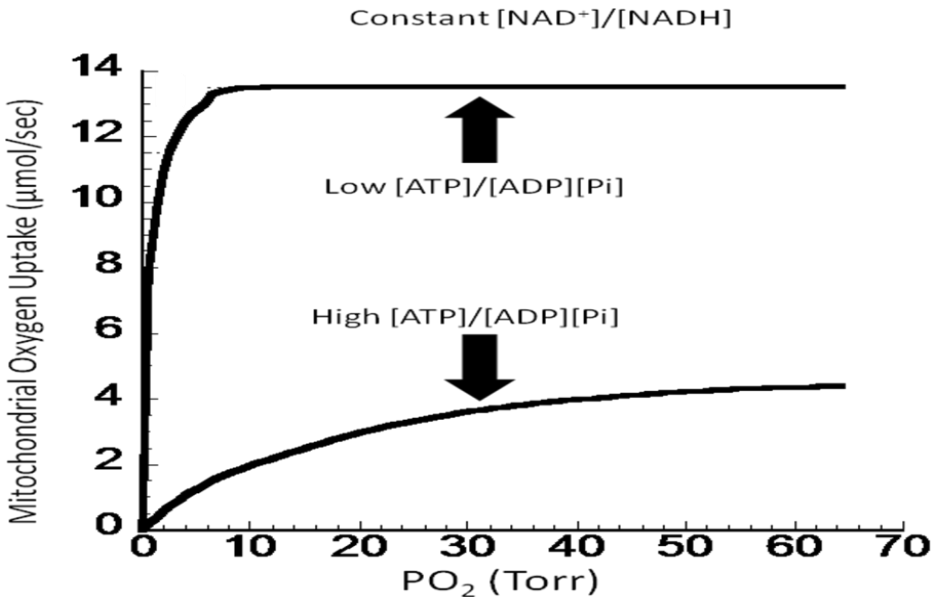

Figure 5A: The predicted dependence of mitochondrial respiration on oxygen tension and "energy charge" ([ATP]/[ADP][Pi]) of the cell. In this scenario, the redox state is held constant. Note that as oxygen tension falls, a greater decline in energy charge is needed for any given respiration rate. Adapted from Wilson et al. (99-102).

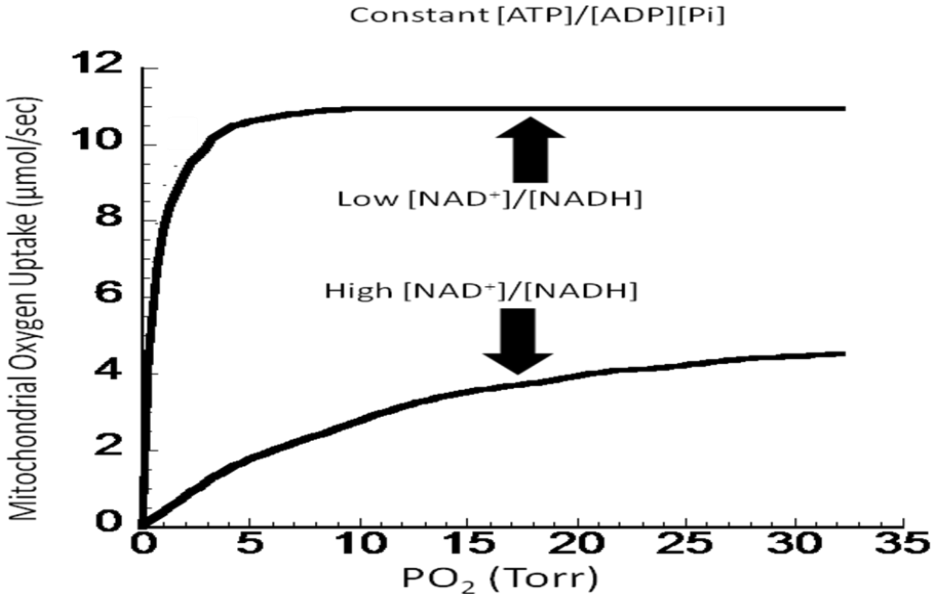

Figure 5B: The predicted dependence of mitochondrial respiration on oxygen tension and "redox state" ([NAD^+]/[NADH]) of the cell. In this scenario, the energy charge is held constant. Note that as oxygen tension falls, a greater decline in redox state is needed for any given respiration rate. Adapted from Wilson et al. (99-102).

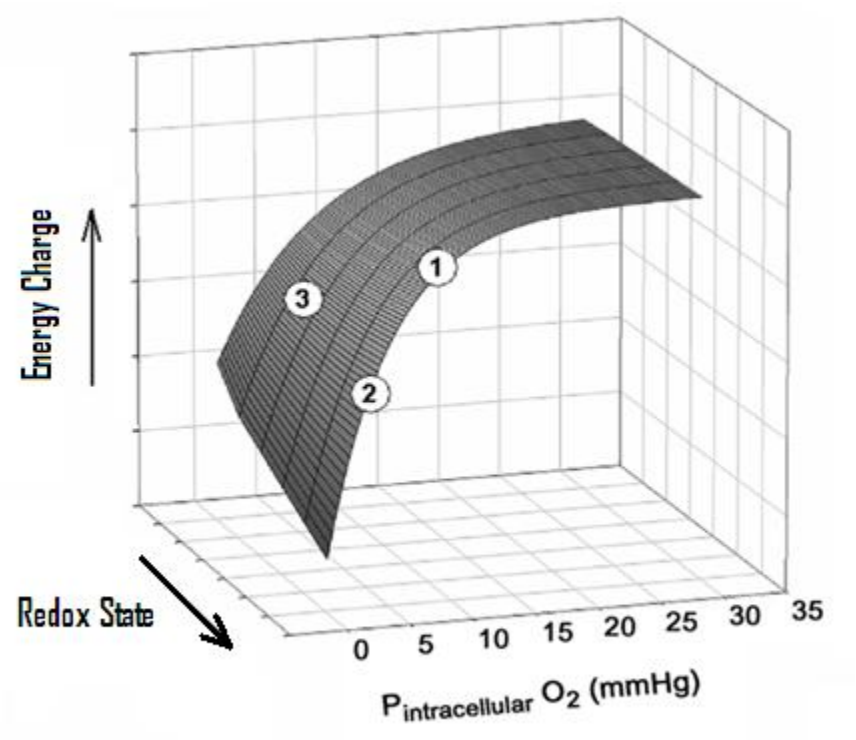

Figure 5C: The interaction of PO_2, energy charge, and redox state for any given respiration rate. The flat portion of this three dimensional wave represents the same respiration rate. In this example, the Y-axis represents energy charge, the X-axis represents intracellular PO_2, and the Z-axis represents redox state. Moving from 1 to 2 (redox state constant), as PO_2 declines, energy charge must decline further to attain a given respiration rate. Moving from 1 to 3, as PO_2 declines, redox state must decline further to attain a given respiration rate. Modified from Hughson (52).

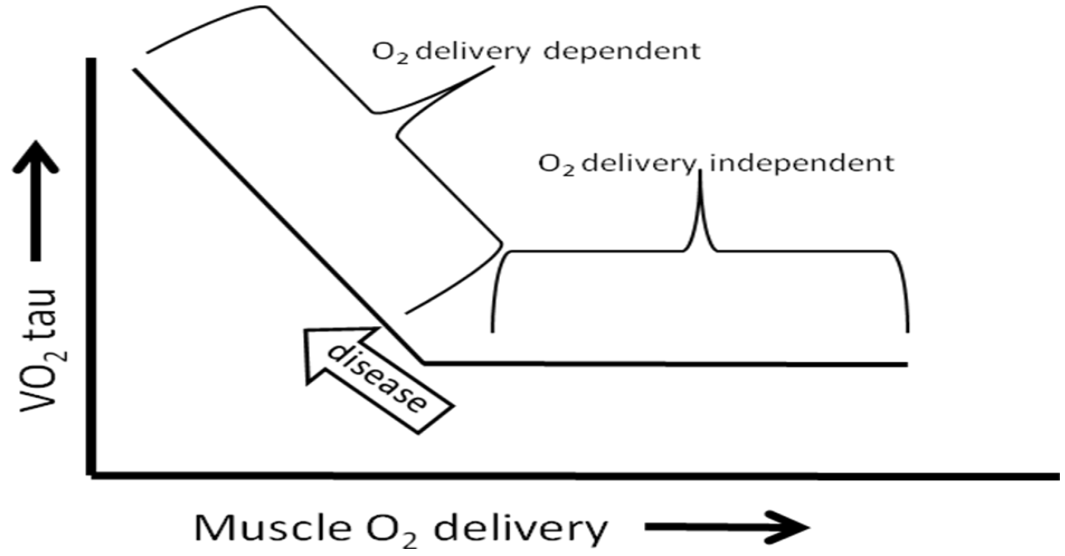

Figure 5D: Cartoon illustrating the relationship between O_2 delivery and the VO_2 time constant for the onset of submaximal exercise. Certain disease states can move patients from being in the O_2 delivery-independent zone into the O_2 delivery-dependent zone. Redrawn from Poole et al. (79).

TOWARDS AN O_2-DEPENDENT UNDERSTANDING OF VO_2 ON-KINETICS

In 1999, Tschakovsky and Hughson perhaps said it best, "If (muscle O_2 consumption) kinetics truly were limited only by intrinsic metabolic inertia or extrinsic O_2 transport inertia in a mutually exclusive manner, it is unlikely that such a degree of conflict would exist" (91). If mitochondrial PO_2 begins to decrease with exercise onset, then energy charge and redox state of the cell must change in order to achieve the desired mitochondrial respiration rate (as shown in Figure 5C). Although Chance and Williams (19) found the Km for O_2 to be ~0.03-0.1 Torr in isolated mitochondria, experimental evidence in other models has shown redox state and energy charge to be altered at what are presumed to be much higher PO_2 levels (4, 22, 49, 56, 61, 100, 101, 103). Wilson et al. (103) show that intracellular PO_2 levels of ~30 Torr and lower warrant significant changes in energy charge or redox state (as compared to intracellular PO_2 values higher than 30 Torr) in order to achieve a particular respiration rate.

This O_2-dependence of mitochondrial respiration has presented many interesting challenges. For example, this model allows the same respiration rate to be achieved at varying O_2 availability levels. Thus, during transitions to higher work rates, if O_2 availability is less than optimal, the required respiration rate can still be achieved by altering the cytosolic milieu (energy charge, redox state) more. This O_2-dependence issue can be examined by analyzing VO_2 on-kinetics – the more altered the cytosolic milieu must become to achieve the appropriate VO_2, the longer the response time will be (91). In human and dog skeletal muscle, attempts to speed the transition to new submaximal steady-state work rates via more O_2 delivery have been unsuccessful, suggesting adequate O_2 delivery during these transitions (36, 55, 69, 98). How much beyond "the tipping point" O_2 delivery is during these transitions is unknown (Figure 6).

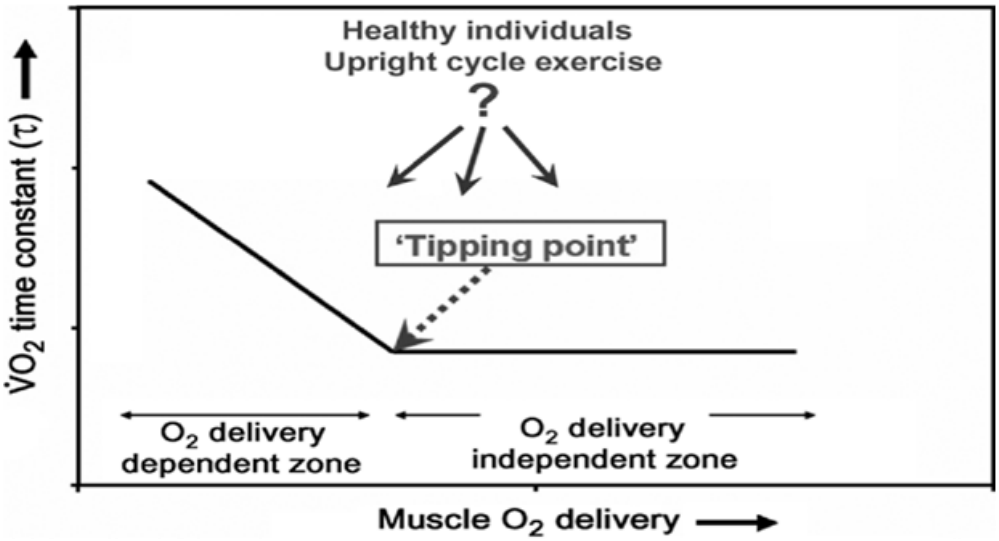

Figure 6: The proposed "tipping point." In transitions to submaximal work rates, evidence suggests that healthy subjects are in the O_2 delivery-independent zone. However, sufficient reductions in O_2 delivery have been shown to increase the VO_2 time constant. It is unclear to what degree O_2 delivery must be impaired for this to happen. From Poole et al. (79).

ROLE OF O_2 DELIVERY IN VO_2 ON-KINETICS

Pathologically, many patients who exhibit slower VO_2 on-kinetics (and thus larger O_2 deficits and decreased activity tolerance) also exhibit altered O_2 delivery to the working muscles (80). For example, in addition to VO_2 on-kinetics being slowed, oxygen delivery is impaired in COPD patients (75), in some chronic heart failure patients (2), in chronic respiratory disease patients (74), in peripheral vascular disease patients (6, 7), and in diabetics (81). Is the slow VO_2 on-response due to a metabolic impairment, impairment in O_2 delivery as shown in Figure 5D (showing movement from O_2-independence to O_2-dependence); or is slower VO_2 on-kinetics in a patient a result of both a metabolic impairment *and* an impaired ability to adequately deliver O_2? It has been shown that the faster VO_2 on-kinetics response seen with training is manifested within days of training, before any changes in oxidative enzyme activity, suggesting that the improvement might have more to do with O_2 delivery (78).

When O_2 consumption by the mitochondria exceeds O_2 delivery to the cell, intracellular PO_2 will decline, and thus capillary PO_2 should decline accordingly (8). With the phosphorescence quenching technique (85), a phosphorescent probe is bound to albumin in the blood and allowed to equilibrate throughout the plasma (~15 min). Then microvascular (~80% capillary) PO_2 can be assessed and analyzed

by the phosphorescence of the probe. For a complete review of this technique, the reader is directed to Rumsey et al. (85).

In 2001, Behnke et al. (8) used phosphorescence quenching techniques to examine microvascular PO_2 during transitions from rest to contractions at 1 Hz in isolated spinotrapezius muscles in rat. Interestingly, there was a 15-20 sec delay before a monoexponential decrease in PO_2 (8). Combined with earlier findings that blood flow is rapidly increased during contractions onset (25, 42), this result suggests that increases in O_2 delivery and O_2 usage are uniquely matched at the onset of contractions in this muscle. If O_2 delivery exceeded usage at contractions onset, then PO_2 would increase transiently; if O_2 delivery did not meet usage at contractions onset, then PO_2 should decrease transiently.

Hogan et al. (47, 48) extended these findings by adapting the phosphorescent quenching technique to single muscle fibers. In these studies, the probe was injected into the isolated frog myocytes, and measurements were made during transitions to contractions while extracellular PO_2 was kept constant at ~30 Torr (to approximate mean capillary PO_2). Interestingly, intracellular PO_2 did not fall immediately, suggesting unqiue matching of O_2 supply to demand. When a prior bout of contractions was used with the same extracellular solution, the time delay until the decrease in PO_2 and the half-time were both significantly shorter, suggesting that "metabolic inertia" played a major role in adjusting to the new ATP demand (47). Using the same technique, Kindig et al. (64) showed that when the extracellular PO_2 is maintained between 20-60 Torr, there is still a time delay on the order of 15-20 sec (64). According to the Fick principle of diffusion, it is difficult to imagine that O_2 diffuses from extracellular space into the cell without an increase in gradient via some decrease in intracellular PO_2. When the phosphoresecent probe is placed in the extracellular fluid instead, and PO_2 is allowed to decrease during transitions (rather than kept constant), PO_2 declines with very little delay (~ 2 sec) (65). These studies suggest that "O_2 delivery" as approximated by an extracellular PO_2 of ~30 Torr uniquely matches the early O_2 demand. The delay in intracellular PO_2 decline when extracellular PO_2 is maintained at ~30 Torr suggests that O_2 delivery is not limiting.

Both DeLorey et al. (24) and Grassi et al. (41) have used near infrared spectroscopy (NIRS) to show a delay in PO_2 decline with contractions onset, suggesting that in normal situations O_2 delivery is not limiting. DeLorey et al. (24) had subjects transition from light exercise to a below-LT work rate on the

cycle ergometer while NIRS (sampling at 2 Hz) was used to monitor oxygenation of the quadriceps vastus lateralis muscle during these transitions. The major finding of this study was that there was a delay (13 ± 2 sec) before the increase in muscle deoxygenation as measured by the reduced hemoglobin signal (24). Grassi et al. (41) performed similar experiments (sampling at 2 Hz), having subjects transition from unloaded pedaling to some below-VT work rate. In these experiments, in agreement with DeLorey et al., NIRS showed an 8.9 ± 0.5 sec delay before a change in the deoxygenation signal was seen (41).

Because it is thought that the NIRS deoxygenation signal (HHb) is a function of the muscle O_2 uptake-to-muscle blood flow ratio (23, 41), and the pulmonary "phase two" response of VO_2 is thought to accurately represent muscle VO_2, Ferreira et al. (30) modified the Fick equation and used these variables to estimate capillary blood flow kinetics where:

Capillary blood flow = VO_2 as measured in phase 2/(a-v)O_2 diff. (approximated by HHb signal)

In subjects who were transitioning from 20 W to 90% of LT on the cycle ergometer, Ferreira et al. (30) showed that capillary blood flow was tightly coupled to VO_2 on-kinetics. This matching of VO_2 kinetics with blood flow kinetics during transitions to below-LT exercise is in agreement with several studies (41, 66). However, other studies have shown blood flow delivery to be faster (30, 38, 58, 71). The authors are careful to point out that this matching of VO_2 to capillary blood flow does not distinguish between either a limitation by O_2 delivery or metabolic inertia (30). Furthermore, the errors associated with these estimates have been questioned (63). In all these measurements though, the O_2 delivery appears *at least* as fast as the VO_2 on-kinetics.

HYPOXEMIA/HYPEROXEMIA

Many studies have sought to examine the role of convective O_2 delivery to the working muscles during work rate transitions, either by altering the amount of O_2 in the blood (hypoxemia/hyperoxemia) or by altering the rate of blood flow delivery. In transitions to submaximal work rates, it has been shown that breathing a hypoxic gas mixture can slow the VO_2 on-kinetics response (29, 72, 88). In 1989, Murphy et al. (72) examined the effect of breathing a 14% O_2 gas on the resultant VO_2 on-kinetics response during transitions from light to moderate cycling exercise. While the gain in VO_2 was the same in both control and hypoxic conditions, the VO_2 on-kinetics response was slower during hypoxia. Springer et al. (88)

supported these findings by showing that both children and adults exhibited slower VO_2 on-kinetics in transitions from rest to moderate exercise when breathing a 15% O_2 gas, despite the fact that normoxia steady state VO_2 was still achieved (88). Other studies since 1991 have shown this same effect; breathing a hypoxic gas (~13-15%) slows the VO_2 on-kinetics response during transitions from rest or light exercise to moderate exercise (20, 55).

Richardson et al. (82) used ^1H NMR to detect myoglobin (Mb) saturation in human quadriceps during exercise at different work rates (50% to 100% VO_{2peak}). The myoglobin desaturation signal indicated a mitochondrial PO_2 of ~5 Torr at rest. This value then declined to an average value of ~3.1 Torr for the remaining exercise intensities (82). When hypoxic gas (12% O_2) was breathed instead of room air, this average PO_2 value fell to ~2.3 Torr. Gayeski et al. (31) measured Mb saturation spectroscopically in dog gracilis muscle that was frozen during transitions from rest to ~70% of VO_{2peak}. During these transitions, PO_2 appeared to decline to as low as ~1.5 Torr. These results suggest that inadequate O_2 delivery during transitional periods can lower intracellular PO_2 enough to significantly slow VO_2 on-kinetics (79, 103).

In 1995, Hughson and Kowalchuk (55) provided evidence that increasing the O_2 delivery did not speed the VO_2 on-kinetics response during transitions to submaximal work rates. While VO_{2max} did increase while subjects inspired a 70% O_2 gas, the VO_2 on-kinetics response was unchanged (55). In 2006, Wilkerson et al. (97) showed that when young healthy subjects (26 ± 4 yr) breathed a hyperoxic gas (50% O_2) during transitions from light to moderate cycling, the VO_2 on-kinetics response was not altered (97).

In 1997, MacDonald et al. (70) examined whether supplying more O_2 during on-transitions to below-VT work rates in healthy subjects would speed VO_2 on-kinetics. In this study (70), subjects breathed either room air or a 70% O_2 gas mixture during transitions from cycling at 25 W to 80% of VT and during transitions from 25 W to half way between VT and VO_{2peak}. Although the hyperoxic gas contributed to a faster VO_2 on-kinetics response during the latter, heavier work rate conditions, it did not affect the VO_2 on-kinetics response during transitions to 80% of VT (70).

Finally, Grassi et al. (37) used the isolated canine gastrocnemius muscle *in situ* to examine the role of hyperoxia in transitions from rest to submaximal work rates. With blood flow already elevated, three conditions were carried out during these transitions: 1) control, 2) ventilation with 100% O_2, and 3)

ventilation with 100% O_2 plus administration of a drug to rightward shift the oxyhemoglobin dissociation curve (2-[4-(((3,5-dimethylanilino)carbonyl)methyl)phenoxy]-2-methylpropionic acid ("RSR-13"), Allos Therapeutics). All trials showed the same VO_2 on-kinetics response, providing further evidence against the idea that hyperoxia can speed the VO_2 on-kinetics response during transitions to submaximal work rates (37). Transitions to higher work rates (maximal, above-VT, above-LT) produce different results, although as mentioned this is beyond the scope of this review.

BLOOD FLOW

Preliminary evidence concerning O_2 and blood delivery as it relates to VO_2 on-kinetics was provided in the form of observations made on cardiac output adjustment as compared to VO_2 adjustment. In 1972 Davies et al. (22) showed that in transitions from rest to moderate work rates, the cardiac output on-kinetics response was faster than the VO_2 on-kinetics response. In 1994 Yoshida et al. (104) provided similar evidence. More indirect evidence that the VO_2 on-kinetics response was not dependent on the blood flow on-kinetics response but rather on some metabolic condition was provided when it was shown that VO_2 on-kinetics mirror PCr on-kinetics, suggesting that intracellular conditions cause the VO_2 on-kinetics response (95). In fact, if the small amounts of ATP contribution from glycolysis are taken out, mathematical models have shown that VO_2 on-kinetics should always mirror PCr on-kinetics (11, 91). However, this VO_2 "mirroring" of PCr kinetics does not necessarily mean that the slow VO_2 response is independent of blood flow; it is possible that low O_2 delivery is the cause for increased reliance on splitting intramuscular phosphate bonds, and O_2 usage then gradually increases as PCr usage gradually decreases until a steady state is achieved. The PCr splitting could be a result of insufficient O_2 availability, and thus PCr kinetics would mirror VO_2 kinetics because O_2 is not adequate. More simply, this correlation does not necessarily prove causation; PCr could be acting as a "primary controller of respiration" or as a temporal ATP buffer (51, 91). In this scenario, PCr rapidly rephosphorylates ADP to ATP to maintain a high intracellular energy charge. However, the Wilson model (99, 102, 103) of varying redox states, energy charges, and PO_2 values to achieve similar respiration rates should be borne in mind. Thus the argument is not over O_2 transport versus metabolic inertia, but rather over when PO_2 is sufficiently low such that other conditions in the cell must adjust more than they would with an adequate PO_2 in order to achieve the

appropriate respiration rate (91). Although the work by Wilson et al. (99, 102, 103) has concerned steady-state respiration, it is logical to assume that the same controls are at work in transitions between metabolic rates (91).

In 1981, Twentyman et al. (92) provided early evidence that slower blood flow adjustment (with β-blockade) resulted in slower VO_2 on-kinetics, although this study was not specifically designed to examine kinetics data. Later, Petersen et al. (77) used β-blockade to examine gas exchange in males during transitions from rest to constant work rate cycling at approximately the "anaerobic threshold"; the VO_2 on-kinetics response was slowed ~49% with β-blockade (τ of 38.4 sec without blockade, 57.2 sec with blockade), although the final VO_2 was the same. In these studies, estimated cardiac output during constant work rate cycling was reduced by 2.1 L/min after β-blockade, an ~13.4% reduction in O_2 delivery. Thus it appears that while O_2 delivery does not affect the final O_2 uptake at this work rate, it does affect the matching of O_2 delivery to demand during the on-transient. However, blood flow on-kinetics to working muscles was not measured.

In 1984 Hughson (50) administered a β-blocker to six males and examined the pulmonary VO_2 kinetics during transitions to and from a work rate below VT. Steady state VO_2 was unaltered; however, much like the earlier work, the VO_2 on-kinetics response was slower (τ slower by ~43%) in the β-blockade group (50). Again, blood flow on-kinetics was not examined. Also in 1984, Convertino et al. (21) showed that the half-time during transition from resting to a submaximal work rate was significantly greater during supine pedaling. In 1986 Hughson and Inman (54) showed that occlusion of nonworking legs during transitions to supine arm cycling resulted in faster VO_2 kinetics, presumably due to more O_2 being available to the working arm muscles. Hughson et al. (60) provided more evidence in 1991 by showing that during step changes in work rate between 25 W and 105 W, VO_2 responded more slowly during supine cycling (as compared to upright).

The implication from these studies was that supine positioning (or β-blockade) resulted in a slowed VO_2 on-kinetics response due to a slower blood flow on-kinetics response, which was based on either assumed or estimated cardiac output. However, no group had yet demonstrated a "restoration" of the control VO_2 on-kinetics response by changing the O_2 delivery conditions back to the control (e.g. in supine cycling, administer lower body negative pressure so that blood flow approximates that of upright cycling).

Hughson et al. (53) followed this line of inquiry in 1993 by examining VO_2 on-kinetics during supine below-VT exercise with and without lower body negative pressure. In this study, subjects showed the slowed on-kinetics response during supine cycling as was shown earlier (τ slower by ~33%), and then lower body negative pressure was applied to normalize the blood flow on-kinetics response. This negative pressure resulted in a VO_2 on-kinetics response similar to control – more evidence for slower rate of blood flow adjustment leading to a slower VO_2 on-kinetics response. Despite the utility of this study, the blood flow on-kinetics was still uncharacterized; the available techniques were not sophisticated enough to follow non-steady state transitions (1).

Grassi and colleagues (42) tackled the issue of assessing blood flow during on-transitions by modifying the constant-infusion thermodilution technique that had been used previously during steady state conditions (1). Subjects in this (42) study transitioned from unloaded pedaling to a work rate ~50 W lower than VT. This transition was made five times for each of the six subjects, with leg blood flow analysis during three of the transitions and blood gas analysis during the other two transitions (42). Blood flow on-transitions appeared to be faster than VO_2 on-transitions (Figure 7), suggesting no O_2 delivery limitation in healthy subjects at below-VT work rates. This study showed that bulk blood flow during normal transitions to below-VT exercise appeared to be sufficient for O_2 delivery to meet O_2 demand. The limitation implicit in the design is that leg blood flow and leg VO_2 were measured, not muscle blood flow or muscle VO_2 *per se*; and blood flow measurements and VO_2 measurements were not made during the same trial.

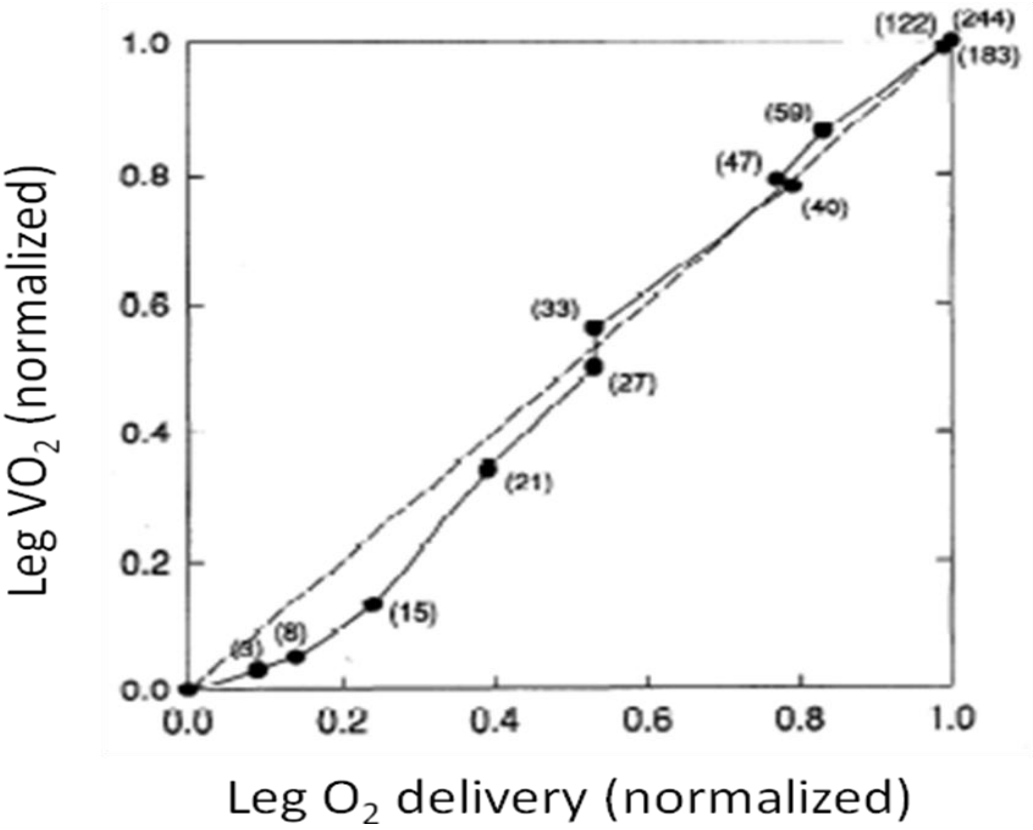

Figure 7: Time course of VO_2 response as compared to blood flow response during upright cycling. Variables were normalized so that the steady state value was 1.0 and the baseline value was 0. In parentheses is the time for each data point. Note that blood flow adjusts more rapidly. Adapted from Grassi et al. (42).

Also in 1996, Hughson et al. (58) examined blood flow and VO_2 on-transitions. In this experiment blood flow to the forearm was altered during transitions from rest to moderate work by performing with the arm either 50° above or 50° below horizontal body position. When O_2 delivery via blood flow was enhanced (50° below horizontal) compared to impeded (50° above horizontal), the VO_2 on-kinetics response was faster. In fact, the response time of VO_2 seemed to match the blood flow response time quite well. Blood flow was calculated by utilizing pulsed-Doppler ultrasound (for blood velocity) and echo Doppler (for vessel diameter). Thus, blood flow was calculated as:

Blood flow = velocity • πr^2

In 1997, Grassi et al. (39) studied the response of 82 heart transplant recipients during on-transitions to moderate exercise. In agreement with earlier work (15, 16), the transplant patients had a slower VO_2 on-kinetics response. In this study, only a short rest was allowed between exercise to allow for

a "priming" of O_2 delivery going into the second bout of exercise (i.e. elevated HR and blood flow). While the on-transition for cardiac output (as measured by impedance cardiography) was speeded during the second bout, the VO_2 on-kinetics response was unchanged. Of course, estimating cardiac output is a less direct measure than measuring blood flow to a particular limb (femoral blood flow), and an even less direct measure than examining blood flow across a working muscle. Furthermore, the time course of splanchnic blood supply vasoconstriction at contractions onset is relatively unknown (56). Thus, while these data appear to argue against the role of convective O_2 delivery as the reason that heart transplant patients have a slowed VO_2 on-kinetics response, they are limited in their scope.

To take a more direct approach, Grassi et al. (36) examined the role of excess O_2 delivery during transitions to submaximal work rates in the isolated canine muscle *in situ*. This approach circumvents two major problems seen in other models. First, muscle VO_2 does not have to be inferred from pulmonary VO_2 (VO_2 is measured directly across the muscle). Second, no "priming exercise" or body positioning is needed to elevate blood flow (these methods may alter the cytosolic milieu). In this study (36), blood flow to the isolated canine gastrocnemius muscle complex was elevated 15-30 sec before contractions onset to the blood flow corresponding to final blood flow levels for that metabolic rate (a submaximal metabolic rate (~60-70% VO_{2peak})). In this manner, any potential limit imposed by convective O_2 delivery is removed. Figure 8 shows the resultant VO_2 on-kinetics data; there was no significant difference in VO_2 on-kinetics response between the control condition and the elevated O_2 delivery condition (36). This was perhaps the clearest demonstration to date that in transitions to submaximal metabolic rates, O_2 delivery does not appear to limit the VO_2 on-kinetics response. However, the question as to how much the blood flow on-kinetics response could be slowed before a slowing of the VO_2 on-kinetics response is seen still remained. In other words, if providing excess blood flow does not speed the VO_2 on-kinetics response, how much could blood flow rate be reduced before the VO_2 on-kinetics response is slowed?

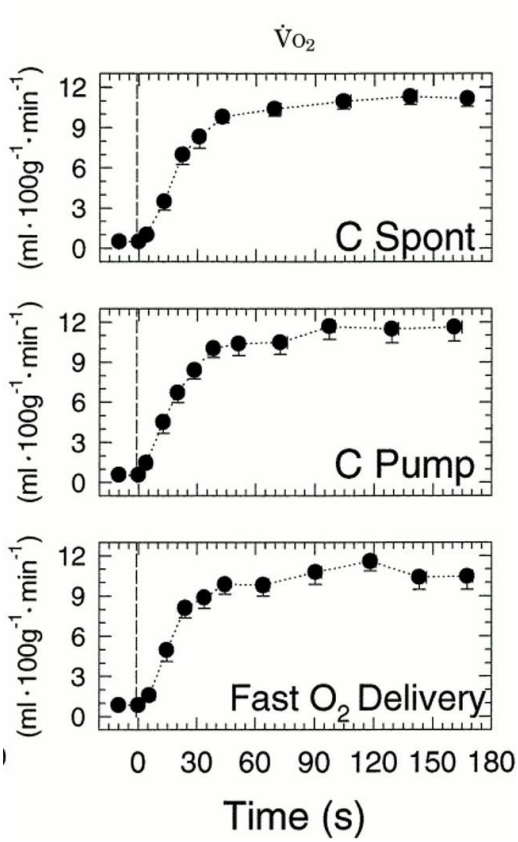

Figure 8: VO_2 on-kinetics in the isolated canine gastrocnemius muscle complex *in situ* during three blood flow conditions. Top: Spontaneous blood flow. Middle: Pump perfusion at spontaneous blood flow rate. Bottom: Blood flow was elevated to steady state level before contractions onset. Note that there was no significant difference between any of the trials. From Grassi et al. (36).

In 1998 MacDonald et al. (71) investigated blood flow on-kinetics and the resultant VO_2 on-kinetics response. In this study (71), subjects performed electrically-braked knee extension and flexion on an ergometer that provided resistance on both movements and set the rate of movement at ~44 cycles per leg per minute at ~40 W. Pulsed and echo Doppler were used to calculate blood flow per equation 3. In this study (71), the VO_2 on-kinetics response and the blood flow on-kinetics response in upright cycling were both faster than during supine cycling. Furthermore, the mean response time (time to ~63.2%) of the blood flow on-kinetics response slowed by ~60% in the supine position, while the VO_2 on-kinetics response only slowed by ~35% (71). In both cycling positions the mean response time of the blood flow on-kinetics response was ~10-12 sec faster than for the VO_2 on-kinetics response. Thus it appears that some "reservoir" of blood flow response may exist such that slowing the blood flow response may not alter the "normal" VO_2 on-kinetics response. Can the blood flow on-response be slowed and the patient/subject

still exhibit normal VO_2 on-kinetics? Does a slower adjustment of blood flow always lead to a more appropriately "disturbed" cytosolic milieu in order to achieve the needed VO_2 changes?

Williamson et al. (98) provided indirect evidence that the blood flow on-kinetics response can be reduced without necessarily reducing the VO_2 on-kinetics response. In this study, the authors administered lower body positive pressure during transitions to moderate intensity exercise. The resultant VO_2 on-kinetics response was not different from controls (atmospheric pressure). This positive pressure was administered in such a manner as to reduce mean flow to the leg on the order of 13-20% (89). However, the blood flow on-kinetics response was not actually assessed in this study.

Shoemaker et al. (86) attempted to quantify and correlate changes in skeletal muscle blood blow, cardiac output, and VO_2 on-kinetics during transitions to submaximal work rates (although it should be noted that blood velocity, not blood flow *per se*, was measured, as no attempt was made at assessing the artery diameter). Subjects performed transitions from rest to dynamic knee extensor exercise (lifting and lowering a weight that was 10% of maximal voluntary contraction through a 2 sec cycle; ~45 W). This knee extensor work rate was similar to submaximal cycling at 45 W. Femoral artery blood velocity was assessed by pulsed Doppler ultrasound, cardiac output was estimated using impedance cardiography, and gas exchange at the mouth was measured breath by breath (86). During these knee extensor transitions, the mean blood velocity on-response (τ of 34.5 ± 3.9 sec) as measured in the femoral artery responded significantly faster than the resultant VO_2 on-kinetics response (τ of 72.2 ± 11.2 sec) (cardiac output τ was 67.1 ± 20.0 sec). In fact, the prolonged τ measured for the VO_2 on-kinetics response was sufficiently long to suggest that this exercise was above the VT (76, 96). Due to 1) no measure of diameter of the femoral artery and thus no blood flow estimate and 2) the resultant work rate appeared to exceed the VT, these data are of limited value other than to demonstrate that blood flow *appears* to adjust to new work rates faster than VO_2.

In an effort to investigate the "central" blood flow adjustment (cardiac output) as compared to the "local" blood flow adjustment (vasodilation) Hayashi et al. (43) examined the VO_2 on-kinetics response during cycling transitions from unloaded pedaling to submaximal work rates (~80% VT) with a delayed vagal withdrawal. This delayed vagal withdrawal was accomplished by applying a cold-water-filled bag to the face during transitions, stimulating bradycardia through the trigeminal-vagal-cardiac pathways. In this

manner the parasympathetic circulatory response is affected (delayed withdrawal); this technique has little effect on the vasculature local to the working skeletal muscle like a β-blocker might (43), yet should slow the rate of heart rate increase. When the desired reduction in rate of cardiac output on-response was achieved in this manner (measured via impedance cardiography), the VO_2 on-kinetics response was not affected (43). This suggested that the adjustment of cardiac output did not necessarily slow the VO_2 on-kinetics response.

This study by Hayashi et al. (43) provided evidence against the 1983 study by Hughson and Morrissey (56) in which transitions from rest (or unloaded pedaling) to 80% VT were compared to 1) transitions from rest to 40% VT (mainly the parasympathetic response), 2) rest to 80% VT (parasympathetic and sympathetic responses), and 3) 40%VT to 80%VT (mainly the sympathetic response). The VO_2 on-kinetics response was slower in the 40-80% transition yet faster in the 0 to 40% transition, in agreement with the different time responses of the sympathetic nervous system and the parasympathetic nervous system. Both the Hayashi et al. (43) and Hughson and Morrissey (56) results are in agreement with other studies (27, 57) and the idea that the parasympathetic nervous system plays a dominant role in transitions from rest to lower work rates, while the sympathetic nervous system plays a dominant role in transitions when heart rate is greater than 100 (84). However, the Hayashi group slowed cardiac output and did not alter the VO_2 on-kinetics, while Hughson and Morrissey speeded and slowed the HR and as a result speeded and slowed the VO_2 on-kinetics response (43, 56).

Hayashi et al. (43) go on to suggest that their results (showing no alteration in VO_2 on-kinetics despite a decrease in HR) are perhaps divergent from other earlier studies because those earlier studies were utilizing β-blockade. They suggest that β-blockers are inappropriate when attempting to specifically alter the cardiac ouput. It is pointed out that while parasympathetic effects on the heart (as in their study) are mainly chronotropic, β-blockade could result in other outcomes. For example, 1) β-blockers affect both stroke volume and vasomotor tone in addition to HR, and 2) splanchnic, cutaneous, and renal blood flow are all influenced by sympathetic outflow. Finally, the authors (43) mention that other studies utilizing body positioning, hypoxia, and/or β-blockade may have changed local blood flow in addition to central blood flow, and thus conclusions drawn about O_2 delivery are limited (43).

The main point though, is that slowing the central blood flow on-kinetics response does not necessarily slow the VO_2 on-kinetics response (the blood flow MRT was reduced by ~32% in the Hayashi study (43) with no resultant slowing of the VO_2 on-kinetics response). If an isolated muscle were used, would reducing the blood flow on-response result in a slower VO_2 on-kinetics response? The Hayashi data suggest that perhaps it would not affect the VO_2 on-kinetics. It must be kept in mind that this paper (43) clearly described the VO_2 on-kinetics response as a result of delayed cardiac output; it is possible and even suggested that the VO_2 on-kinetics response is not delayed in this case due to local O_2 delivery adjusting accordingly (43). It should be pointed out that different groups have gotten vastly different responses when examining transitions to moderate work rates from light exercise or from rest (14, 22, 26, 28, 56). Some of the disagreement has been attributed to exercise modality. Given the disagreement over this, it is logical to suggest that blood flow changes to the muscle are best investigated by directly altering blood flow to the muscle and not having to rely on changes in cardiac output and/or heart rate as surrogates for muscle blood flow and/or O_2 delivery. Thus, full examination would best take place across a single, isolated muscle, in which blood flow changes can be directly controlled and VO_2 changes can be directly assessed.

PURPOSE

A substantial body of evidence now supports the idea that during transitions to submaximal work rates 1) an excess of O_2 delivered to the working muscle does not speed the VO_2 on-kinetics response, and 2) the VO_2 on-kinetics response can be slowed via sufficient reductions in O_2 delivery to the working muscle. The question then arises: what "buffer" of O_2 delivery exists during these transitions? Thus, the purpose of this study was to examine the resultant VO_2 on-kinetics response when O_2 delivery is slowed by slowing blood flow delivery. To what degree must the blood flow on-kinetics response be slowed in order to see a resultant slowed VO_2 on-kinetics response? In this study, blood flow on-kinetics (tau) will be slowed by 25 sec and 50 sec. Based on the literature to date, we hypothesize that some excess O_2/blood delivery ("buffer") exists during these transitions.

III. JOURNAL MANUSCRIPT

VO_2 ON-KINETICS IN ISOLATED CANINE MUSCLE *IN SITU* DURING SLOWED CONVECTIVE O_2 DELIVERY

ABSTRACT

With respect to O_2 delivery and VO_2 on-kinetics, current evidence suggests that a "tipping point" exists; increasing O_2 delivery above this point will not speed VO_2 on-kinetics while slowing O_2 delivery below this point will slow VO_2 on-kinetics. The purpose of this study was to examine the resultant VO_2 on-kinetics when the blood flow on-response was slowed by 25 and 50 sec. The isolated gastrocnemius muscle complex *in situ* in 6 anesthetized dogs was studied during transitions from rest to submaximal contractions. Four trials were performed: 1) A Control Trial (CT), in which resting blood flow and steady state blood flow were established, 2) Control Trial 20 (CT20), in which blood flow on-kinetics tau was set at 20 sec, 3) Experimental Trial 45 (EX45), in which blood flow on-kinetics tau was set at 45 sec, and 4) Experimental Trial 70 (EX70), in which the blood flow on-kinetics tau was set at 70 sec. Average mean response time (tau + time delay = MRT) values for CT20, EX45, and EX70 were (mean ± SD) 19.9 ± 3.8, 26.3 ± 5.9, and 31.7 ± 4.1 sec, respectively (all significantly different). Slowing O_2 delivery via slowing blood flow on-kinetics resulted in a linear slowing of the VO_2 on-kinetics response (R=0.99997); this suggests that either 1) the appropriate levels of metabolites needed to stimulate the control VO_2 at any time could not be reached, or 2) the appropriate levels of metabolites needed to stimulate the control VO_2 at any time were reached, yet the O_2 was not available. These results show that in our current experimental model, muscle VO_2 and blood flow/O_2 delivery are very closely matched during the transition period from rest to steady state contractions.

.

INTRODUCTION

Despite almost 100 years of investigation into the controls of oxidative phosphorylation (OxPhos) at the onset of exercise/muscle contractions (42), it is still a much-debated topic (18, 37, 52). In particular, the role of O_2 delivery on OxPhos response time has been an area of recent discussion and experimentation (40, 52). This has garnered interest from both basic and applied scientists, in part because many patients who present with slower oxygen uptake (VO_2) on-kinetics also exhibit altered blood flow on-kinetics to the working muscles (53) {(e.g. COPD patients (49), some chronic heart failure patients (10, 24), chronic respiratory disease patients (47), peripheral vascular disease patients (5, 6), and diabetics (54)}. (Note that "VO_2" is used here to represent "oxygen uptake per minute"; traditionally this is represented as "VO_2" with a dot over the V.)

Studies utilizing hypoxic/hyperoxic breathing during transitions to submaximal work rates have shown that breathing hypoxic gas during these transitions can slow the VO_2 on-kinetics response (12, 35, 46, 59), yet breathing a hyperoxic gas does not speed the VO_2 on-kinetics response (21, 35, 43, 62). When examining the same principle (altered O_2 delivery) in studies of blood flow alterations, similar results are obtained. For example, when subjects performed transitions while under β-blockade (and presumably slower blood flow adjustments), the VO_2 on-kinetics response was slowed when compared to control non-β-blockade trials (32). Similarly, when subjects performed cycling transitions while in the supine position, the VO_2 on-kinetics response was slowed when compared to upright cycling (13, 34, 38, 44). However, many of these studies did not directly assess blood flow or VO_2 across a working muscle, instead relying on cardiac output, limb blood flow, and pulmonary VO_2 on-kinetics as estimates. To date, most studies in this area have relied on pulmonary VO_2 measured at the mouth as a proxy for muscle VO_2 and limb blood flow or even cardiac output as a proxy for muscle blood flow. For mechanistic investigations, a more direct approach is needed.

In 1998, Grassi et al. (20) addressed this problem by examining the resultant VO_2 on-kinetics during transitions to submaximal metabolic rates during conditions of increased O_2 delivery in the isolated canine gastrocnemius muscle complex *in situ*. In this study, blood flow to the working muscle was elevated to the steady state level prior to contractions onset, thus eliminating any delay in convective O_2

delivery to the contracting muscle. Despite the increased O_2 availability to the muscle at contractions onset, the VO_2 on-kinetics response was not significantly altered (20).

Furthermore, it has been shown that in human whole body exercise, limb blood flow appears to adjust with a faster relative time course when compared to VO_2 (27, 44), suggesting that some blood flow adjustment "buffer" exists. While Hughson and Morrissey (36) speeded and slowed HR and as a result speeded and slowed VO_2 on-kinetics, other studies suggest that blood flow can be reduced and yet VO_2 on-kinetics may remain unaltered (28, 63). Perhaps the conflicting results are due to the inherent limitations of making inferences from indirect, whole-body measurements. For example, β-blockade or supine positioning may alter more than just blood flow across a single muscle bed. Also, HR changes may be more indicative of changes in central blood flow rather than local blood flow, and limb blood flow may differ from muscle blood flow (28).

Overall, there appears to be a "tipping point" at which increasing convective O_2 delivery does not further speed VO_2 on-kinetics while decreasing O_2 delivery will slow VO_2 on-kinetics (40, 52) (Figure 1). Given the debate and disagreement that surrounds this topic, emphasis should be placed on mechanistic investigations across a single, isolated muscle, where blood flow changes can be directly controlled and VO_2 changes can be directly assessed. Grassi et al. (20) used the isolated canine gastrocnemius muscle complex *in situ* to directly measure whether speeding O_2 delivery would speed the VO_2 on-kinetics response; it did not. It is the purpose of the current study to use this same direct approach to examine the other side of the "tipping point"; does slowing convective blood flow delivery slow VO_2 on-kinetics? In this study, the blood flow on-kinetics response (tau) was slowed by 25 and 50 sec, and the resultant VO_2 on-kinetics response was analyzed.

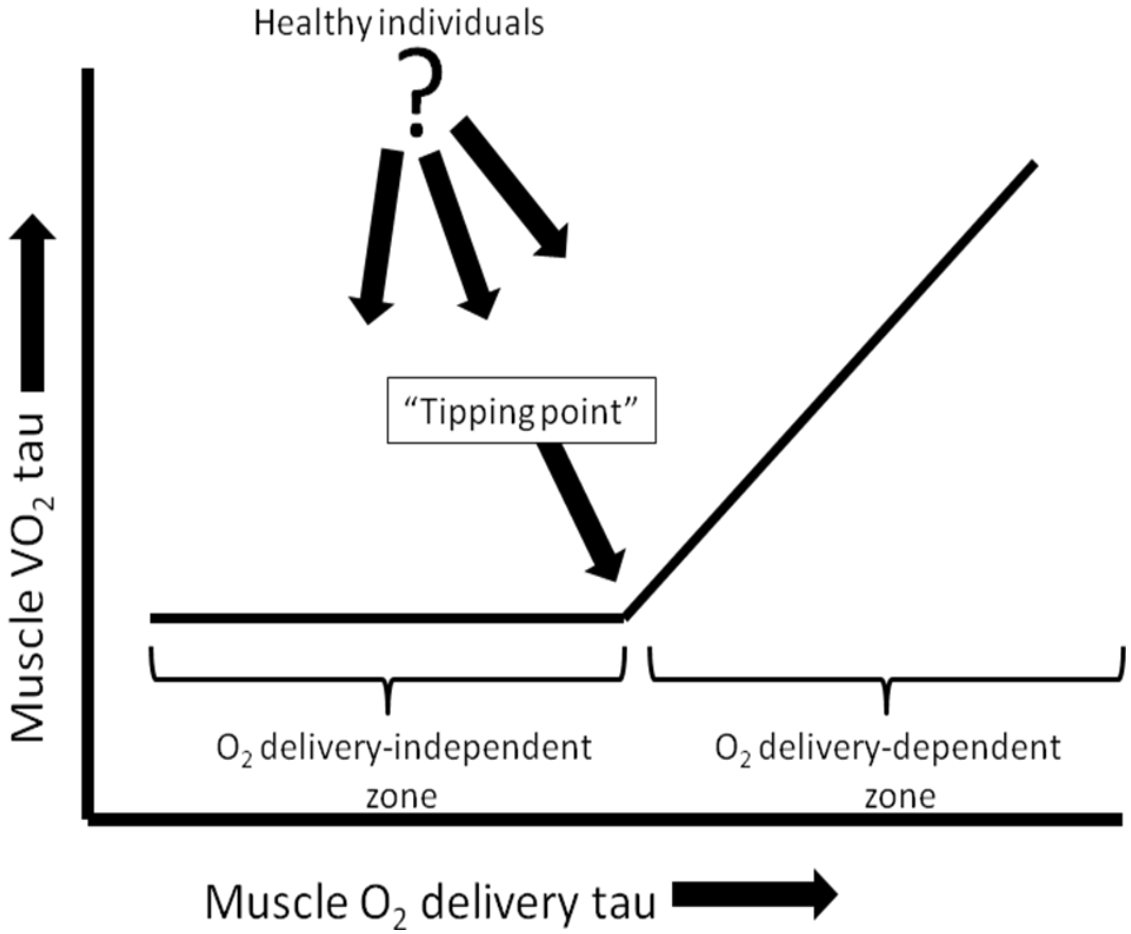

Figure 1: The proposed "tipping point." In transitions to submaximal work rates, evidence suggests that healthy subjects performing upright exercises are in the O_2-delivery-independent zone. However, sufficient reductions in O_2 delivery appear to increase the VO_2 time constant. It is unclear to what degree O_2 delivery must be impaired for this to happen. Adapted from Poole et al. (52).

METHODS AND PROCEDURES

This study was conducted with the approval of the Institutional Animal Care and Use Committee of Auburn University, Auburn, Alabama, where experiments were performed. Eleven adult dogs (beagles) of either sex were anesthetized with sodium pentobarbital (30 mg • kg^{-1}), with maintenance doses given as required (palpebral and plantar reflexes were monitored). Dogs were intubated with an endotracheal tube and ventilated with a respirator (model 613, Harvard Apparatus). Rectal temperatures were maintained at 37°C with a heating pad. Subsequent to surgical preparation, all dogs were treated with heparin (3,000 U/kg). Ventilation was maintained at a level that maintained "normal" arterial PO_2, PCO_2, and pH.

Surgical Preparation. Data for this study were obtained utilizing the gastrocnemius muscle complex (gastrocnemius + superficial digital flexor) as described in detail previously (60). Briefly, a medial incision was made through the skin of the left hindlimb from midthigh to the ankle. All muscles which overlie the gastrocnemius (sartorius, gracilis, semitendinosus, and semimembranosus) were cut with a cauterizing blade (electric soldering gun) at their insertions and laid back. Venous outflow from the GP was isolated by ligating all veins draining into the popliteal vein except the GP veins. The popliteal vein was cannulated, and this venous blood flow was returned to the animal via a reservoir attached to a cannula in the left jugular vein. Arterial circulation to the GP was isolated by ligation of all vessels from the popliteal artery that do not enter the GP. The right femoral artery was also isolated and cannulated. Blood from this artery was passed through tubing to a peristaltic pump (Gilson Minipuls 3, Gilson Inc., Middleton, WI) and through another cannula into the contralateral, isolated popliteal artery supplying the GP. A T-connector in the tubing to the GP was connected to a pressure transducer (model RP-1500, Narco Biosystems) for measurement of perfusion pressure.

A portion of the calcaneus, with the two tendons from the GP attached, was cut away at the heel and clamped around a metal rod for connection to an isometric myograph via a load cell (Interface SM-250) and a universal joint coupler. The universal joint coupler allowed the muscle to always pull in a direct line with the load cell and thus prevented the development of significant torque. The other end of the muscle remained attached to its origin. Both the femur and the tibia were fixed to the base of the myograph by bone nails. A turnbuckle strut was placed parallel to the muscle between the tibial bone and the arm of the myograph to minimize flexing of the myograph.

The sciatic nerve was exposed and isolated near the GP. The distal stump of the nerve, ~1.5-3.0 cm in length, was pulled through a small epoxy electrode containing two wire loops for stimulation. Exposed tissues were covered with saline-soaked gauze and a thin plastic sheet to minimize drying and cooling. After each experiment, the muscle was removed from the animal, cleared of surface connective tissue and weighed both before and after drying. Weight was used to normalize some variables to muscle mass. All dogs were euthanized at the end of the experiment with an overdose of sodium pentobarbital and potassium chloride.

At the start of each experiment, the muscle was set at optimal length (L_o) by progressively lengthening it until a peak in developed tension was obtained (stimulated at a rate of 0.2 Hz). Once L_o was obtained, five minutes of rest were allowed before studies began.

Experimental Design. Five dogs were used in a preliminary study to determine the spontaneous blood flow on-response. Six dogs were used in the experimental trials below. Resting and steady state flow rates to the GP were determined in a Control Trial (CT) by adjusting the flow pump during contractions to obtain a reasonable pressure for rest (90-120 Torr) and contractions (130-160 Torr) while minimizing fatigue. Flow rate was subsequently controlled with the pump in experimental trials. Overall, four trials were performed, each separated by ~35 minutes of rest: 1) The Control Trial (CT) in which resting blood flow and steady state blood flow were selected by beginning contractions and adjusting the flow in a manner to maintain adequate pressure, 2) Control Trial 20 (CT20) in which pump-perfusion was used to deliver blood to the muscle with a tau of 20 sec, 3) Experimental Trial 45 (EX45) in which the blood flow on-kinetics response to the GP was slowed by 25 sec (tau = 45 sec) via pump perfusion, and 4) Experimental Trial 70 (EX70) in which the blood flow on-kinetics response to the GP was slowed by 50 sec (tau = 70 sec) via pump perfusion. Because arterial [O_2] (CaO_2) was kept constant, O_2 delivery was changed by altering blood flow. For all trials, stimulation was via the sciatic nerve, using trains of stimuli (4.0 V, 200-ms duration, 50-Hz frequency) at a rate of one per two seconds to evoke isometric tetanic contractions that elicit ~60-70% of VO_{2peak} in this model (20). Blood flow was controlled via a Gilson Minipuls 3 high flow peristaltic pump. For experimental trials final blood flow in the steady state remained the same, but the rate of achieving that steady state was progressively slowed. Thus, the time constant was changed appropriately in order to achieve the slower blood flow adjustments. A laptop with software (706 developer's kit, Gilson) and a program developed in-house were used to drive the pump via an interface box (RS-232 to RS-485 converter; 508 box, Gilson).

Measurements. Outputs from the pressure transducer and load cell (first through strain gauge couplers), flowmeter (T206, Transonic Systems, Ithaca, New York; first through a transducer coupler), and indwelling Abbott Oximeter probe (Oximetrix 3) were fed into a computerized data acquisition system (Oxymon MkIII, Artinis Medical Systems BV). All signals were sampled at a rate of 125 Hz. The load

cell reaches 90% of full response within 1 ms while the flowmeter was set to a pulsatile cutoff frequency of 100 Hz. The load cell was calibrated with known weights prior to each experiment. The flowmeter was manually calibrated with a graduated cylinder and clock during and after each experiment. The Oximetrix 3 sampled percent hemoglobin saturation (SO_2, %) at a rate of 244 samples per second, averaged the samples each second, and then gave an output of a 5-sec rolling average each second. This output has a 90% response time of 5 sec. The time response of this output was further speeded via mathematical deconvolution based on the Oximetrix 3's response to square wave changes induced by rapidly moving the probe between two tubes of blood containing different SO_2 values.

Samples of arterial blood entering the muscle and of venous blood from the popliteal vein were drawn anaerobically into 3.0 mL plastic syringes. Since the arterial values varied only slightly throughout each experiment, arterial samples were taken at before and after each contraction period. Venous blood samples were collected from the catheter draining the muscle at rest (~10 sec before the onset of each contraction period) and during the steady state near the end of each contraction period; these samples were used to calibrate the indwelling Oximetrix 3 signal. Blood samples were immediately stored in ice water and analyzed within 30 min of collection. Both arterial and venous blood samples were analyzed at 37 °C for PO_2, PCO_2 and pH by a blood gas, pH analyzer (Instrumentation Laboratories GEM Premium 3000), and for hemoglobin concentration ([Hb]) and SO_2 with a CO-Oximeter (IL 682, Instrumentation Laboratories), set for dog blood. These instruments were calibrated before and during each experiment.

VO_2 of the gastrocnemius was calculated by Fick's principle as $VO_2 = Q \bullet C(a\text{-}v)O_2$, where $C(a\text{-}v)O_2$ is the difference in O_2 concentration between arterial blood (CaO_2) and venous blood (CvO_2) and Q is blood flow. Samples for blood flow and venous SO_2 (following deconvolution) were averaged over each contraction cycle (2 sec), allowing calculation of VO_2 on a contraction-by-contraction time frame. Blood samples were also taken before experimental trials to ensure proper arterial values. Sodium bicarbonate and oxygen were administered and ventilation adjusted as required to maintain appropriate pH, PCO_2, and PO_2.

Kinetics analysis. VO_2 data were fitted by an equation (KaleidaGraph 4.0) of the type:

$$y(t) = y_{BAS} + A\,[1 - e^{-(t - TD)/\tau}]$$

In this equation, y*BAS* indicates the baseline value obtained at rest before contraction onset, A indicates the amplitude between y*BAS* and the steady-state value at the end of the contraction period, TD the time delay and τ the time constant of the function. The half-time ($t_{50\%}$) of the on-kinetics exponential function can be calculated by multiplying τ by 0.693. To facilitate a comparison with the results reported by previous studies (20-23, 27), τ and TD were added together to calculate the mean response time (MRT) of the overall response. Similarly, blood flow data were fit by an equation of the type:

$$y(t) = y_{BAS} + A\,[1 - e^{-(t)/\tau}]$$

NIRS. Muscle oxygenation was analyzed with a continuous wave near-infrared spectroscopy (NIRS) system (Oxymon MkIII, Artinis Medical Systems BV). Briefly, two fiber-optic bundles communicate between the data acquisition system and the muscle. At the end of one cable, NIR light is emitted from an optode in two wavelengths (860 and 784nm); at the end of the other cable, NIR light is absorbed through an optode and transmitted back to the data acquisition center. Because deoxyhemoglobin (HHb) and oxyhemoglobin (O_2Hb) absorb NIR light maximally at different wavelengths, it is possible to distinguish between the relative oxygenation of these chromophores. Currently, controversy still exists over how much myoglobin (Mb) contributes to the NIRS signal (8, 11, 45, 48, 56). For a more thorough review, the reader is directed to Elwell (16). In current experiments, the optodes were fixed in place on the GP muscle and retained in place by a Velcro strap. Opaque black plastic was placed over the optodes to block external light. Signals are relative (μM), and were biased to zero prior to each contraction period. Signals were averaged over each contraction cycle.

Statistical Analysis. All data are presented as means ± SD. The data were analyzed using a one-way repeated measures analysis of variance (ANOVA). In some circumstances the data were analyzed using student t-tests to determine differences between means. Student Newman-Keuls post hoc testing was used to determine where any significant differences occurred. The level of significance was set at $p<0.05$.

RESULTS

The weight of the GP muscles was 44.5±9 g (10.1±1.9 g dried, indicating an average water percentage of 77.2±0.7%).

Resting and Steady State values. Resting and steady state values pertinent to our study are shown in Tables 1 and 2, respectively. There was no significant difference between any of these variables between trials. There were also no significant differences between trials with respect to temperature of blood draining the muscle. Differences in temperature did occur when analyzing temperature changes across time (0-180 sec). However, the temperature changes seen from 0-180 sec were all less than 1°C.

Table 1: Resting average values.

Variable	Condition		
	CT20	EX45	EX70
PaO_2 (Torr)	122±21	118±17	139±31
$PaCO_2$ (Torr)	30±3	30±4	30±5
PvO_2 (Torr)	53±4	49±6	55±8
CaO_2 ($mL \cdot dL^{-1}$)	26.9±3.6	26.4±3.1	26.6±3.2
CvO_2 ($mL \cdot dL^{-1}$)	22.1±4.4	20.8±3.3	22.2±3.6
CaO_2-CvO_2 ($mL \cdot dL^{-1}$)	4.8±1.2	5.6±1.5	4.4±1.2
Blood Flow (Q) ($mL \cdot kg^{-1} \cdot min^{-1}$)	102±17.4	101.4±12.4	97.7±10.5
Q x CaO_2 ($mL \cdot kg^{-1} \cdot min^{-1}$)	27.3±5.7	26.8±5.0	26.1±5.3
VO_2 ($mL \cdot kg^{-1} \cdot min^{-1}$)	3.7±2.3	4.5±1.7	3.8±1.6
Muscle Perfusion Pressure (Torr)	121.2±18.2	124.9±27.5	134.8±25.3
tHb ($g \cdot dL^{-1}$)	19.9±3.1	19.5±2.5	19.5±2.6
arterial pH	7.34±0.06	7.37±0.02	7.36±0.06

Data are presented as means ± SD; n=6. CT20 = trial with blood flow delivery tau = 20 sec; EX45 = trial with blood flow delivery tau = 45 sec; EX70 = trial with blood flow delivery tau = 70 sec. There were no significant differences between any of these variables at the $p<0.05$ level.

Table 2: Steady state average values.

Variable	Condition		
	CT20	EX45	EX70
PaO_2 (Torr)	126±17	126±20	142±30
PaCO2 (Torr)	27±3	27±6	28±7
PvO_2 (Torr)	25±6	25±5	25±5
CaO_2 ($mL \cdot dL^{-1}$)	27±4	26±3	27±3
CvO_2 ($mL \cdot dL^{-1}$)	9.6±3.8	9.2±3.5	9.0±2.6
CaO_2-CvO_2 ($mL \cdot dL^{-1}$)	17.3±4.2	17.2±3.7	17.5±3.7
Blood Flow (Q) ($mL \cdot kg^{-1} \cdot min^{-1}$)	811±207	831±204	804±205†
Q x CaO_2 ($mL \cdot kg^{-1} \cdot min^{-1}$)	214±42	220±44	210±38
VO_2 ($mL \cdot kg^{-1} \cdot min^{-1}$)	129.9±12.1	135.9±10	131.5±11.1
Muscle Perfusion Pressure (Torr)	158.6±37.9	151.2±38.8	149.7±29.1
tHb ($g \cdot dL^{-1}$)	19.6±2.7	19.8±2.3	19.7±2.5
arterial pH	7.34±0.07	7.35±0.02	7.35±0.08
Time to 50% peak force (sec)	102.7±11.5	76±24.9*	72±19.4*†
Peak Force (N)	266.4±63.5	265.2±63.8	256.2±56

Data are presented as means ± SD; n=6. CT20 = trial with blood flow delivery tau = 20 sec; EX45 = trial with blood flow delivery tau = 45 sec; EX70 = trial with blood flow delivery tau = 70 sec. *Denotes statistical significance from CT20 at the $p<0.05$ level. †Denotes significance from EX45 at the $p<0.05$ level. Note that "steady state blood flow" in trial EX70 was significantly lower than in EX45 ($p=0.0351$). This difference is most likely due to the fact that the manual blood flow calibration was taken at around 3 min of each trial. In EX70 (tau=70 sec), blood flow would be lower at 3 min because of the very large tau (tau of 70 sec; at 3 min, only 2.6 tau will have elapsed – representing ~92% of final response). In any case, note that steady state VO_2 values were not significantly different, and the pump-controlled blood flow patterns were verified by fitting the blood flow curves with a monoexponential function (Table 3).

Kinetics of Blood Flow and VO_2. The experimental trials were designed to yield blood flow tau values of 20, 45, and 70 sec for CT20, EX45, and EX70 respectively. The actual values matched our planned values quite well (Figure 2 shows data from an example dog; means were 22.6 ± 1.7, 46.8 ± 4.4, and 67.8 ± 5.6 sec for CT20, EX45, and EX70 respectively). The experimental trials were carried out without a spontaneous blood flow run (i.e. all trials involved pump-perfusing the muscle). However, pilot experiments were done (n=5) in which the muscles were spontaneously perfused. In these experiments the average MRT value of the blood flow/O_2 delivery was determined to be 15.6 ± 8.6 sec. This was not significantly different from the blood flow/O_2 delivery MRT in the experimental trials during CT20. The average VO_2 MRT value during these pilot experiments was 19.2 ± 6.3 sec, also not significantly different from CT20 MRT value.

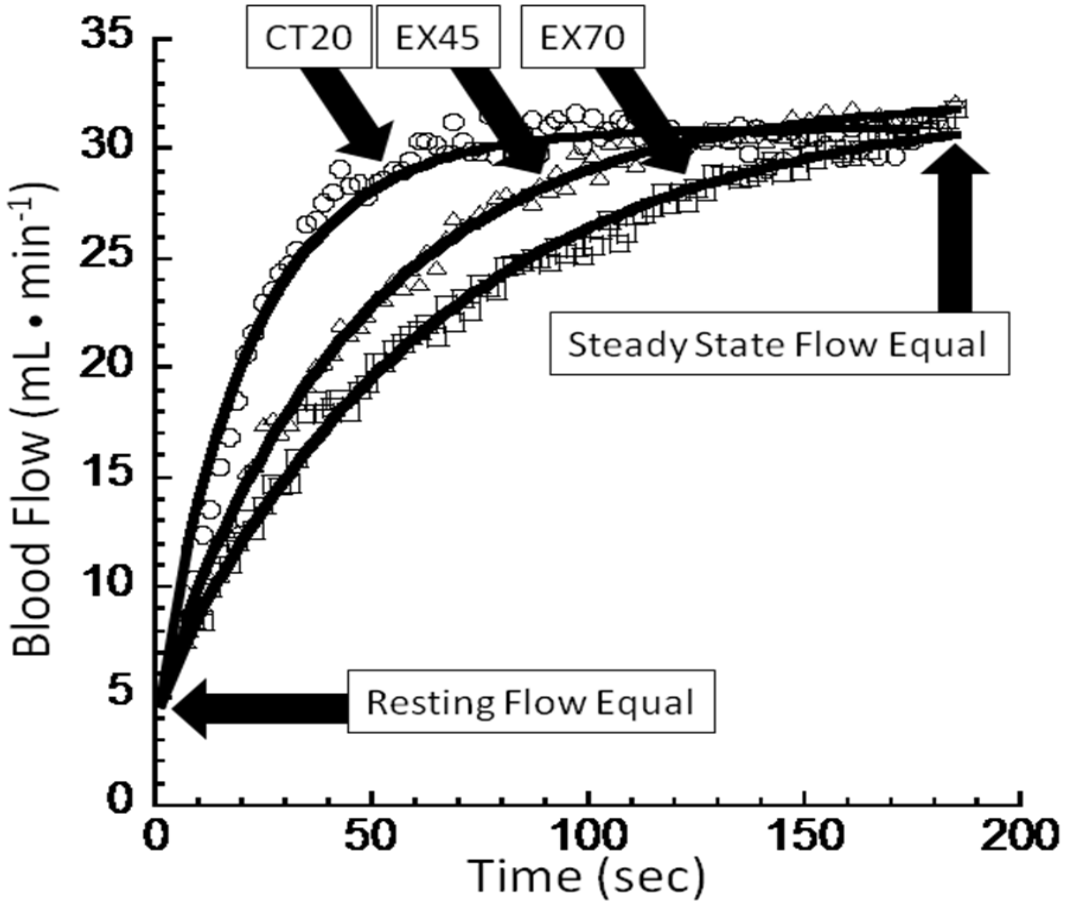

Figure 2: Alterations in blood flow on-kinetics. Four trials were run. A Control Trial (CT) allowed spontaneous perfusion of the muscle in order to determine appropriate resting and steady state blood flows. Control trial 20 (CT20) entailed pump-perfusing the muscle with a tau of 20 sec. Also, an experimental trial with a pump-perfused tau of 45 sec was performed (EX45) and an experimental trial with a pump-perfused tau of 70 sec was performed (EX70). Note that steady state blood flow and resting blood flow are the same in all trials. (These are real data from Dog 2 in this study.)

Because flow rate was pump-controlled and then actually measured as it left the muscle venously, approximately the first five seconds of flow data were artificially inflated due to the muscle pump squeezing blood from the muscle (this was determined in pilot work by clamping the arterial inflow and then eliciting contractions while measuring blood flow leaving the ischemic muscle). Thus, the first 6 seconds of data were omitted and the rest of the data were fit with the monoexponential curve with no time delay (and thus tau=MRT for blood flow data).

As planned (illustrated in Figure 2), EX45 exhibited significantly slower blood flow delivery than CT20 ($p<0.0001$) and EX70 exhibited significantly slower blood flow delivery than both CT20 ($p<0.0001$) and EX45 ($p<0.0001$). Because our concern was O_2 delivery *per se* (mL O_2 • min^{-1}), it was calculated by multiplying the blood flow by the arterial O_2 concentration. However, O_2 delivery and blood flow kinetics are mentioned interchangeably, since blood flow increased exponentially while CaO_2 did not change from rest to steady state contractions.

Because the VO_2 on-response includes an early divergence from the monoexpoential rise that may be due to 1) the muscle pump elevating blood flow, 2) some transit delay from the mitochondrial response to a corresponding signal in the venous blood, or 3) some other delay yet to be fully explained, the response was fit with an equation that included the TD. VO_2 was calculated over each contraction cycle (2 sec) to provide contraction-by-contraction values.

There were no significant differences for TD values between any of the conditions, nor were there any significant differences between the steady state VO_2 values between any of the conditions. Mean tau values for CT20, EX45, and EX70 were 13.1 ± 4.9, 18.5 ± 5.2, and 23.3 ± 4.5 sec respectively. EX70 exhibited significantly larger tau values when compared to CT20 ($p=0.003$). EX45 also exhibited significantly larger tau values when compared to CT20 ($p=0.04$). The difference between EX45 and EX70 tau values were not significant, although the p-value should be noted ($p=0.06$).

Average mean response time (TD + tau = MRT) values for CT20, EX45, and EX70 were 19.9 ± 3.8, 26.3 ± 5.9, and 31.7 ± 4.1 sec respectively. EX70 exhibited significantly larger MRT values when compared to EX45 ($p=0.01$) and CT20 ($p<0.0001$). EX45 was also significantly different from CT20 ($p=0.003$). VO_2 on-response data are presented in table 3. Fits for all VO_2 on-kinetics in CT20, EX45, and EX70 are illustrated in panels 3A, 3B, and 3C, respectively. Figure 4 shows the normalized VO_2 responses averaged over all trials. Table 3 shows O_2 delivery and VO_2 values.

3A

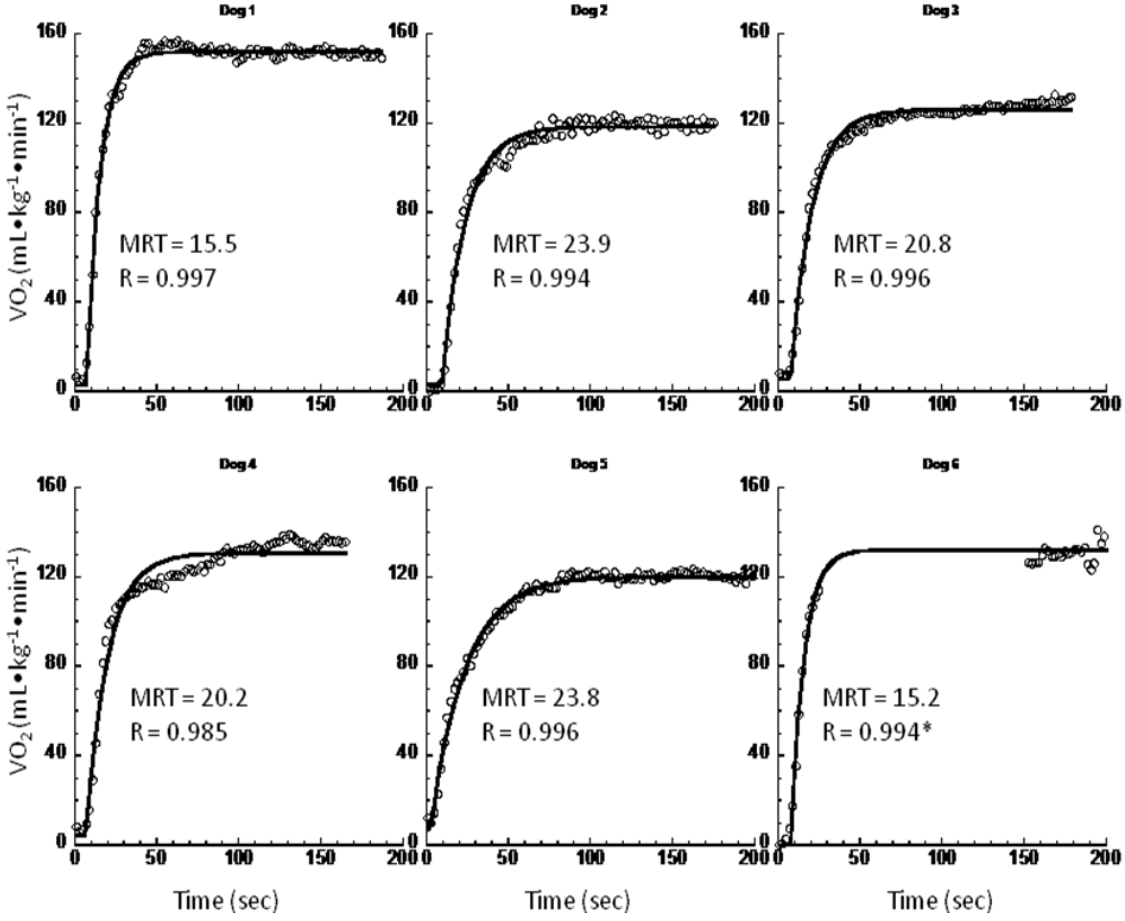
Dog 1
Dog 2
Dog 3
Dog 4
Dog 5
Dog 6
MRT = 15.5
R = 0.997
MRT = 23.9
R = 0.994
MRT = 20.8
R = 0.996
MRT = 20.2
R = 0.985
MRT = 23.8
R = 0.996
MRT = 15.2
R = 0.994*
VO2 (mL•kg-1•min-1)
Time (sec)

3B

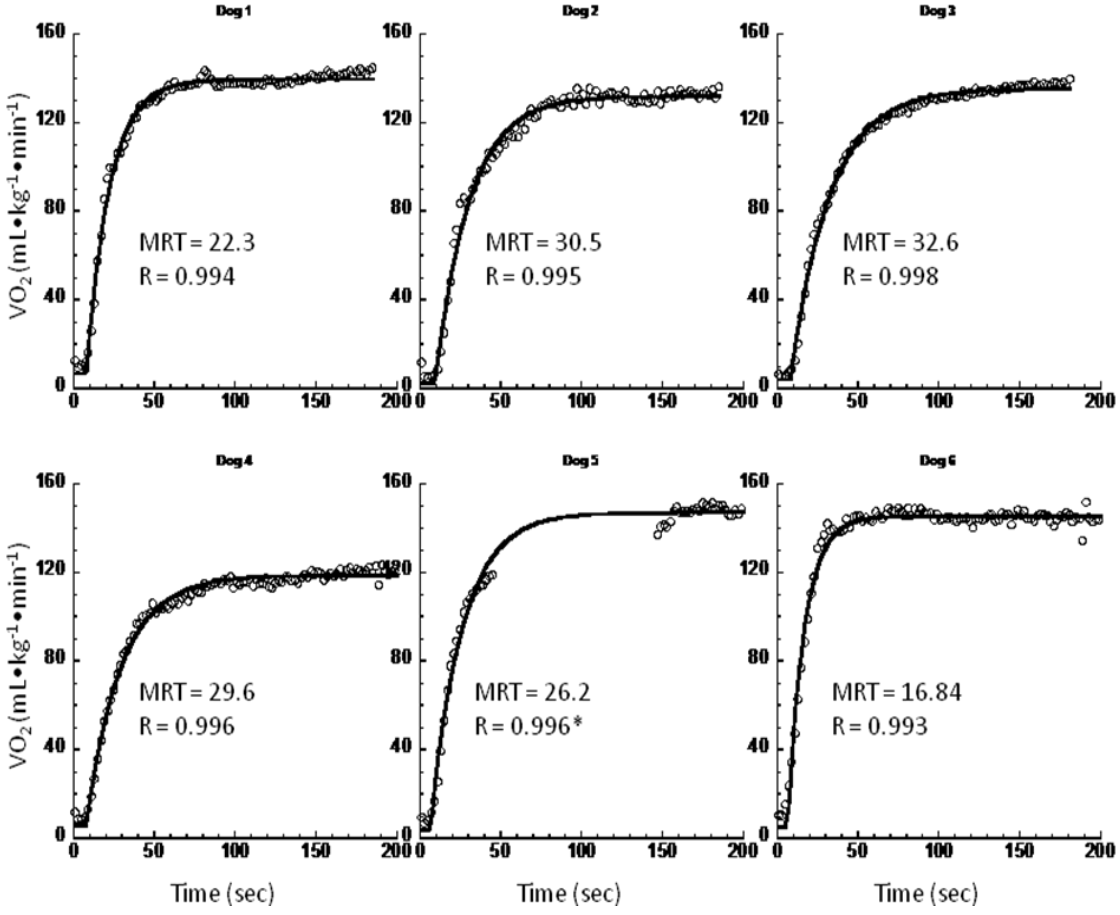
Dog 1
Dog 2
Dog 3
Dog 4
Dog 5
Dog 6
MRT = 22.3
R = 0.994
MRT = 30.5
R = 0.995
MRT = 32.6
R = 0.998
MRT = 29.6
R = 0.996
MRT = 26.2
R = 0.996*
MRT = 16.84
R = 0.993
VO2 (mL•kg-1•min-1)
Time (sec)

3C

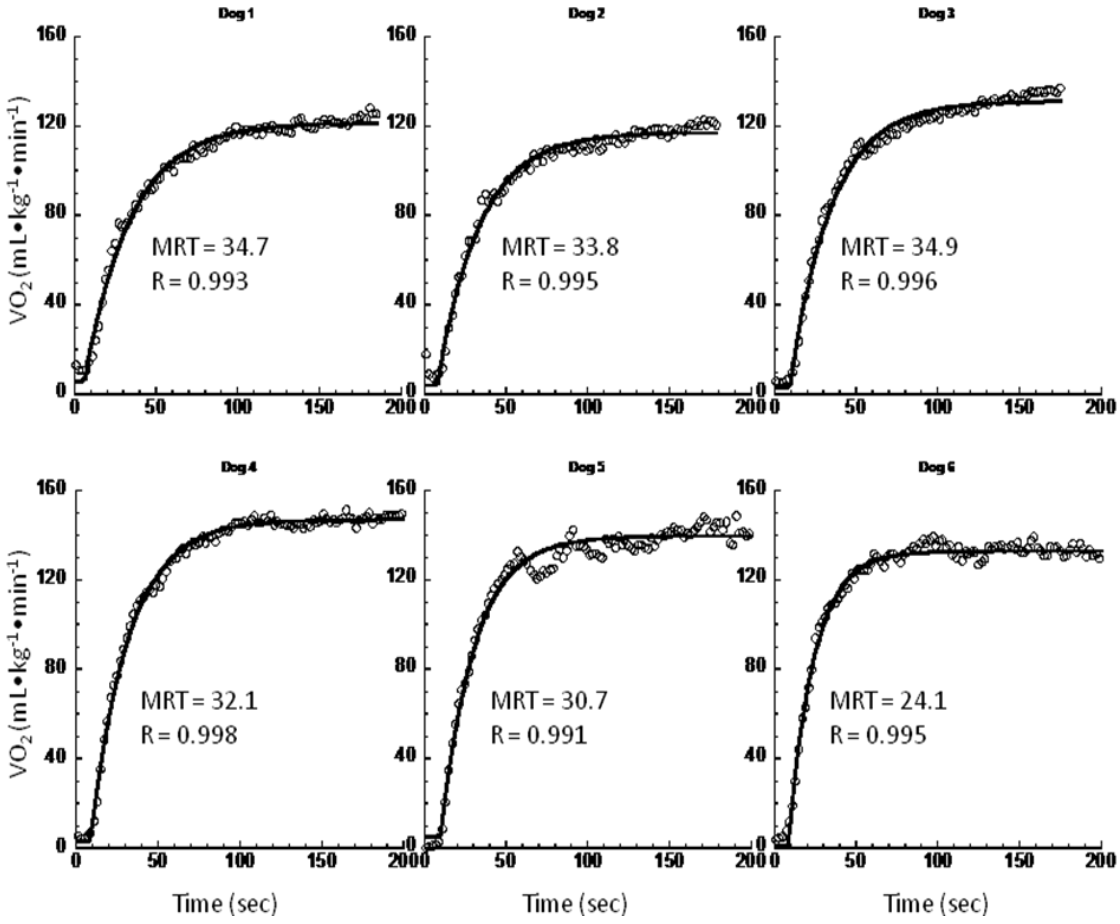

Figure 3(A-C): VO_2 on-response fits for all experiments (3A=CT20, 3B=EX45, 3C=EX70). Each plot contains MRT and correlation coefficient for the fit. VO_2 is given in mL of O_2 per kg muscle per minute. Note that in 2 (dog6, trial CT20 and dog5, trial EX45; these are marked with asterisks (*****) next to the R value) of the 18 trials, data were clipped out due to apparent malfunctioning of the Oximetrix 3 (non-physiological dips or spikes in data). In each of these cases enough data were available for a confident curve fit.

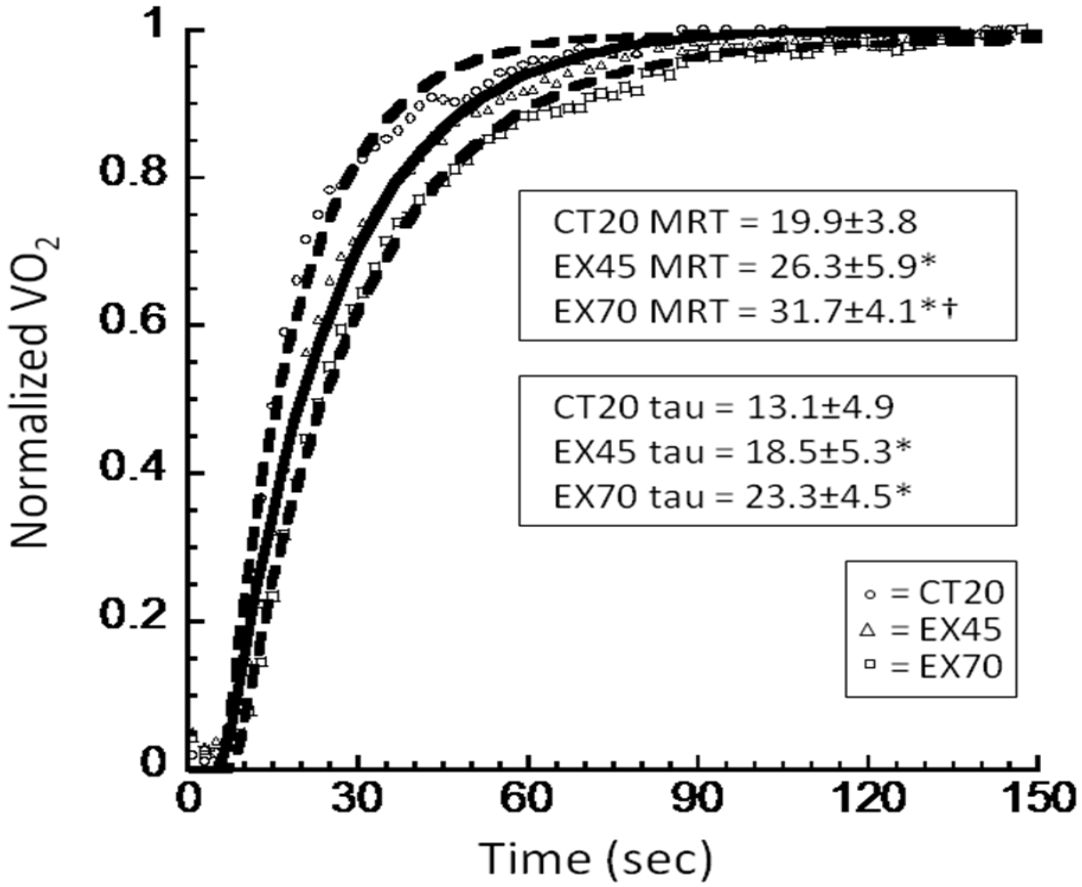

Figure 4: The VO_2 on-response normalized and averaged for all six dogs. Resting VO_2 was set equal to 0 and steady state VO_2 was set equal to 1. Open circles represent CT20, open triangles represent EX45, and squares represent EX70. Tau and MRT values are shown. *Denotes statistical significance from CT20 at the $p<0.05$ level. †Denotes statistical significance from EX45 at the $p<0.05$ level.

Table 3: Average values pertinent to oxygen delivery and uptake.

Variable	CT20	EX45	EX70
Blood Flow/O_2 delivery tau/MRT (sec)	**22.6±1.7**	**46.8±4.4***	**67.8±5.6*†**
VO_2 tau (sec)	**13.1±4.9**	**18.5±5.2***	**23.3±4.5***
VO_2 TD (sec)	**6.8±2.3**	**7.8±1.2**	**8.4±1.2**
VO_2 MRT (sec)	**19.9±3.8**	**26.3±5.9***	**31.7±4.1*†**

Data are presented as means ± SD; n=6. CT20 = trial with blood flow delivery tau = 20 sec; EX45 = trial with blood flow delivery tau = 45 sec; EX70 = trial with blood flow delivery tau = 70 sec. *Denotes statistical significance from CT20 at the $p<0.05$ level. †Denotes significance from EX45 at the $p<0.05$ level.

The blood flow/O_2 delivery on-kinetics response was highly correlated with the VO_2 on-kinetics response. Figure 5 shows the relationship between O_2 delivery tau and VO_2 tau. Figure 6 shows the relationship between O_2 delivery MRT and VO_2 MRT.

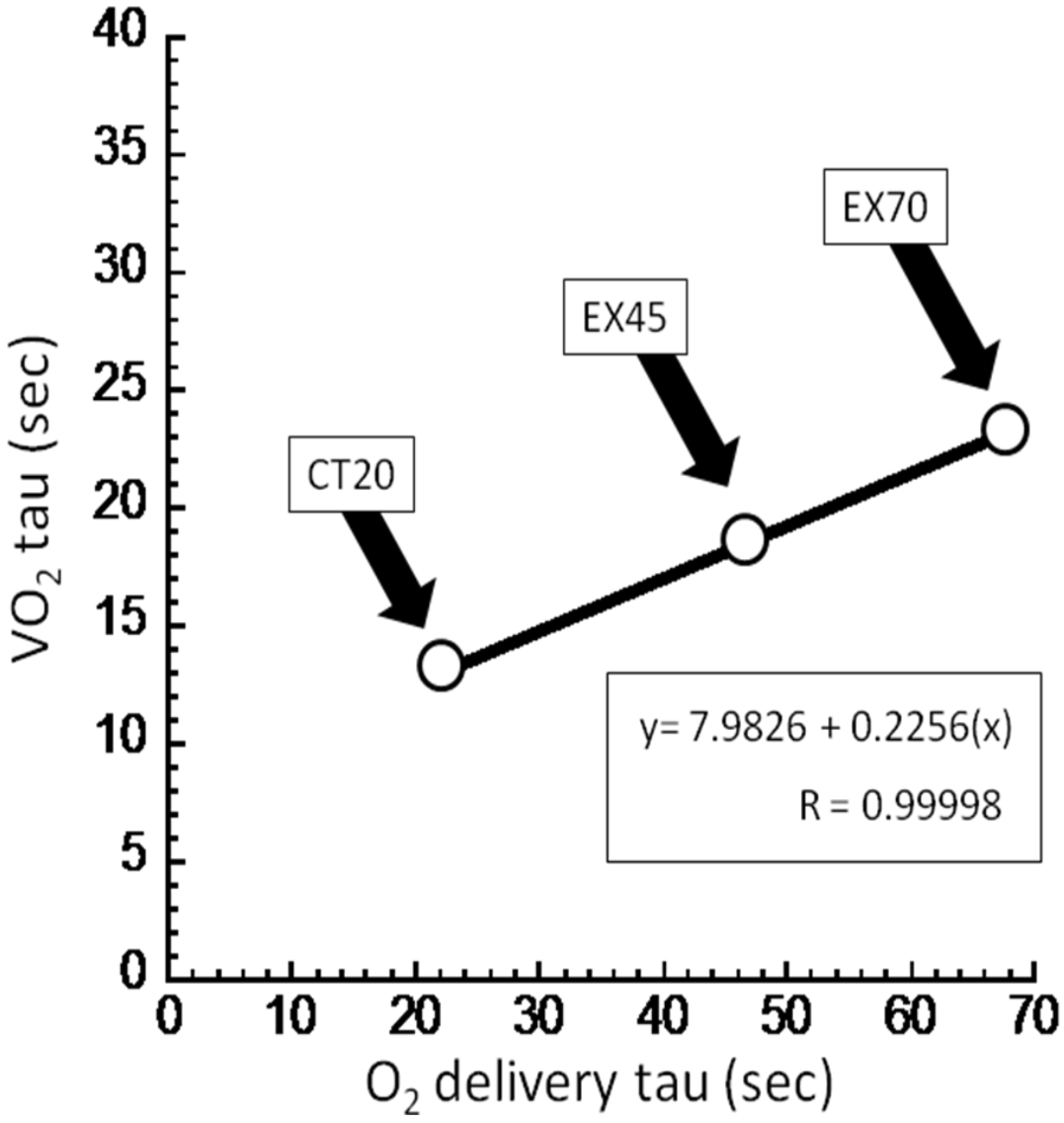

Figure 5: The relationship between VO_2 tau values and O_2 delivery tau values.

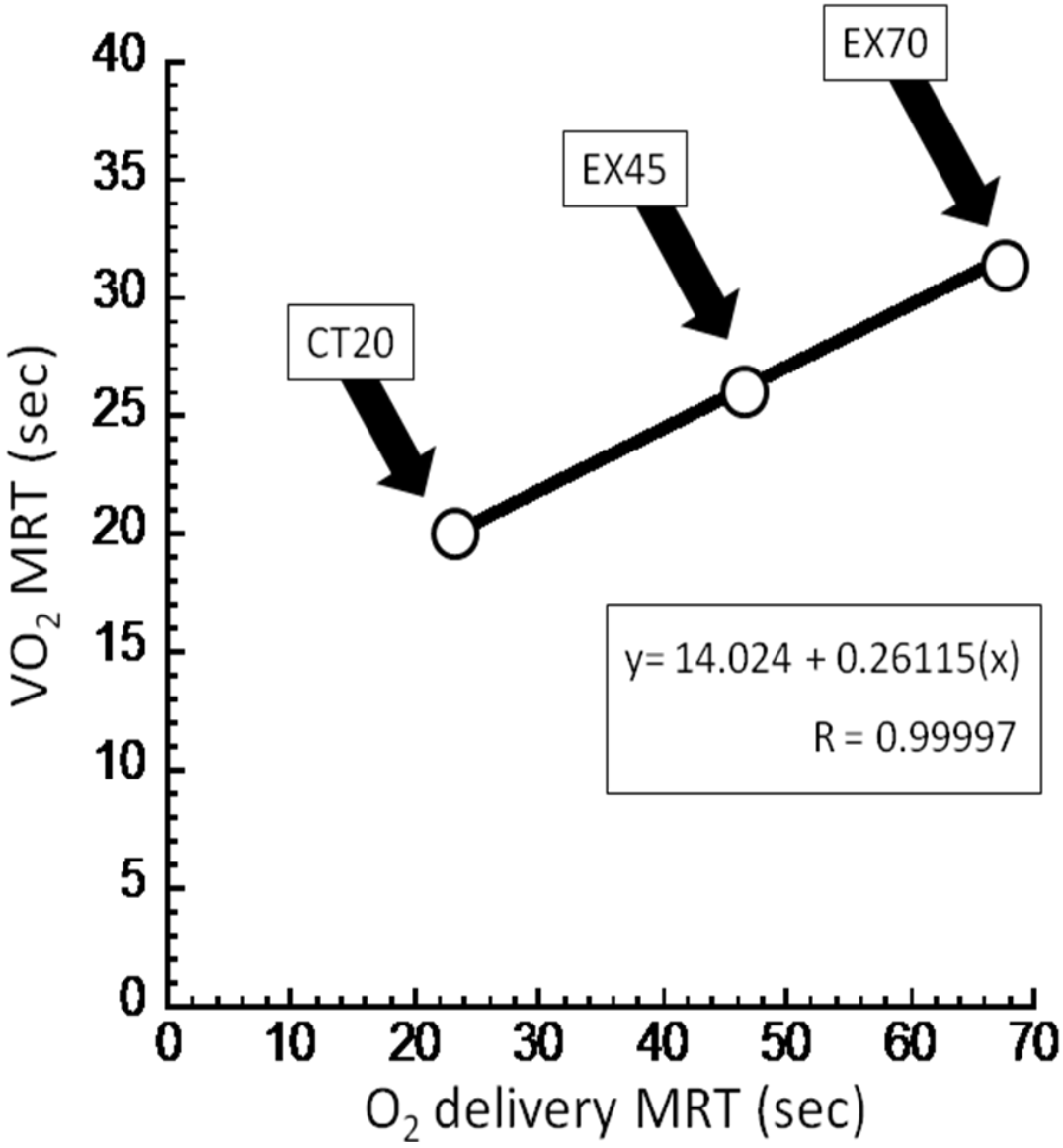

Figure 6: The relationship between VO_2 MRT values and O_2 delivery MRT values.

NIRS Responses. Figure 7 shows the average Δ[HHb] response for all six dogs. There was a statistical difference in Δ[HHb] from resting [HHb] to peak [HHb] between trials CT20 and EX70 (p=0.0006) and between trials CT20 and EX45 (p=0.0036), but not between trials EX45 and EX70 (p=0.1045). The "overshoot" of the [HHb] signal was calculated as ((peak[HHb] – steady state[HHb])/(steady state [HHb] – resting[HHb])). There were no significant differences between any of [HHb] overshoots. There were also no significant differences between any of the trials for Δ[HHb] from resting to steady state. Pertinent NIRS [HHb] data are given in Table 4.

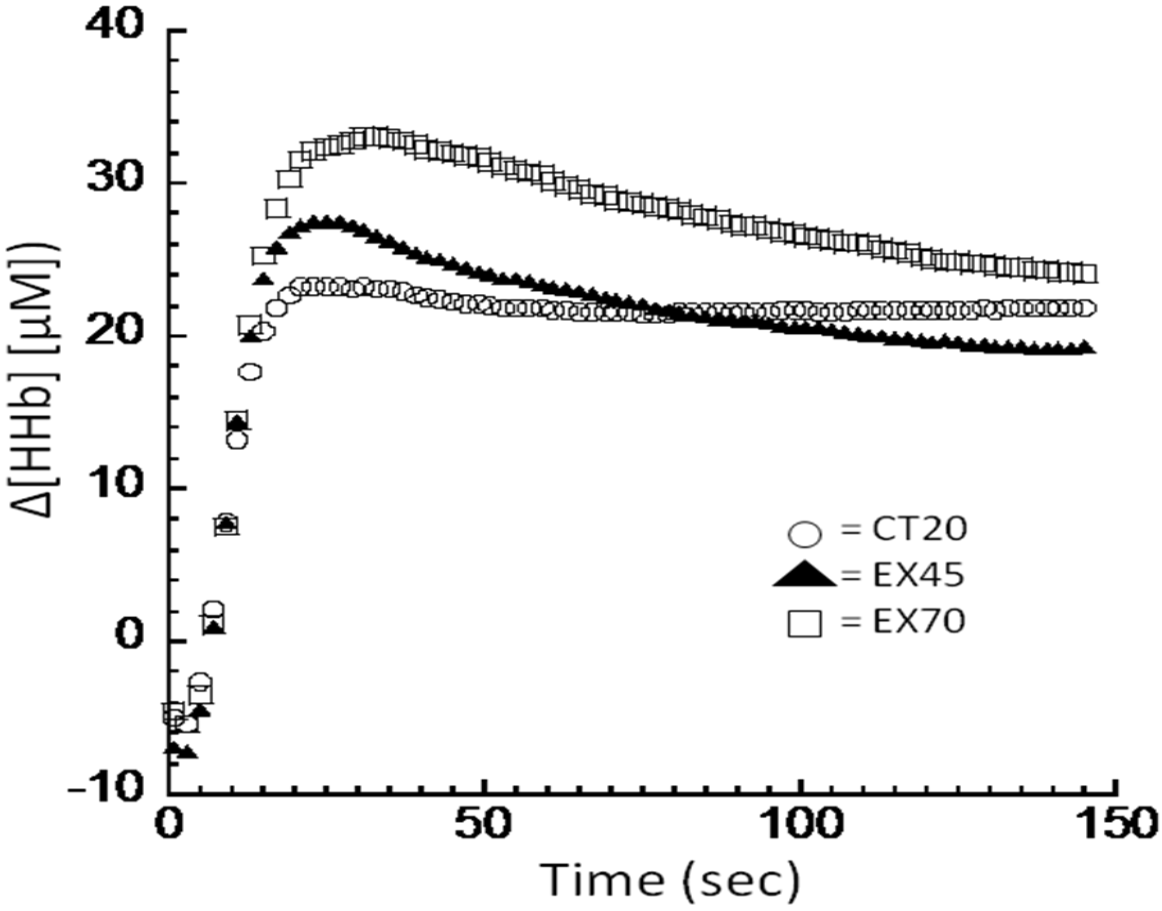

Figure 7: Change in [HHb] averaged for each trial, averaged for all six dogs. There was a significant difference between change in [HHb] from resting[HHb] to peak[HHb] between CT20 and EX45 (p=0.0036) and between CT20 and EX70 (p=0.0006). Also note that there were no significant differences between resting[HHb], steady state[HHb], or change in [HHb] from resting to steady state.

Table 4: Variables of interest for [HHb] at contractions onset.

Variable	CT20	EX45	EX70
Baseline [HHb] (µM)	**1.4±1.6**	**0.4±4.6**	**2.2±4.8**
Peak[HHb] (µM)	**24.3±8.8**	**28±10.1**	**33.2±8.9**
SteadyState[HHb]-Resting[HHb] (µM)	**19.6±8.5**	**19.5±9.3**	**21.1±11.9**
% overshoot Δ[HHb]	**24.9±26.5**	**34.4±33**	**46.6±83.8**
Peak[HHb]-Resting[HHb] (µM)	**24.3±8.8**	**28±10.1***	**33.2±8.9***
Tau, FIT1	**6.2±2.9**	**6.4±1.6**	**6.4±1.7**
Tau, FIT2	**9.2±3.4**	**9.4±3.9**	**10.5±3.6**
Time delay (TD), FIT1	**7.3±0.8**	**7.1±0.9**	**8.3±1.7**
Time delay (TD), FIT2	**4.6±0.1**	**5.1±0.7**	**5.8±0.8***
MRT (tau+TD), FIT1	**13.4±3.0**	**13.6±1.8**	**14.7±2.1**
MRT (tau+TD), FIT2	**13.9±3.4**	**14.5±3.5**	**16.3±3.9**

Data are presented as means ± SD; n=6. CT2 = trial with blood flow delivery tau = 20 sec; EX45 = trial with blood flow delivery tau = 45 sec; EX70 = trial with blood flow delivery tau = 70 sec. Formula for % overshoot and methods for FIT1 and FIT2 are given in the text. *Denotes statistical significance from CT20 at the $p<0.05$ level.

Figure 8 shows typical [HHb], [O_2Hb], and [tHb] responses for each trial (8A=CT20, 8B=EX45, 8C=EX70). While some trials exhibited an "overshoot" in [HHb] and others did not, [O_2Hb] appeared to mirror [HHb] in all cases. Because the [HHb] signal appeared to immediately decrease (from the resting [HHb] – an average of the previous 5 sec) and then rapidly increase at contractions onset and some trials exhibited an "overshoot" while others did not, the primary [HHb] response (~first 20-30 sec) was fit two different ways: 1) The response was fit with a mono-exponential curve in which a time delay was included (starting from the resting [HHb]) to account for the time from contractions onset until the [HHb] signal increased and went beyond the resting [HHb] signal, and 2) The response was fit with a mono-exponential curve in which the fitting program was allowed to pick what [HHb] the time delay started from (i.e. not

from the resting [HHb]). The MRT values derived from these two different fits were not significantly different. Tau values were not significantly different between Fit 1 and Fit 2 except for EX70 (p=0.04). TD values were significantly different between Fit 1 and Fit 2 for CT20 (p=0.0005), and EX45 (p=0.0015), but not for EX70 (p=0.065). Figure 9 shows an example of each of these fits.

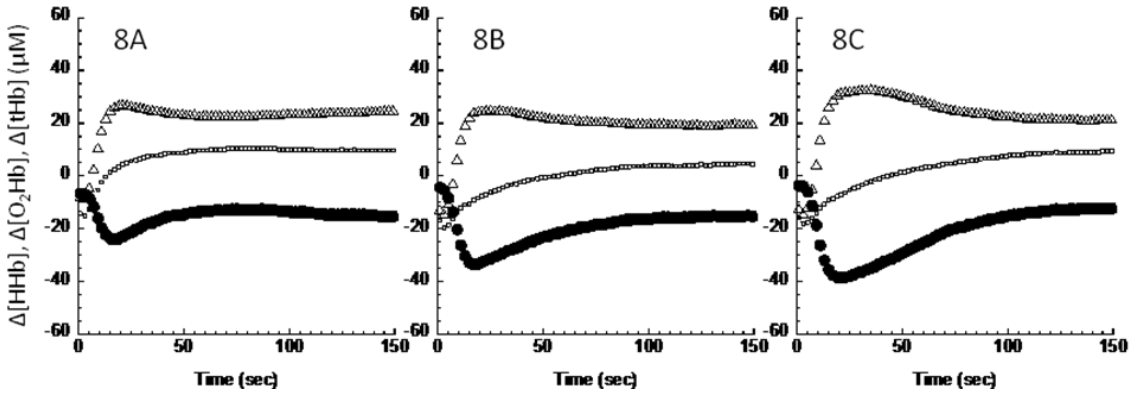

FIGURE 8: Typical Δ[HHb](open triangles), Δ[O_2Hb](filled circles), and Δ[tHb](squares; middle line) (dog 4); 8A=CT20, 8B=EX45, 8C=EX70. Note that all concentrations are given in μM and represent change in concentration from a zero baseline set prior to contractions onset. Also note that [O_2Hb] tends to mirror [HHb].

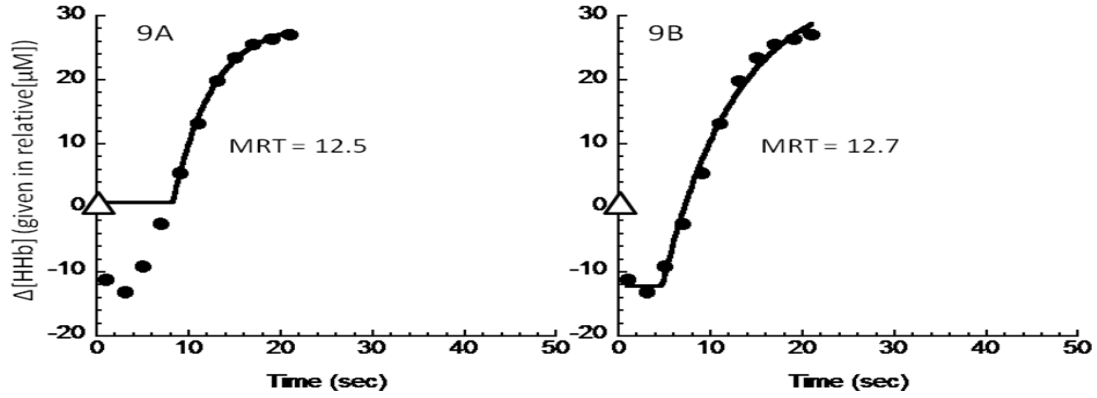

FIGURE 9: Two different methods used for fitting the Δ[HHb] upon contractions onset. 9A shows fitting with a monoexponential curve in which a time delay is used to "ignore" the immediate drop and subsequent rebound of [HHb] to resting levels (resting [HHb] was determined by averaging the 5 sec prior to contractions; resting [HHb] is represented in both 9A and 9B with the open triangle on the y-axis). 9B shows fitting with a monoexponential curve in which the fitting program was allowed to choose the [HHb] value from which to begin. As mentioned in the text and shown here, the MRT values derived from the two fitting methods were not statistically different.

DISCUSSION

Principal finding pertaining to VO_2. For the first time to our knowledge, only the monoexponential rise in the O_2 delivery rate has been slowed across a contracting muscle; resting and steady state O_2 delivery were not different between trials. This novel procedure allows unique insight into the role of convective O_2 delivery during the transition from a resting to a contracting metabolic rate. The principal finding of this investigation was that when convective O_2 delivery is slowed across an isolated canine muscle at the onset of contractions, the VO_2 on-kinetics response is slowed in a linear manner (Figures 6 and 7). The pilot experiemtents (spontaneous blood flow) are represented in Figure 10 as the open square ("spontaneous"). In 1998, Grassi et al. (20) used this same muscle preparation to examine the effect of elevating blood flow to the steady state level prior to contractions onset. In that study, the delay in O_2 delivery was eliminated, and yet the VO_2 on-kinetics response was not significantly different from that observed under spontaneous blood flow conditions. These results argued against O_2 delivery as a limitation at contractions onset, as providing more O_2 to the muscle via convective delivery did not change the VO_2 on-kinetics. This suggested that some change in OxPhos stimulators within the cell (called "metabolic inertia" by some) determined the rate of VO_2 on-kinetics. Accounting for this previous work (20), we speculate that spontaneously-perfused muscle lives at the nexus of sufficient and insufficient O_2 delivery (see Figure 10).

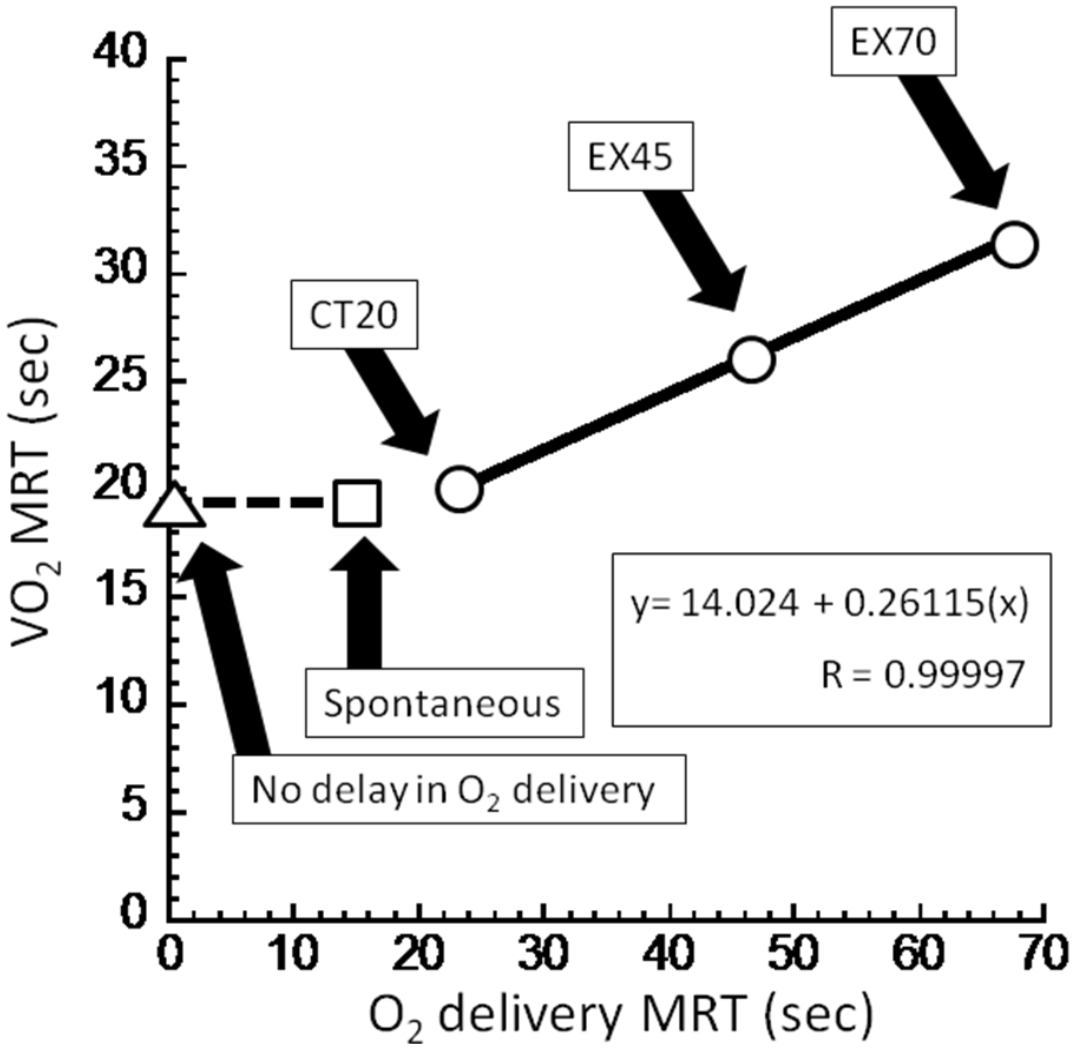

Figure 10: The relationship between VO_2 MRT values and O_2 delivery MRT values. Open circles are average results from current study. The square represents the average spontaneous blood flow response MRT values (no tubing or pumps) and average VO_2 MRT values measured in pilot work for the current study (n=5). The spontaneous blood flow MRT values (O_2 delivery) were not significantly faster than our CT20 blood flow MRT values (p=0.1438) and the VO_2 MRT values for these pilot experiments were not significantly faster than CT20 VO_2 MRT values (p=0.8349). The triangle represents our prediction of what would happen if the delay in O_2 delivery in this set of experiments were removed. This is based on work by Grassi et al. (20) with the same model used in this study and their finding of no significant speeding of the VO_2 on-response when blood flow was elevated to steady state levels prior to contractions onset.

These results hold specific application to those disease states in which the VO_2 on-kinetics response is slowed (1, 4-6, 9, 10, 19, 24, 25, 47, 53, 54, 58) and/or the rate of convective O_2 delivery at the onset of contractions is impaired (1, 5, 6, 47, 49, 54). Specifically, we have shown that this isolated muscle operates precariously close to the "tipping point" whereby any slowing of O_2 delivery slows the VO_2 on-kinetics. In reference to disease, several studies have shown how certain diseases present with both impaired VO_2 on-kinetics and impaired O_2 delivery on-kinetics. Interestingly, untrained subjects exhibit faster VO_2 on-kinetics after undergoing endurance training, and these changes begin within days of training (51). This time course (before any changes in oxidative enzyme capacity) suggests that improvements in untrained subjects may be due to improvements in O_2 delivery to the muscle.

Do the current results apply to lowly-oxidative muscle? Similarly to VO_2 on-kinetics, debate over what limits VO_{2max} has involved an "O_2 delivery versus O_2 utilization" approach. However, recent evidence suggests that O_2 delivery and usage (by mitochondria) interact to determine VO_{2max}. Hepple et al. (29) found that when mitochondrial content or O_2 delivery was reduced, VO_{2max} was reduced. However, when both O_2 delivery and mitochondrial content were reduced, the decrease in VO_{2max} was more than additive (29). Is there a similar interaction between O_2 delivery and mitochondrial content/oxidative capacity during the on-kinetics transition from rest to contractions/exercise? Given that particular patients may present with relatively "untrained" muscle (less oxidative) *and* impaired O_2 delivery on-kinetics, more lowly-oxidative muscle might be more indicative of many diseased patients.

Specifically, in COPD patients (49), when hyperoxic gas is given during transitions to submaximal metabolic rates, the VO_2 time constant is reduced, suggesting an O_2 delivery limitation (49). In chronic heart failure patients (1) there is a reduced ability to deliver adequate blood flow to working musculature and in heart transplant patients a sluggish adjustment of cardiac output (10), suggesting a major role for reduced O_2 delivery in the causation of the slowed VO_2 on-kinetics. In chronic respiratory disease patients, it has been suggested that the slower fundamental monoexponential component of the VO_2 on-kinetics response appears to be due to a slowed cardiovascular response rather than respiratory function *per se* (47). In peripheral arterial disease (PAD) patients, Auchincloss et al. (2, 3) concluded that PAD patients exhibit slower VO_2 on-kinetics as a result of impaired peripheral blood flow. However, when Bauer et al. (6)

specifically examined this, there was no relationship between worsening severity of PAD patients and slowed VO_2 on-kinetics responses, clouding the picture of O_2 delivery and/or metabolic impairment. When type II diabetic women (without clinical presentation of cardiovascular disease) transitioned to submaximal work rates, the VO_2 on-kinetics response and the HR on-kinetics response were slowed (54). Finally, in two patients who underwent surgical procedures to improve impaired pulmonary hemodynamics, the VO_2 on-kinetics response subsequently improved (57), further demonstrating the importance of O_2 delivery in disease. Our experiments bring clarity to these clinical data. To the extent that our isolated muscle results apply to intact humans, healthy muscle appears to operate precariously close to the "tipping point", such that any O_2 delivery impairment can slow the VO_2 on-kinetics response and further compound any metabolic impairment present. The interaction of O_2 delivery limitations with O_2 utilization impairments (e.g. reduced mitochondria) in healthy or diseased muscle is yet to be fully elucidated.

Our results also agree with work done utilizing phosphorescence quenching techniques in animal models (7, 30, 31, 41). If O_2 delivery to the cell exceeds O_2 usage, then capillary PO_2 should increase accordingly. Conversely, if O_2 usage exceeds O_2 delivery, then capillary PO_2 should decrease. In 2001, Behnke et al. (7) used this technique to examine capillary PO_2 on-kinetics in isolated spinotrapezius muscles in rat. In their study (7) there was a 15-20 sec delay at the onset of contractions during which PO_2 was constant, suggesting that O_2 delivery precisely matched O_2 usage at contractions onset (operating at "the tipping point"). Hogan et al. (30, 31) and Kindig et al. (41) extended these findings with phosphorescence quenching studies in single fibers. Similarly to the results of Behnke et al. (7), there was a delay before intracellular PO_2 decreased, suggesting a unique matching of O_2 supply to O_2 demand at contractions onset. DeLorey et al. (15) and Grassi et al. (26) both used NIRS to show a delay in the increase in the deoxygenation signal (HHb) in human leg muscle during cycling transitions, supporting the notion that O_2 supply precisely meets O_2 demand at contracts onset.

Many studies have utilized hypoxia as a method for decreasing O_2 delivery during transitions between work rates in humans. In fact, both Murphy et al. (46) and Springer et al. (59) have shown that inspiring a hypoxic gas (14-15% O_2) slows the VO_2 on-kinetics response, despite the fact that the same steady state VO_2 is reached. Other data have also shown a slowing of VO_2 on-kinetics during hypoxic

breathing (12, 35). When subjects breathed hyperoxic gas during similar transitions, the VO_2 on-kinetics response was not speeded (12, 35, 43, 62). These studies also support our current study by suggesting that O_2 delivery is very tightly coupled to the muscle's ability to use O_2 during contractions onset.

Much of the work that has been done in an effort to reduce the blood flow on-kinetics response (and thus the O_2 delivery on-kinetics response) has utilized less specific means than those used in the current study. For example, numerous studies have been conducted in which the VO_2 on-kinetics response is analyzed in subjects undergoing β-blockade (32, 50, 61) or supine pedaling/lower body pressure alterations (13, 34, 38, 44, 63). While most of these studies show a slowing of VO_2 on-kinetics with either β-blockade or supine pedaling, some have had divergent results. MacDonald et al. (44) found that subjects had a blood flow on-response that was slowed by ~60% during supine pedaling, yet the VO_2 on-kinetics response was only slowed by ~35%. Furthermore, the blood flow on-kinetics response was ~10-12 sec faster than the VO_2 on-kinetics response, suggesting that some "buffer" of O_2 delivery exists. Williamson et al. (63) used lower body positive pressure to slow the blood flow on-kinetics, and found no slowing of VO_2 on-kinetics during these conditions. Finally, Hayashi et al. (28) have argued that the effects of β-blockade and supine pedaling are too nonspecific, and thus results should be interpreted with caution. To circumvent this, these authors (28) used a cold-water-filled bag that was applied to subjects' faces during transitions, thus delaying vagal withdrawal through the trigeminal-vagal-cardiac pathway. When this protocol was performed rather than supine pedaling or β-blockade, the VO_2 on-kinetics response was unaltered. However, when Hughson and Morrissey (36) attempted to investigate more specific ways of altering HR changes, they found that faster HR adaptations led to faster VO_2 on-kinetics and slower HR changes led to slower VO_2 on-kinetics (faster HR changes were achieved by transitions from 0 to 40% of VT (mainly parasympathetic removal) while slower HR changes were achieved by transitions from 40 to 80% VT (mainly sympathetic stimulation)).

Now, for the first time to our knowledge, we have performed experiments that avoid the major problems associated with attempting to alter O_2 delivery rate while accurately measuring VO_2. The current studies were unique in that they utilized pump-perfusion control to slow the on-kinetics of O_2 delivery while still matching both the resting and steady state O_2 delivery rate. This allowed specific investigation

into the role of O_2 delivery rate on VO_2 on-kinetics. Also, the isolated muscle *in situ* allows *direct measurement of* blood flow to the muscle rather than having to rely on limb blood flow or central blood flow measurements as surrogates. This model also allowed us to calculate VO_2 of the muscle from direct measures of a-vO_2 difference and muscle blood flow rather than relying on limb VO_2 or pulmonary VO_2 as indices of muscle VO_2. Our results, taken in concert with those of Grassi et al. (20) lead us to conclude that this highly-oxidative muscle operates remarkably close to the proposed "tipping point" (52).

NIRS data. The NIRS-derived [HHb] signal (Δ[deoxy(hemoglobin+myoglobin)]) is generally thought to reflect O_2 extraction, giving an indication of the balance between O_2 delivery and O_2 utilization (14, 17, 26, 39). Given our current interest in balance between O_2 delivery and O_2 utilization, this was the primary NIRS component analyzed. Given the results of the VO_2 on-kinetics response, we expected that the [HHb] signal would exhibit progressively slower kinetics when O_2 delivery/blood flow was slowed. However, regardless of the fitting method employed, the MRT values for [HHb] on-kinetics response was not significantly different between any of the groups (Figure 9, Table 4). It is worth noting that the while the change from resting [HHb] to steady state [HHb] was not different, the change in resting [HHb] to peak [HHb] was different between CT20 and EX45 and between CT20 and EX70 (but not between EX45 and EX70). This suggests that while the time course of deoxygenation is unchanged when O_2 delivery is slowed, the muscle experiences a greater degree of deoxygenation.

Although the deoxygenation of the muscle appear to happen "as fast" in EX70 as they did in CT20, the muscle becomes more deoxygenated in EX45 and EX70 than in CT20. This suggests simply that for any given time on the curve, CT20 VO_2 cannot be met in the EX45 and EX70 trials because of an O_2 limitation. One then wonders why the VO_2 on-response was slower in EX70 than in EX45, when the rest-to-peak [HHb] was not significantly different. These results may follow a more logical pattern when viewed in the context of the "Wilson" model of oxidative metabolism (64-67). Wilson et al. (64-67) determined in isolated mitochondria that the same VO_2 can be achieved at different PO_2 values depending on the "redox potential" ($[NAD^+]$/[NADH]) and the "energy charge" ([ATP]/[ADP]X[Pi]). This model has recently been adapted by Hughson (33) to apply to transitions from rest to submaximal exercise. During

these transitions from rest to some submaximal work rate, the VO_2 is determined by the interplay of redox state ([NAD^+]/[NADH]), energy charge ([ATP]/[ADP]X[Pi]), and PO_2.

Thus, during transitions to exercise, when O_2 delivery is reduced, one should expect that energy charge and/or redox state would adjust more to achieve the desired VO_2. If they do not adjust fast enough or to a great enough degree, the VO_2 for that time cannot be met and the resultant VO_2 on-kinetics response is slowed. It would be interesting to know what was happening to energy charge and/or redox state during the transitional phases such that the VO_2 on-kinetics response was slowed as O_2 delivery was slowed, yet the [HHb] on-kinetics response was unchanged. While the deoxygenation of the muscle proceeds with the same course despite the condition (faster than even the CT20 VO_2 response (~13 sec vs. ~20 sec)), perhaps no adjustment within the cell can "stimulate" O_2 uptake if enough O_2 is simply not available. [HHb] increases "maximally" in EX45, such that EX70 [HHb] changes are not statistically significant from EX45 [HHb]. However, the VO_2 on-response is almost perfectly linear depending on the O_2 availability.

Our results suggest that in EX45 and EX70 trials as compared to CT20 trials (CT20 trials were not significantly different from pilot work (n=5) spontaneous perfusion trials) either 1) the signals needed to increase VO_2 at any time were present, yet the O_2 was not available, or 2) the signals to increase VO_2 at any time (redox potential and/or energy charge) had already adjusted as much as possible in CT20 and thus could not stimulate greater O_2 usage in EX45 or EX70. In either scenario, the VO_2 on-kinetics response would show a linear slowing with reduction in O_2 delivery rate, as was shown. As has been hypothesized by other authors (27), blood flow on-kinetics seem to be very closely matched to VO_2 on-kinetics. Perhaps future studies will elucidate whether the signals that stimulate VO_2 adjust as much as possible during spontaneous-perfusion transitions from rest to submaximal metabolic rates.

Another interesting facet of this study was the [HHb] change in the first few seconds of contractions (a representative example is shown in Figure 11A). While others have shown a delay in the increase in [HHb] (15, 26), we recorded an immediate decline in [HHb] followed by an increase. By averaging the previous 5 seconds before contractions (after biasing everything to ~0), a resting [HHb] value was obtained. From this baseline, [HHb] decreased with the first contraction. This is consistent with mechanisms of the "muscle pump". Figure 11B shows the same [HHb] changes in Figure 11A, but with

changes in [O_2Hb] and [tHb] as well. As shown, all concentrations decrease as the muscle contracts and pumps blood out. However, the muscle has a greater decrease in [HHb] than [O_2Hb] upon contractions onset. This can also be explained in view of the muscle pump. That is, given that the [HHb] signal is mainly due to the capillaries surrounding the muscle fibers and given that blood flows in one direction (from the muscle back toward the heart), as the muscle contracts it pumps out more relatively deoxygenated blood and maintains relatively more oxygenated blood. Thus we see a very brief decline in [HHb] before it begins to increase. As seen in Figure 9, if we fit this curve from resting [HHb] or from the lower [HHb], we get delay times of 4.6 and 5.2 sec, respectively. A delay time in this model is consistent with other models (15, 26, 27, 31, 41, 55) that also show a delay time before an exponential increase or decrease in a variable (e.g. delay in the increase in [HHb] in muscle groups *in vivo*, delay in the decrease in PO_2 in single fibers, etc.).

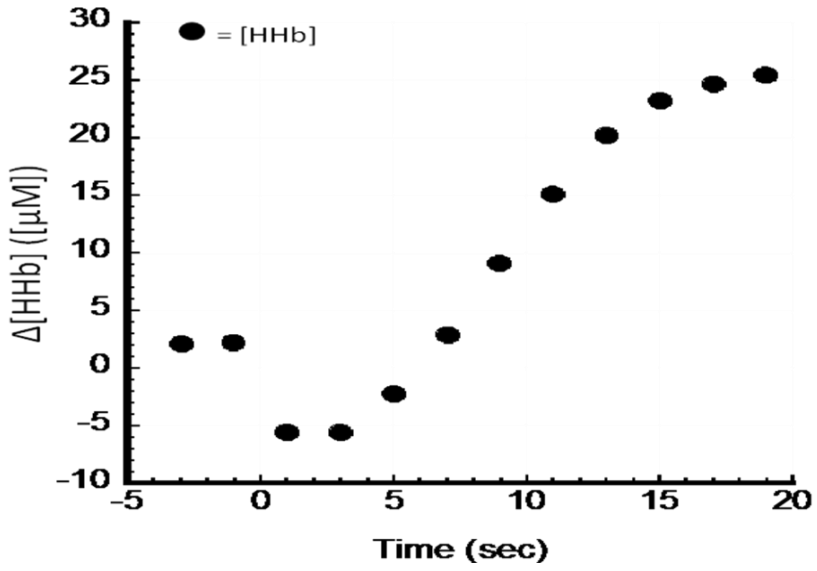

Figure 11A: A typical change in [HHb] at contractions onset. Contractions start when time=0. Values were averaged over 2 sec.

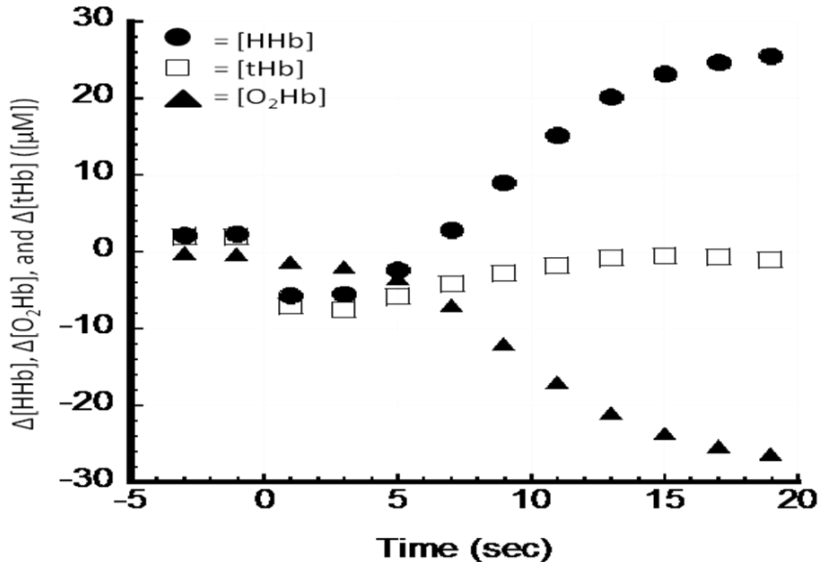

Figure 11B: The same example shown in 11A, yet also showing changes in [O_2Hb] and [tHb]. As can be seen, all signals decrease upon muscle contraction due to the muscle pump, although [HHb] decreases more than [O_2Hb].

***Limitations of study*.** Some limitations are inherent in the isolated canine GP muscle preparation *in situ*. The canine GP muscle is highly-oxidative and thus conclusions drawn from this model must be interpreted with caution. Also, this model uses electrical stimulation of the sciatic nerve to invoke muscle contractions. The electrical current stimulates all motor units synchronously, not progressively recruiting motor units as would be done *in vivo*. Finally, no work is actually done in these studies, as the muscle is attached to a force transducer that is mounted on a stereotactic frame. Thus, these contractions are isometric and produced at a rate that elicits approximately 60-70% of VO_{2peak} and mimics "submaximal exercise". Also, bulk blood flow is controlled, but we cannot control the microcirculation of the muscle in this model. Despite these limitations, the isolated canine GP muscle preparation *in situ* allows many advantages. This model allows direct control of blood flow to an isolated working muscle, allowing us to directly alter the blood flow as well as circumventing any reliance on cardiac output or limb blood flow as a surrogate for blood flow measures. Furthermore, the isolation of the muscle allows direct measurement of VO_2 across the working muscle, circumventing the reliance on pulmonary VO_2 or limb VO_2 as surrogates for muscle VO_2.

Conclusions. Overall, it appears that the canine GP muscle *in situ* operates very close to the "tipping point" between O_2 delivery dependence and O_2 delivery independence under normal, spontaneous transitions from rest to a submaximal metabolic rate. We have demonstrated a linear relationship between O_2 delivery on-kinetics and VO_2 on-kinetics. Despite this linear relationship, the time course of [HHb] changes at contractions onset were not significantly different between trials. This suggests that during the on-transition either 1) the appropriate levels of metabolites needed to stimulate the control VO_2 at any time could not be reached, or 2) the appropriate levels of metabolites needed to stimulate the control VO_2 at any time were reached, yet the O_2 was not available. These results show that in our current experimental model, muscle VO_2 and blood flow/O_2 delivery are very closely matched during contractions onset.

REFERENCES

1. **Arena R, Humphrey R, and Peberdy MA**. Measurements of oxygen consumption on-kinetics during exercise: implications for patients with heart failure. *J Card Fail* 7: 302-310, 2001.

2. **Auchincloss JH, Ashutosh K, Rana S, Peppi D, Johnson LW, and Gilbert R**. Effect of cardiac, pulmonary, and vascular disease on one-minute oxygen uptake. *Chest* 70: 486-493, 1976.

3. **Auchincloss JHJ, Meade JW, Gilbert R, and Chamberlain BE**. One minute oxygen uptake in peripheral ischemic vascular disease. *Ann Surg* 191: 203-206, 1980.

4. **Babcock MA, Paterson DH, Cunningham DA, and Dickinson JR**. Exercise on-transient gas exchange kinetics are slowed as a function of age. *Med Sci Sports Exerc* 26: 440-446, 1994.

5. **Barker GA, Green S, Green AA, and Walker PJ**. Walking performance, oxygen uptake kinetics and resting muscle pyruvate dehydrogenase complex activity in peripheral arterial disease. *Clin Sci (Lond)* 106: 241-249, 2004

6. **Bauer TA, Regensteiner JG, Brass EP, and Hiatt WR**. Oxygen uptake kinetics during exercise are slowed in patients with peripheral arterial disease. *J Appl Physiol* 87: 809-816, 1999.

7. **Behnke BJ, Kindig CA, Musch TI, Koga S, and Poole DC**. Dynamics of microvascular oxygen pressure across the rest-exercise transition in rat skeletal muscle. *Respir Physiol* 126: 53-63, 2001.

8. **Boushel R, and Piantadosi CA**. Near-infrared spectroscopy for monitoring muscle oxygenation. *Acta Physiol Scand* 168: 615-622, 2000.

9. **Cade WT, Fantry LE, Nabar SR, Shaw DK, and Keyser RE**. Impaired oxygen on-kinetics in persons with human immunodeficiency virus are not due to highly active antiretroviral therapy. *Arch Phys Med Rehabil* 84: 1831-1838, 2003

10. **Cerretelli P, Grassi B, Colombini A, Caru B, and Marconi C**. Gas exchange and metabolic transients in heart transplant recipients. *Respir Physiol* 74: 355-371, 1988.

11. **Chance B, Dait MT, Zhang C, Hamaoka T, and Hagerman F**. Recovery from exercise-induced desaturation in the quadriceps muscles of elite competitive rowers. *Am J Physiol Cell Physiol* 262: C766-C775, 1992.

12. **Cleuziou C, Perrey S, Lecoq AM, Candau R, Courteix D, and Obert P**. Oxygen uptake kinetics during moderate and heavy intensity exercise in humans: the influence of hypoxia and training status. *Int J Sports Med* 26: 356-362, 2005.

13. **Convertino VA, Goldwater DJ, and Sandler H**. Oxygen uptake kinetics of constant-load work: upright vs. supine exercise. *Aviat Space Environ Med* 55: 501-506, 1984.

14. **DeLorey DS, Kowalchuk JM, and Paterson DH**. Effects of prior heavy-intensity exercise on pulmonary O2 uptake and muscle deoxygenation kinetics in young and older adult humans. *J Appl Physiol* 97: 998-1005, 2004.

15. **DeLorey DS, Kowalchuk JM, and Paterson DH**. Relationship between pulmonary O_2 uptake kinetics and muscle deoxygenation during moderate-intensity exercise. *J Appl Physiol* 95: 113-120, 2003.

16. **Elwell C**. A Practical User's Guide To Near Infrared Spectroscopy. London: Hamatsu Photonics KK, 1995, p. 1-155.

17. **Ferrari M, Binzoni T, and Quaresima V**. Oxidative metabolism in muscle. *Philos Trans R Soc Lond B Biol Sci* 352: 677-683, 1997.

18. **Grassi B**. Regulation of oxygen consumption at exercise onset: is it really controversial? . *Exerc Sport Sci Rev* 29: 134-138, 2001.

19. **Grassi B, Ferretti G, Xi L, Rieu M, Meyer M, Marconi C, and Cerretelli P**. Ventilatory response to exercise after heart and lung denervation in humans. *Respir Physiol* 92: 289-304, 1993.

20. **Grassi B, Gladden LB, Samaja M, Stary CM, and Hogan MC**. Faster adjustment of O_2 delivery does not affect VO_2 on-kinetics in isolated in situ canine muscle. *J Appl Physiol* 85: 1394-1403, 1998.

21. **Grassi B, Gladden LB, Samaja M, Stary CM, Wagner PD, and Hogan MC**. Peripheral O_2 diffusion does not affect VO_2 on-kinetics in isolated in situ canine muscle *J Appl Physiol* 85: 1404-1412, 1998.

22. **Grassi B, Hogan MC, Greenhaff PL, Hamann JJ, Kelley KM, Aschenbach WG, Constantin-Teodosiu D, and Gladden LB**. Oxygen uptake on-kinetics in dog gastrocnemius in situ following activation of pyruvate dehydrogenase by dichloroacetate. *J Physiol* 538: 195-207, 2002.

23. **Grassi B, Hogan MC, Kelley KM, Aschenbach WG, Hamann JJ, Evans RK, Patillo RE, and Gladden LB**. Role of convective O_2 delivery in determining VO_2 on-kinetics in canine muscle contracting at peak VO_2. *J Appl Physiol* 89: 1293-1301, 2000.

24. **Grassi B, Marconi C, Meyer M, Rieu M, and Cerretelli P**. Gas exchange and cardiovascular kinetics with different exercise protocols in heart transplant recipients. *J Appl Physiol* 82: 1952-1962, 1997.

25. **Grassi B, Morandi L, Pogliahi S, Rampichini S, Marconi C, and Cerretelli P**. Functional evaluation of patients with metabolic myopathies during exercise. *Med Sci Sports Exerc* 34: S78, 2002.

26. **Grassi B, Pogliahi S, Rampichini S, Quaresima V, Ferrari M, Marconi C, and Cerretelli P**. Muscle oxygenation and pulmonary gas exchange kinetics during cycling exercise on-transitions in humans. *J Appl Physiol* 95: 149-158, 2003.

27. **Grassi B, Poole DC, Richardson RS, Knight DR, Erickson BK, and Wagner PD**. Muscle O_2 uptake kinetics in humans: implications for metabolic control. *J Appl Physiol* 80: 988-998, 1996.

28. **Hayashi N, Tanaka A, Ishihara M, and Yoshida T**. Delayed vagal withdrawal slows circulatory but not oxygen uptake responses at work increase. *Am J Physiol Regul Integr Comp Physiol* 274: R1268-R1273, 1998.

29. **Hepple RT, Hagen JL, and Krause DJ**. Oxidative capacity interacts with oxygen delivery to determine maximal O_2 uptake in rat skeletal muscles *in situ*. *J Physiol* 541: 1003-1012, 2002.

30. **Hogan MC**. Fall in intracellular PO_2 at the onset of contractions in Xenopus single skeletal muscle fibers. *J Appl Physiol* 90: 1871-1876, 2001.

31. **Hogan MC**. Phosphorescence quenching method for measurement of intracellular PO_2 in isolated skeletal muscle fibers. *J Appl Physiol* 86: 720-724, 1999.

32. **Hughson RL**. Alterations in the oxygen deficit-oxygen debt relationships with β-adrenergic receptor blockade in man. *J Appl Physiol* 349: 375-387, 1984.

33. **Hughson RL**. Regulation of VO_2 on-kinetics by O_2 delivery. In: *Oxygen uptake kinetics in sport, exercise and medicine*, edited by Jones AM, and Poole DC. New York: Routledge, 2005, p. 185-211.

34. **Hughson RL, Cochrane JE, and Butler GC**. Faster O_2 uptake kinetics at onset of supine exercise with than without lower body negative pressure. *J Appl Physiol* 75: 1962-1967, 1993.

35. **Hughson RL, and Kowalchuk JM**. Kinetics of oxygen uptake for submaximal exercise in hyperoxia, normoxia, and hypoxia. *Can J Appl Physiol* 20: 198-210, 1995.

36. **Hughson RL, and Morrisey MA**. Delayed kinetics of VO_2 in the transition from prior exercise. Evidence for O_2 transport limitation of VO_2 kinetics: a review. *Int J Sports Med* 4: 31-39, 1983.

37. **Hughson RL, Tschakovsky ME, and Houston ME**. Regulation of oxygen consumption at the onset of exercise. *Exerc Sport Sci Rev* 29: 129-133, 2001.

38. **Hughson RL, Xing HC, Borkhoff C, and Butler GC**. Kinetics of ventilation and gas exchange during supine and upright cycle exercise. *Eur J Appl Physiol Occup Physiol* 63: 300-307, 1991.

39. **Jones AM, Fulford J, and Wilkerson DP**. Influence of prior exercise on muscle [phosphorylcreatine] and deoxygenation kinetics during high-intensity exercise in men. *Exp Physiol* 93: 468-478, 2008.

40. **Jones AM, and Poole DC**. *Oxygen uptake kinetics in sport, exercise and medicine*. New York: Routledge, 2005.

41. **Kindig CA, Howlett RA, and Hogan MC**. Effect of extracellular PO_2 on the fall in intracellular PO_2 in contracting single myocytes. *J Appl Physiol* 94: 1964-1970, 2003.

42. **Krogh A, and Lindhard J**. The regulation of respiration and circulation during the initial stages of muscular work. *J Physiol* 47: 112-136, 1913.

43. **Macdonald M, Pedersen PK, and Hughson RL**. Acceleration of VO_2 kinetics in heavy submaximal exercise by hyperoxia and prior high-intensity exercise. *J Appl Physiol* 83: 1318-1325, 1997.

44. **Macdonald MJ, Shoemaker JK, Tschakovsky ME, and Hughson RL**. Alveolar oxygen uptake and femoral artery blood flow dynamics in upright and supine leg exercise in humans. *J Appl Physiol* 85: 1622-1628, 1998.

45. **Mancini DM, Bolinger L, Li H, Kendrick K, Chance B, and Wilson JR**. Validation of near-infrared spectroscopy in humans. *J Appl Physiol* 77: 2740-2747, 1994.

46. **Murphy PC, Cuervo LA, and Hughson RL**. A study of cardiorespiratory dynamics with step and ramp exercise tests in normoxia and hypoxia. *Cardiovasc Res* 23: 825-832, 1989.

47. **Nery LE, Wasserman K, Andrews JD, Huntsman DJ, Hansen JE, and Whipp BJ**. Ventilatory and gas exchange kinetics during exercise in chronic airways obstruction. *J Appl Physiol* 53: 1594-1602, 1982.

48. **Nighswander-Rempel SP, Kupriyanov VV, and Shaw RK**. Relative contributions of hemoglobin and myoglobin to near-infrared spectroscopic images of cardiac tissue. *Appl Spectrosc* 59: 190-193, 2005.

49. **Palange P, Galassetti P, Mannix ET, Farber MO, Manfredi F, Serra P, and Carlone S**. Oxygen effect on O2 deficit and VO2 kinetics during exercise in obstructive pulmonary disease. *J Appl Physiol* 78: 2228-2234, 1995.

50. **Petersen ES, Whipp BJ, Davis JA, Huntsman DJ, Brown HV, and Wasserman K**. Effects of β-adrenergic blockade on ventilation and gas exchange during exercise in humans. *J Appl Physiol Respirat Environ Exercise Physiol* 54: 1306-1313, 1983.

51. **Phillips SM, Green H, Macdonald MJ, and Hughson RL**. Progressive effect of endurance training on VO_2 kinetics at the onset of submaximal exercise. *J Appl Physiol* 79: 1914-1920, 1995.

52. **Poole DC, Barstow TJ, McDonough P, and Jones AM**. Control of oxygen uptake during exercise. *Med Sci Sports Exerc* 40: 462-474, 2008.

53. **Poole DC, Kindig CA, and Behnke BJ**. VO_2 kinetics in different disease states. In: *Oxygen uptake kinetics in sport, exercise and medicine*, edited by Jones AM, and Poole DC. New York: Routledge, 2005, p. 353-372.

54. **Regensteiner JG, Bauer TA, Reusch JE, Brandenburg SL, Sippel JM, Vogelsong AM, Smith S, Wolfel EE, Eckel RH, and Hiatt WR**. Abnormal oxygen uptake kinetic response in women with type II diabetes mellitus. *J Appl Physiol* 85: 310-317, 1998.

55. **Rossiter HB, Ward SA, Doyle VL, Howe FA, Griffiths JR, and Whipp BJ**. Inferences from pulmonary O_2 uptake with respect to intramuscular [phosphocreatine] kinetics during moderate exercise in humans. *J Physiol* 518: 921-932, 1999.

56. **Seiyama A, Hazeki O, and Tamura M**. Noninvasive quantitative analysis of blood oxygenation in rat skeletal muscle. *J Biochem* 103: 419-424, 1988.

57. **Sietsema KE**. Oxygen uptake kinetics in response to exercise in patients with pulmonary vascular disease. *Am Rev Respir Dis* 145: 1052-1057, 1992.

58. **Sietsema KE, Ben-Dov I, Zhang YY, Sullivan C, and Wasserman K**. Dynamics of oxygen uptake for submaximal exercise and recovery in patients with chronic heart failure. *Chest* 105: 1693-1700, 1994.

59. **Springer C, Barstow TJ, Wasserman K, and Cooper DM**. Oxygen uptake and heart rate responses during hypoxic exercise in children and adults. *Med Sci Sports Exerc* 23: 71-79, 1991.

60. **Stainsby WN, and Welch HG**. Lactate metabolism of contracting dog skeletal muscle in situ. *Am J Physiol* 211: 177-183, 1966.

61. **Twentyman OP, Disley A, Gribbin HR, Alberti KGMM, and Tattersfield AE**. Effect of β-adrenergic blockade on respiratory and metabolic responses to exercise. *J Appl Physiol Respirat Environ Exercise Physiol* 51: 788-793, 1981.

62. **Wilkerson DP, Berger NJA, and Jones AM**. Influence of hyperoxia on pulmonary O2 uptake kinetics following the onset of exercise in humans. *Respir Physiol Neurobiol* 153: 92-106, 2006.

63. **Williamson JW, Raven PB, and Whipp BJ**. Unaltered oxygen uptake kinetics at exercise onset with lower-body positive pressure. *Exp Physiol* 81: 695-705, 1996.

64. **Wilson DF**. Factors affecting the rate and energetics of mitochondrial oxidative phosphorylation. *Med Sci Sports Exerc* 26: 37-43, 1994.

65. **Wilson DF, Erecinska M, Nuutinen EM, and Silver IA**. Dependence of cellular metabolism and local oxygen delivery on oxygen tension. *Adv Exp Med Biol* 180: 629-634, 1984.

66. **Wilson DF, Owen CS, and Erecinska M**. Quantitative dependence of mitochondrial oxidative phosphorylation on oxygen concentration: a mathematical model. *Arch Biochem Biophys* 195: 494-504, 1979.

67. **Wilson DF, and Rumsey WL**. Factors modulating the oxygen dependence of mitochondrial oxidative phosphorylation. *Adv Exp Med Biol* 222: 121-131, 1988.

CUMULATIVE REFERENCES

1. **Andersen P, and Saltin B**. Maximal perfusion of skeletal muscle in man. *J Physiol* 366: 233-249, 1985.

2. **Arena R, Humphrey R, and Peberdy MA**. Measurements of oxygen consumption on-kinetics during exercise: implications for patients with heart failure. *J Card Fail* 7: 302-310, 2001.

3. **Babcock MA, Paterson DH, Cunningham DA, and Dickinson JR**. Exercise on-transient gas exchange kinetics are slowed as a function of age. *Med Sci Sports Exerc* 26: 440-446, 1994.

4. **Balaban RS**. Regulation of oxidative phosphorylation in the mammalian cell. *Am J Physiol Cell Physiol* 258: C377-C389, 1990.

5. **Bangsbo J**. Muscle oxygen uptake in humans at onset of and during intense exercise. *Acta Physiol Scand* 168: 457-462, 2000.

6. **Barker GA, Green S, Green AA, and Walker PJ**. Walking performance, oxygen uptake kinetics and resting muscle pyruvate dehydrogenase complex activity in peripheral arterial disease. *Clin Sci (Lond)* 106: 241-249, 2004.

7. **Bauer TA, Regensteiner JG, Brass EP, and Hiatt WR**. Oxygen uptake kinetics during exercise are slowed in patients with peripheral arterial disease. *J Appl Physiol* 87: 809-816, 1999.

8. **Behnke BJ, Kindig CA, Musch TI, Koga S, and Poole DC**. Dynamics of microvascular oxygen pressure across the rest-exercise transition in rat skeletal muscle. *Respir Physiol* 126: 53-63, 2001.

9. **Bell C, Paterson DH, Kowalchuk JM, Padilla J, and Cunningham DA**. A comparison of modeling techniques used to characterise oxygen uptake kinetics during the on-transient of exercise. *Exp Physiol* 86: 667-676, 2001.

10. **Berg WE**. Individual differences in respiratory gas exchange during recovery from moderate exercise. *Am J Physiol* 149: 597-610, 1947.

11. **Binzoni T, Ferretti G, Schenker K, and Cerretelli P**. Phosphocreatine hydrolysis by 31P-NMR at the onset of constant-load exercise in humans. *J Appl Physiol* 73: 1644-1649, 1992.

12. **Brooks GA, Fahey TD, and Baldwin KM**. *Exercise Physiology: Human Bioenergetics and Its Applications, 4th Ed*. New York: McGraw Hill, 2005.

13. **Cade WT, Fantry LE, Nabar SR, Shaw DK, and Keyser RE**. Impaired oxygen on-kinetics in persons with human immunodeficiency virus are not due to highly active antiretroviral therapy. *Arch Phys Med Rehabil* 84: 1831-1838, 2003.

14. **Casaburi R, Whipp BJ, Wasserman K, Beaver WL, and Koyal SN**. Ventilatory and gas-exchange dynamics in response to sinusoidal work. *J Appl Physiol* 42: 300-311, 1977.

15. **Cerretelli P, Grassi B, Colombini A, Caru B, and Marconi C**. Gas exchange and metabolic transients in heart transplant recipients. *Respir Physiol* 74: 355-371, 1988.

16. **Cerretelli P, Marconi C, Meyer M, Ferretti G, and Grassi B**. Gas exchange kinetics in heart transplant recipients. *Chest 101* Suppl 1: 199S-205S, 1992.

17. **Cerretelli P, Sikand R, and Farhi LE**. Readjustments in cardiac output and gas exchange during onset of exercise and recovery. *J Appl Physiol* 21: 1345-1350, 1966.

18. **Chance B, Leigh JS, Clark BJ, Maris J, Kent J, Nioka S, and Smith D**. Control of oxidative metabolism and oxygen delivery in human skeletal muscle: a steady-state analysis of the work/energy cost transfer function. *Proc Natl Acad Sci* 82: 8383-8388, 1985.

19. **Chance B, and Williams GR**. The respiratory chain and oxidative phosphorylation. *Adv Enzymol Relat Subj Biochem* 17: 65-134, 1956.

20. **Cleuziou C, Perrey S, Lecoq AM, Candau R, Courteix D, and Obert P**. Oxygen uptake kinetics during moderate and heavy intensity exercise in humans: the influence of hypoxia and training status. *Int J Sports Med* 26: 356-362, 2005.

21. **Convertino VA, Goldwater DJ, and Sandler H**. Oxygen uptake kinetics of constant-load work: upright vs. supine exercise. *Aviat Space Environ Med* 55: 501-506, 1984.

22. **Davies CT, Di Prampero PE, and Cerretelli P**. Kinetics of cardiac output and respiratory gas exchange during exercise and recovery. *J Appl Physiol* 32: 618-625, 1972.

23. **DeLorey DS, Kowalchuk JM, and Paterson DH**. Effects of prior heavy-intensity exercise on pulmonary O2 uptake and muscle deoxygenation kinetics in young and older adult humans. *J Appl Physiol* 97: 998-1005, 2004.

24. **DeLorey DS, Kowalchuk JM, and Paterson DH**. Relationship between pulmonary O_2 uptake kinetics and muscle deoxygenation during moderate-intensity exercise. *J Appl Physiol* 95: 113-120, 2003.

25. **Delp MD**. Control of skeletal muscle perfusion at the onset of dynamic exercise. *Med Sci Sports Exerc* 31: 1011-1018, 1999.

26. **Di Prampero PE, Davies CTM, Cerretelli P, and Margaria R**. An analysis of O_2 debt contracted in submaximal exercise. *J Appl Physiol* 29: 547-551, 1970.

27. **Di Prampero PE, Mahler PB, Giezendanner D, and Cerretelli P**. Effects of priming exercise on VO_2 kinetics and O_2 deficit at the onset of stepping and cycling. *J Appl Physiol* 66: 2023-2031, 1989.

28. **Diamond LB, Casaburi R, Wasserman K, and Whipp BJ**. Kinetics of gas exchange and ventilation in transitions from rest to prior exercise. *J Appl Physiol* 43: 704-708, 1977.

29. **Engelen M, Porszasz J, Riley M, Wasserman K, Maehara K, and Barstow TJ**. Effect of hypoxic hypoxia on O2 uptake and heart rate kinetics during heavy exercise. *J Appl Physiol* 81: 2500-2508, 1996.

30. **Ferreira LF, Townsend DK, Lutjemeier BJ, and Barstow TJ**. Muscle capillary blood flow kinetics estimated from pulmonary O_2 uptake and near-infrared spectroscopy. *J Appl Physiol* 98: 1820-1828, 2005.

31. **Gayeski TE, Connett RJ, and Honig CR**. Oxygen transport in rest-work transition illustrates new functions for myoglobin. *Am J Physiol Heart Circ Physiol* 248: H914-H921, 1985.

32. **Gladden LB**. Lactate metabolism during exercise. In: *Principles of Exercise Biochemistry, Medicine and Sport Science*, edited by Poortmans JR. Basel: Karger, 2003, p. 322-360.

33. **Grassi B**. Oxygen uptake kinetics: old and recent lessons from experiments on isolated muscle in situ. *Eur J Appl Physiol* 90: 242-249, 2003.

34. **Grassi B**. Regulation of oxygen consumption at exercise onset: is it really controversial? *Exerc Sport Sci Rev* 29: 134-138, 2001.

35. **Grassi B, Ferretti G, Xi L, Rieu M, Meyer M, Marconi C, and Cerretelli P**. Ventilatory response to exercise after heart and lung denervation in humans. *Respir Physiol* 92: 289-304, 1993.

36. **Grassi B, Gladden LB, Samaja M, Stary CM, and Hogan MC**. Faster adjustment of O_2 delivery does not affect VO_2 on-kinetics in isolated in situ canine muscle. *J Appl Physiol* 85: 1394-1403, 1998.

37. **Grassi B, Gladden LB, Samaja M, Stary CM, Wagner PD, and Hogan MC**. Peripheral O_2 diffusion does not affect VO_2 on-kinetics in isolated in situ canine muscle *J Appl Physiol* 85: 1404-1412, 1998.

38. **Grassi B, Hogan MC, Greenhaff PL, Hamann JJ, Kelley KM, Aschenbach WG, Constantin-Teodosiu D, and Gladden LB**. Oxygen uptake on-kinetics in dog gastrocnemius in situ following activation of pyruvate dehydrogenase by dichloroacetate. *J Physiol* 538: 195-207, 2002.

39. **Grassi B, Marconi C, Meyer M, Rieu M, and Cerretelli P**. Gas exchange and cardiovascular kinetics with different exercise protocols in heart transplant recipients. *J Appl Physiol* 82: 1952-1962, 1997.

40. **Grassi B, Morandi L, Pogliahi S, Rampichini S, Marconi C, and Cerretelli P**. Functional evaluation of patients with metabolic myopathies during exercise. *Med Sci Sports Exerc* 34: S78, 2002.

41. **Grassi B, Pogliahi S, Rampichini S, Quaresima V, Ferrari M, Marconi C, and Cerretelli P**. Muscle oxygenation and pulmonary gas exchange kinetics during cycling exercise on-transitions in humans. *J Appl Physiol* 95: 149-158, 2003.

42. **Grassi B, Poole DC, Richardson RS, Knight DR, Erickson BK, and Wagner PD**. Muscle O_2 uptake kinetics in humans: implications for metabolic control. *J Appl Physiol* 80: 988-998, 1996.

43. **Hayashi N, Tanaka A, Ishihara M, and Yoshida T**. Delayed vagal withdrawal slows circulatory but not oxygen uptake responses at work increase. *Am J Physiol Regul Integr Comp Physiol* 274: R1268-R1273, 1998.

44. **Henry FM**. Aerobic oxygen consumption and alactic debt in muscular work. *J Appl Physiol* 3: 427-438, 1951.

45. **Henry FM, and DeMoor JC**. Lactic and alactic oxygen consumption in moderate exercise of graded intensity. *J Appl Physiol* 8: 608-614, 1955.

46. **Hochachka PW**. *Muscles as molecular and metabolic machines*. Boca Raton: CRC Press, Inc., 1994.

47. **Hogan MC**. Fall in intracellular PO_2 at the onset of contractions in Xenopus single skeletal muscle fibers. *J Appl Physiol* 90: 1871-1876, 2001.

48. **Hogan MC**. Phosphorescence quenching method for measurement of intracellular PO_2 in isolated skeletal muscle fibers. *J Appl Physiol* 86: 720-724, 1999.

49. **Hogan MC, Nioka S, Brechue WF, and Chance B**. ^{31}P-NMR study of tissue respiration in working dog muscle during reduced O_2 delivery conditions. *J Appl Physiol* 73: 1662-1670, 1992.

50. **Hughson RL**. Alterations in the oxygen deficit-oxygen debt relationships with β-adrenergic receptor blockade in man. *J Appl Physiol* 349: 375-387, 1984.

51. **Hughson RL**. Exploring cardiorespiratory control mechanisms through gas exchange dynamics. *Med Sci Sports Exerc* 22: 72-79, 1990.

52. **Hughson RL**. Regulation of VO_2 on-kinetics by O_2 delivery. In: *Oxygen uptake kinetics in sport, exercise and medicine*, edited by Jones AM, and Poole DC. New York: Routledge, 2005, p. 185-211.

53. **Hughson RL, Cochrane JE, and Butler GC**. Faster O_2 uptake kinetics at onset of supine exercise with than without lower body negative pressure. *J Appl Physiol* 75: 1962-1967, 1993.

54. **Hughson RL, and Imman (sic) RD**. Faster kinetics of VO_2 during arm exercise with circulatory occlusion of the legs. *Int J Sports Med* 7: 22-25, 1986.

55. **Hughson RL, and Kowalchuk JM**. Kinetics of oxygen uptake for submaximal exercise in hyperoxia, normoxia, and hypoxia. *Can J Appl Physiol* 20: 198-210, 1995.

56. **Hughson RL, and Morrisey MA**. Delayed kinetics of VO_2 in the transition from prior exercise. Evidence for O_2 transport limitation of VO_2 kinetics: a review. *Int J Sports Med* 4: 31-39, 1983.

57. **Hughson RL, and Morrissey MA**. Delayed kinetics of respiratory gas exchange in the transition from prior exercise. *J Appl Physiol Respirat Environ Exercise Physiol* 52: 921-929, 1982.

58. **Hughson RL, Shoemaker JK, Tschakovsky ME, and Kowalchuk JM**. Dependence of muscle VO_2 on blood flow dynamics at onset of forearm exercise. *J Appl Physiol* 81: 1619-1626, 1996.

59. **Hughson RL, Tschakovsky ME, and Houston ME**. Regulation of oxygen consumption at the onset of exercise. *Exerc Sport Sci Rev* 29: 129-133, 2001.

60. **Hughson RL, Xing HC, Borkhoff C, and Butler GC**. Kinetics of ventilation and gas exchange during supine and upright cycle exercise. *Eur J Appl Physiol Occup Physiol* 63: 300-307, 1991.

61. **Idstrom JP, Subramanian VH, Chance B, Schersten T, and Bylund-Fellenius AC**. Oxygen dependence of energy metabolism in contracting and recovering rat skeletal muscle. *Am J Physiol Heart Circ Physiol* 248: H40-H48, 1985.

62. **Jones AM, and Poole DC**. *Oxygen uptake kinetics in sport, exercise and medicine*. New York: Routledge, 2005.

63. **Kemp G**. Kinetics of muscle oxygen use, oxygen content, and blood flow during exercise. *J Appl Physiol* 99: 2463-2468, 2005.

64. **Kindig CA, Howlett RA, and Hogan MC**. Effect of extracellular PO_2 on the fall in intracellular PO_2 in contracting single myocytes. *J Appl Physiol* 94: 1964-1970, 2003.

65. **Kindig CA, Kelley KM, Howlett RA, Stary CM, and Hogan MC**. Assessment of O_2 uptake dynamics in isolated single skeletal myocytes. *J Appl Physiol* 94: 353-357, 2003.

66. **Koga S, Poole DC, Shiojiri T, Kondo N, Fukuba Y, Miura A, and Barstow TJ**. Comparison of oxygen uptake kinetics during knee extension and cycle exercise. *Am J Physiol Regul Integr Comp Physiol* 288: R212-R220, 2005.

67. **Korzeniewski B, and Zoladz JA**. Factors determining the oxygen consumption rate (VO_2) on-kinetics in skeletal muscles. *Biochem J* 379: 703-710, 2004.

68. **Krogh A, and Lindhard J**. The regulation of respiration and circulation during the initial stages of muscular work. *J Physiol* 47: 112-136, 1913.

69. **Laughlin MH**. Skeletal muscle blood flow capacity: the role of the muscle pump in exercise hyperemia. *Am J Physiol Heart Circ Physiol* 253: H296-H306, 1987.

70. **Macdonald M, Pedersen PK, and Hughson RL**. Acceleration of VO_2 kinetics in heavy submaximal exercise by hyperoxia and prior high-intensity exercise. *J Appl Physiol* 83: 1318-1325, 1997.

71. **Macdonald MJ, Shoemaker JK, Tschakovsky ME, and Hughson RL**. Alveolar oxygen uptake and femoral artery blood flow dynamics in upright and supine leg exercise in humans. *J Appl Physiol* 85: 1622-1628, 1998.

72. **Murphy PC, Cuervo LA, and Hughson RL**. A study of cardiorespiratory dynamics with step and ramp exercise tests in normoxia and hypoxia. *Cardiovasc Res* 23: 825-832, 1989.

73. **Nelson DL, and Cox MM**. *Lehninger Principles of Biochemistry 4th Ed.* New York: W.H. Freeman and Company, 2005.

74. **Nery LE, Wasserman K, Andrews JD, Huntsman DJ, Hansen JE, and Whipp BJ**. Ventilatory and gas exchange kinetics during exercise in chronic airways obstruction. *J Appl Physiol* 53: 1594-1602, 1982.

75. **Palange P, Galassetti P, Mannix ET, Farber MO, Manfredi F, Serra P, and Carlone S**. Oxygen effect on O2 deficit and VO2 kinetics during exercise in obstructive pulmonary disease. *J Appl Physiol* 78: 2228-2234, 1995.

76. **Paterson DH, and Whipp BJ**. Asymmetries of oxygen uptake transients at the on- and offset of heavy exercise in humans *J Physiol Lond* 443: 575-586, 1991.

77. **Petersen ES, Whipp BJ, Davis JA, Huntsman DJ, Brown HV, and Wasserman K**. Effects of β-adrenergic blockade on ventilation and gas exchange during exercise in humans. *J Appl Physiol Respirat Environ Exercise Physiol* 54: 1306-1313, 1983.

78. **Phillips SM, Green H, Macdonald MJ, and Hughson RL**. Progressive effect of endurance training on VO_2 kinetics at the onset of submaximal exercise. *J Appl Physiol* 79: 1914-1920, 1995.

79. **Poole DC, Barstow TJ, McDonough P, and Jones AM**. Control of oxygen uptake during exercise. *Med Sci Sports Exerc* 40: 462-474, 2008.

80. **Poole DC, Kindig CA, and Behnke BJ**. VO_2 kinetics in different disease states. In: *Oxygen uptake kinetics in sport, exercise and medicine*, edited by Jones AM, and Poole DC. New York: Routledge, 2005, p. 353-372.

81. **Regensteiner JG, Bauer TA, Reusch JE, Brandenburg SL, Sippel JM, Vogelsong AM, Smith S, Wolfel EE, Eckel RH, and Hiatt WR**. Abnormal oxygen uptake kinetic response in women with type II diabetes mellitus. *J Appl Physiol* 85: 310-317, 1998.

82. **Richardson RS, Noyszewski EA, Kendrick KF, Leigh JS, and Wagner PD**. Myoglobin O_2 desaturation during exercise. Evidence of limited O_2 transport. *J Clin invest* 96: 1916-1926, 1995.

83. **Rossiter HB, Ward SA, Doyle VL, Howe FA, Griffiths JR, and Whipp BJ**. Inferences from pulmonary O_2 uptake with respect to intramuscular [phosphocreatine] kinetics during moderate exercise in humans. *J Physiol* 518: 921-932, 1999.

84. **Rowell LB**. *Human Cardiovascular Control*. New York: Oxford Univ Press, 1993.

85. **Rumsey WL, Vanderkooi JM, and Wilson DF**. Imaging of phosphorescence: a novel method for measuring oxygen distribution in perfused tissue. *Science* 241: 1649-1651, 1988.

86. **Shoemaker JK, Hodge L, and Hughson RL**. Cardiorespiratory kinetics and femoral artery blood velocity during dynamic knee extension exercise. *J Appl Physiol* 77: 2625-2632, 1994.

87. **Sietsema KE, Ben-Dov I, Zhang YY, Sullivan C, and Wasserman K**. Dynamics of oxygen uptake for submaximal exercise and recovery in patients with chronic heart failure. *Chest* 105: 1693-1700, 1994.

88. **Springer C, Barstow TJ, Wasserman K, and Cooper DM**. Oxygen uptake and heart rate responses during hypoxic exercise in children and adults. *Med Sci Sports Exerc* 23: 71-79, 1991.

89. **Sundberg CJ, and Kauser L**. Effects of graded restriction of perfusion on circulation and metabolism in the working leg; quantification of a human ischaemia-model. *Acta Physiol Scand* 146: 1-9, 1992.

90. **Tonkongi M, and Sahlin K**. Physical exercise and mitochondrial function in human skeletal muscle. *Exerc Sport Sci Rev* 30: 129-137, 2002.

91. **Tschakovsky ME, and Hughson RL**. Interaction of factors determining oxygen uptake at the onset of exercise. *J Appl Physiol* 86, 1101-1113, 1999.

92. **Twentyman OP, Disley A, Gribbin HR, Alberti KGMM, and Tattersfield AE**. Effect of β-adrenergic blockade on respiratory and metabolic responses to exercise. *J Appl Physiol Respirat Environ Exercise Physiol* 51: 788-793, 1981.

93. **van Beek JH, and Westerhof N**. Response time of cardiac mitochondrial oxygen consumption to heart rate steps. *Am J Physiol* 260: H613-H625, 1991.

94. **Wasserman K**. Diagnosing cardiovascular and lung pathophysiology from exercise gas exchange. *Chest* 112: 1091-1101, 1997.

95. **Whipp BJ, and Mahler PB**. Dynamics of pulmonary gas exchange during exercise. In: *Pulmonary Gas Exchange*, edited by West JB. New York: Academic, 1980, p. 33-95.

96. **Whipp BJ, and Ward SA**. Physiological determinants of pulmonary gas exchange kinetics during exercise. *Med Sci Sports Exerc* 22: 62-71, 1990.

97. **Wilkerson DP, Berger NJA, and Jones AM**. Influence of hyperoxia on pulmonary O2 uptake kinetics following the onset of exercise in humans. *Respir Physiol Neurobiol* 153: 92-106, 2006.

98. **Williamson JW, Raven PB, and Whipp BJ**. Unaltered oxygen uptake kinetics at exercise onset with lower-body positive pressure. *Exp Physiol* 81: 695-705, 1996.

99. **Wilson DF**. Factors affecting the rate and energetics of mitochondrial oxidative phosphorylation. *Med Sci Sports Exerc* 26: 37-43, 1994.

100. **Wilson DF, Erecinska M, Nuutinen EM, and Silver IA**. Dependence of cellular metabolism and local oxygen delivery on oxygen tension. *Adv Exp Med Biol* 180: 629-634, 1984.

101. **Wilson DF, Erecinska M, and Silver IA**. Metabolic effects of lowering oxygen tension in vivo. *Adv Exp Med Biol* 159: 293-301, 1983.

102. **Wilson DF, Owen CS, and Erecinska M**. Quantitative dependence of mitochondrial oxidative phosphorylation on oxygen concentration: a mathematical model. *Arch Biochem Biophys* 195: 494-504, 1979.

103. **Wilson DF, and Rumsey WL**. Factors modulating the oxygen dependence of mitochondrial oxidative phosphorylation. *Adv Exp Med Biol* 222: 121-131, 1988.

104. **Yoshida T, and Whipp BJ**. Dynamic asymmetries of cardiac output transients in response to muscular exercise in man. *J Physiol* 480: 355-359, 1994.

(ADDITIONAL REFERENCES ONLY IN JOURNAL ARTICLE)

105. **Auchincloss JH, Ashutosh K, Rana S, Peppi D, Johnson LW, and Gilbert R.** Effect of cardiac, pulmonary, and vascular disease on one-minute oxygen uptake. *Chest* 70: 486-493, 1976.

106. **Auchincloss JHJ, Meade JW, Gilbert R, and Chamberlain BE.** One minute oxygen uptake in peripheral ischemic vascular disease. *Ann Surg* 191: 203-206, 1980.

107. **Boushel R, and Piantadosi CA.** Near-infrared spectroscopy for monitoring muscle oxygenation. *Acta Physiol Scand* 168:615-622, 2000.

108. **Chance B, Dait MT, Zhang C, Hamaoka T, and Hagerman F.** Recovery from exercise-induced desaturation in the quadriceps muscles of elite competitive rowers. *Am J Physiol Cell Physiol* 262: C766 C775, 1992.

109. **Elwell C.** A Practical User's Guide To Near Infrared Spectroscopy. London: Hamatsu Photonics KK, 1995, p. 1-155.

110. **Ferrari M, Binzoni T, and Quaresima V.** Oxidative metabolism in muscle. *Philos Trans R Soc Lond B Biol Sci* 352:677-683, 1997.

111. **Grassi B, Hogan MC, Kelley KM, Aschenbach WG, Hamann JJ, Evans RK, Patillo RE, and Gladden LB.** Role of convective O_2 delivery in determining VO_2 on-kinetics in canine muscle contracting at peak VO_2. *J Appl Physiol* 89: 1293-1301, 2000.

112. **Hepple RT, Hagen JL, and Krause DJ.** Oxidative capacity interacts with oxygen delivery to determine maximal O_2 uptake in rat skeletal muscles *in situ*. *J Physiol* 541: 1003-1012, 2002.

113. **Jones AM, Fulford J, and Wilkerson DP.** Influence of prior exercise on muscle [phosphorylcreatine] and deoxygenation kinetics during high-intensity exercise in men. *Exp Physiol* 93: 468-478, 2008.

114. **Mancini DM, Bollinger L, Li H, Kendrick K, Chance B, and Wilson JR.** Validation of near infrared spectroscopy in humans. *J Appl Physiol* 77: 2740-2747, 1994.

115. **Nighswander-Rempel SP, Kupriyanov VV, and Shaw RK.** Relative contributions of hemoglobin and myoglobin to near-infrared spectroscopic images of cardiac tissue. *Appl Spectrosc* 59: 190-193, 2005.

116. **Seiyama A, Hazeki O, and Tamura M.** Noninvasive quantitative analysis of blood oxygenation in rat skeletal muscle. *J Biochem* 103: 419-424, 1988.

117. **Sietsema KE.** Oxygen uptake kinetics in response to exercise in patients with pulmonary vascular disease. *Am Rev Respir Dis* 145: 1052-1057, 1992.

118. **Stainsby WN, and Welch HG.** Lactate metabolism of contracting dog skeletal muscle in situ. *Am J Physiol* 211:177-183, 1966.

APPENDIX A

Working Protocol for Dog Studies June-Oct 2008; Slowed O_2 delivery

Weeks Before

1. Be sure cartridge for blood gas machine has been ordered.
2. Be sure reagents for solutions in study have been ordered.
3. Be sure that dogs have been ordered.
4. Be sure that other lab members are aware of upcoming experiment days and have planned accordingly.
5. Contact any undergrad/masters students that may be assisting with data collection.
6. Run any pilot work that can be run without an animal to ensure equipment is working.
7. Be sure someone has obtained a keycard to kennel facilities so that we can be admitted before 7am.

Day Before

8. Benchtop paper on table and dog board.
9. Heating pad on dog board.
10. Strings cut for tying limbs of dog to board.
11. Surgical equipment clean and placed on tray.
12. Soldering guns cleaned, checked, and working.
13. Blood gas and CO-Ox machines turned on and working.
14. Syringes for blood samples labeled and arranged.
15. Plastic tubes for muscle samples labeled and arranged.
16. Set up Oxymon for appropriate measurements.
17. Be sure that ice and liquid N_2 are available.
18. Check that sutures, umbilical tape and string are in ample supply.
19. Check that sufficient pentobarbital has been diluted from 324 mg/mL to 65 mg/mL.
20. Check that sufficient normal saline (0.9% or 0.9g/100mL) is available and soak flow probe in saline.
21. Check that sufficient saturated KCl solution is available for euthanasia.
22. Check the laptop with "flow program" is ready and working.

Day of Getting Dog

23. Double-check the anesthesia toolbox.
    a. Catheters
    b. Syringes
    c. Needles
    d. Stopcocks
    e. Gauze
    f. Gloves
    g. Pentobarbital
    h. Endotracheal tubes
    i. Flashlight
    j. Muzzle
    k. Leash
    l. Calculator
    m. Extension Cord

n. Clippers
o. Keys to kennel
p. Key/card to enter facility if before 7:30am
q. Scale
r. White Coats

24. Take any frozen carcass with you and drop off at incinerator
25. Walk dog from kennel to examination room

26. Obtain weight, anesthetize animal:
    s. Anesthesia dosage:

$$\frac{30\text{mg}}{(?)\text{ Kg animal Wt.}} \times \frac{1\text{ mL sol'n}}{65\text{ mg sol'n}} = \text{mL's sol'n per Kg dog Wt.}$$

27. Insert endotracheal tube.
28. Transport dog via cart to lab.

Setting up in lab

29. Place dog on table.
30. Shave hair from surgical areas while vacuuming.
31. Place heating pad under dog and maintain at 37°C.
32. Place rectal probe through anus into rectum and check temperature.
33. Tie limbs to table and begin Surgery (steps 35-37).
34. While surgery is being performed:
    a. Set up jugular reservoir with saline.
    b. Prepare heparin syringe (3,000 Units per Kg dog Wt).
    c. Check blood gas, pH, and CO-Ox machines (run cal dyes on CO-Ox).
    d. Turn on all equipment (Flowmeter, indwelling oximeter, physiograph, data acquisition center, laptop for pump-control, pumps) and prepare accordingly.
    e. Set up perfusion pump by pumping saline through all of the tubing until all bubbles are removed.
    f. Top off liquid N_2 in small flask.
    g. Put fresh blade in scalpel.
    h. Discuss politics and religion.
35. Surgically isolate the left-side GP.
36. Surgically isolate the jugular vein.
37. Surgically isolate the right-side femoral artery.
38. Place 12" X 12" plastic sheet under isolated GP and into V-groove of board.
39. Drive bone nails.
40. Andres – take muscle sample
41. Place connector on Achilles tendon
42. Insert jugular reservoir catheter into jugular vein and suspend on ring stand.
43. **IMMEDIATELY add heparin to jugular reservoir**.
44. Insert catheter into popliteal vein and attach oxicath, flow probe, and tubing to jugular reservoir.
45. Thread sciatic nerve through stimulator cuff.
46. Run data acquisition calibration:
    a. Pressure – 0 and 100 mmHg pressure
    b. Force – 0 and 198 N on load cell.
    c. Flow – 0 and 1,000 mL/min on the flowmeter.
    d. Indwelling Oximeter is set to alternately output 0 and 100% saturation throughout the 30 sec of calibration.
47. Set up muscle myograph and attach Achilles tendon connector to the load cell.
48. Set up Oxymon and attach optodes to the muscle with elastic.

49. Place dog on ventilator and check appropriate settings: tidal volume = 20 mL/kg, 50% inspiration, 15-20 breaths/min.
50. Insert catheter from perfusion pump into right side femoral artery.
51. Allow blood to move through tubing and be sure bubbles are removed.
52. Insert catheter from perfusion pump into the left popliteal artery supplying the GP using Goodwin method:
    a. Turn pump on so that blood is dripping out of end of catheter to be inserted into popliteal artery.
53. After inserting catheter, turn on perfusion pump and set flow. Set the flow such that pressure is reasonable (~100-120 torr).
54. Quickly attack the pressure transducer to the sidearm of the catheter supplying the GP so that perfusion pressure can be measured. Adjust perfusion flow to give about 100 mmHg perfusion pressure. Continue to adjust flow with time to maintain reasonable pressure and in the neighborhood of 5-10mL/min.
55. Set optimal length of muscle. Use titanic stimuli (8.0 V, 0.2 ms duration, trains at 50 Hz for 200ms duration).
56. Before continuing, cut down on right side gastroc and take muscle biopsy if desired.
57. Check blood gas, pH, Hb, O_2Sat values and adjust as necessary according to the following algorithm:
    a. <u>"Normal" arterial dog values in this prep and how to fix problems:</u>
        i. **pH = ~7.38 – 7.4**
            1. If pH is lower than 7.38 – 7.40, then:
                a. If PCO_2 is adequate or high, consider increasing ventilation (perhaps 5-10 breaths/min per 0.03 pH units?).
                b. If PCO_2 is adequate or low, consider adding bicarbonate (use a 1.0 M bicarb solution and titrate ~10 mL per hour per 0.05 pH units).
            2. If pH is higher than 7.38 – 7.4, then:
                a. If PCO_2 is lower than 28-35 Torr, consider decreasing ventilation (perhaps 5-10 breath/min per 0.03 pH units?).
                b. If PCO_2 is higher than usual, then slow ventilation slightly and add acid. This would be most unusual!
        ii. **PCO_2 = ~28-35 Torr**
            1. If pH is normal and PCO_2 is higher, then we probably do not need to worry too much about it. Ventilation could be speeded slightly.
            2. If pH is normal and PCO_2 is lower, then we probably do not need to worry too much about it. Ventilation could be slowed slightly.
        iii. **O_2 Sat = 95-98%**
            1. If O_2Sat is below 94, consider giving titrating small amounts of 100% O_2 flow into ventilator until 95-98% is reached.
        iv. **If PCO_2 is high and pH is very low, or anything else looks really goofy** – check to be sure that trach tube cuff is properly inflated.
58. Throughout, check blood gas, pH, Hb, and O_2Sat and adjust as needed.
59. Throughout, check palpebral and plantar reflexes throughout and add maintenance doses of pentobarbital as needed (usually in 1-2 mL dosages).
60. Sometime during the day be sure to copy dog tag and place with strip chart recording at end of day.
61. Be sure to speak up if you think someone has done something wrong! (clamped the wrong tube, gotten the trials out of order, etc)
62. THROUGHOUT THE DAY BE SURE TO do the following before administering Pento:
    a. ASK the group if anyone has done so recently.
    b. CHECK the strip chart to see if any is marked down.
    c. MARK any pentobarbital that is given on the strip chart (e.g. "1 mL Pento at 11:35am") AND announce this to the group! (e.g. "I just gave the dog 1mL of Pento).

Experimental Protocol; Trials will be randomized according to the following chart:
A=CT2, B=EX25, C=EX50

Trial Order →	**1**	**2**	**3**	**4**	**5(?)**	6(?)
Dog# ↓						
1	CT1	A	B	C	Flow-steps	
2	CT1	B	C	A	Flow-steps	
3	CT1	C	A	B	Flow-steps	
4	CT1	A	C	B	Flow-steps	
5	CT1	B	A	C	Flow-steps	
6	CT1	C	B	A	Flow-steps	
7	FT1	A	B	C	Flow-steps, MC	10%?
8	FT1	B	C	A	Flow-steps, MC	10%?
9	FT1	C	A	B	Flow-steps, MC	10%?
10	FT1	A	C	B	Flow-steps, MC	10%?
11	FT1	B	A	C	Flow-steps, MC	10%?
12	FT1	C	B	A	Flow-steps, MC	10%?
13	FT1	A	B	C	Flow Steps, MC	
14	FT1	B	C	A	Flow Steps, MC	

Sample Run to Set Flow (FT1)

63. Do a faux run of ~2 minutes to determine an appropriate resting flow (before the run) and an appropriate steady state flow. Use pressure to gauge what is appropriate.
64. Be sure to write down what the pump is set on (what the flow is) for each of these!! These will be the flow for the remaining resting and steady state trials.

Pump-controlled run (CT2)

65. MARKERS: Draw A1 and V1 blood samples.
66. Get pump set up correctly and enter needed variables.
67. For CT2 we will use a tau of 20 seconds and run for 6 tau.
68. MARKER: Start contractions at 1 tetanic contraction every 2 seconds (4.0 V, 200 ms, 50 Hz) AT THE SAME TIME that we start the blood flow response.
    a. **Goodwin: Countdown and start flow program**
    b. **Gladden: Start contractions**
    c. **Hernandez: Event Marker**
69. MARKER: In last 30 sec of run, draw venous blood sample V2.
70. Allow run to go for at least 6 tau (so we will let it run for 4-5 min).
71. MARKER: Turn contractions off and continue to collect off-kinetics data for 3 min.
72. **Watch the pressure – do not let it get too high here!**
73. MARKER: End run.
74. MARKER: Draw A2.
75. Allow muscle to recover for 30-35 min after end of contractions.

Pump-controlled run, tau 25sec longer (EX25)

76. MARKERS: Draw A3 and V3 blood samples.
77. Get pump set up correctly and enter needed variables.
78. For EX25 we will use a tau of 45 seconds.
79. MARKER: Start contractions at 1 tetanic contraction every 2 seconds (4.0 V, 200 ms, 50 Hz) AT THE SAME TIME that we start the blood flow response.
    a. **Goodwin: Countdown and start flow program**
    b. **Gladden: Start contractions**
    c. **Hernandez: Event Marker**
80. MARKER: In last 30 sec of run, draw venous blood sample V4.

81. Allow run to go for at least 6 tau (so we will let it run for 4-5 min).
82. MARKER: Turn contractions off and continue to collect off-kinetics data for 3 min.
83. **Watch the pressure – do not let it get too high here!**
84. MARKER: End run.
85. MARKER: Draw A4.
86. Allow muscle to recover for 30-35 min after end of contractions.

Pump-controlled run, tau 50sec longer (EX50)

87. MARKERS: Draw A5 and V5 blood samples.
88. Get pump set up correctly and enter needed variables.
89. For EX50 we will use tau of 70 seconds.
90. MARKER: Start contractions at 1 tetanic contraction every 2 seconds (4.0 V, 200 ms, 50 Hz) AT THE SAME TIME that we start the blood flow response.
    a. **Goodwin: Countdown and start flow program**
    b. **Gladden: Start contractions**
    c. **Hernandez: Event Marker**
91. MARKER: In last 30 sec of run, draw venous blood sample V6.
92. Allow run to go for at least 6 tau (so we will let it run for 4-5 min).
93. MARKER: Turn contractions off and continue to collect off-kinetics data for 3 min.
94. **Watch the pressure – do not let it get too high here!**
95. MARKER: End run.
96. MARKER: Draw A6.
97. Allow muscle to recover for 30-35 min after end of contractions.

*****FOR WHICHEVER CONDITION IS THE LAST TRIAL OF THE DAY:**

98. **After you have reached 6 tau, let the trial continue**
99. **Leave contractions going**
100. **Leave flow steady**
101. **MARKER: Take a manual flow cal**
102. **MARKER: Draw Arterial sample**
103. **MARKER: Step up flow SS+25% from steady state flow for 90 sec**
104. **MARKER: Step down to steady state flow for 90 sec**
105. **MARKER: Step up flow to SS+50% from steady state flow for 90 sec**
106. **MARKER: Step down to steady state flow for 90 sec**
107. **MARKER: Step up flow to SS+75% from steady state flow for 90 sec**
108. **MARKER: Manual flow cal here**
109. **MARKER: Step down to steady state for 90 sec**
110. **MARKER: Stop contractions**
111. **Leave flow elevated for around 2 more min.**
112. **End run.**

Determine how much blood leaves muscle once contractions start

113. With flow still elevated clamp arterial inflow to muscle and start a few contractions at the same time. Mark this on record as "high flow clamp"
114. Mark on record "flow back" when flow is back down to resting
115. Now, with flow set to resting flow rate, clamp arterial side of blood flow as you begin contractions again.
116. Mark this on record as "low flow clamp"
117. Monitor BF throughout (sensor) so that flow can be analyzed.
118. Let run for a few contractions

IF THE DOG SEEMS OK AND WE FEEL GOOD:

119. **Throw in an EX10 run. We could wait until we have analyzed the first 6 dogs to see if this is necessary (i.e. if EX25 doesn't slow kinetics, we need not do EX10). DON'T THINK THIS IS NECESSARY (6/8/08)**

After experiments

120. Remove dog from ventilator.
121. Release clamping on tubes in pumps and check that tubes are ok for next experiment.
122. Inject remainder of Pentobarbital into animal and then pour saturated KCl into jugular reservoir to stop heart. Check for heart beat as you perform this step to feel it stop.
123. After heart and breathing appear to stop, perform a bilateral pneumothorax to ensure the dog has expired.
124. Remove muscle, trim non-muscle tissue, place onto weighed and labeled aluminum foil, and record weight as follows:
    i. Tare weight: (weight of aluminum foil)
    ii. Total weight: (weight of foil + muscle)
    iii. Net weight: (total weight – tare weight)
125. Place muscle wrapped in aluminum foil into drying oven at 80°C.
126. Record aluminum foil tare weight and muscle weight on recording paper (strip chart).
127. Clean up and place dog in freezer.
128. Turn off all gases used during exp (O_2!!)
129. Turn off other pertinent equipment and shut down, etc.
130. Remove tubes from pumps (unclamp the pumps!)!

PLAN:

1) Do the flow steps for the tmito model for the first 6 dogs
2) Then over July I will analyze all data and see if a 10% slowing of tau is even needed (if 25% reduction did not change VO_2 response, then we don't need to do 10%).
3) For dogs 7-12 (August beagles), we will either do more flow steps as before OR switch to 10% if needed.
   PLAN (9/8/08) = do 5-7 dogs with CT1, CT2 tau = 20 sec, EX25 tau = 45 sec, EX50 tau = 70 sec

APPENDIX B

RAW DATA

For all data tables means are presented ± S.D. Significance at the $p<0.05$ level is denoted with an asterisk (*) if different from CT20 and with a dagger (†) if different from EX45. p-values for selected samples are shown in parentheses.

RAW DATA

MUSCLE WEIGHTS

DOG #	BODY WEIGHT (kg)	MUSCLE WEIGHT (g)	% MUSCLE WATER
1(6)	14.1	49.2	77.2
2(7)	16.3	54.7	78.0
3(8)	13.4	51.0	77.9
4(9)	10.0	33.4	77.5
5(12)	14.8	44.8	76.6
6(14)	11.4	33.8	76.2
MEAN ± SD	13.3±2.3	44.5±9.0	77.2±0.7

TIME TO 50% FATIGUE (sec)

DOG #	CT20	EX45	EX70
1(6)	84	70	88
2(7)	106	70	84
3(8)	96	68	56
4(9)	106	62	82
5(12)	106	126	82
6(14)	118	76	72
MEAN ± SD	102.7±11.5	76±24.9* (p=0.0163)	72±19.4* (p=0.0195)

RAW DATA

RESTING PaO_2 (Torr)

DOG #	CT20	EX45	EX70
1(6)	144	149	137
2(7)	107	102	114
3(8)	106	109	104
4(9)	122	110	127
5(12)	152	123	166
6(14)	103	113	185
MEAN ± SD	122.3±21.1	117.7±16.8	138.8±31.1

RESTING PvO_2 (Torr)

DOG #	CT20	EX45	EX70
1(6)	50	46	44
2(7)	50	45	46
3(8)	57	56	56
4(9)	49	43	57
5(12)	53	57	61
6(14)	59	48	64
MEAN ± SD	53±4.1	49.2±5.9	54.7±8.0

RAW DATA

RESTING $PaCO_2$ (Torr)

DOG #	CT20	EX45	EX70
1(6)	27	25	25
2(7)	27	28	29
3(8)	33	36	34
4(9)	30	32	38
5(12)	33	30	29
6(14)	31	31	26
MEAN ± SD	30±3	30±4	30±5

RESTING CaO_2 (mL O_2 • dL $blood^{-1}$)

DOG #	CT20	EX45	EX70
1(6)	25.1	25.6	24.4
2(7)	27.2	27.4	27
3(8)	30.5	28.6	29.5
4(9)	26.4	24.6	29
5(12)	21.1	21.8	21.2
6(14)	30.8	30.6	28.2
MEAN ± SD	26.9±3.6	26.4±3.1	26.5±3.2

RAW DATA

RESTING CvO_2 (mL O_2 • dL $blood^{-1}$)

DOG #	CT20	EX45	EX70
1(6)	18.5	19.2	18.4
2(7)	23	20.8	21.4
3(8)	27.1	25.4	25.7
4(9)	20.6	17.7	24.5
5(12)	16.4	17.7	17.7
6(14)	26.7	24.2	25.4
MEAN ± SD	22.1±4.4	20.8±3.3	22.2±3.6

RESTING $CaO_2 – CvO_2$ (mL O_2 • dL $blood^{-1}$)

DOG #	CT20	EX45	EX70
1(6)	6.6	6.4	6
2(7)	4.2	6.6	5.6
3(8)	3.4	3.2	3.8
4(9)	5.8	6.9	4.5
5(12)	4.7	4.1	3.5
6(14)	4.1	6.4	2.8
MEAN ± SD	4.8±1.2	5.6±1.5	4.4±1.2

RAW DATA

RESTING BLOOD FLOW ($mL \cdot kg^{-1} \cdot min^{-1}$)

DOG #	CT20	EX45	EX70
1(6)	83.4	101.7	89.5
2(7)	84.2	82.3	91.5
3(8)	119.7	117.7	117.7
4(9)	98.7	92.8	92.8
5(12)	125.1	107.2	93.8
6(14)	100.7	106.6	100.7
MEAN ± SD	102±17.4	101.4±12.4	97.7±10.5

RESTING BLOOD FLOW X CaO_2 ($mL\ O_2 \cdot kg^{-1} \cdot min^{-1}$)

DOG #	CT20	EX45	EX70
1(6)	20.9	26.0	21.8
2(7)	22.9	22.6	24.7
3(8)	36.5	33.7	34.7
4(9)	26.1	22.8	26.9
5(12)	26.4	23.4	19.9
6(14)	31.0	32.6	28.4
MEAN ± SD	27.3±5.7	26.8±5.0	26.1±5.3

RAW DATA

RESTING MUSCLE PERFUSION PRESSURE (Torr)

DOG #	CT20	EX45	EX70
1(6)	126.7	125.8	127.1
2(7)	88.4	100.8	92.1
3(8)	130.2	125	143.9
4(9)	115.9	98.3	155.2
5(12)	123.8	124.4	127.9
6(14)	142.2	174.9	162.6
MEAN ± SD	121.2±18.2	124.9±27.5	134.8±25.3

RESTING TOTAL [Hb] ($g \cdot dL^{-1}$)

DOG #	CT20	EX45	EX70
1(6)	18.2	18.6	18.1
2(7)	20.5	20.9	19.8
3(8)	23.3	21.5	22.3
4(9)	19.8	18.1	21.6
5(12)	14.9	15.7	15.2
6(14)	22.9	22.3	19.9
MEAN ± SD	19.9±3.1	19.5±2.5	19.5±2.6

RAW DATA

RESTING ARTERIAL pH

DOG #	CT20	EX45	EX70
1(6)	7.24	7.36	7.4
2(7)	7.38	7.37	7.41
3(8)	7.4	7.39	7.33
4(9)	7.37	7.37	7.31
5(12)	7.34	7.33	7.3
6(14)	7.33	7.37	7.43
MEAN ± SD	7.34±0.06	7.34±0.02	7.36±0.06

RAW DATA

STEADY STATE PaO_2 (Torr)

DOG #	CT20	EX45	EX70
1(6)	139	148	137
2(7)	104	111	144
3(8)	120	105	91
4(9)	125	146	136
5(12)	152	138	161
6(14)	117	110	182
MEAN ± SD	126±17	126±20	142±30

STEADY STATE PvO2 (Torr)

DOG #	CT20	EX45	EX70
1(6)	23	24	22
2(7)	16	17	18
3(8)	23	23	23
4(9)	23	23	26
5(12)	32	30	30
6(14)	32	31	29
MEAN ± SD	24.8±6.2	24.7±5.2	24.7±4.5

RAW DATA

STEADY STATE $PaCO_2$ (Torr)

DOG #	CT20	EX45	EX70
1(6)	29	27	28
2(7)	27	26	20
3(8)	26	36	37
4(9)	25	18	32
5(12)	33	24	28
6(14)	24	31	20
MEAN ± SD	27±3	27±6	28±7

STEADY STATE CaO_2 (mL O_2 • dL $blood^{-1}$)

DOG #	CT20	EX45	EX70
1(6)	25.1	25.6	24.4
2(7)	27.2	27.4	27
3(8)	30.5	28.6	29.5
4(9)	26.4	24.6	29
5(12)	21.1	21.8	21.2
6(14)	30.8	30.6	28.2
MEAN ± SD	26.9±3.6	26.4±3.1	26.6±3.2

RAW DATA

STEADY STATE CvO_2 (mL O_2 • dL blood^{-1})

DOG #	CT20	EX45	EX70
1(6)	6.6	8.1	6.8
2(7)	4.9	4.8	6.2
3(8)	10.8	9.2	8.8
4(9)	8.5	7.5	9.2
5(12)	11.1	10.3	9.6
6(14)	15.6	15.3	13.5
MEAN ± SD	9.6±3.8	9.2±3.5	9.0±2.6

STEADY STATE $CaO_2 – CvO_2$ (mL O_2 • dL blood^{-1})

DOG #	CT20	EX45	EX70
1(6)	18.5	17.5	17.6
2(7)	22.3	22.6	20.8
3(8)	19.7	19.4	20.7
4(9)	17.9	17.1	19.8
5(12)	10	11.5	11.6
6(14)	15.2	15.3	14.7
MEAN ± SD	17.3±4.2	17.2±3.7	17.5±3.7

RAW DATA

STEADY STATE BLOOD FLOW ($mL \cdot kg^{-1} \cdot min^{-1}$)

DOG #	CT20	EX45	EX70
1(6)	803	793	742
2(7)	549	585	567
3(8)	687	726	687
4(9)	778	778	778
5(12)	1161	1184	1161
6(14)	888	918	888
MEAN ± SD	811±207	831±204	804±204*

STEADY STATE BLOOD FLOW X CaO2 ($mL\ O_2 \cdot kg^{-1} \cdot min^{-1}$)

DOG #	CT20	EX45	EX70
1(6)	202	203	181
2(7)	149	160	153
3(8)	209	208	203
4(9)	205	191	226
5(12)	245	258	246
6(14)	274	281	251
MEAN ± SD	214±42	217±45	210±38

RAW DATA

STEADY STATE MUSCLE PERFUSION PRESSURE (Torr)

DOG #	CT20	EX45	EX70
1(6)	135.4	141.3	138.9
2(7)	107.4	113.8	103.5
3(8)	151.3	124.6	134.6
4(9)	153.5	131.7	173.8
5(12)	193	181	169.3
6(14)	211	214.9	178
MEAN ± SD	158.6±37.9	151.2±38.8	149.7±29.1

STEADY STATE TOTAL [Hb] ($g \cdot dL^{-1}$)

DOG #	CT20	EX45	EX70
1(6)	18.9	18.8	18.2
2(7)	20.5	19.9	19.7
3(8)	22.2	21.4	22.4
4(9)	18.3	19.7	21.4
5(12)	15.3	16	15.6
6(14)	22.6	22.7	20.7
MEAN ± SD	19.6±2.7	19.8±2.3	19.7±2.5

RAW DATA

STEADY STATE ARTERIAL pH

DOG #	CT20	EX45	EX70
1(6)	7.23	7.36	7.37
2(7)	7.37	7.38	7.44
3(8)	7.37	7.36	7.31
4(9)	7.43	7.35	7.25
5(12)	7.34	7.32	7.29
6(14)	7.31	7.34	7.42
MEAN ± SD	7.34±0.07	7.35±0.02	7.35±0.08

RAW DATA

RESTING VO_2 ($mL \cdot kg^{-1} \cdot min^{-1}$)

DOG #	CT20	EX45	EX70
1(6)	2.9	6.8	5.9
2(7)	3	2.1	3.9
3(8)	5.2	4.1	3.2
4(9)	4.3	5.7	3
5(12)	6.8	3.4	5.1
6(14)	0.02	5.1	1.5
MEAN ± SD	3.7±2.3	4.5±1.7	3.8±1.6

STEADY STATE VO_2 ($mL \cdot kg^{-1} \cdot min^{-1}$)

DOG #	CT20	EX45	EX70
1(6)	152	139.4	121.5
2(7)	118.5	132	117.1
3(8)	125.9	135.2	131.2
4(9)	130.7	118.6	147
5(12)	120.2	144.9	139.5
6(14)	132	145.3	132.7
MEAN ± SD	129.9±12.1	135.9±10.0	131.5±11.1

RAW DATA

DOG 1 VENOUS BLOOD TEMPERATURE (°C)

TIME (sec)	CT20	EX45	EX70
0	35.6	35.8	35.8
15	36.1	35.8	35.8
30	35.9	35.7	35.8
45	35.7	35.7	35.8
60	35.5	35.3	35.8
90	35.4	34.8	35.8
120	35.4	34.7	35.8
180	35.8	34.8	36
(CORE)	(37.3)	(36.3)	(37.3)
MEAN ± SD	35.7±0.2	35.3±0.5	35.8±0.1

RAW DATA

DOG 2 VENOUS BLOOD TEMPERATURE (°C)

TIME (sec)	CT20	EX45	EX70
0	32.8	33.3	33.4
15	32.8	33.4	33.4
30	32.7	33.1	33.4
45	32.8	33.2	33.6
60	32.9	33.3	33.8
90	32.9	33.4	34
120	32.9	33.4	33.9
180	33.4	33.7	33.9
(CORE)	(37.6)	(37.1)	(36.9)
MEAN ± SD	32.9±0.2	33.4±0.2	33.7±0.3

RAW DATA

DOG 3 VENOUS BLOOD TEMPERATURE (°C)

TIME (sec)	CT20	EX45	EX70
0	33.3	32.8	34.1
15	33.5	32.8	34.1
30	33.1	32.7	33.9
45	32.5	32.5	33.9
60	32.3	32.3	33.8
90	32.7	32	33.5
120	33.3	32.1	33.4
180	34.1	33	34.1
(CORE)	(38.7)	(36.9)	(37)
MEAN ± SD	33.1±0.6	32.5±0.4	33.9±0.3

RAW DATA

DOG 4 VENOUS BLOOD TEMPERATURE (°C)

TIME (sec)	CT20	EX45	EX70
0	33.8	33.6	32.5
15	33.9	33.6	32.6
30	33.7	33.5	32.7
45	33.7	33	32.5
60	33.6	32.8	32.2
90	33.3	32.3	31.9
120	33.4	32.3	31.8
180	33.9	33.2	32.8
(CORE)	(36.8)	(37.6)	(38.8)
MEAN ± SD	33.7±0.2	33.0±0.5	32.4±0.4

RAW DATA

DOG 5 VENOUS BLOOD TEMPERATURE (°C)

TIME (sec)	CT20	EX45	EX70
0	33.9	32.6	33.9
15	33.4	32.2	33.4
30	33.1	31.6	33.1
45	33.1	31.4	33.1
60	33.3	31.5	33.3
90	34.3	32.5	34.3
120	34.8	33.5	34.8
180	35.3	34.5	34.3
(CORE)	(37.9)	(38.2)	(37.2)
MEAN ± SD	33.9±0.8	32.5±1.1	33.8±0.6

RAW DATA

DOG 6 VENOUS BLOOD TEMPERATURE (°C)

TIME (sec)	CT20	EX45	EX70
0	33.8	34.9	31.6
15	33.8	34.9	31.6
30	32.7	34.5	31
45	32.3	34.3	30.6
60	32.2	34.2	30.3
90	32.5	34.1	30.2
120	33.4	34.3	30.6
180	34.4	35.1	31.9
(CORE)	(37.4)	(36.8)	(37)
MEAN ± SD	33.1±0.8	34.5±0.4	31.0±0.7

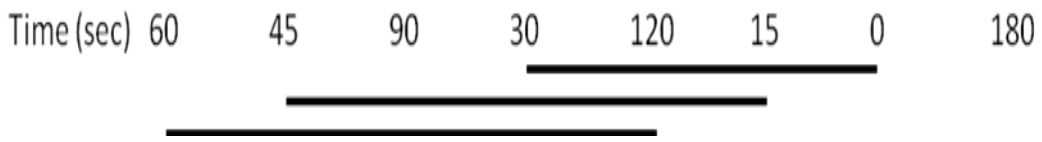

Temperature of blood leaving the muscle was recorded from 0-180 sec during each trial. There were no significant differences between trials (CT20, EX45, and EX70). There were significant differences between times in each trial, yet all varied by less than 1°C. The above lines represent no significant differences between those times.

RAW DATA

BLOOD FLOW ON-KINETICS (tau or MRT in sec)

DOG #	CT20	EX45	EX70
1(6)	22.1	48.3	70.8
2(7)	22.3	46.4	66.0
3(8)	23.0	50.7	75.2
4(9)	24.4	50.5	69.1
5(12)	19.6	38.7	58.4
6(14)	23.9	46.2	67.0
MEAN ± SD	22.6±1.7	46.8±4.4* (p<0.0001)	67.8±5.6*† (p<0.001, p<0.001)

VO_2 ON-KINETICS TIME DELAY (sec)

DOG #	CT20	EX45	EX70
1(6)	7.4	8.2	6.2
2(7)	9.5	9.5	7.9
3(8)	7.8	8.4	9.4
4(9)	6.7	7.8	8.6
5(12)	2.5	6.5	9.7
6(14)	7.0	6.5	8.5
MEAN ± SD	6.8±2.3	7.8±1.2	8.4±1.2

RAW DATA

VO_2 ON-KINETICS tau (sec)

DOG #	CT20	EX45	EX70
1(6)	8.1	14.1	28.5
2(7)	14.4	21.0	25.8
3(8)	13.0	24.3	25.5
4(9)	13.5	21.8	23.5
5(12)	21.3	19.7	21.0
6(14)	8.2	10.3	15.6
MEAN ± SD	13.1±4.9	18.5±5.3* (p=0.04)	23.3±4.5* (p=0.003)

VO_2 ON-KINETICS MRT (sec)

DOG #	CT20	EX45	EX70
1(6)	15.5	22.3	34.7
2(7)	23.9	30.5	33.8
3(8)	20.8	32.6	34.9
4(9)	20.2	29.6	32.1
5(12)	23.8	26.2	30.7
6(14)	15.2	16.8	24.1
MEAN ± SD	19.9±3.8	26.3±5.9* (p=0.003)	31.7±4.1*† (p<0.0001, p=0.01)

CURVE FITS OF $\dot{V}O_2$ ON-RESPONSES

ALL GRAPHS ARE IN UNITS OF TIME (sec) ON THE X-AXIS AND $\dot{V}O_2$ ($mL \cdot kg^{-1} \cdot min^{-1}$) ON THE Y-AXIS

Curves were fit with a monoexponential rise equation of the type:

$$\mathbf{y(t) = y}\boldsymbol{BAS}\mathbf{ + A\,[1 - e^{-(t - TD) / \tau}]}$$

In this equation, y*BAS* indicates the baseline value obtained at rest before contraction onset, A indicates the amplitude between y*BAS* and the steady-state value at the end of the contraction period, TD the time delay and τ the time constant of the function. The half-time ($t_{50\%}$) of the on-kinetics exponential function can be calculated by multiplying τ by 0.693. To facilitate a comparison with the results reported by previous studies, τ and TD were added together to calculate the mean response time (MRT) of the overall response.

Program used: KaleidaGraph 4.0

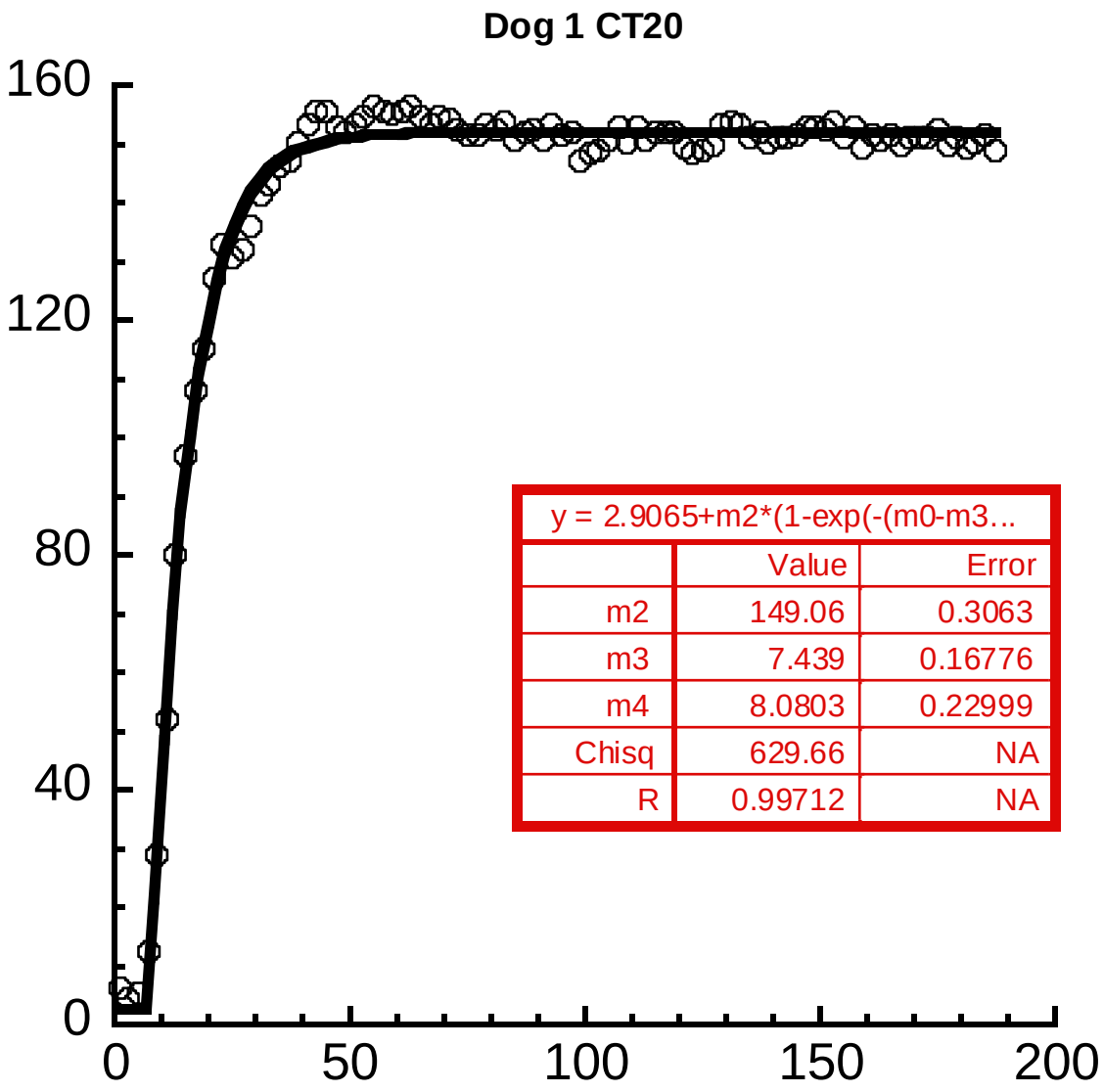
Dog 1 CT20
160
120
80
40
0
0
50
100
150
200
y = 2.9065+m2*(1-exp(-(m0-m3...
Value
Error
m2
149.06
0.3063
m3
7.439
0.16776
m4
8.0803
0.22999
Chisq
629.66
NA
R
0.99712
NA

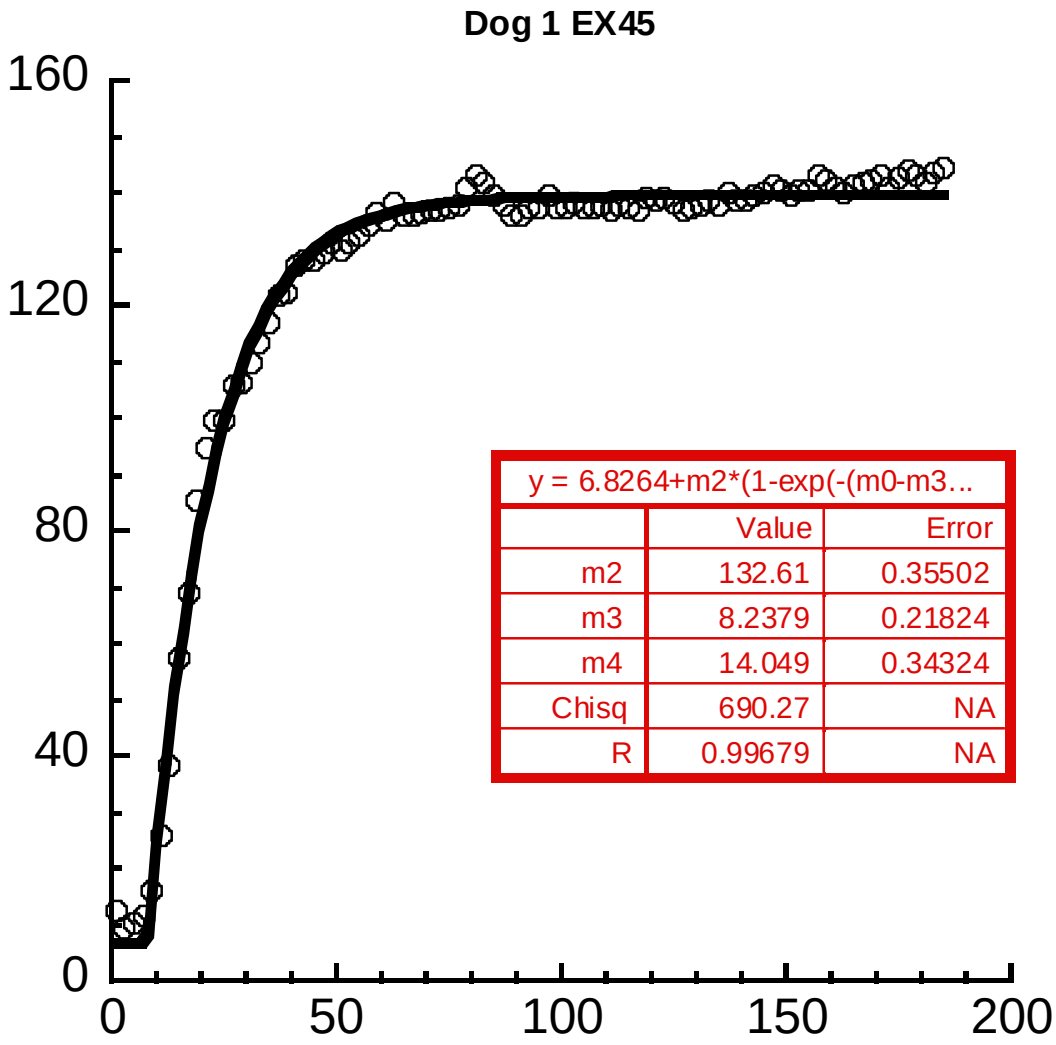
Dog 1 EX45
160
120
80
40
0
0
50
100
150
200
y = 6.8264+m2*(1-exp(-(m0-m3...
Value
Error
m2
132.61
0.35502
m3
8.2379
0.21824
m4
14.049
0.34324
Chisq
690.27
NA
R
0.99679
NA

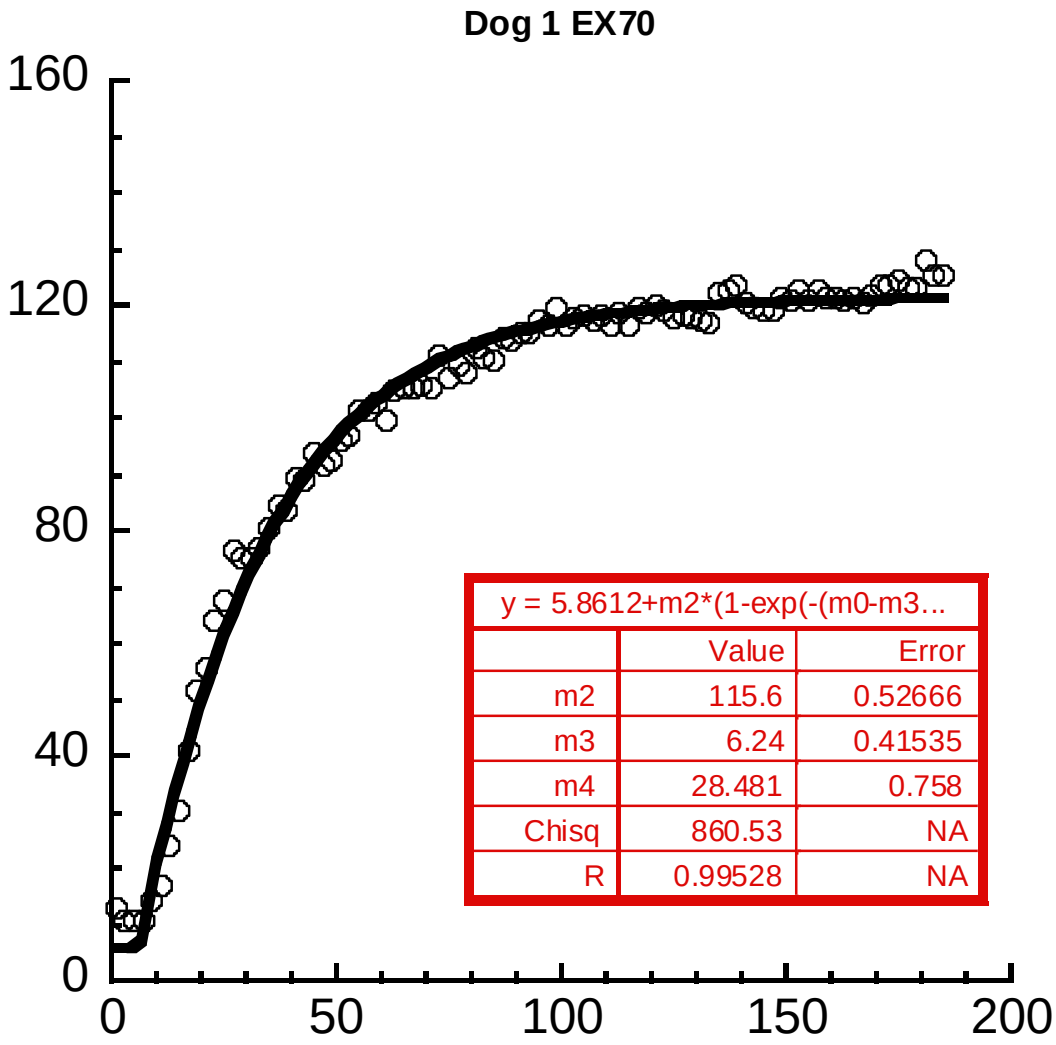
Dog 1 EX70
160
120
80
40
0
0
50
100
150
200
y = 5.8612+m2*(1-exp(-(m0-m3...
Value
Error
m2
115.6
0.52666
m3
6.24
0.41535
m4
28.481
0.758
Chisq
860.53
NA
R
0.99528
NA

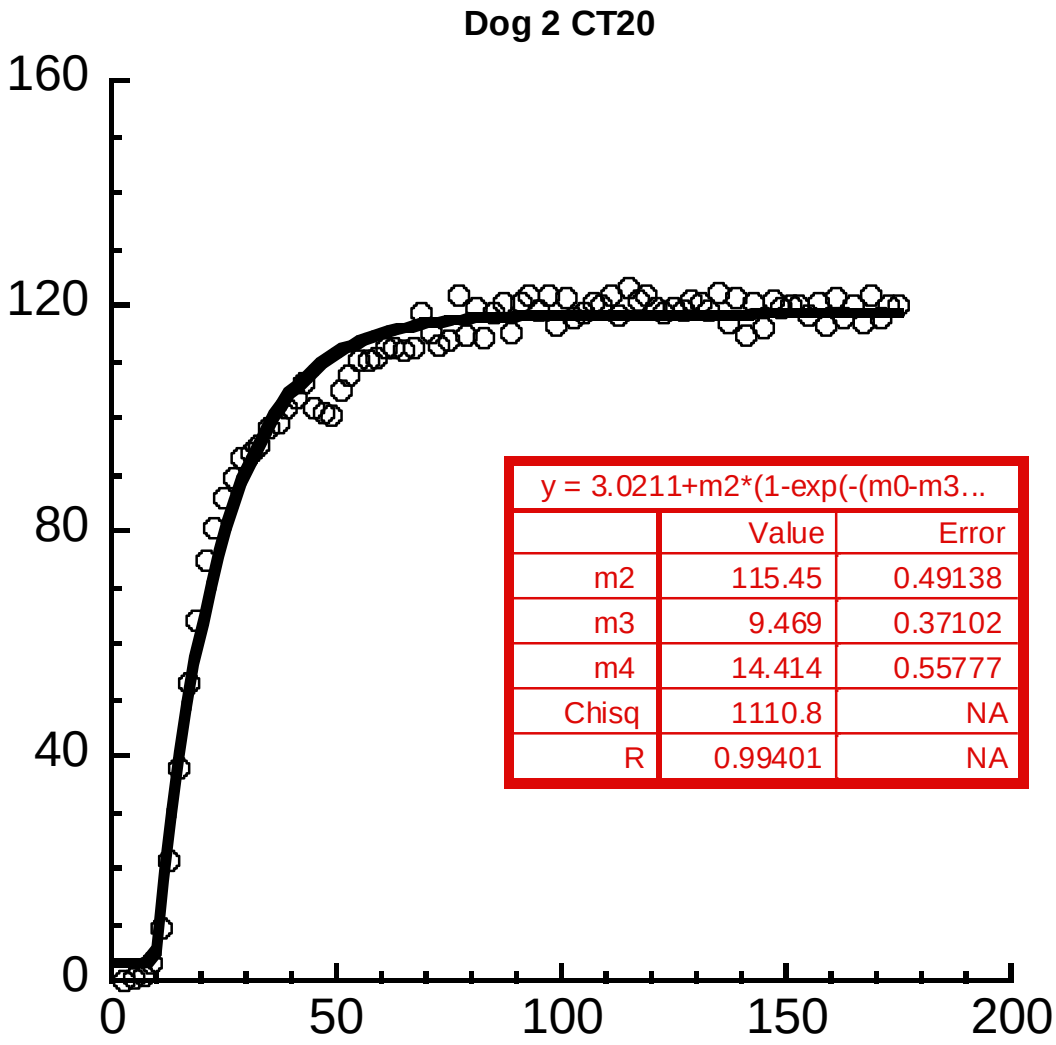
Dog 2 CT20
160
120
80
40
0
0
50
100
150
200
y = 3.0211+m2*(1-exp(-(m0-m3...
Value
Error
m2
115.45
0.49138
m3
9.469
0.37102
m4
14.414
0.55777
Chisq
1110.8
NA
R
0.99401
NA

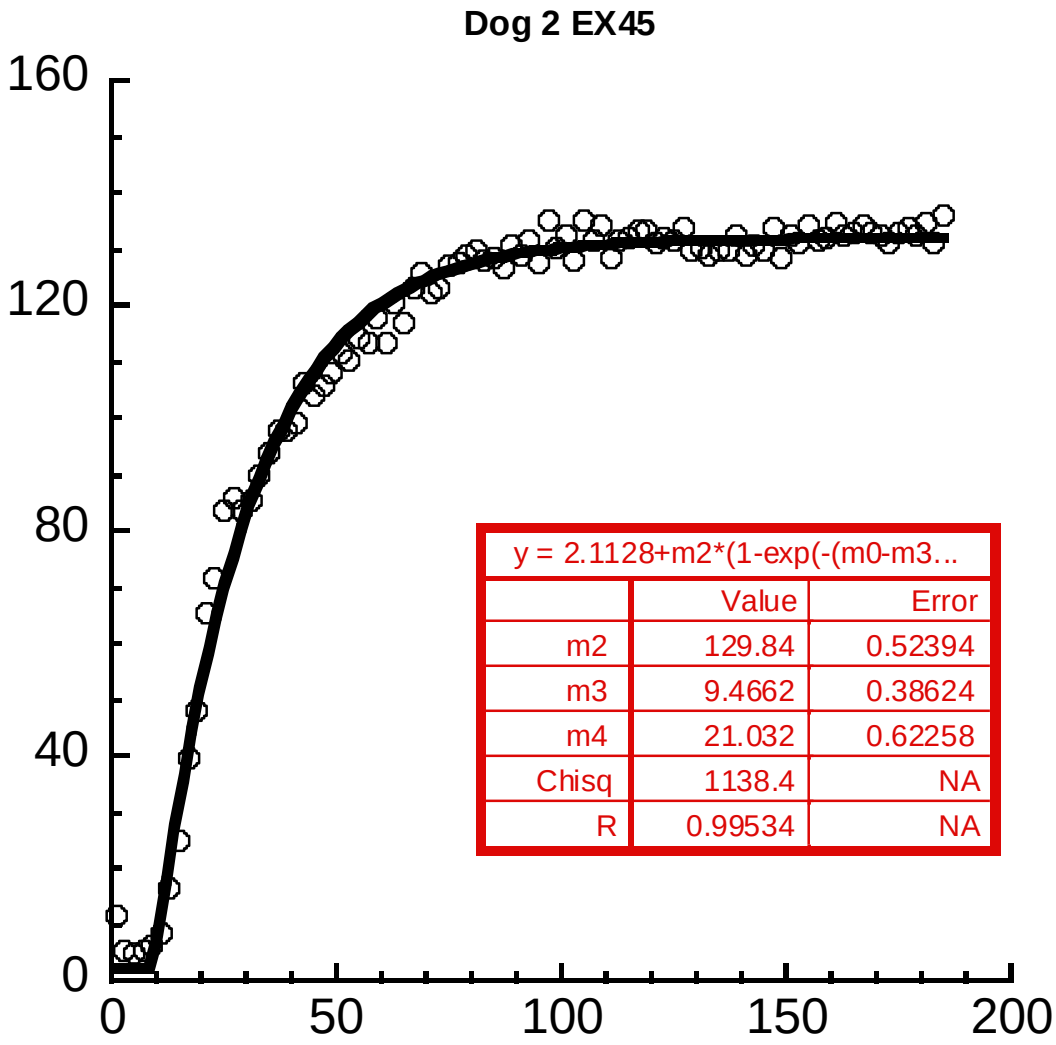
Dog 2 EX45
160
120
80
40
0
0
50
100
150
200
y = 2.1128+m2*(1-exp(-(m0-m3...
Value
Error
m2
129.84
0.52394
m3
9.4662
0.38624
m4
21.032
0.62258
Chisq
1138.4
NA
R
0.99534
NA

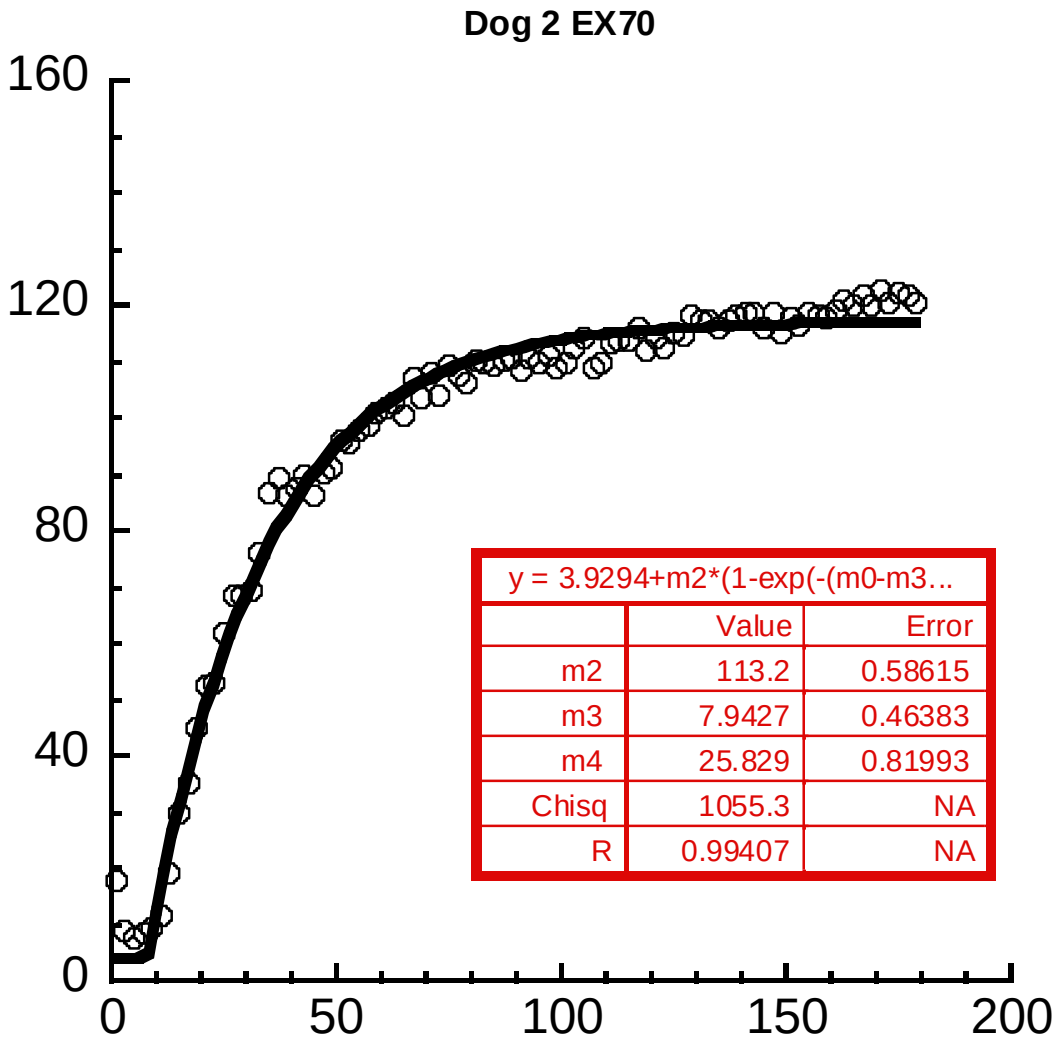
Dog 2 EX70
160
120
80
40
0
0
50
100
150
200
y = 3.9294+m2*(1-exp(-(m0-m3...
Value
Error
m2
113.2
0.58615
m3
7.9427
0.46383
m4
25.829
0.81993
Chisq
1055.3
NA
R
0.99407
NA

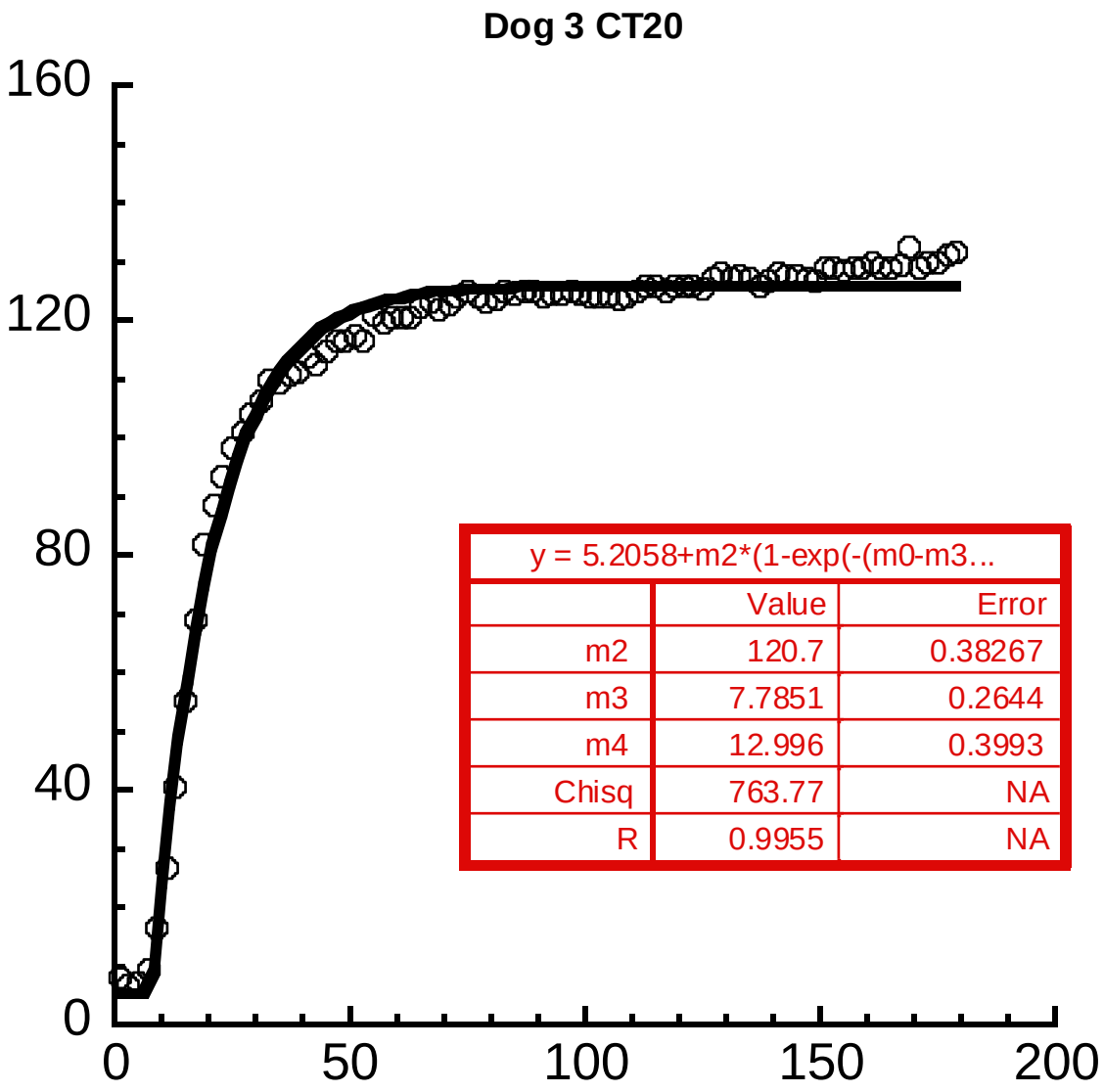
Dog 3 CT20
160
120
80
40
0
0
50
100
150
200
y = 5.2058+m2*(1-exp(-(m0-m3...
Value
Error
m2
120.7
0.38267
m3
7.7851
0.2644
m4
12.996
0.3993
Chisq
763.77
NA
R
0.9955
NA

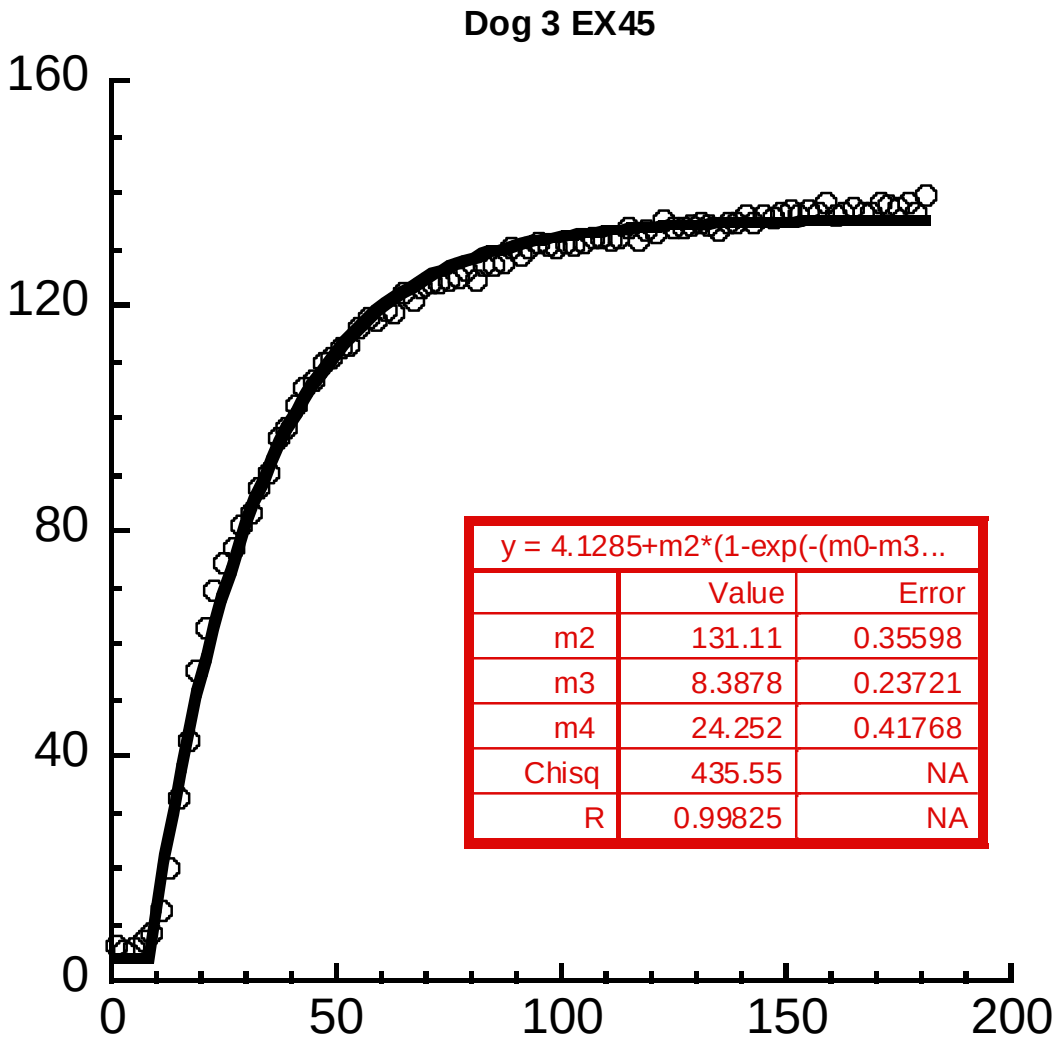
Dog 3 EX45
160
120
80
40
0
0
50
100
150
200
y = 4.1285+m2*(1-exp(-(m0-m3...
Value
Error
m2
131.11
0.35598
m3
8.3878
0.23721
m4
24.252
0.41768
Chisq
435.55
NA
R
0.99825
NA

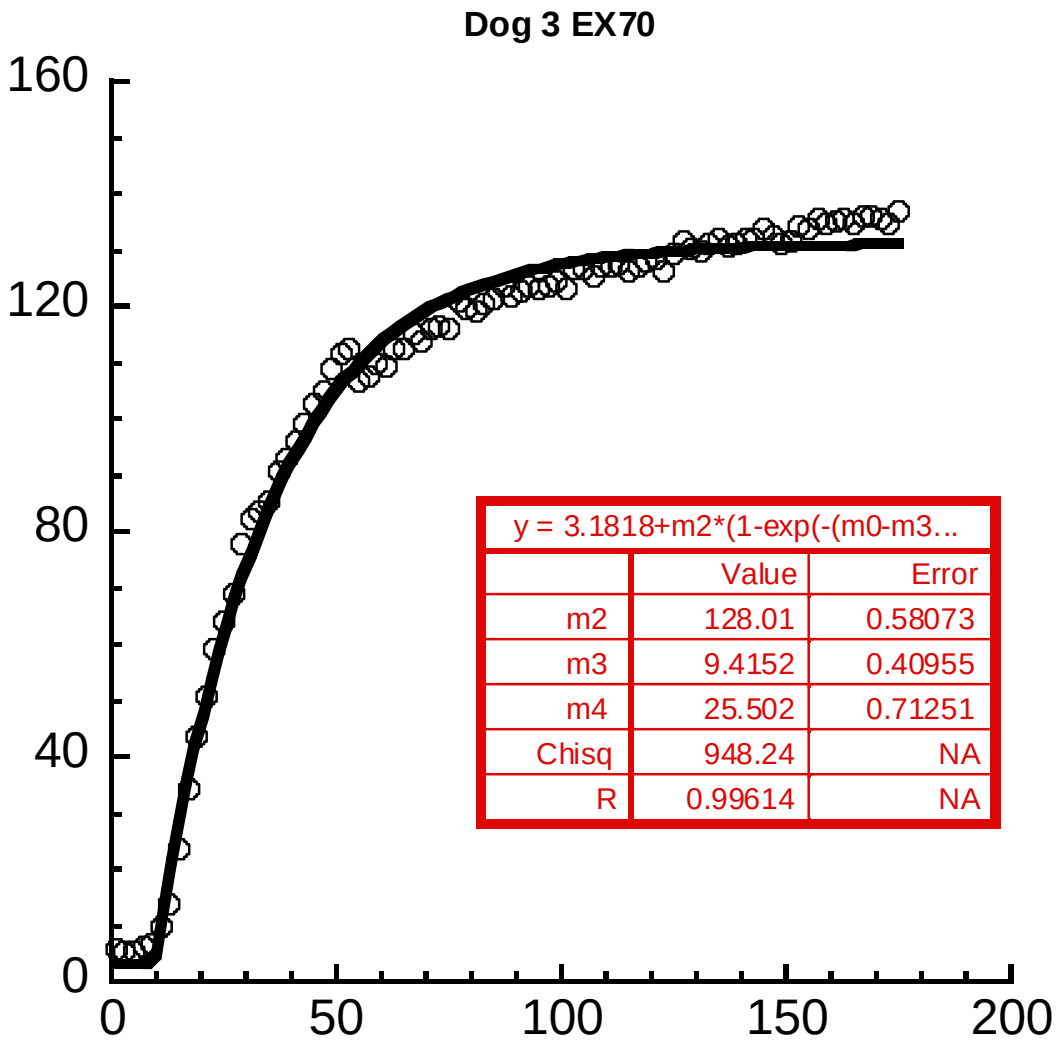
Dog 3 EX70
160
120
80
40
0
0
50
100
150
200
y = 3.1818+m2*(1-exp(-(m0-m3...
Value
Error
m2
128.01
0.58073
m3
9.4152
0.40955
m4
25.502
0.71251
Chisq
948.24
NA
R
0.99614
NA

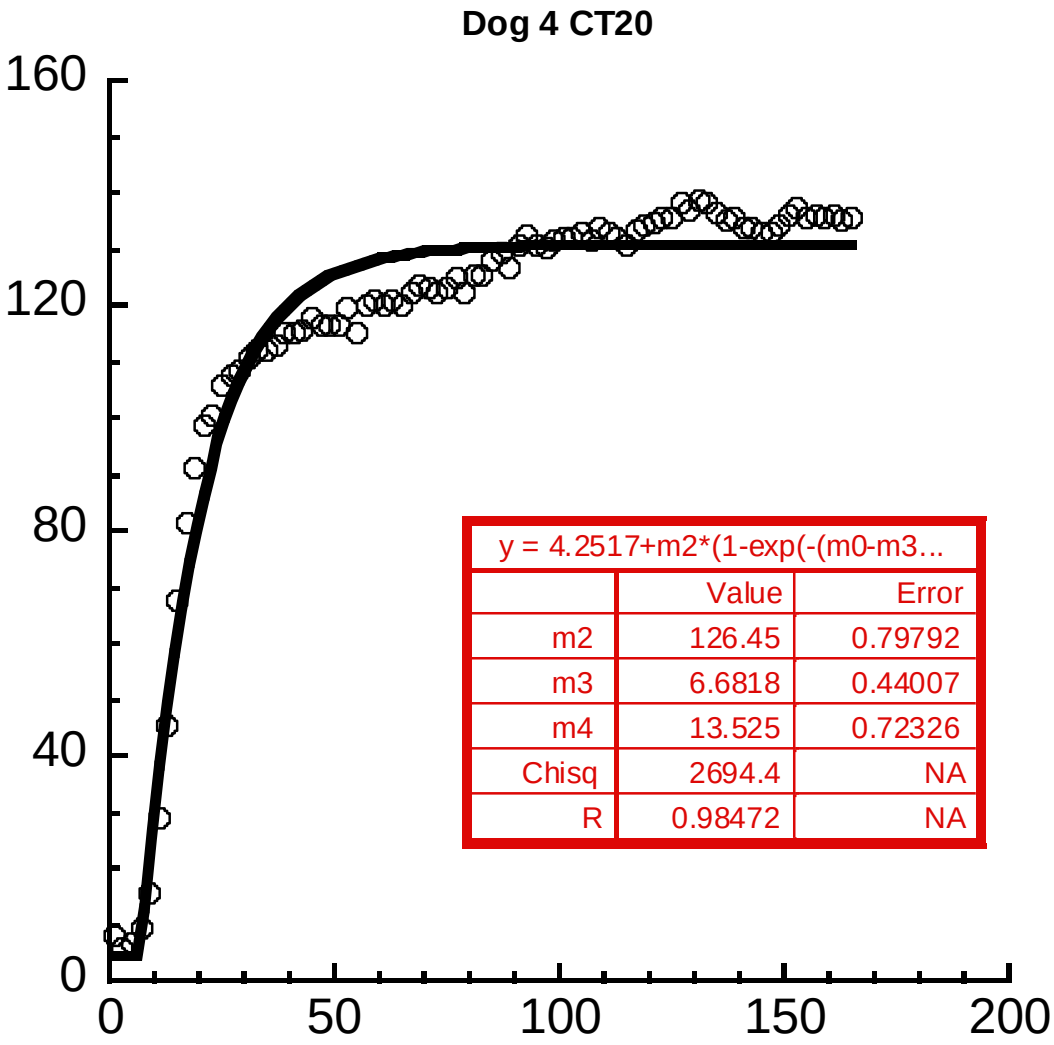
Dog 4 CT20
160
120
80
40
0
0
50
100
150
200
y = 4.2517+m2*(1-exp(-(m0-m3...
Value
Error
m2
126.45
0.79792
m3
6.6818
0.44007
m4
13.525
0.72326
Chisq
2694.4
NA
R
0.98472
NA

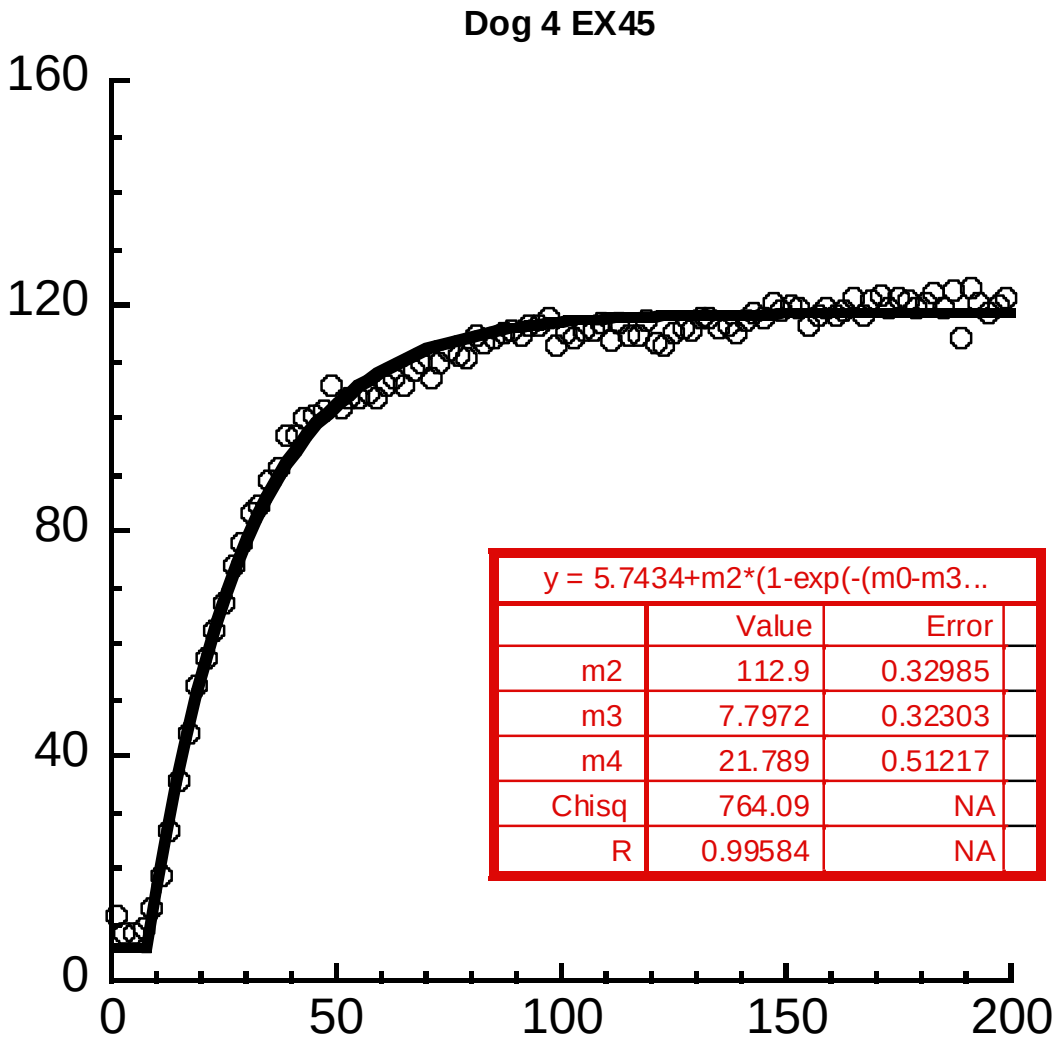
Dog 4 EX45
160
120
80
40
0
0
50
100
150
200
y = 5.7434+m2*(1-exp(-(m0-m3...
Value
Error
m2
112.9
0.32985
m3
7.7972
0.32303
m4
21.789
0.51217
Chisq
764.09
NA
R
0.99584
NA

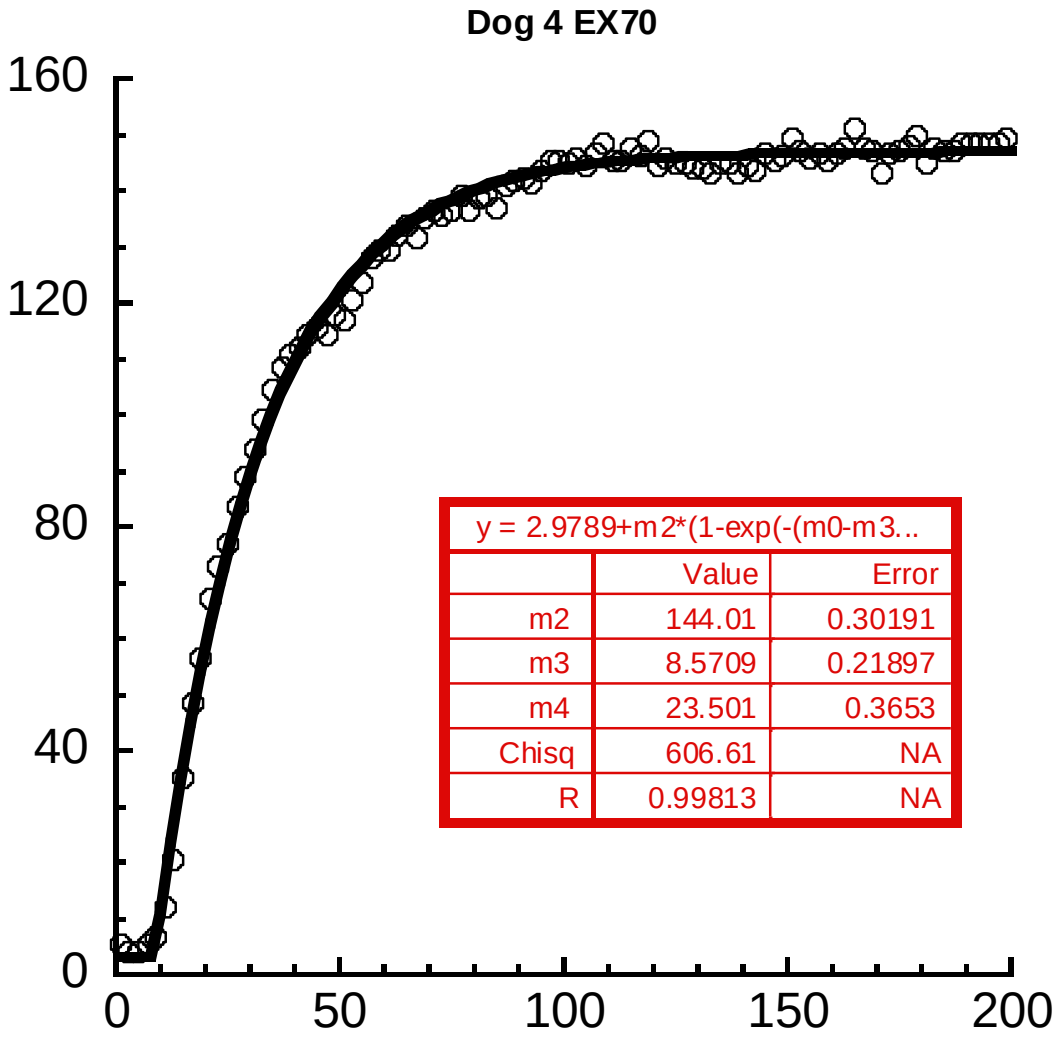
Dog 4 EX70
160
120
80
40
0
0
50
100
150
200
y = 2.9789+m2*(1-exp(-(m0-m3...
Value
Error
m2
144.01
0.30191
m3
8.5709
0.21897
m4
23.501
0.3653
Chisq
606.61
NA
R
0.99813
NA

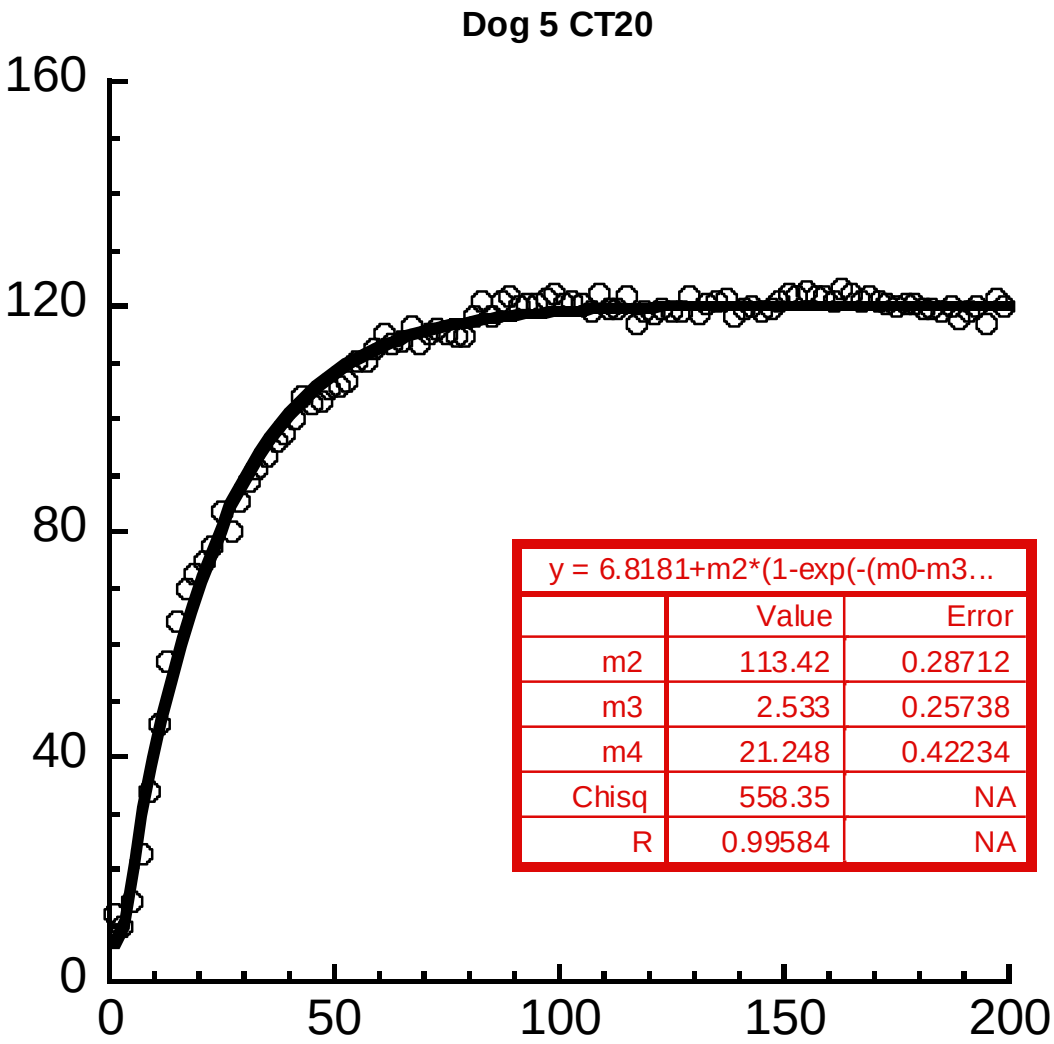
Dog 5 CT20
160
120
80
40
0
0
50
100
150
200
y = 6.8181+m2*(1-exp(-(m0-m3...
Value
Error
m2
113.42
0.28712
m3
2.533
0.25738
m4
21.248
0.42234
Chisq
558.35
NA
R
0.99584
NA

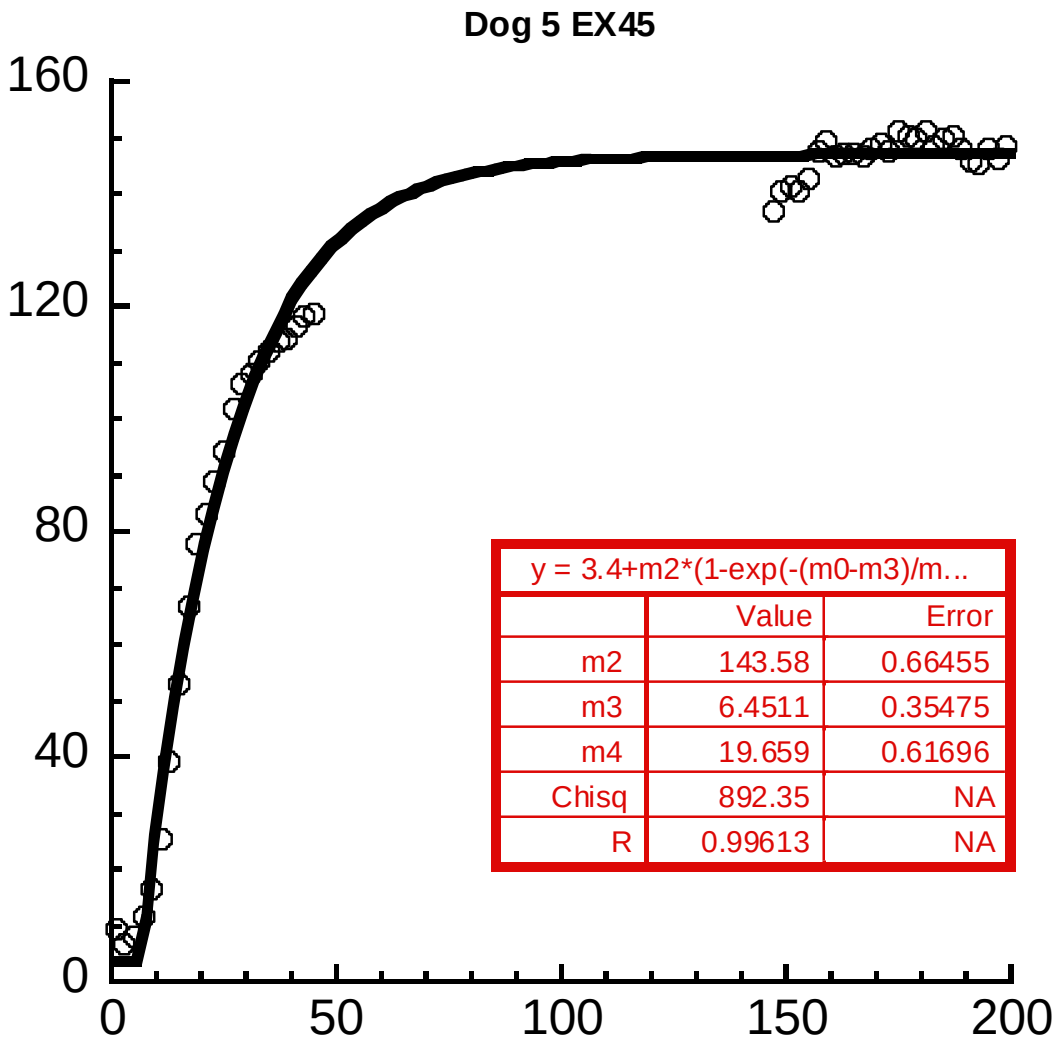
Dog 5 EX45
160
120
80
40
0
0
50
100
150
200
y = 3.4+m2*(1-exp(-(m0-m3)/m...
Value
Error
m2
143.58
0.66455
m3
6.4511
0.35475
m4
19.659
0.61696
Chisq
892.35
NA
R
0.99613
NA

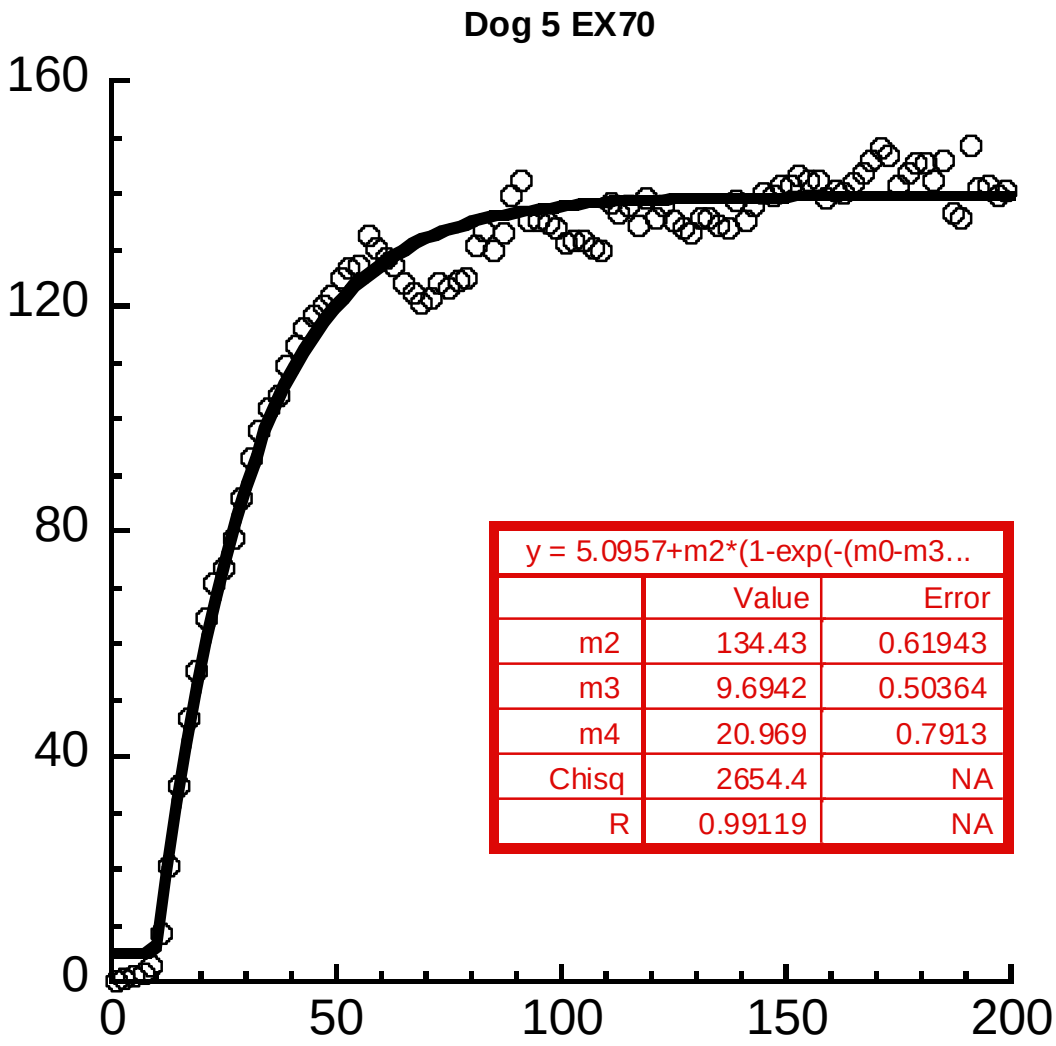
Dog 5 EX70
160
120
80
40
0
0
50
100
150
200
y = 5.0957+m2*(1-exp(-(m0-m3...
Value
Error
m2
134.43
0.61943
m3
9.6942
0.50364
m4
20.969
0.7913
Chisq
2654.4
NA
R
0.99119
NA

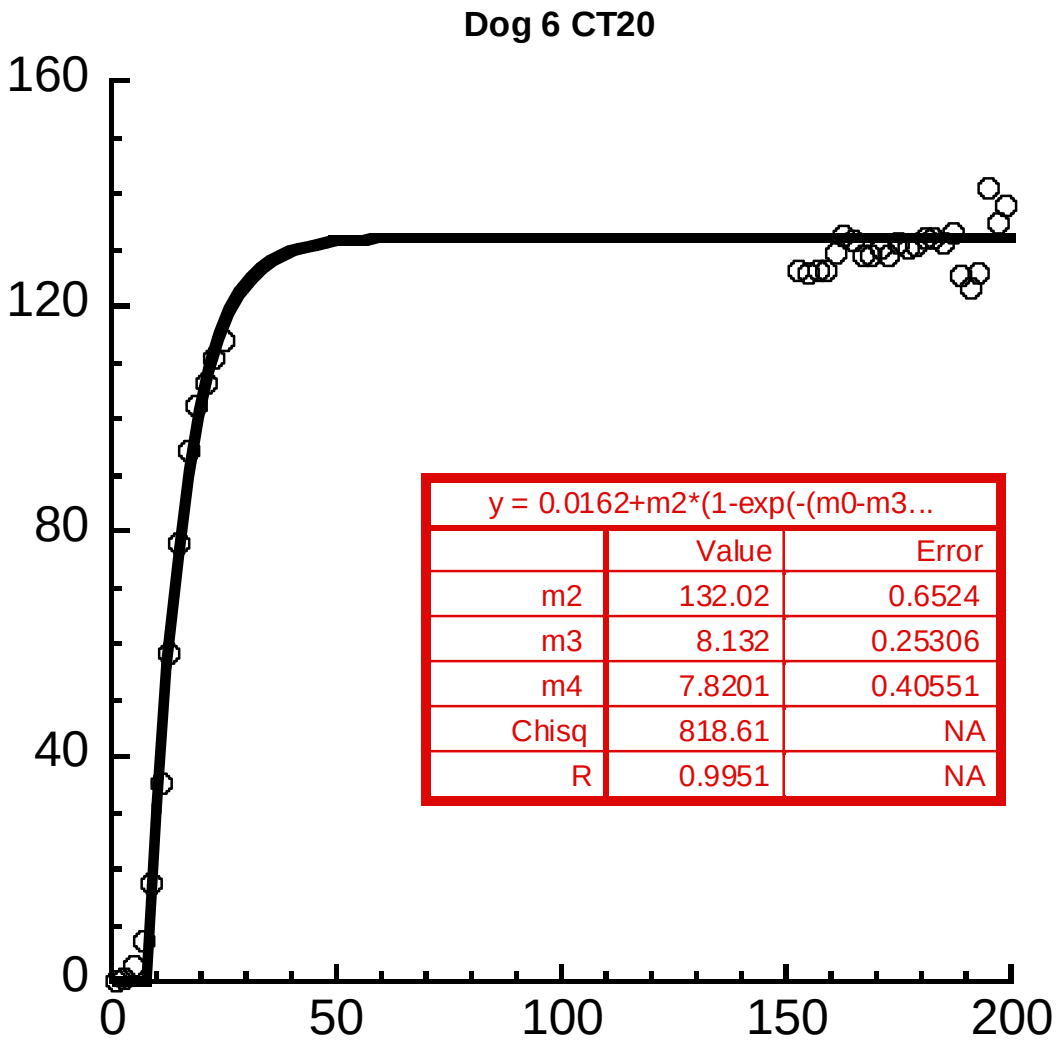
Dog 6 CT20
160
120
80
40
0
0
50
100
150
200
y = 0.0162+m2*(1-exp(-(m0-m3...
Value
Error
m2
132.02
0.6524
m3
8.132
0.25306
m4
7.8201
0.40551
Chisq
818.61
NA
R
0.9951
NA

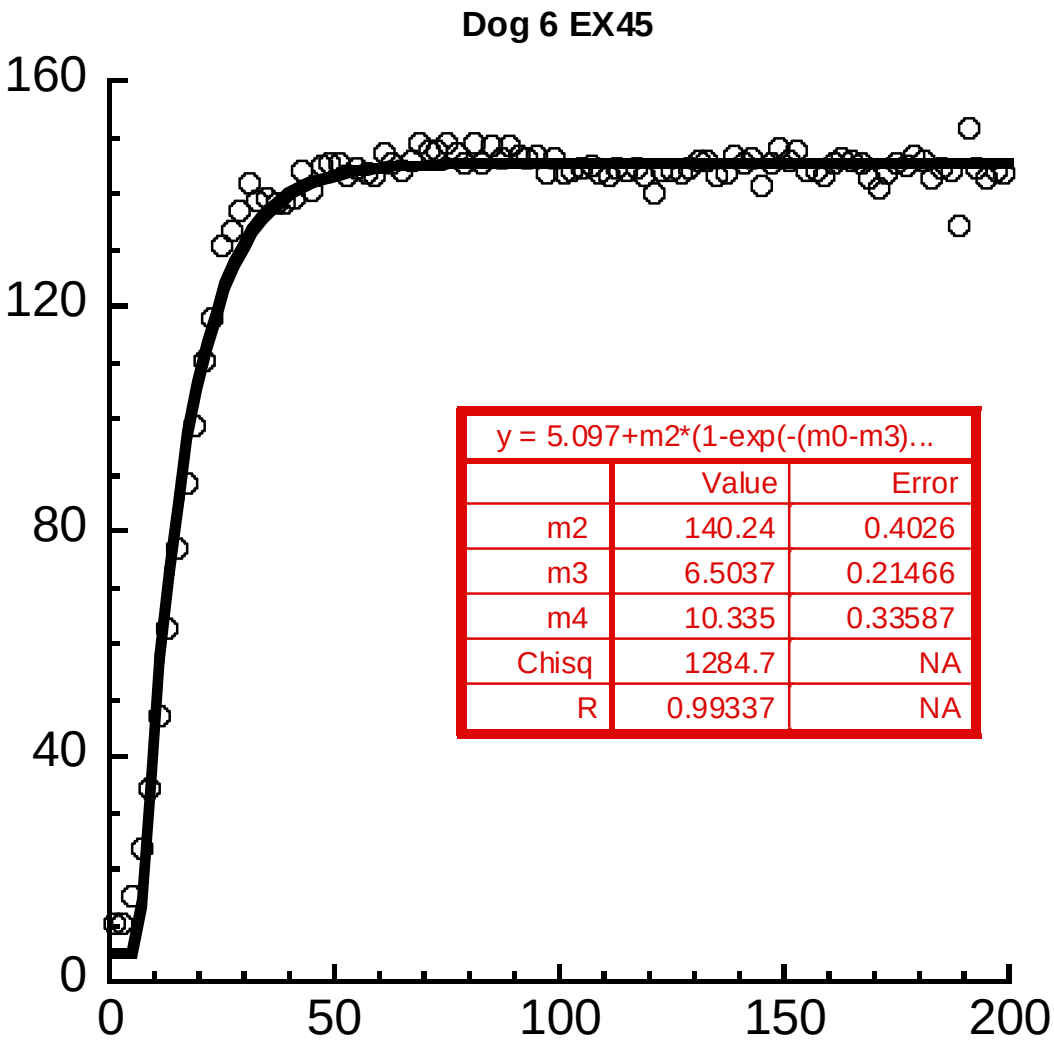
Dog 6 EX45
160
120
80
40
0
0
50
100
150
200
y = 5.097+m2*(1-exp(-(m0-m3)...
Value
Error
m2
140.24
0.4026
m3
6.5037
0.21466
m4
10.335
0.33587
Chisq
1284.7
NA
R
0.99337
NA

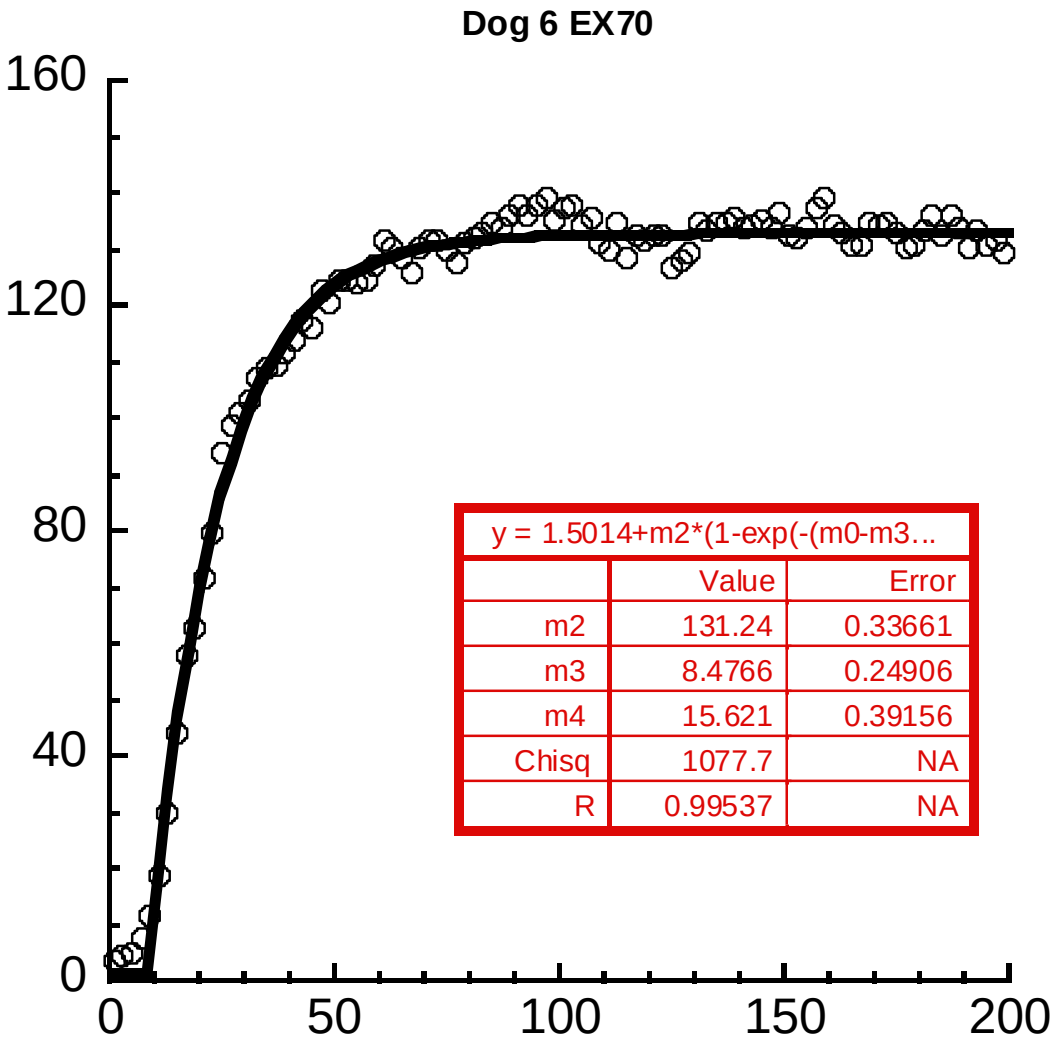
Dog 6 EX70
160
120
80
40
0
0
50
100
150
200
y = 1.5014+m2*(1-exp(-(m0-m3...
Value
Error
m2
131.24
0.33661
m3
8.4766
0.24906
m4
15.621
0.39156
Chisq
1077.7
NA
R
0.99537
NA

NIRS ON-RESPONSES

ALL GRAPHS ARE IN UNITS OF TIME (sec) ON THE X-AXIS AND CONCENTRATION (relative μM) ON THE Y-AXIS

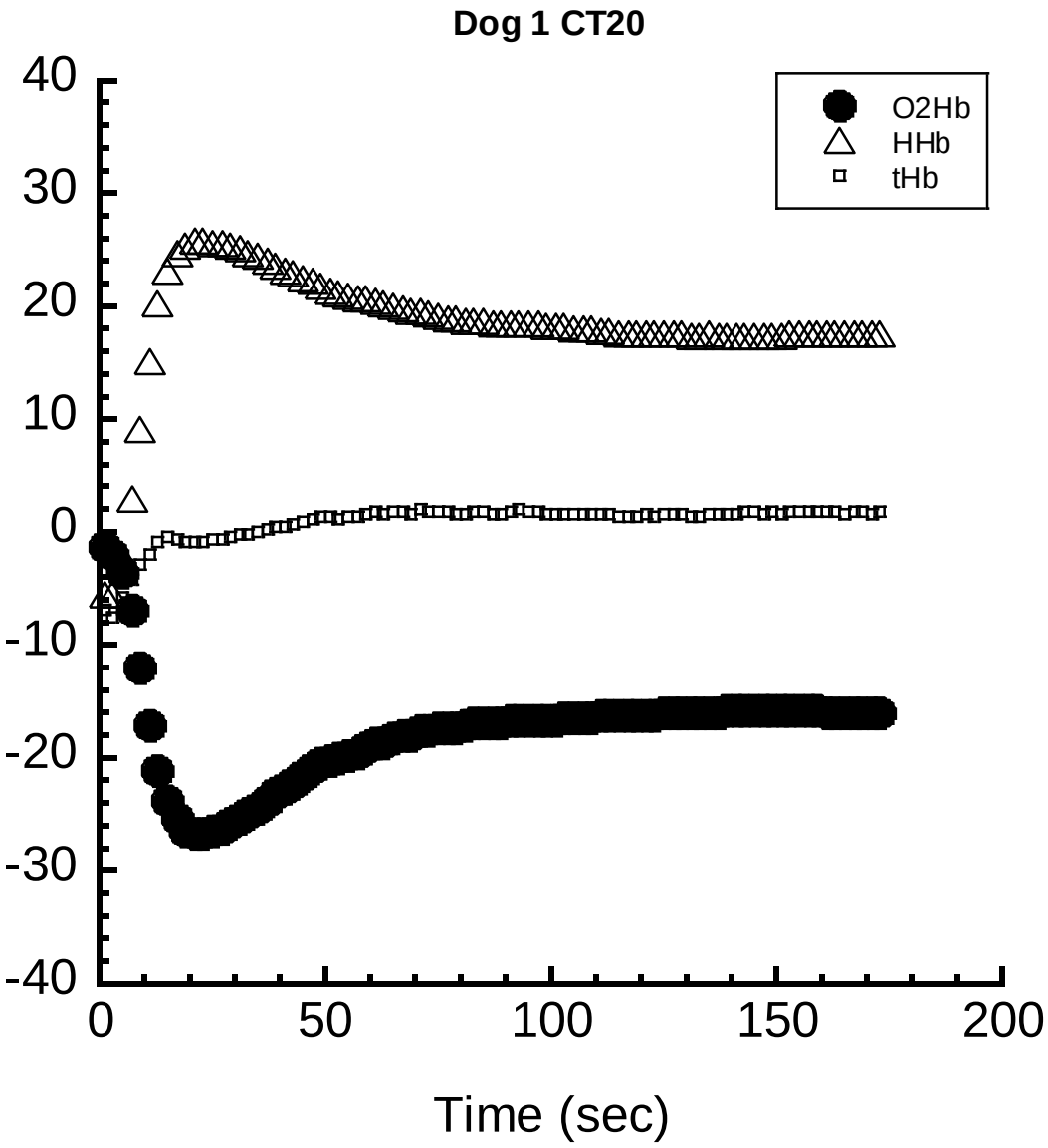
Dog 1 CT20
O2Hb
HHb
tHb
40
30
20
10
0
-10
-20
-30
-40
0
50
100
150
200
Time (sec)

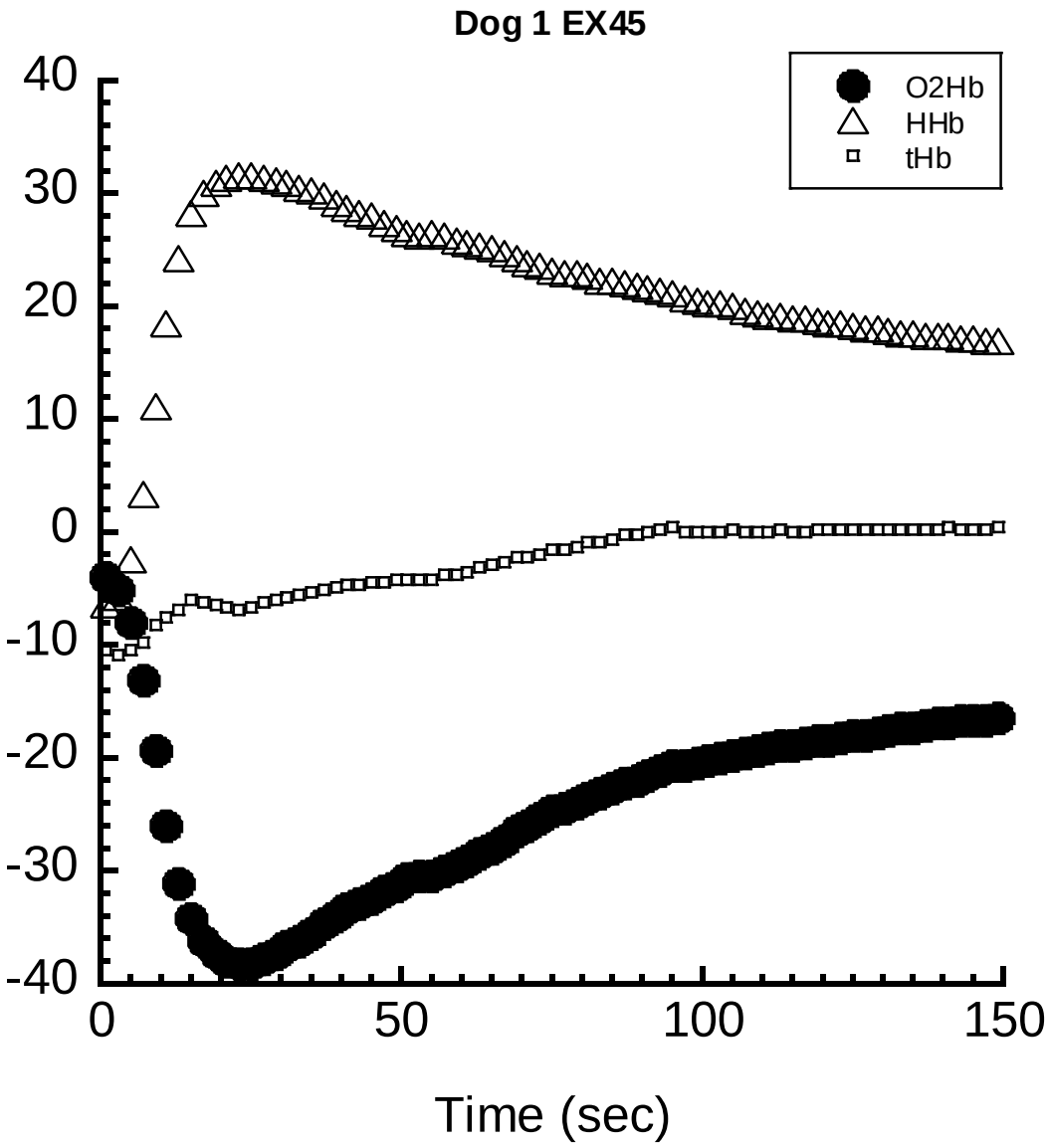
Dog 1 EX45
O2Hb
HHb
tHb
40
30
20
10
0
-10
-20
-30
-40
0
50
100
150
Time (sec)

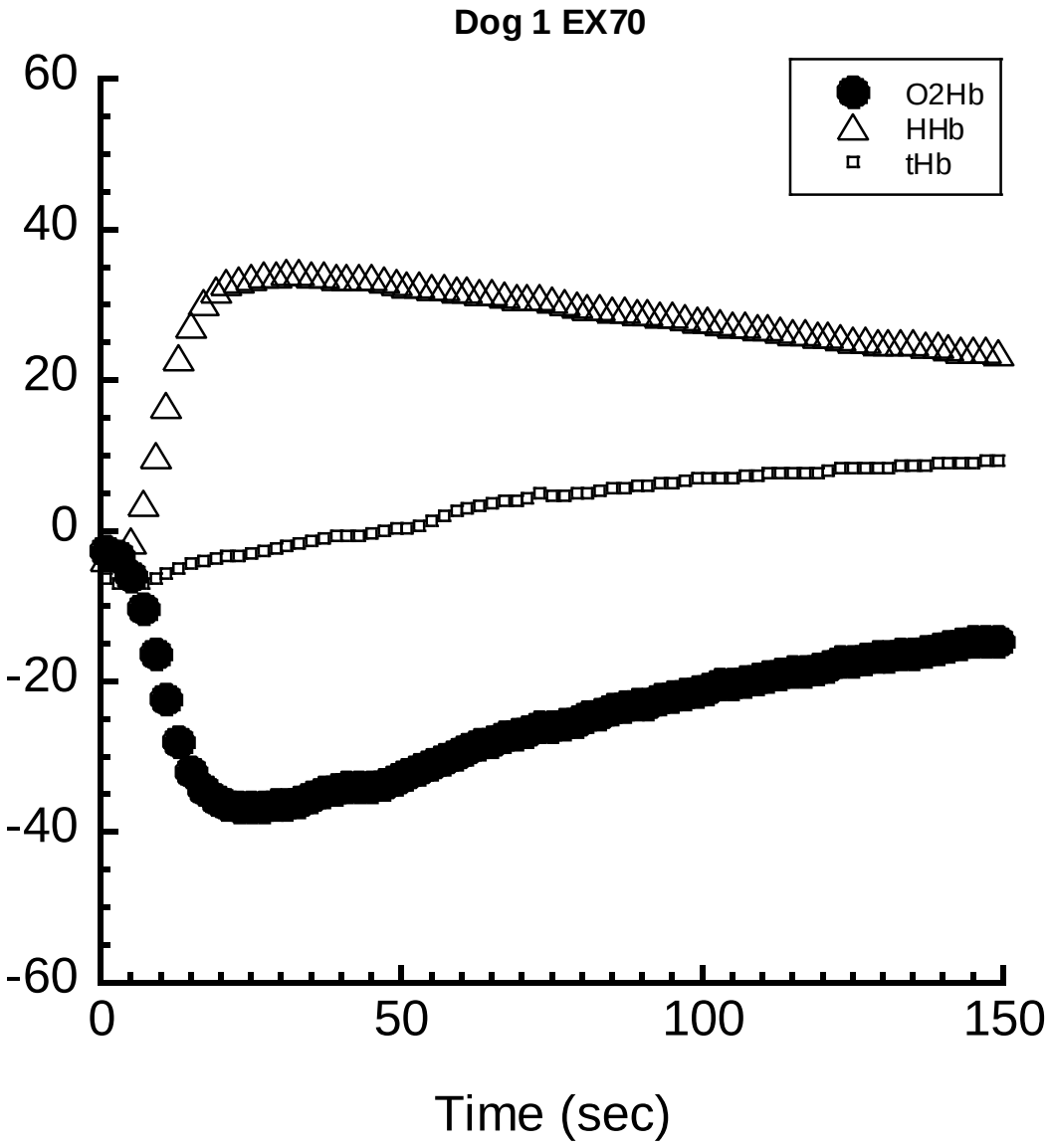
Dog 1 EX70
O2Hb
HHb
tHb
60
40
20
0
-20
-40
-60
0
50
100
150
Time (sec)

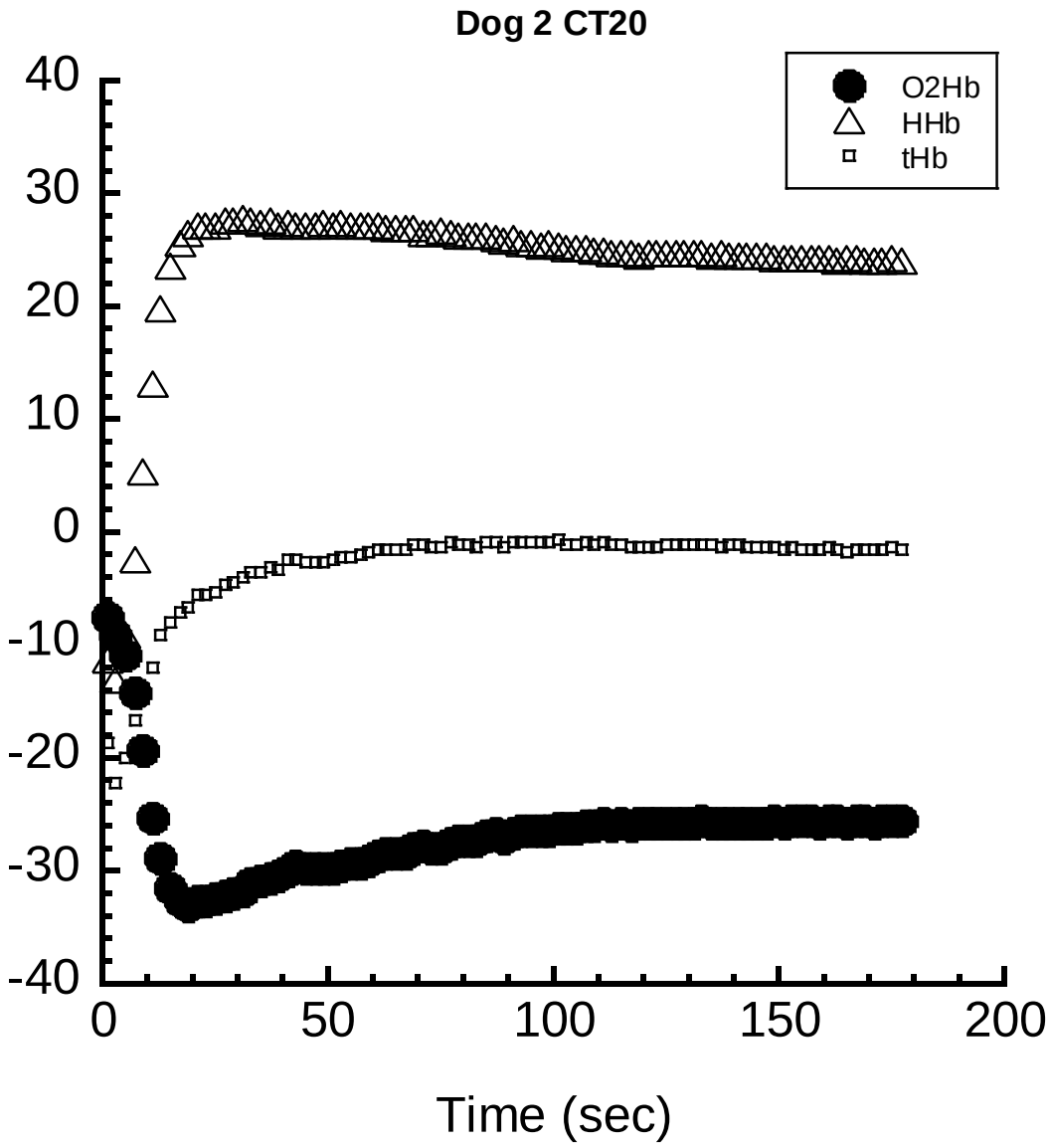
Dog 2 CT20
O2Hb
HHb
tHb
40
30
20
10
0
-10
-20
-30
-40
0
50
100
150
200
Time (sec)

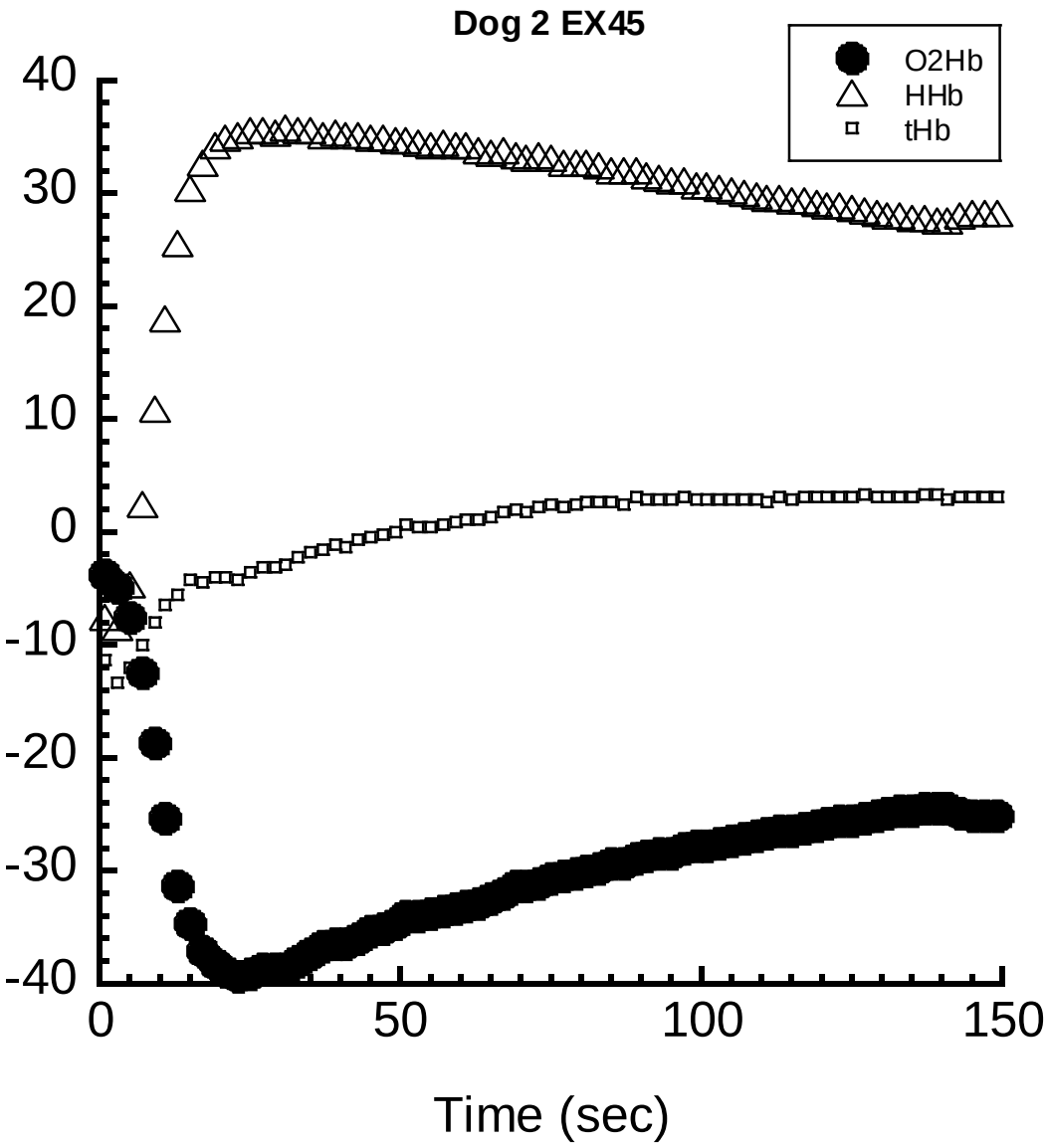
Dog 2 EX45
O2Hb
HHb
tHb
40
30
20
10
0
-10
-20
-30
-40
0
50
100
150
Time (sec)

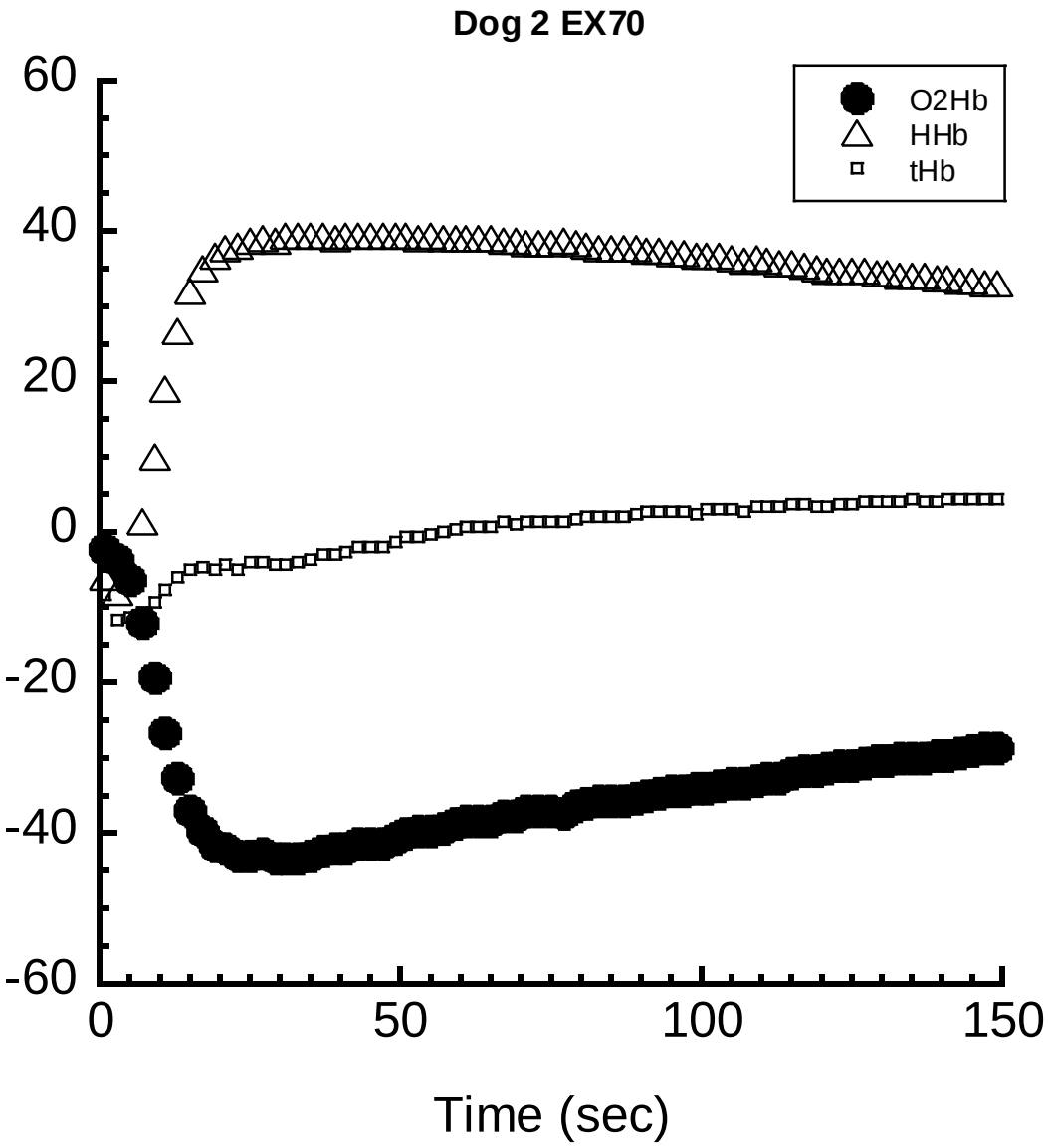
Dog 2 EX70
O2Hb
HHb
tHb
60
40
20
0
-20
-40
-60
0
50
100
150
Time (sec)

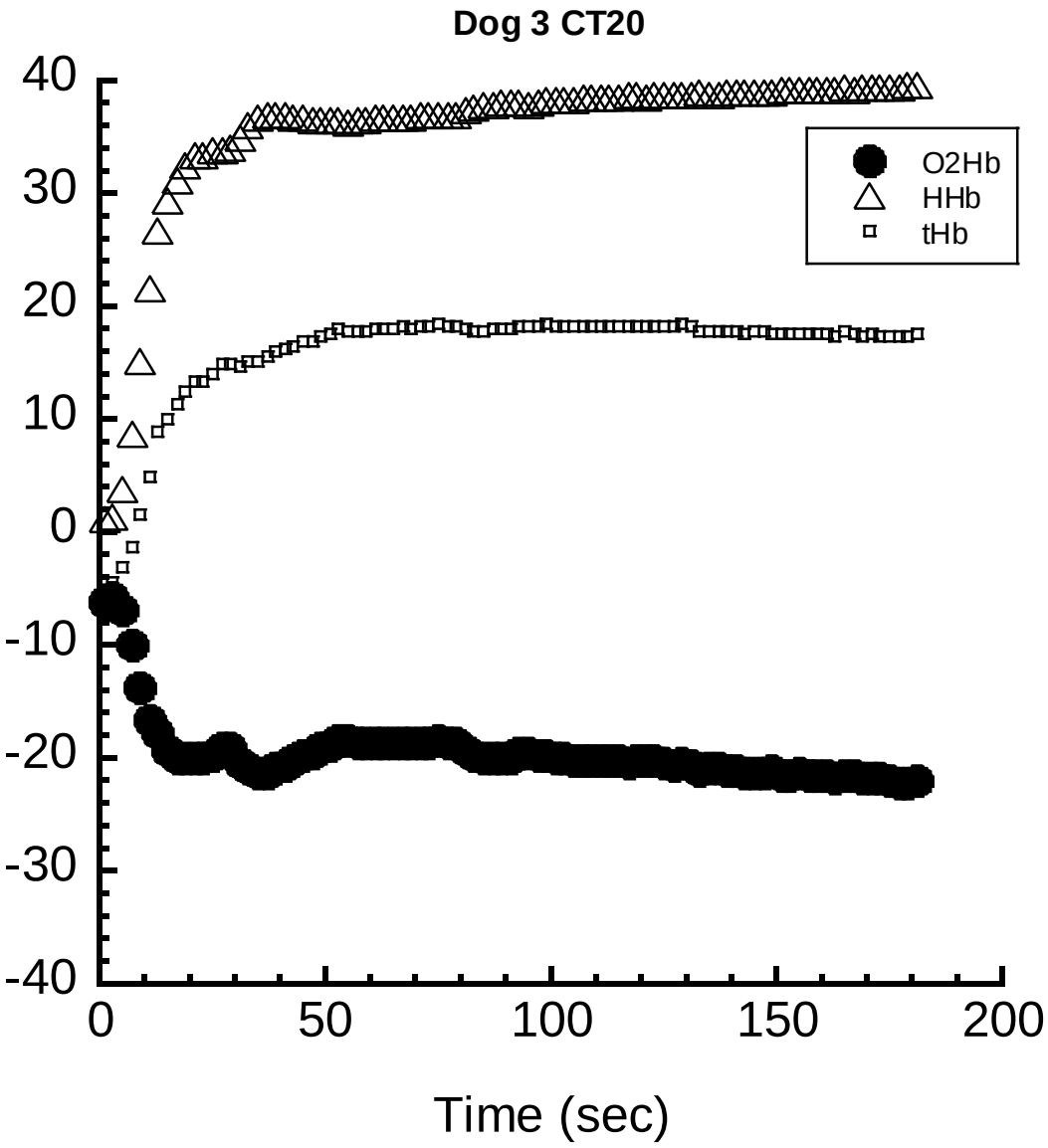
Dog 3 CT20
40
30
20
10
0
-10
-20
-30
-40
0
50
100
150
200
Time (sec)
O2Hb
HHb
tHb

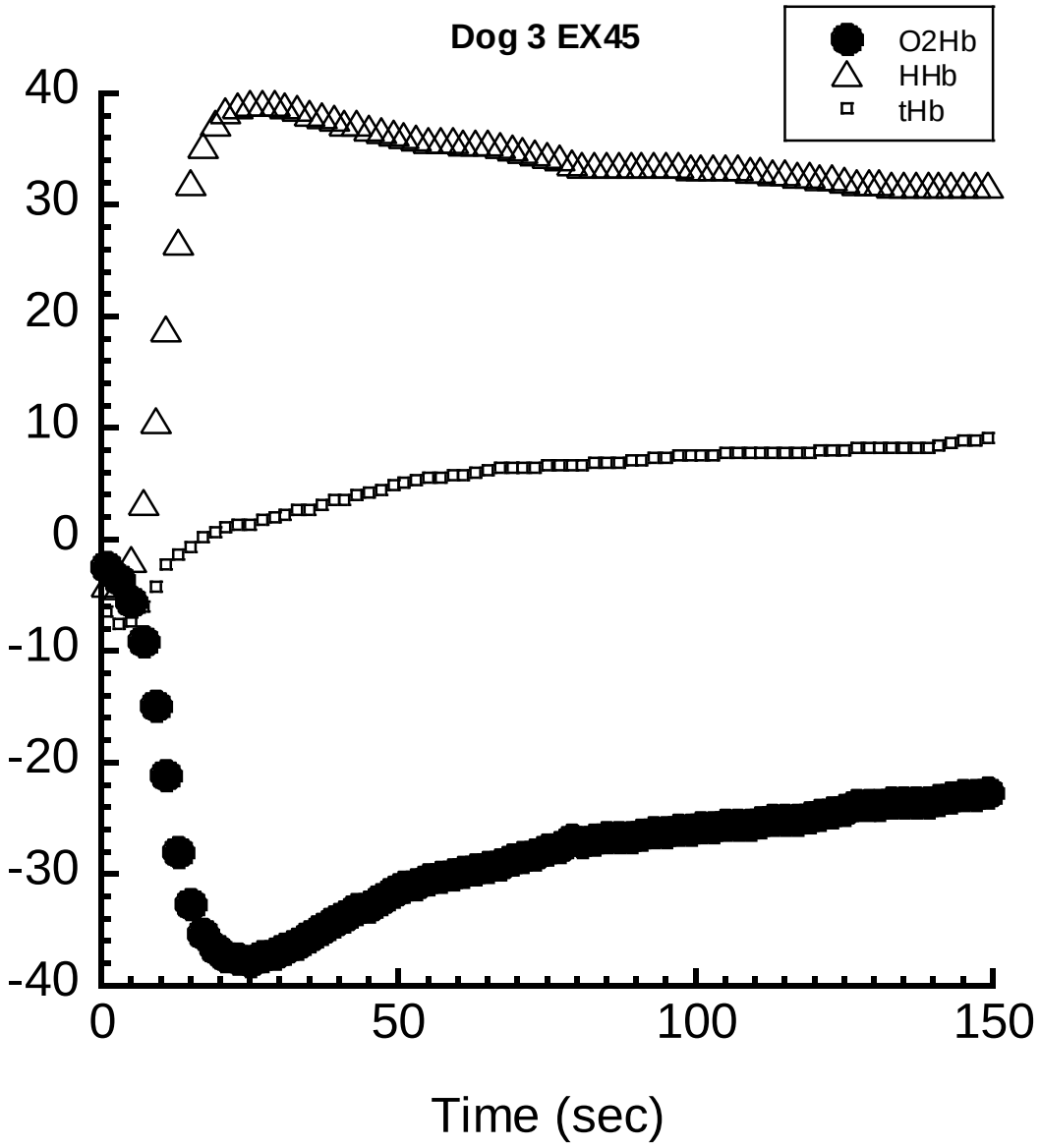
Dog 3 EX45
O2Hb
HHb
tHb
40
30
20
10
0
-10
-20
-30
-40
0
50
100
150
Time (sec)

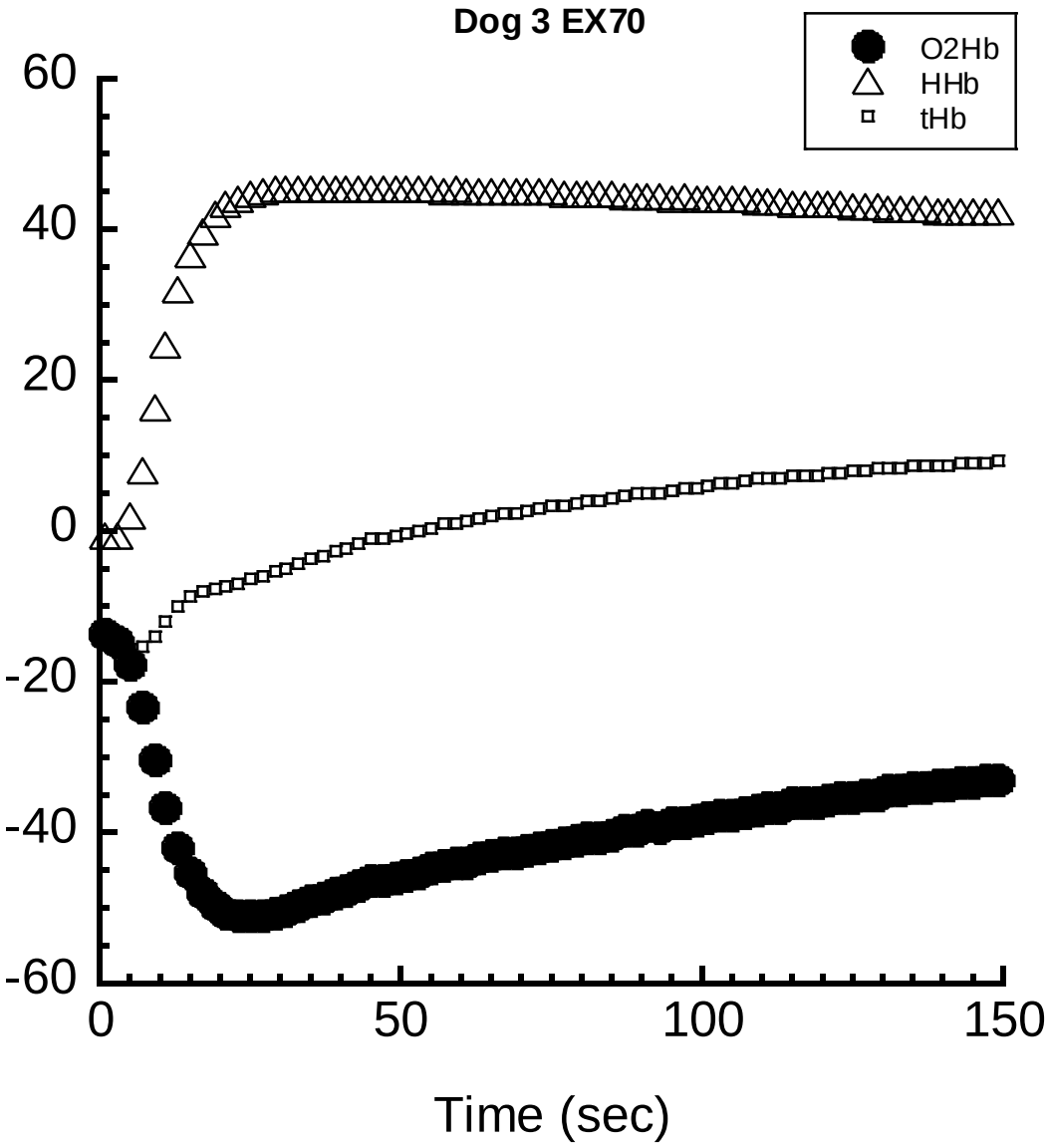
Dog 3 EX70
O2Hb
HHb
tHb
60
40
20
0
-20
-40
-60
0
50
100
150
Time (sec)

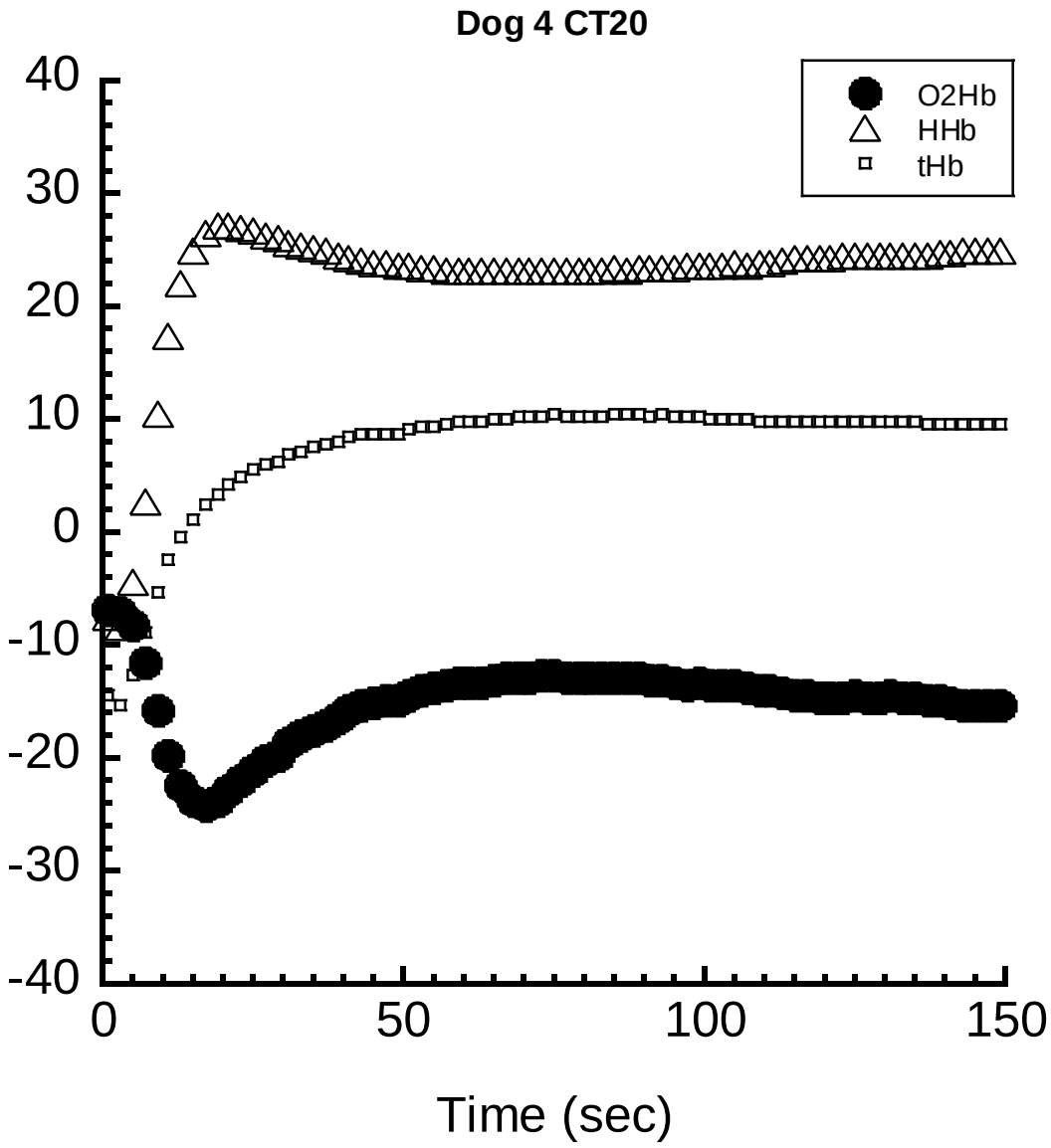
Dog 4 CT20
O2Hb
HHb
tHb
40
30
20
10
0
-10
-20
-30
-40
0
50
100
150
Time (sec)

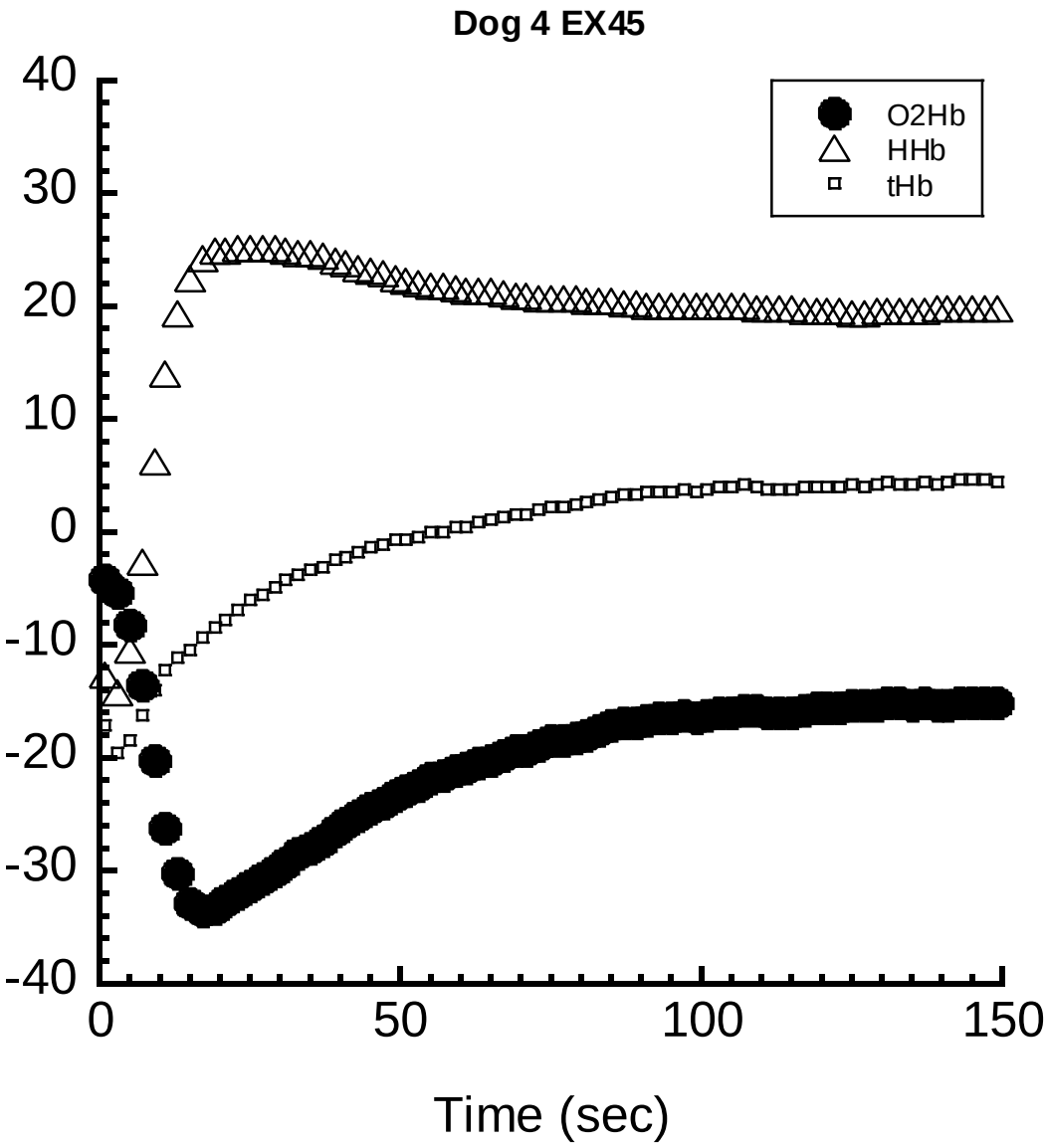
Dog 4 EX45
O2Hb
HHb
tHb
40
30
20
10
0
-10
-20
-30
-40
0
50
100
150
Time (sec)

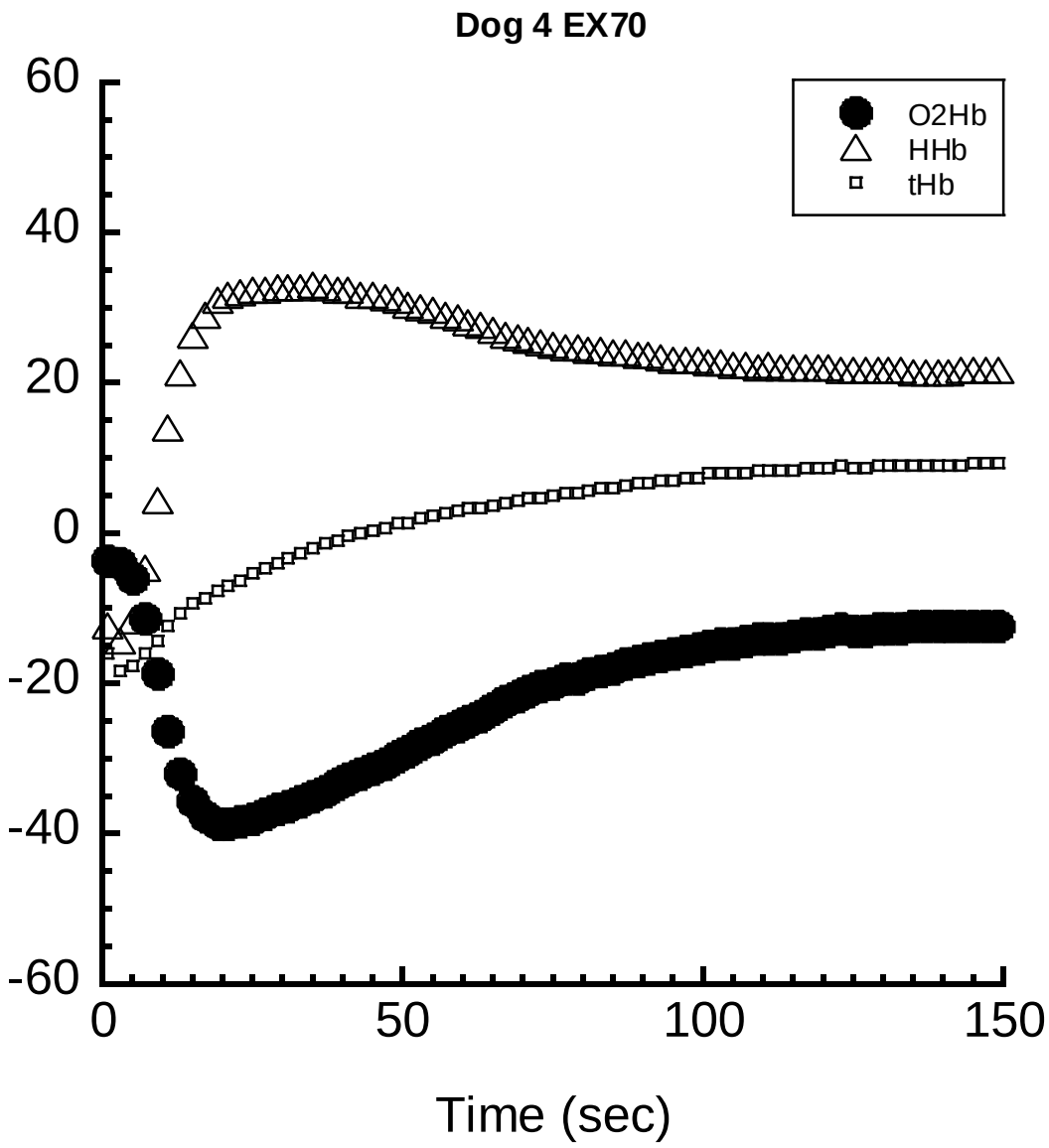
Dog 4 EX70
O2Hb
HHb
tHb
60
40
20
0
-20
-40
-60
0
50
100
150
Time (sec)

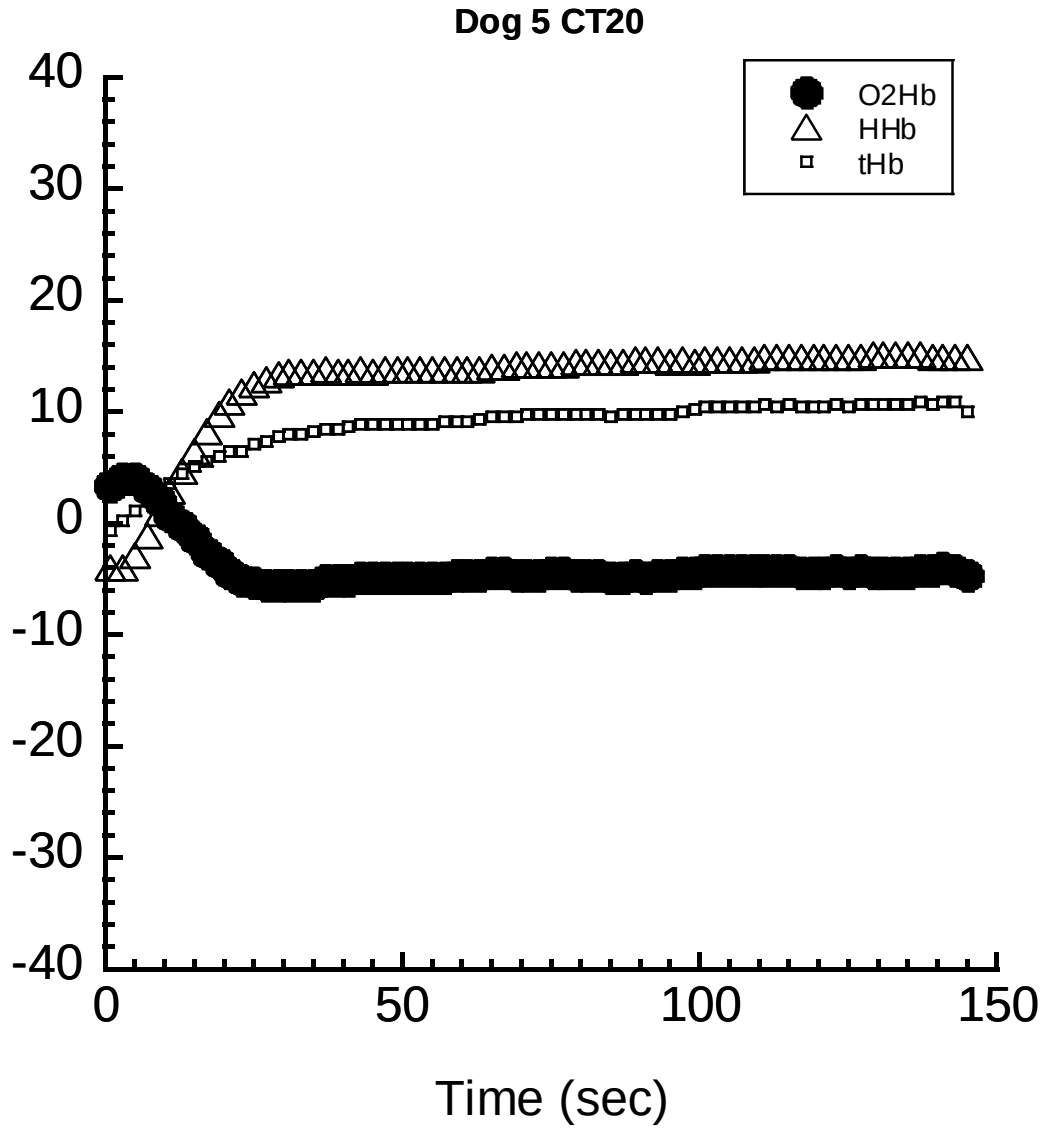
Dog 5 CT20
O2Hb
HHb
tHb
40
30
20
10
0
-10
-20
-30
-40
0
50
100
150
Time (sec)

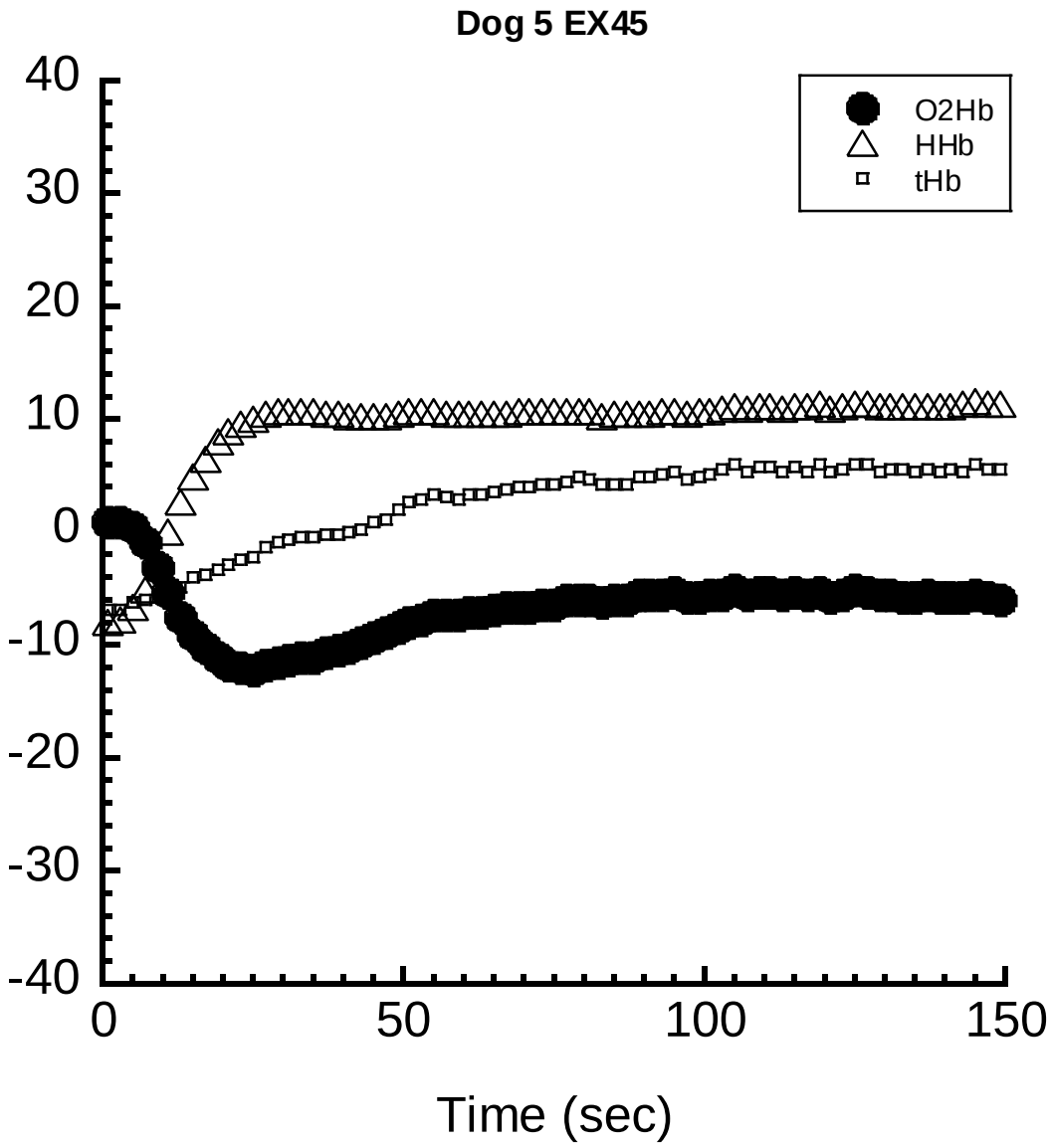
Dog 5 EX45
40
30
20
10
0
-10
-20
-30
-40
0
50
100
150
Time (sec)
O2Hb
HHb
tHb

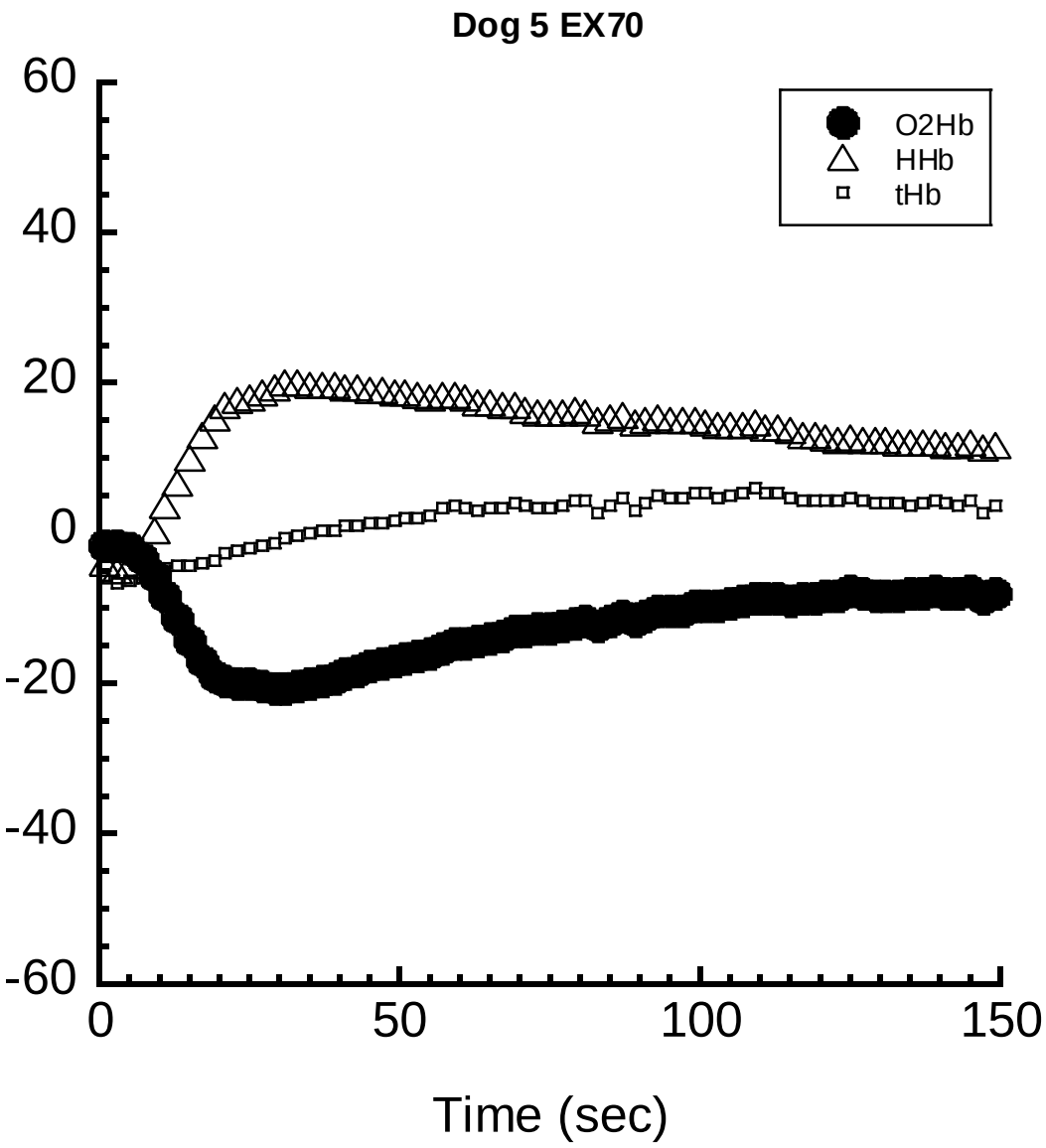
Dog 5 EX70
60
40
20
0
-20
-40
-60
0
50
100
150
Time (sec)
O2Hb
HHb
tHb

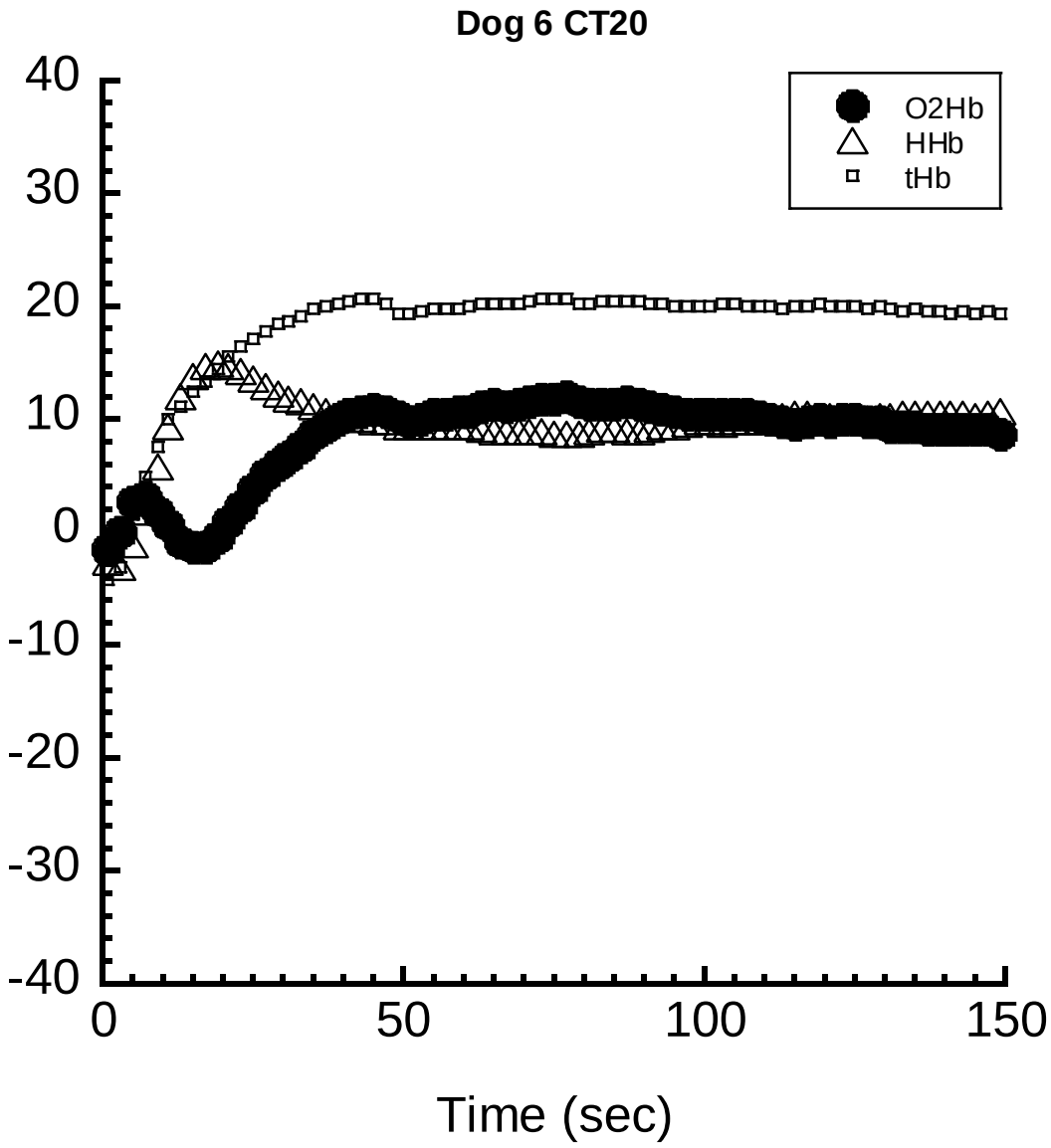
Dog 6 CT20
O2Hb
HHb
tHb
40
30
20
10
0
-10
-20
-30
-40
0
50
100
150
Time (sec)

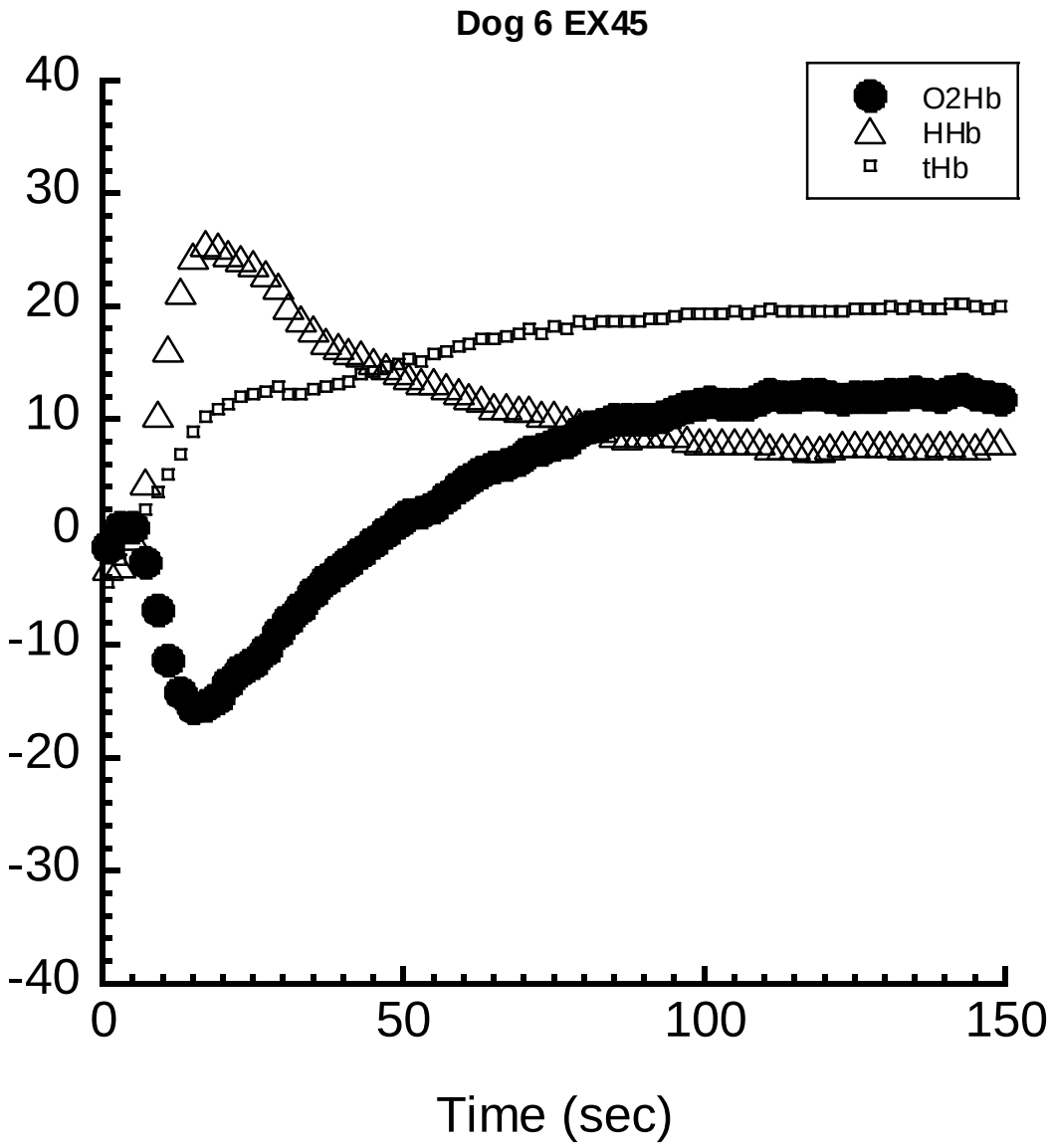
Dog 6 EX45
O2Hb
HHb
tHb
40
30
20
10
0
-10
-20
-30
-40
0
50
100
150
Time (sec)

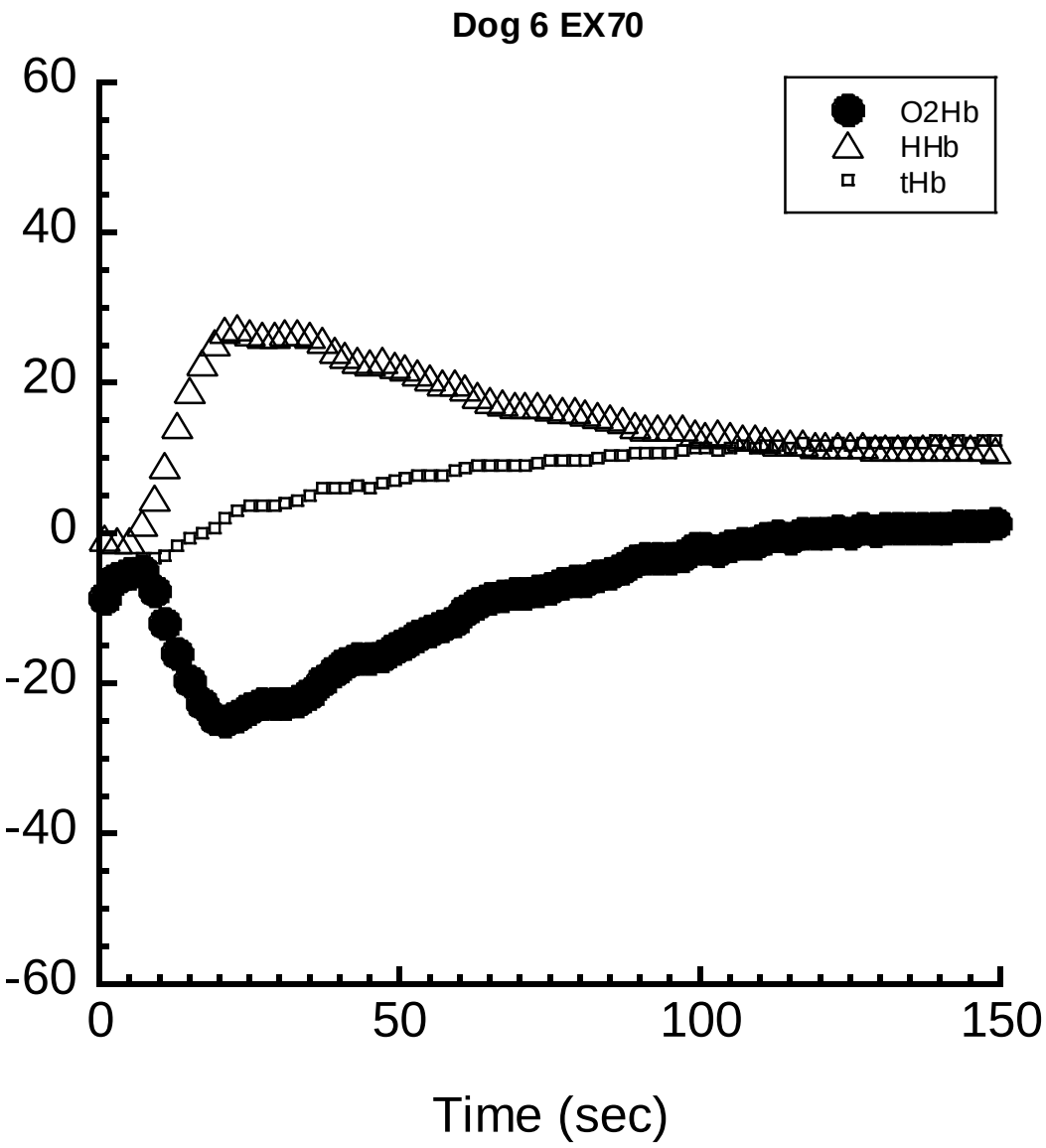
Dog 6 EX70
60
40
20
0
-20
-40
-60
0
50
100
150
Time (sec)
O2Hb
HHb
tHb

CURVE FITS OF NIRS [HHb] ON-RESPONSES

ALL GRAPHS ARE IN UNITS OF TIME (sec) ON THE X-AXIS AND CONCENTRATION (relative μM) ON THE Y-AXIS

"a" = FIT1, time delay starts from resting [HHb]

"b" = FIT2, time delay starts from where program chooses

Curves were fit with a monoexponential rise equation of the type:

$$\mathbf{y(t) = y}\boldsymbol{BAS}\mathbf{ + A\,[1 - e^{-(t - TD) / \tau}]}$$

In this equation, y*BAS* indicates the baseline value obtained at rest before contraction onset, A indicates the amplitude between y*BAS* and the steady-state value at the end of the contraction period, TD the time delay and τ the time constant of the function. The half-time ($t_{50\%}$) of the on-kinetics exponential function can be calculated by multiplying τ by 0.693. To facilitate a comparison with the results reported by previous studies, τ and TD were added together to calculate the mean response time (MRT) of the overall response.

Program used: KaleidaGraph 4.0

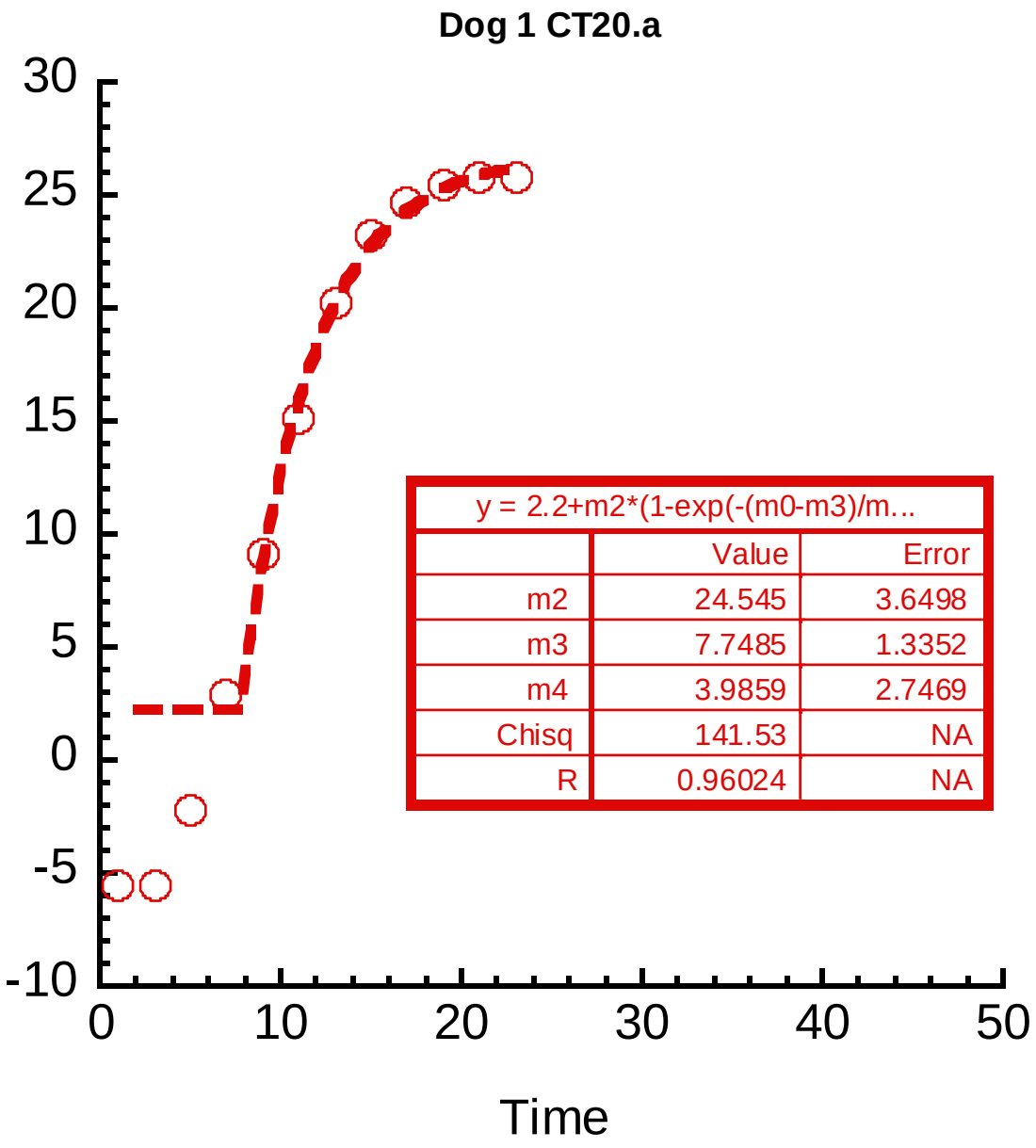
Dog 1 CT20.a
30
25
20
15
10
5
0
-5
-10
0
10
20
30
40
50
Time
y = 2.2+m2*(1-exp(-(m0-m3)/m...
Value
Error
m2
24.545
3.6498
m3
7.7485
1.3352
m4
3.9859
2.7469
Chisq
141.53
NA
R
0.96024
NA

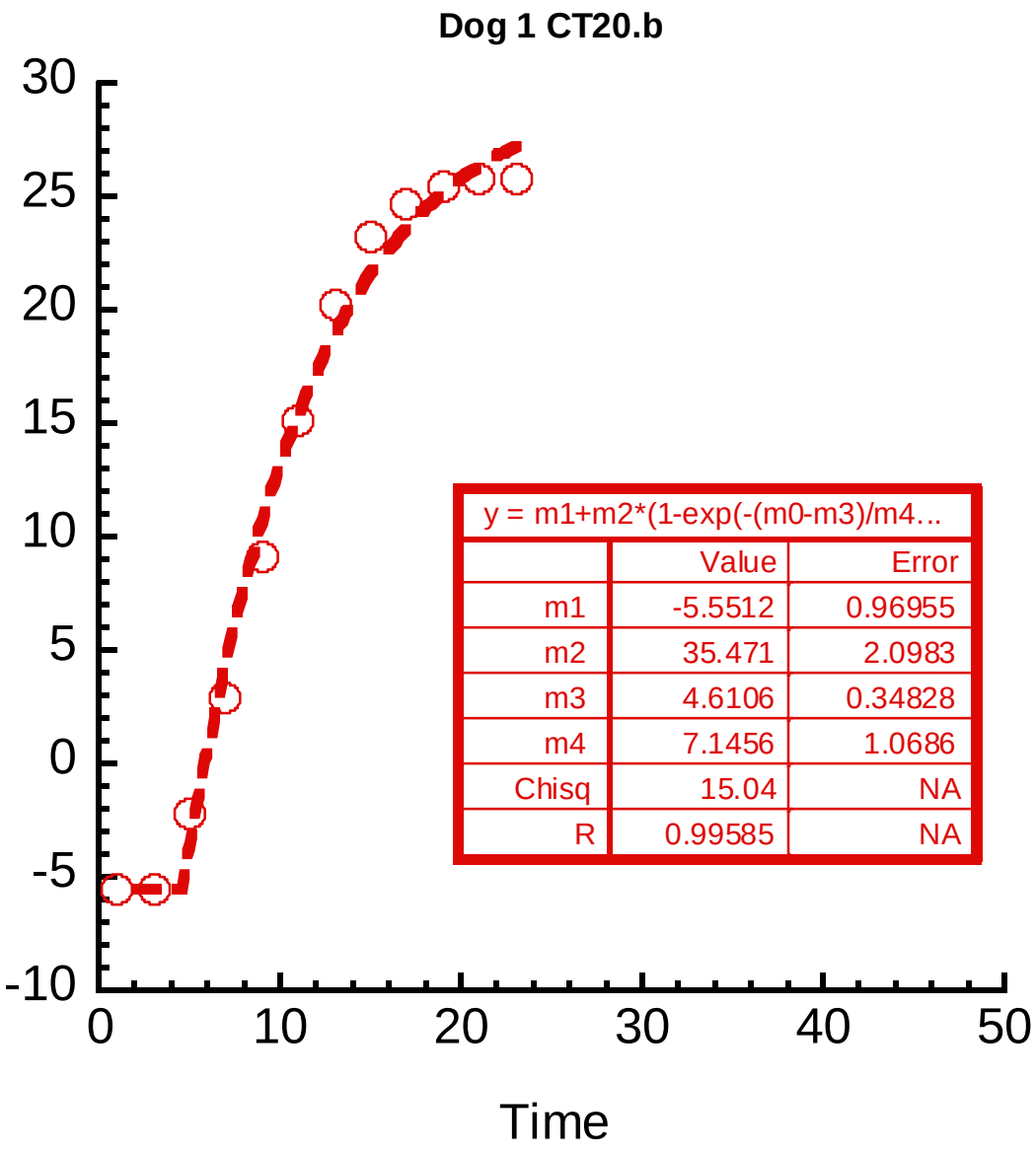
Dog 1 CT20.b
30
25
20
15
10
5
0
-5
-10
0
10
20
30
40
50
Time
y = m1+m2*(1-exp(-(m0-m3)/m4...
Value
Error
m1
-5.5512
0.96955
m2
35.471
2.0983
m3
4.6106
0.34828
m4
7.1456
1.0686
Chisq
15.04
NA
R
0.99585
NA

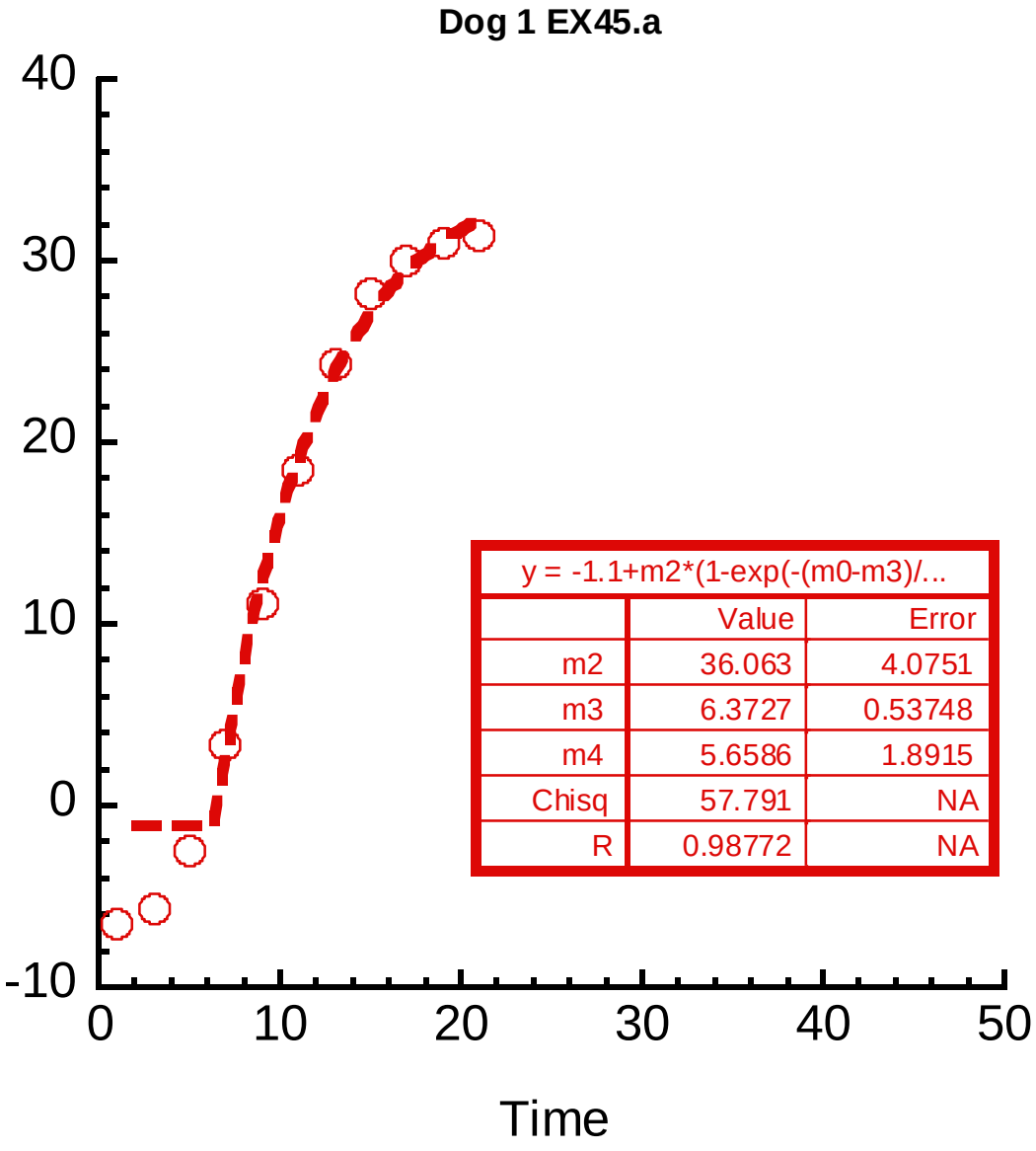
Dog 1 EX45.a
40
30
20
10
0
-10
0
10
20
30
40
50
Time
y = -1.1+m2*(1-exp(-(m0-m3)/...
Value
Error
m2
36.063
4.0751
m3
6.3727
0.53748
m4
5.6586
1.8915
Chisq
57.791
NA
R
0.98772
NA

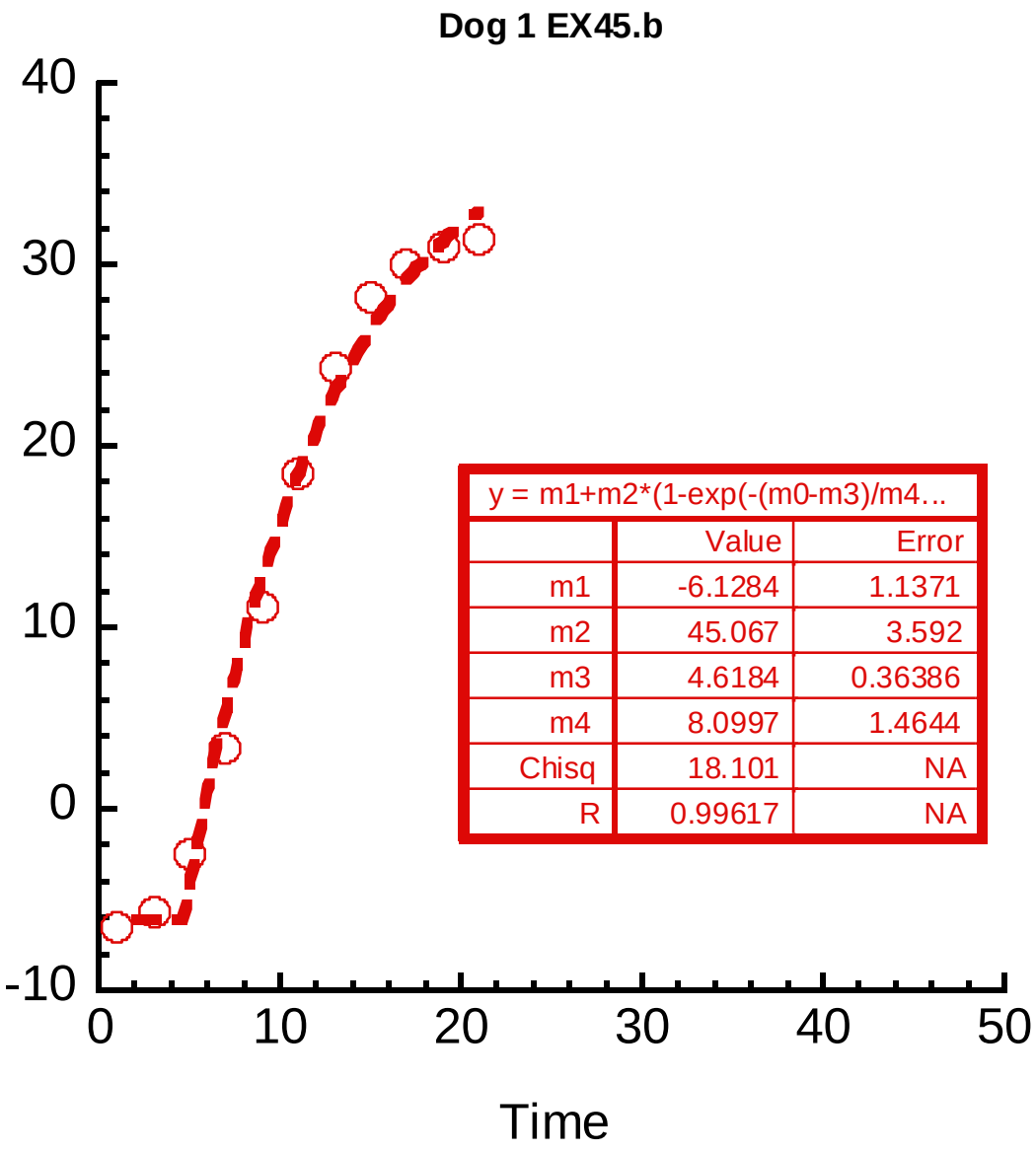
Dog 1 EX45.b
40
30
20
10
0
-10
0
10
20
30
40
50
Time
y = m1+m2*(1-exp(-(m0-m3)/m4...
Value
Error
m1
-6.1284
1.1371
m2
45.067
3.592
m3
4.6184
0.36386
m4
8.0997
1.4644
Chisq
18.101
NA
R
0.99617
NA

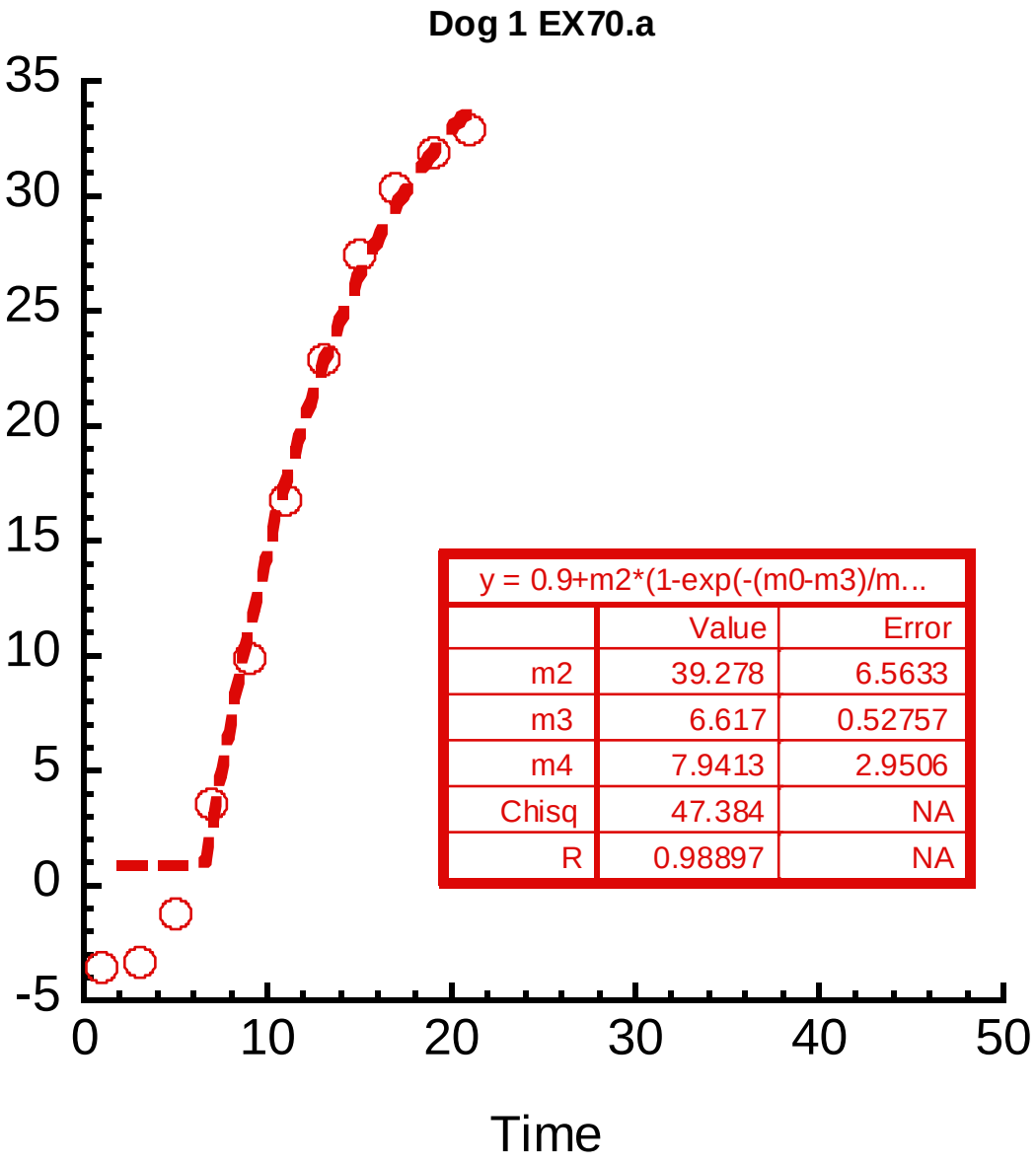
Dog 1 EX70.a
35
30
25
20
15
10
5
0
-5
0
10
20
30
40
50
Time
y = 0.9+m2*(1-exp(-(m0-m3)/m...
Value
Error
m2
39.278
6.5633
m3
6.617
0.52757
m4
7.9413
2.9506
Chisq
47.384
NA
R
0.98897
NA

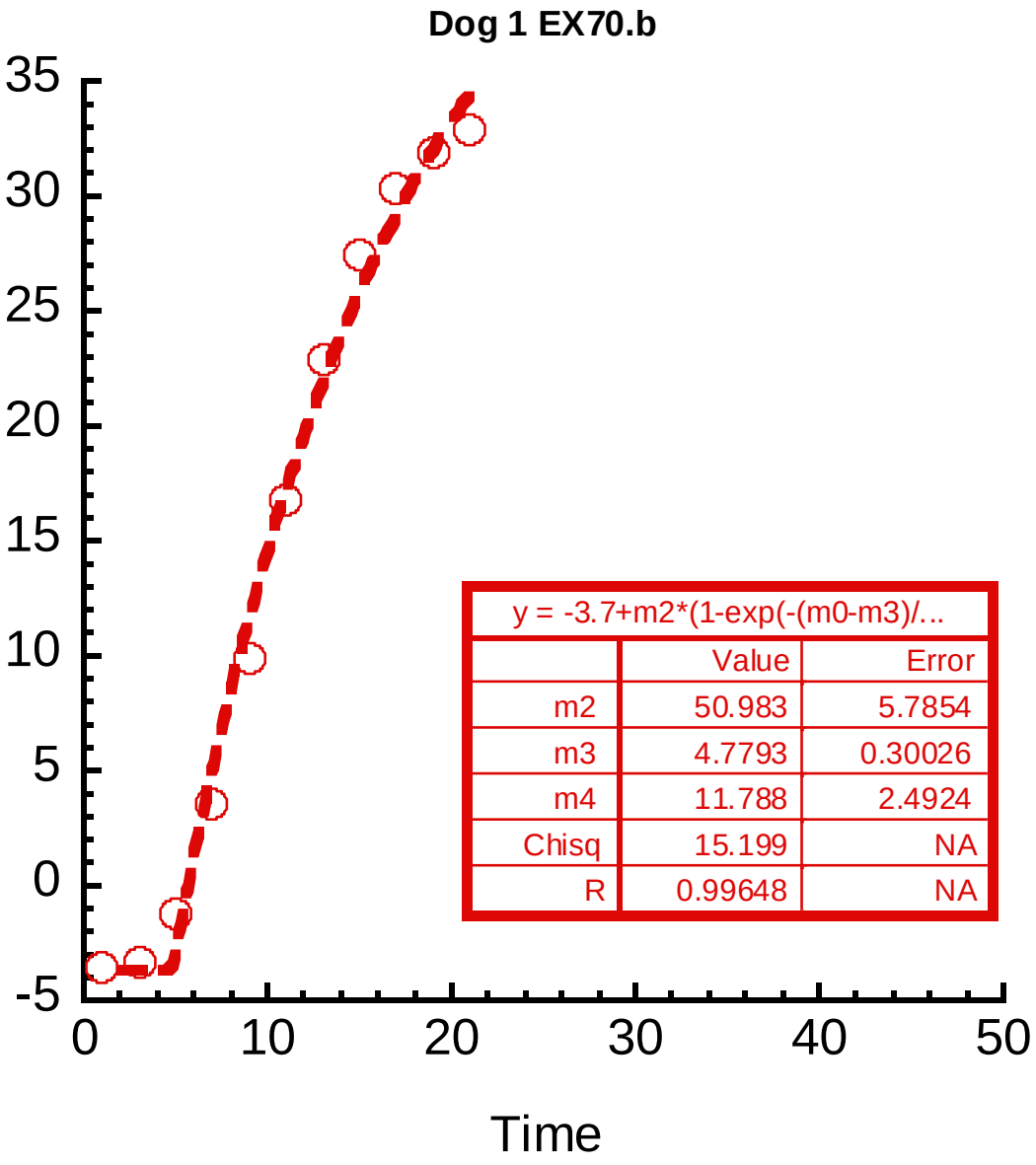
Dog 1 EX70.b
35
30
25
20
15
10
5
0
-5
0
10
20
30
40
50
Time
y = -3.7+m2*(1-exp(-(m0-m3)/...
Value
Error
m2
50.983
5.7854
m3
4.7793
0.30026
m4
11.788
2.4924
Chisq
15.199
NA
R
0.99648
NA

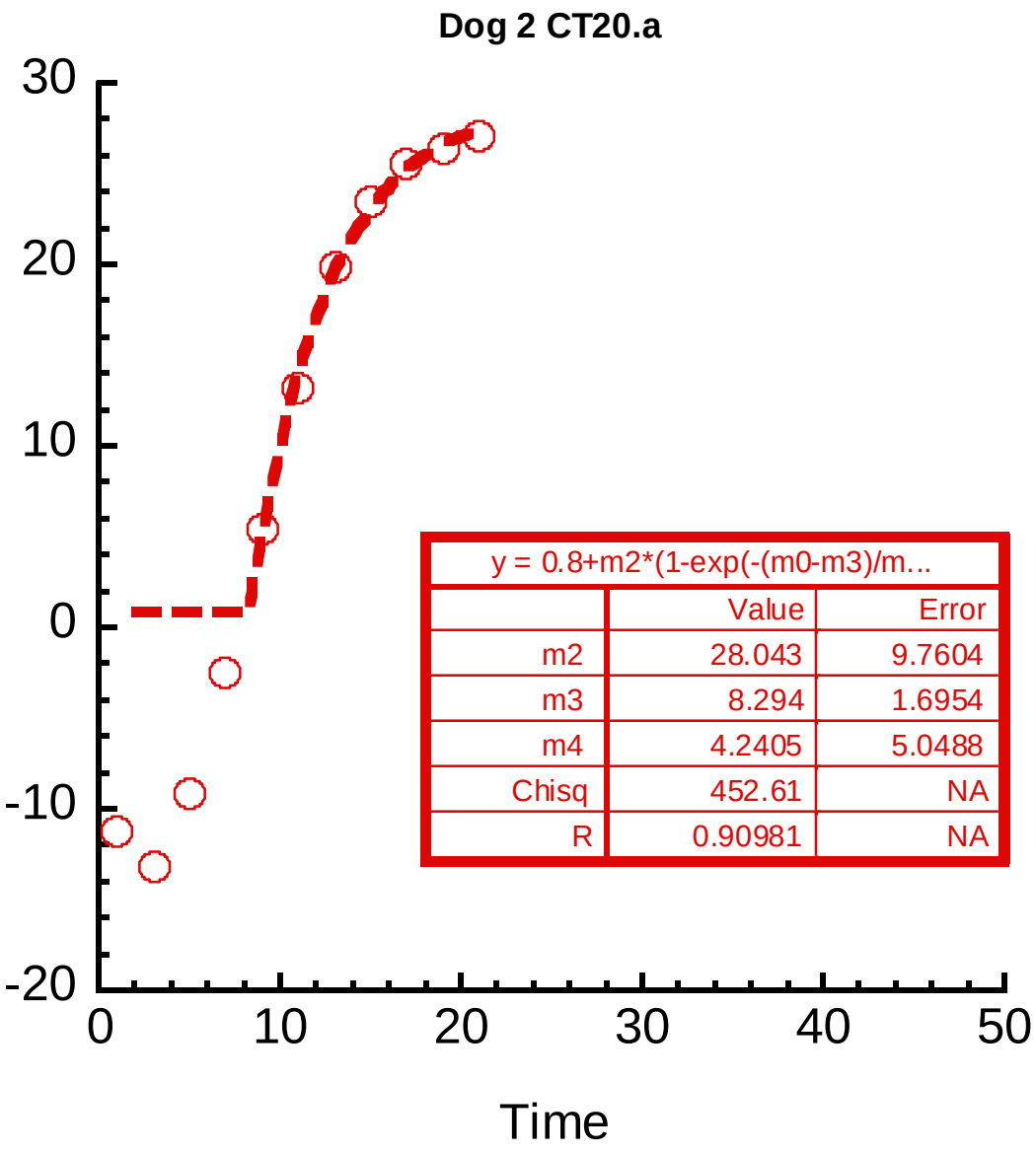
Dog 2 CT20.a
30
20
10
0
-10
-20
0
10
20
30
40
50
Time
y = 0.8+m2*(1-exp(-(m0-m3)/m...
Value
Error
m2
28.043
9.7604
m3
8.294
1.6954
m4
4.2405
5.0488
Chisq
452.61
NA
R
0.90981
NA

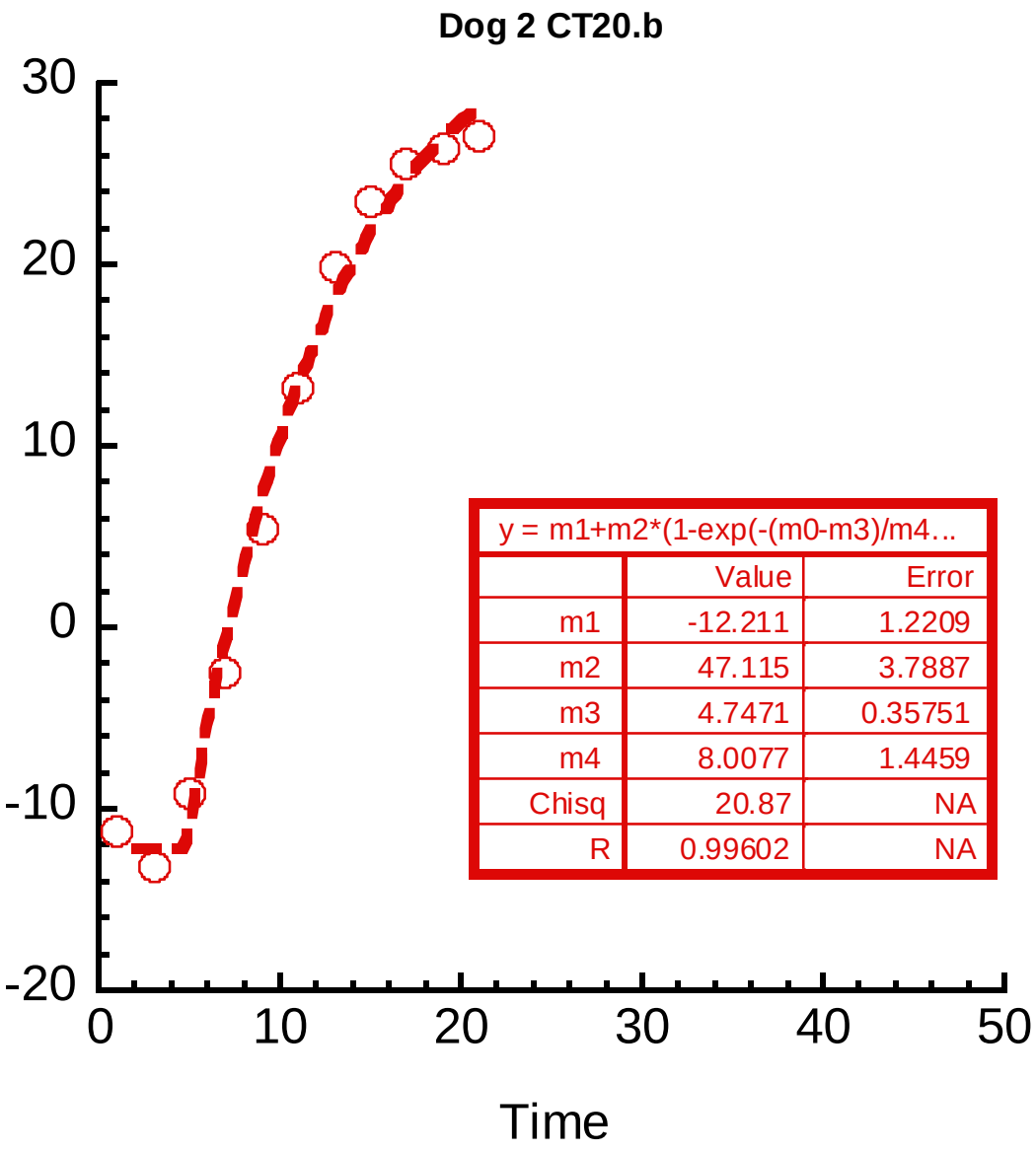
Dog 2 CT20.b
30
20
10
0
-10
-20
0
10
20
30
40
50
Time
y = m1+m2*(1-exp(-(m0-m3)/m4...
Value
Error
m1
-12.211
1.2209
m2
47.115
3.7887
m3
4.7471
0.35751
m4
8.0077
1.4459
Chisq
20.87
NA
R
0.99602
NA

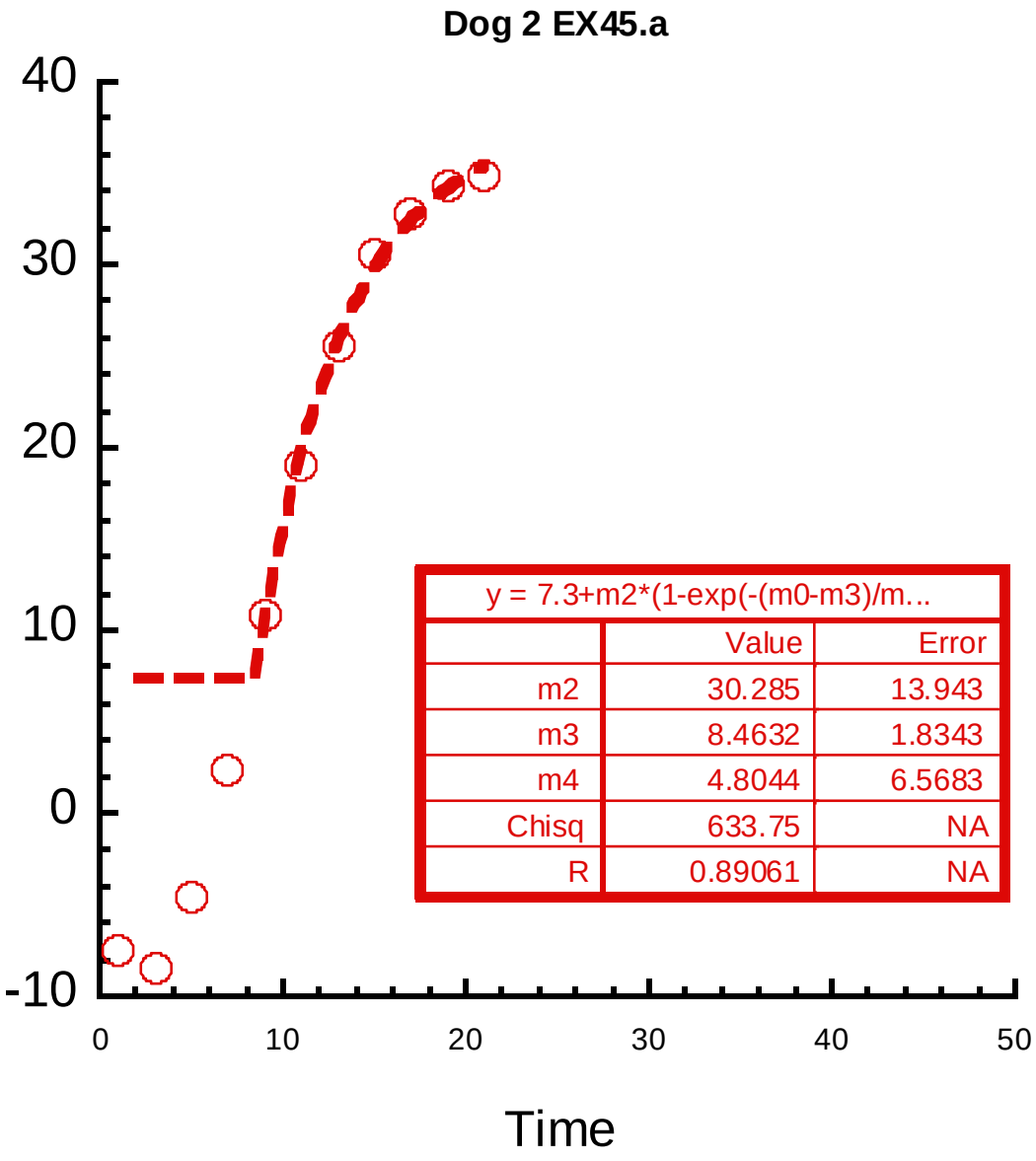
Dog 2 EX45.a
40
30
20
10
0
-10
0
10
20
30
40
50
Time
y = 7.3+m2*(1-exp(-(m0-m3)/m...
Value
Error
m2
30.285
13.943
m3
8.4632
1.8343
m4
4.8044
6.5683
Chisq
633.75
NA
R
0.89061
NA

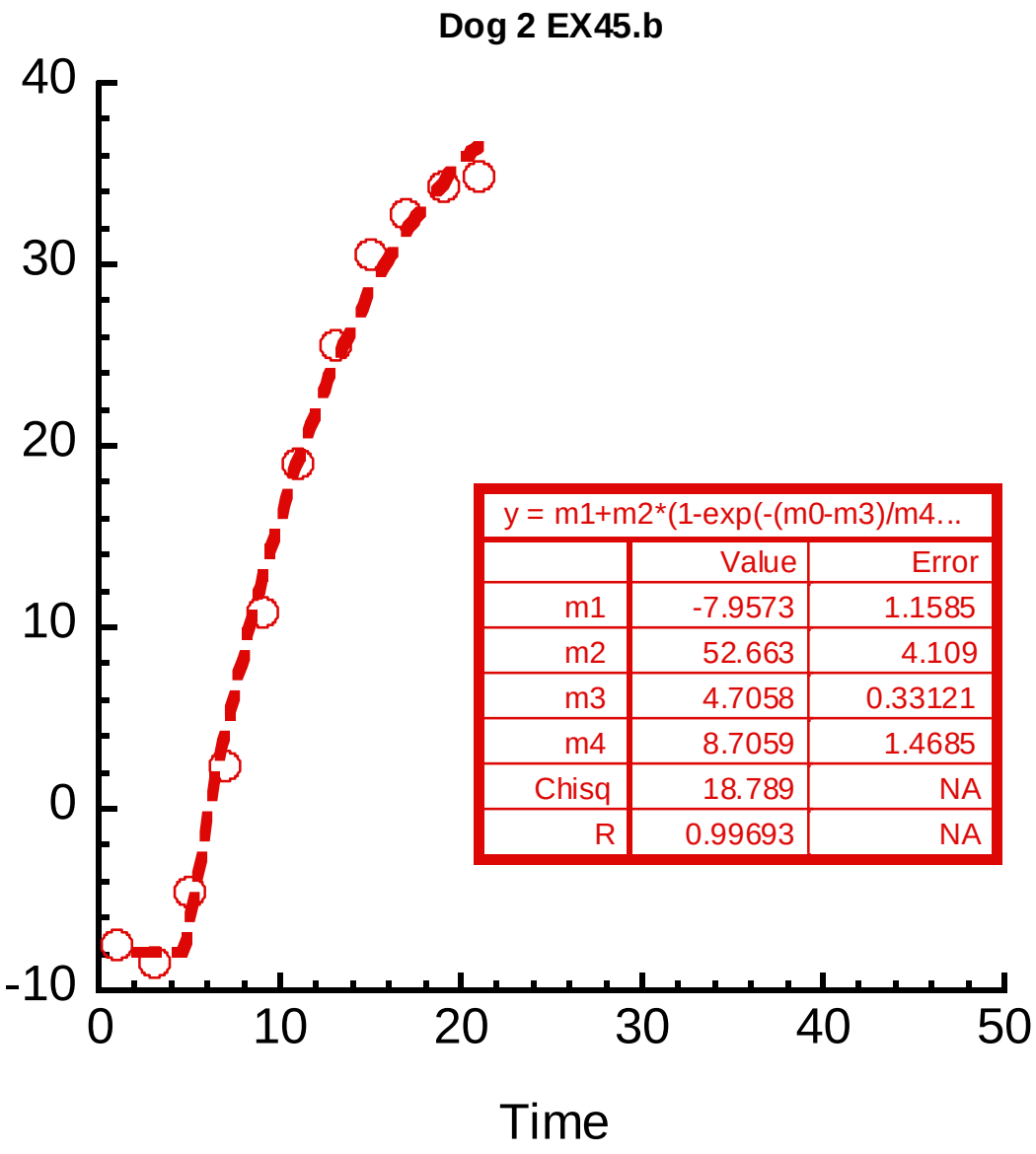
Dog 2 EX45.b
40
30
20
10
0
-10
0
10
20
30
40
50
Time
y = m1+m2*(1-exp(-(m0-m3)/m4...
Value
Error
m1
-7.9573
1.1585
m2
52.663
4.109
m3
4.7058
0.33121
m4
8.7059
1.4685
Chisq
18.789
NA
R
0.99693
NA

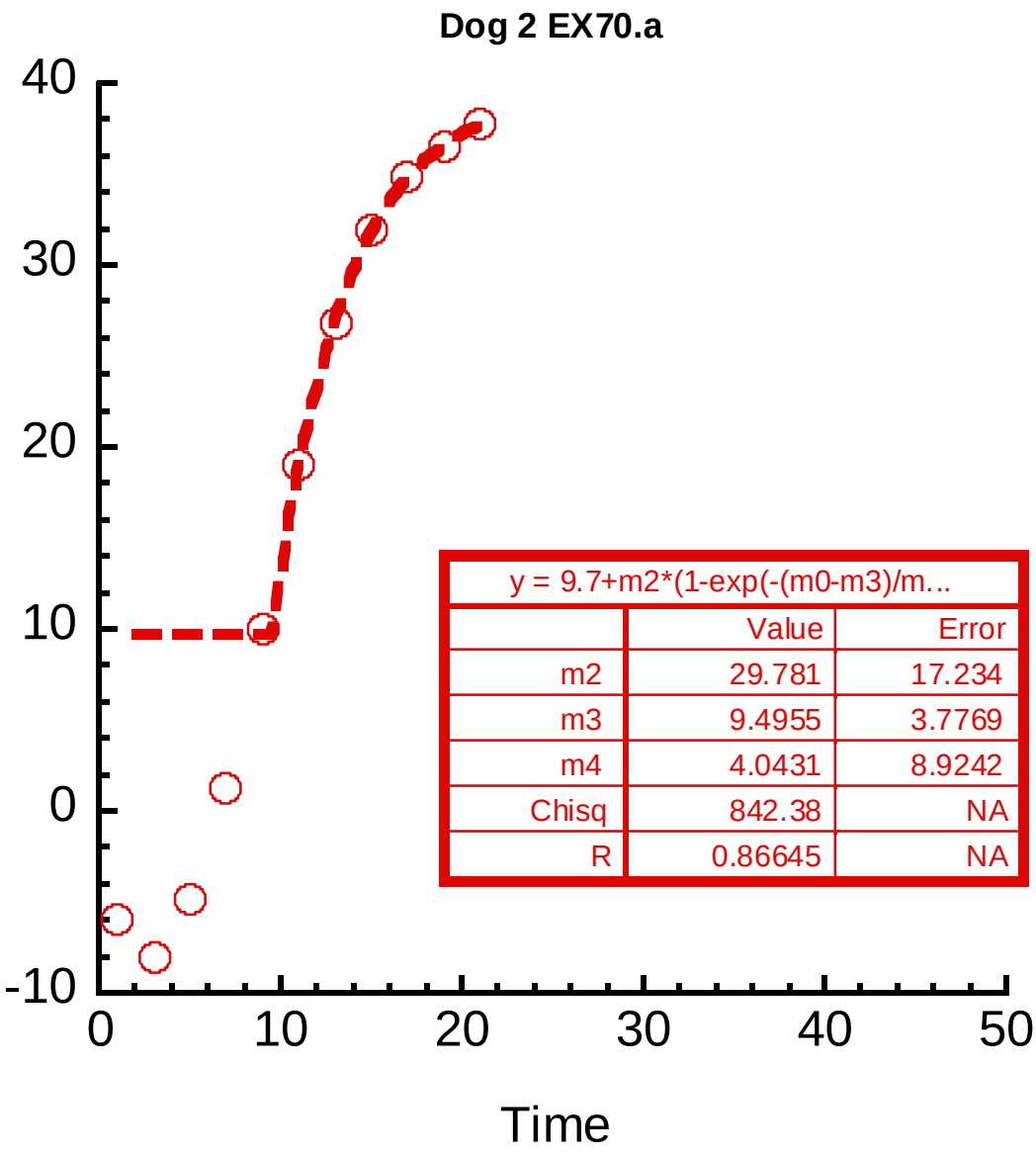
Dog 2 EX70.a
40
30
20
10
0
-10
0
10
20
30
40
50
Time
y = 9.7+m2*(1-exp(-(m0-m3)/m...
Value
Error
m2
29.781
17.234
m3
9.4955
3.7769
m4
4.0431
8.9242
Chisq
842.38
NA
R
0.86645
NA

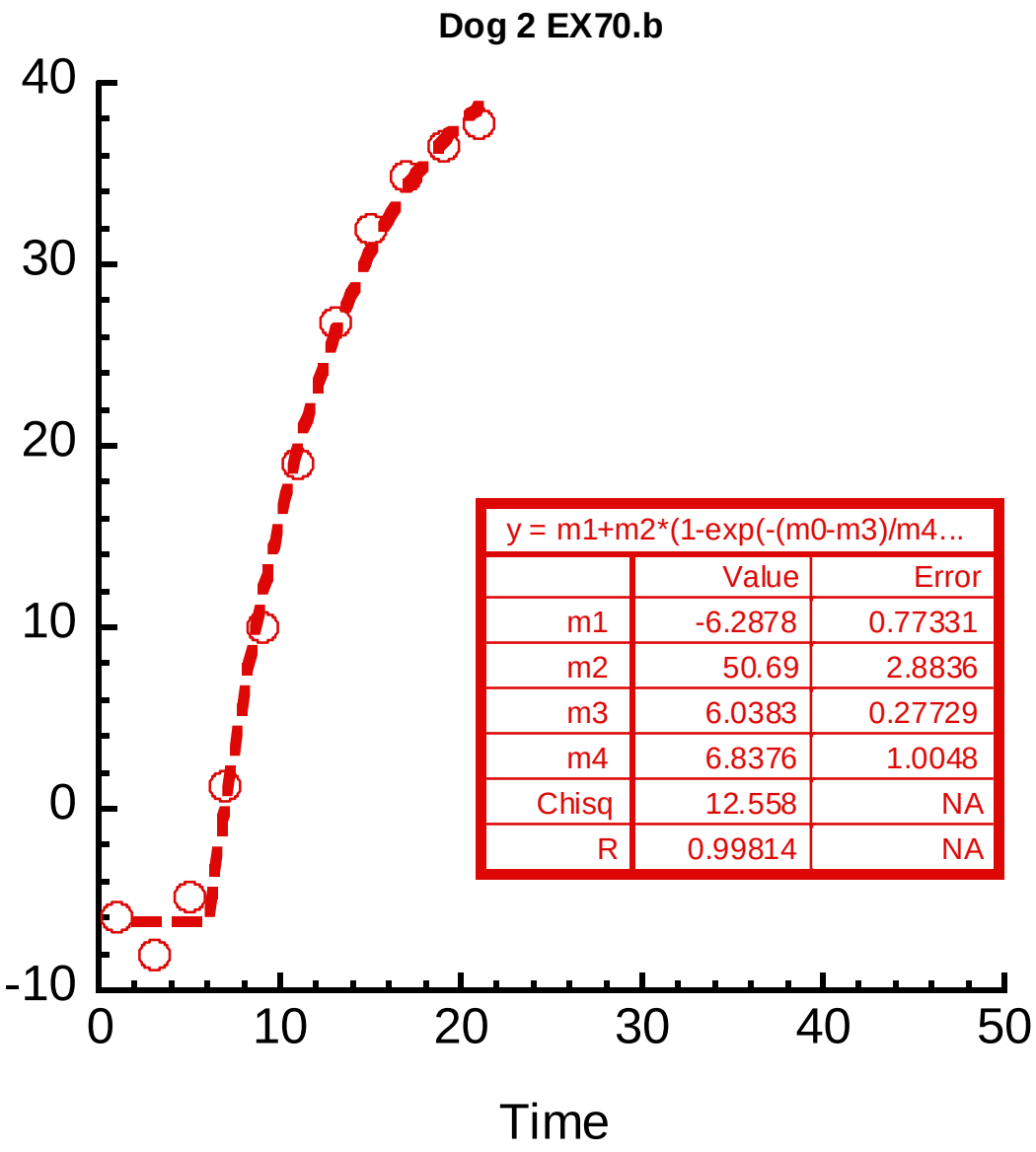
Dog 2 EX70.b
40
30
20
10
0
-10
0
10
20
30
40
50
Time
y = m1+m2*(1-exp(-(m0-m3)/m4...
Value
Error
m1
-6.2878
0.77331
m2
50.69
2.8836
m3
6.0383
0.27729
m4
6.8376
1.0048
Chisq
12.558
NA
R
0.99814
NA

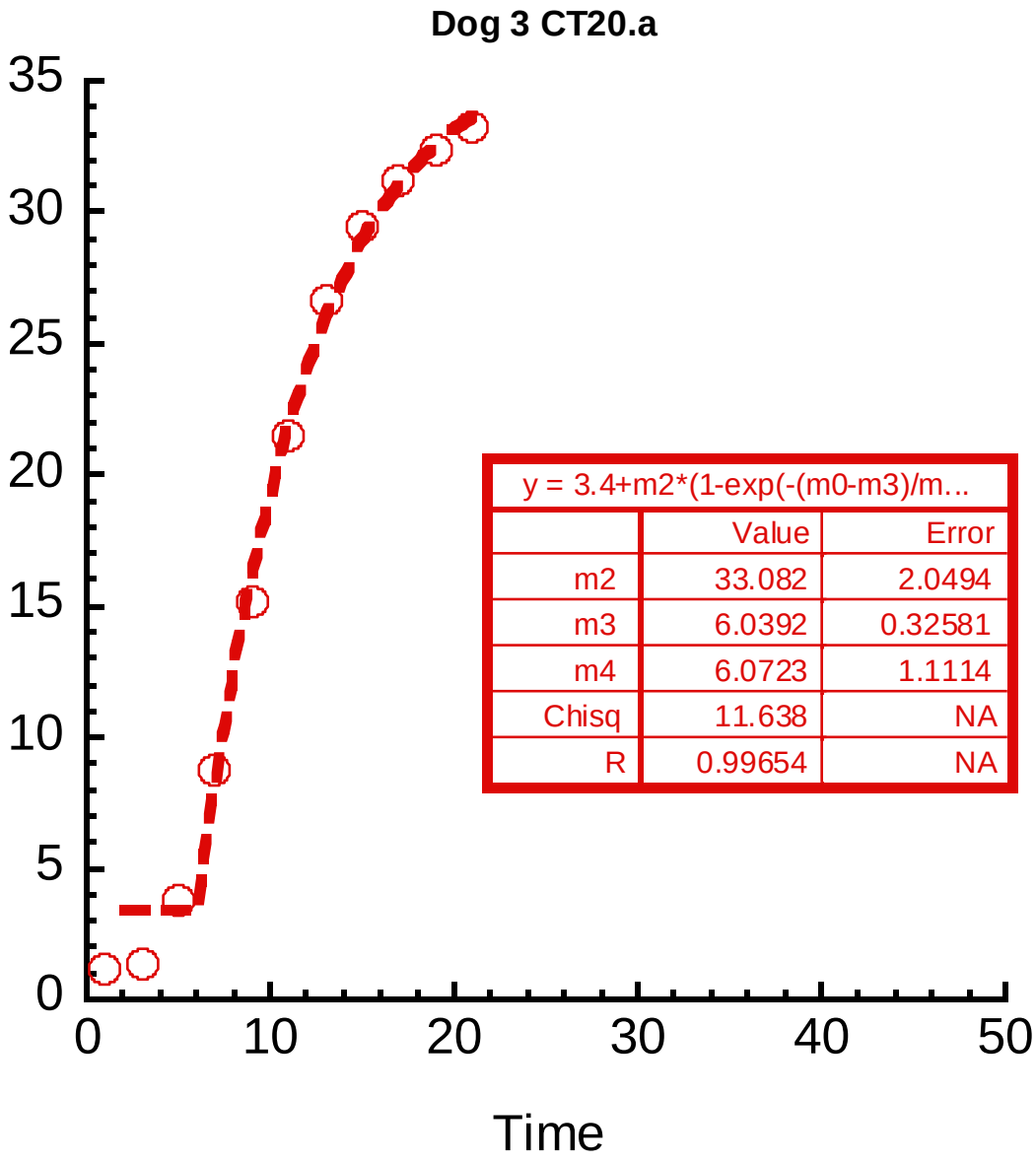
Dog 3 CT20.a
35
30
25
20
15
10
5
0
0
10
20
30
40
50
Time
y = 3.4+m2*(1-exp(-(m0-m3)/m...
Value
Error
m2
33.082
2.0494
m3
6.0392
0.32581
m4
6.0723
1.1114
Chisq
11.638
NA
R
0.99654
NA

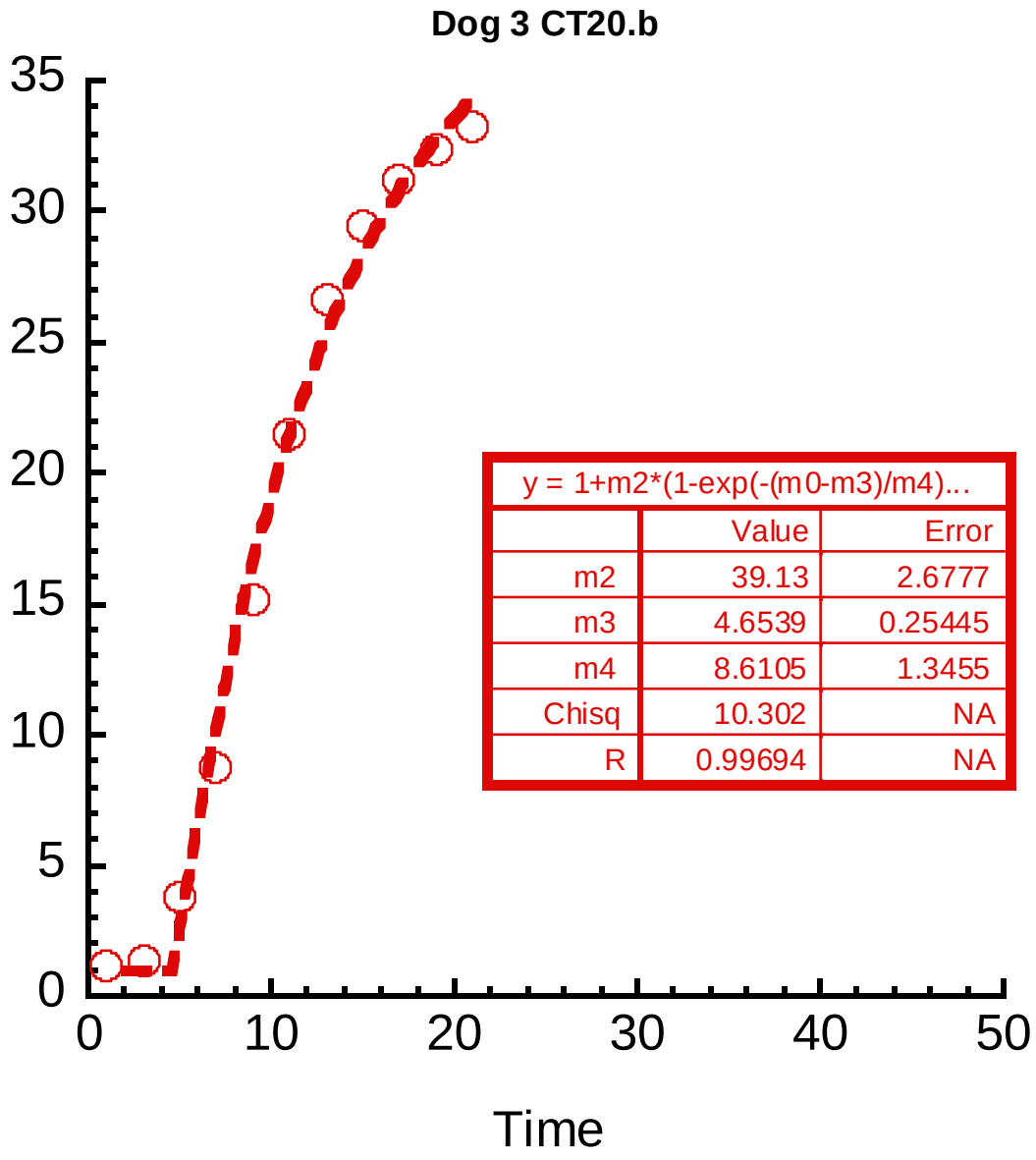
Dog 3 CT20.b
35
30
25
20
15
10
5
0
0
10
20
30
40
50
Time
y = 1+m2*(1-exp(-(m0-m3)/m4)...
Value
Error
m2
39.13
2.6777
m3
4.6539
0.25445
m4
8.6105
1.3455
Chisq
10.302
NA
R
0.99694
NA

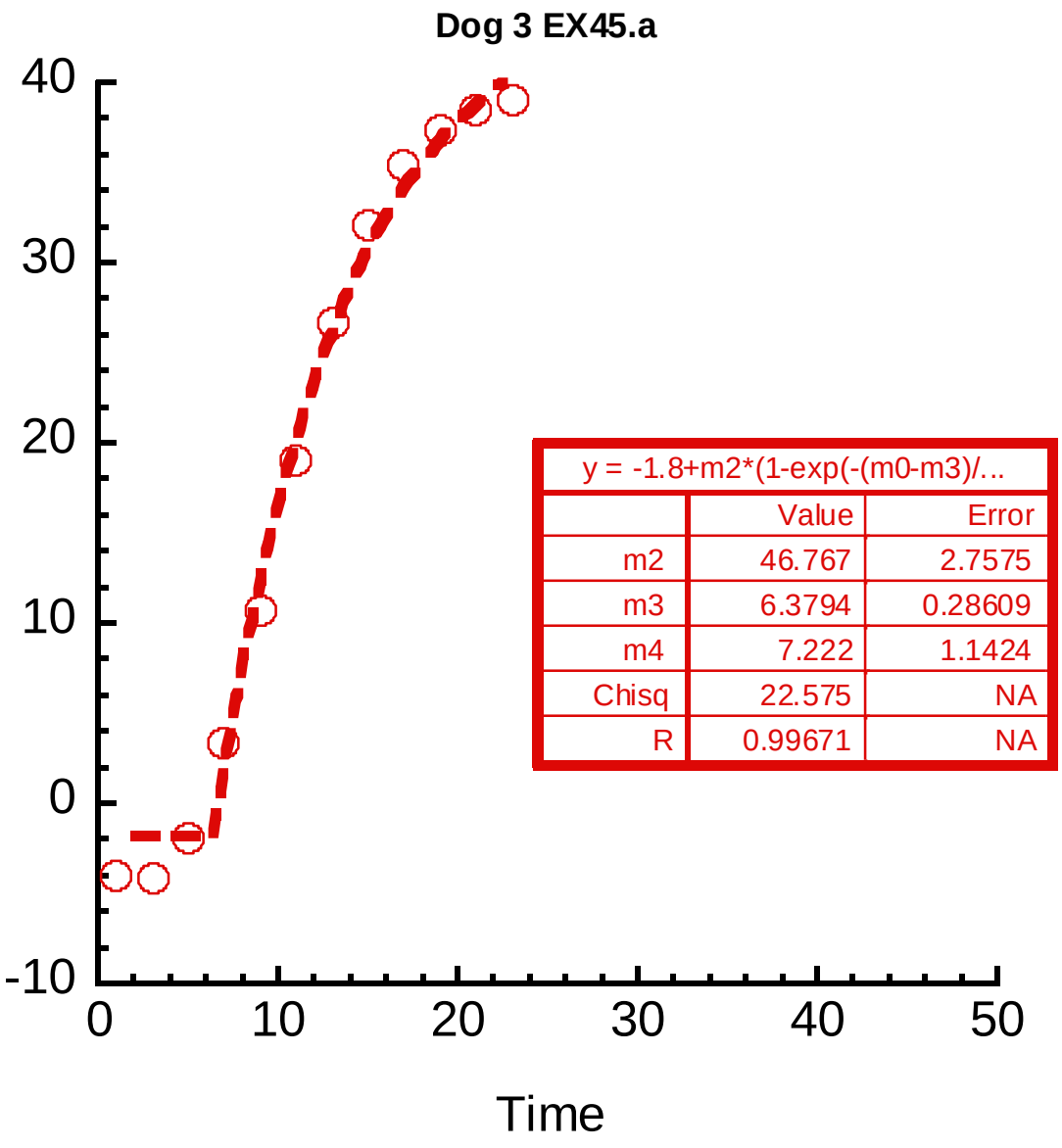
Dog 3 EX45.a
40
30
20
10
0
-10
0
10
20
30
40
50
Time
y = -1.8+m2*(1-exp(-(m0-m3)/...
Value
Error
m2
46.767
2.7575
m3
6.3794
0.28609
m4
7.222
1.1424
Chisq
22.575
NA
R
0.99671
NA

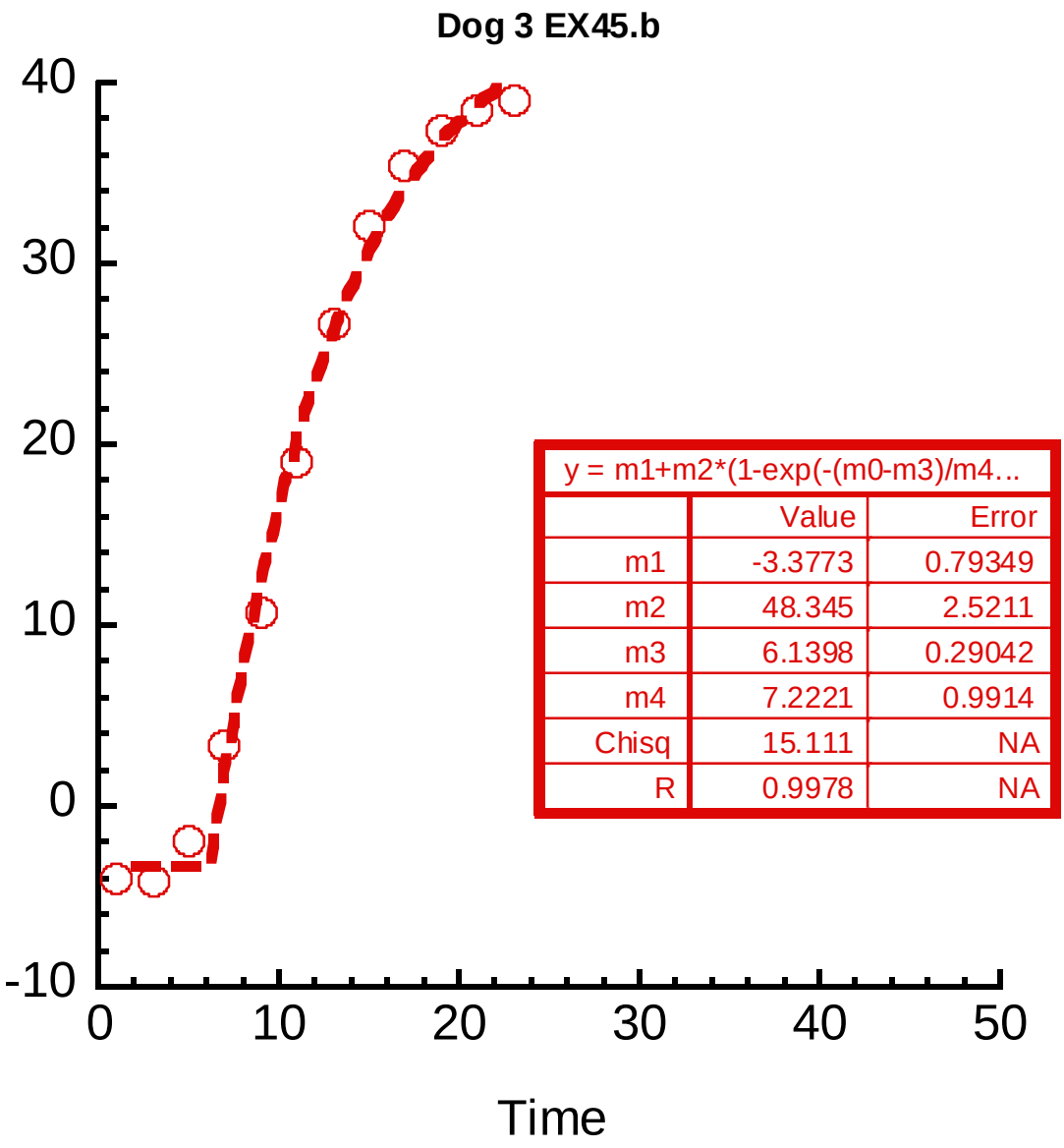
Dog 3 EX45.b
40
30
20
10
0
-10
0
10
20
30
40
50
Time
y = m1+m2*(1-exp(-(m0-m3)/m4...
Value
Error
m1
-3.3773
0.79349
m2
48.345
2.5211
m3
6.1398
0.29042
m4
7.2221
0.9914
Chisq
15.111
NA
R
0.9978
NA

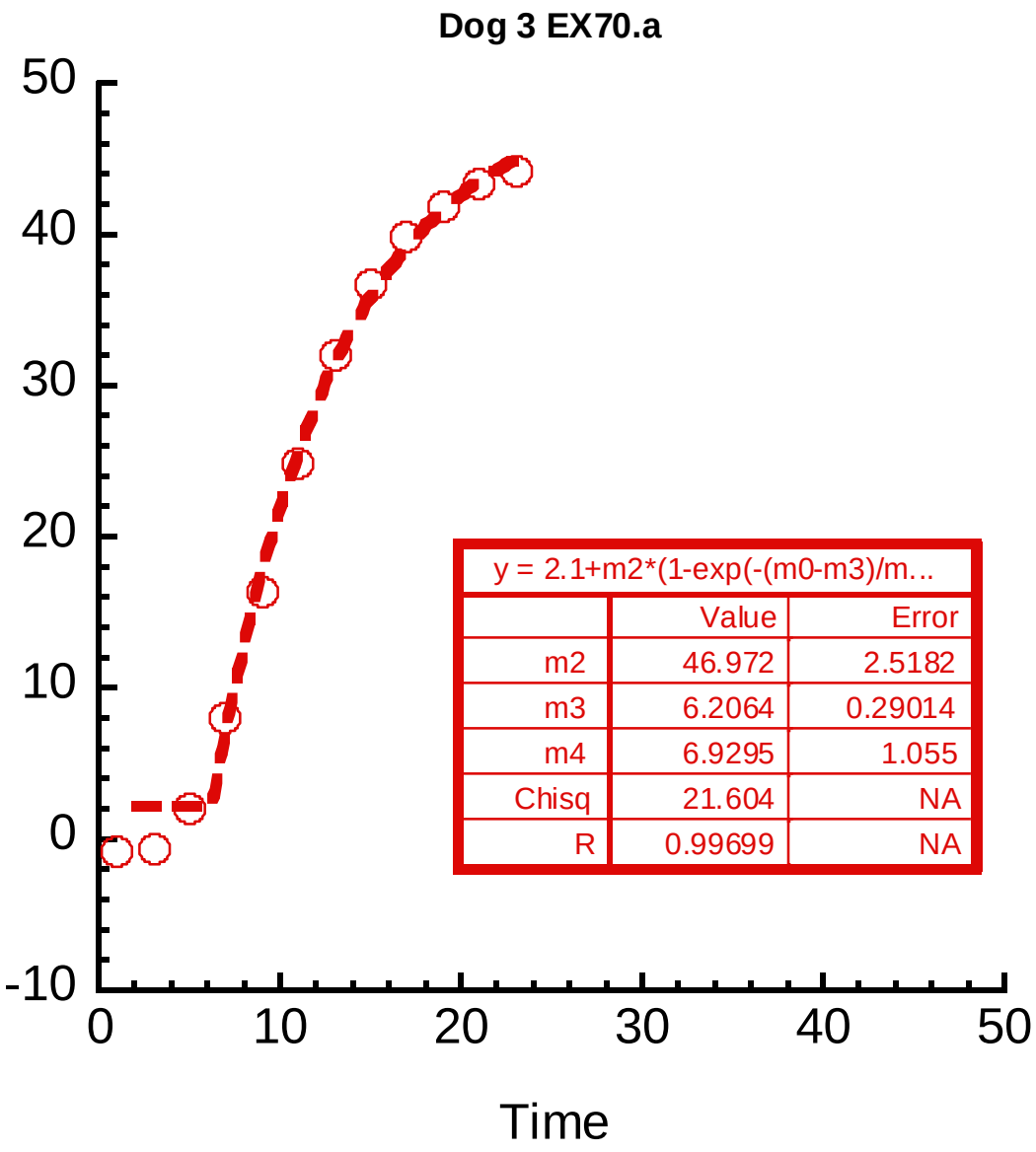
Dog 3 EX70.a
50
40
30
20
10
0
-10
0
10
20
30
40
50
Time
y = 2.1+m2*(1-exp(-(m0-m3)/m...
Value
Error
m2
46.972
2.5182
m3
6.2064
0.29014
m4
6.9295
1.055
Chisq
21.604
NA
R
0.99699
NA

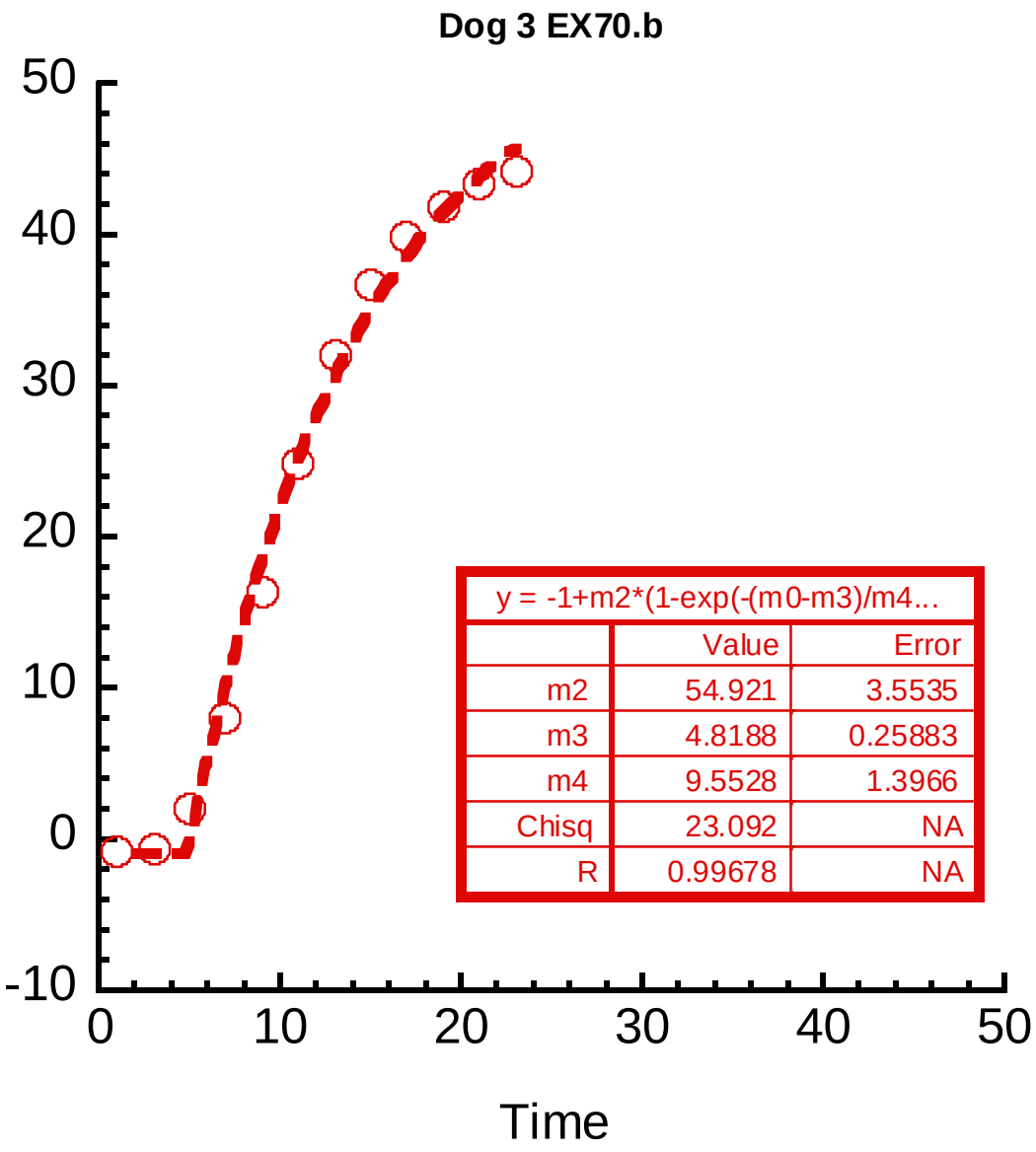
Dog 3 EX70.b
50
40
30
20
10
0
-10
0
10
20
30
40
50
Time
y = -1+m2*(1-exp(-(m0-m3)/m4...
Value
Error
m2
54.921
3.5535
m3
4.8188
0.25883
m4
9.5528
1.3966
Chisq
23.092
NA
R
0.99678
NA

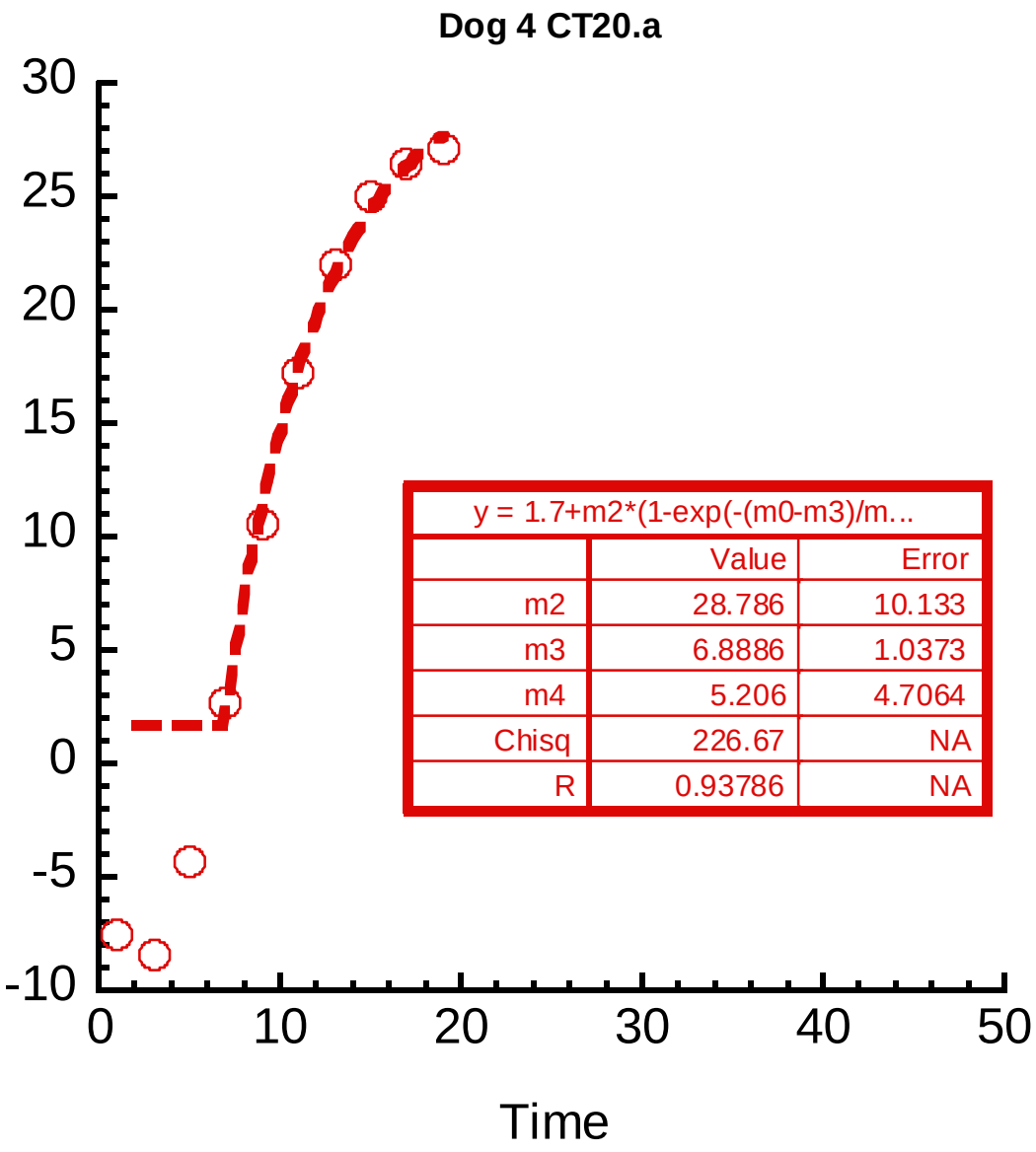
Dog 4 CT20.a
30
25
20
15
10
5
0
-5
-10
0
10
20
30
40
50
Time
y = 1.7+m2*(1-exp(-(m0-m3)/m...
Value
Error
m2
28.786
10.133
m3
6.8886
1.0373
m4
5.206
4.7064
Chisq
226.67
NA
R
0.93786
NA

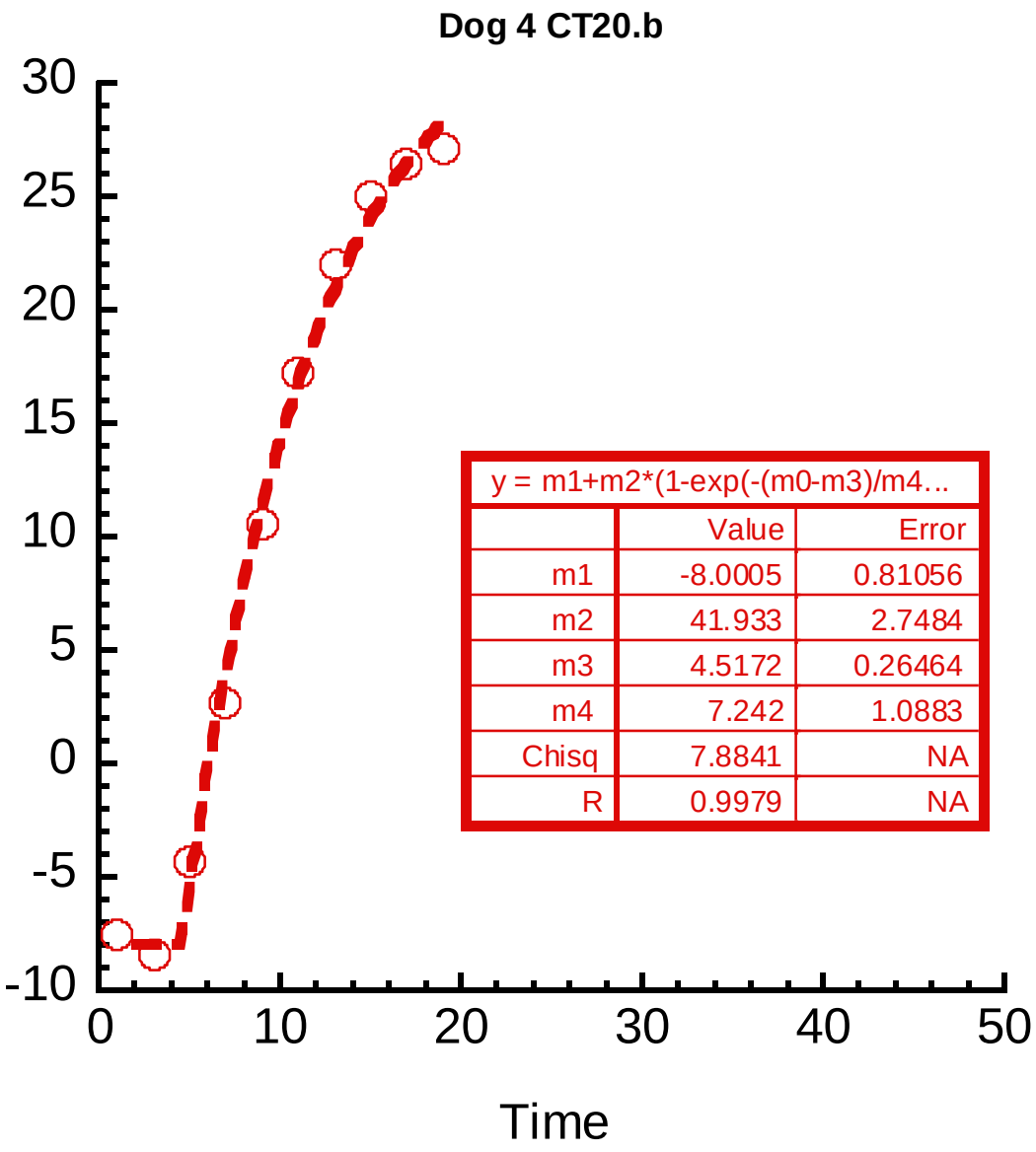
Dog 4 CT20.b
30
25
20
15
10
5
0
-5
-10
0
10
20
30
40
50
Time
y = m1+m2*(1-exp(-(m0-m3)/m4...
Value
Error
m1
-8.0005
0.81056
m2
41.933
2.7484
m3
4.5172
0.26464
m4
7.242
1.0883
Chisq
7.8841
NA
R
0.9979
NA

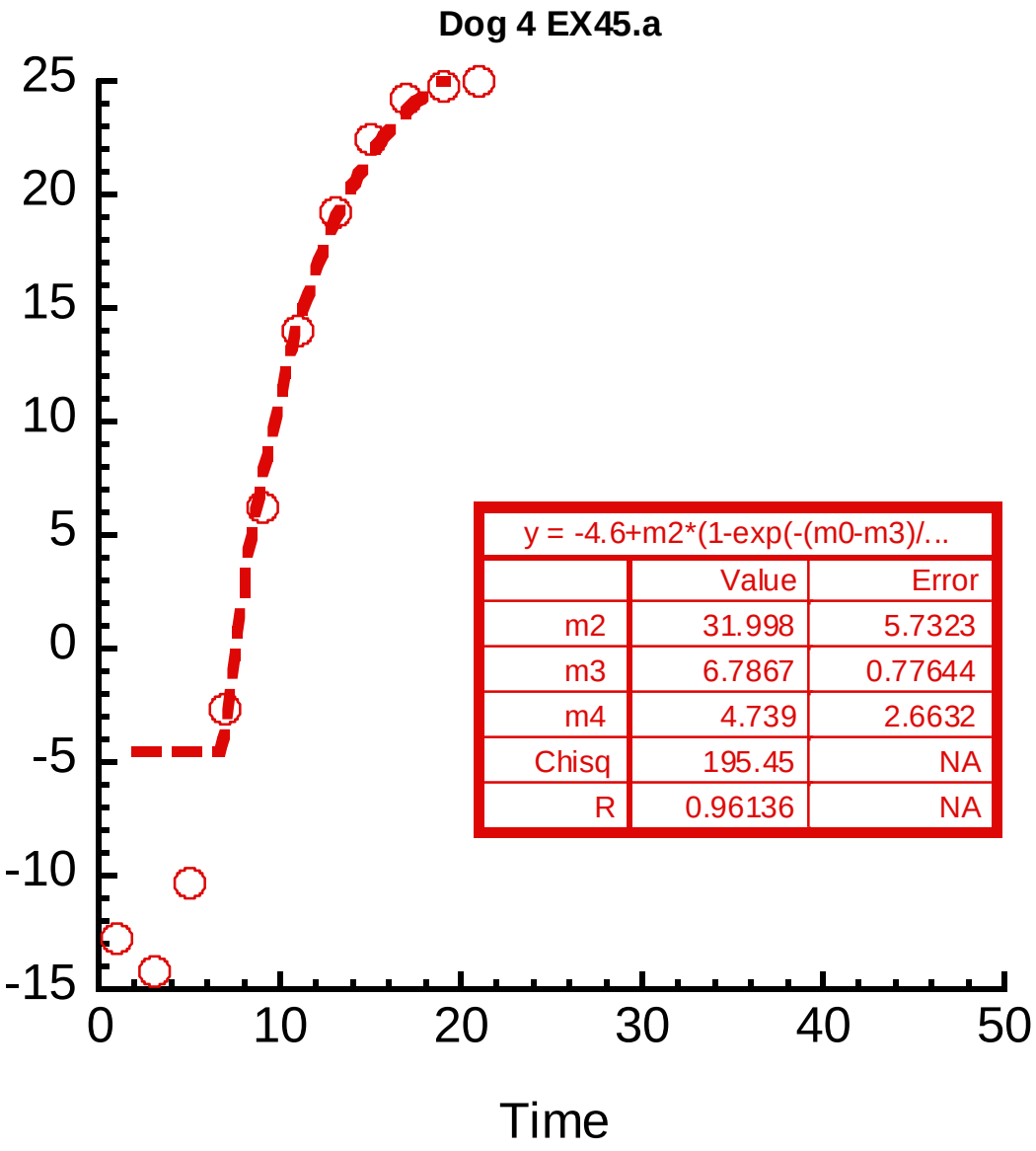
Dog 4 EX45.a
25
20
15
10
5
0
-5
-10
-15
0
10
20
30
40
50
Time
y = -4.6+m2*(1-exp(-(m0-m3)/...
Value
Error
m2
31.998
5.7323
m3
6.7867
0.77644
m4
4.739
2.6632
Chisq
195.45
NA
R
0.96136
NA

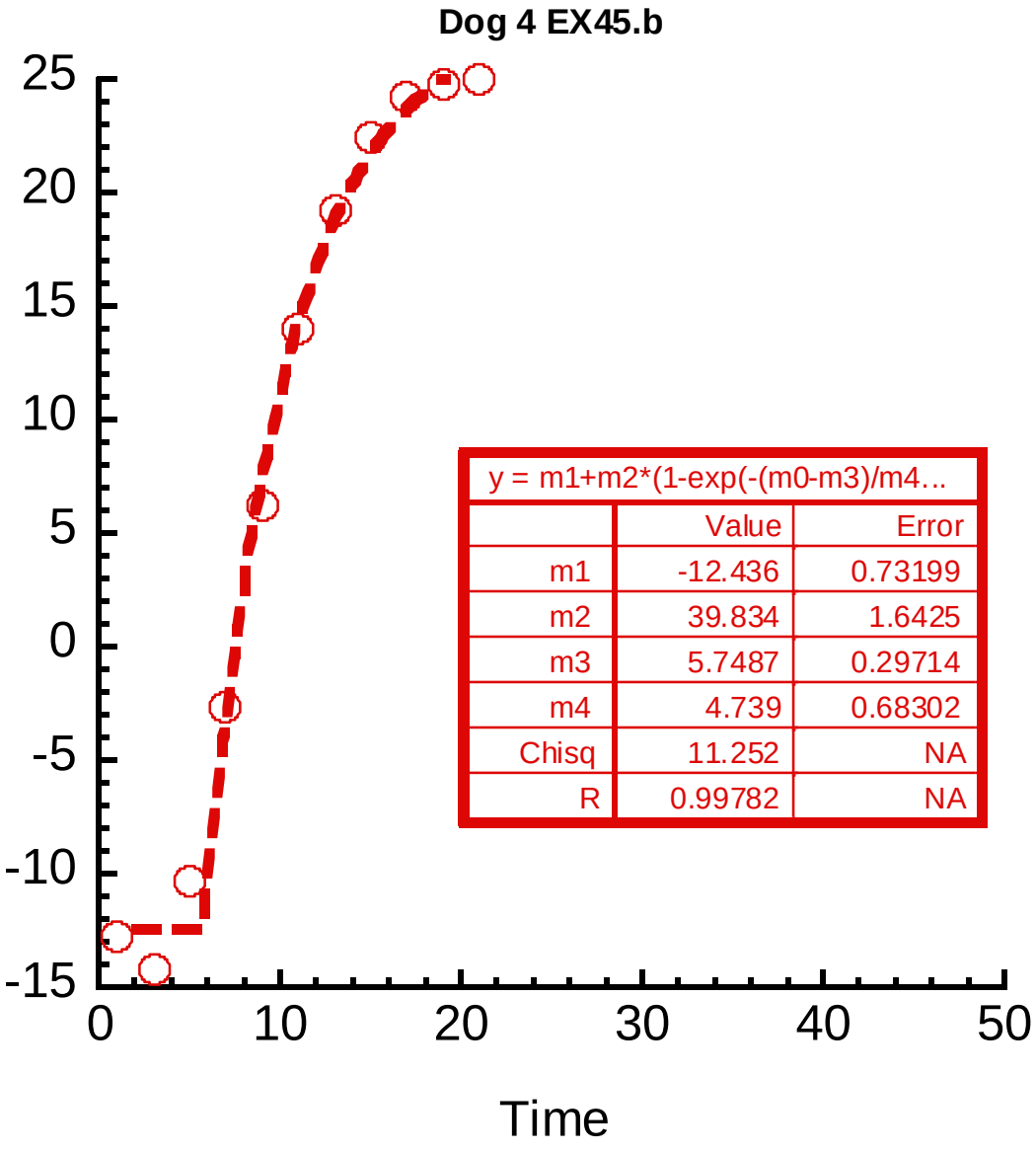
Dog 4 EX45.b
25
20
15
10
5
0
-5
-10
-15
0
10
20
30
40
50
Time
y = m1+m2*(1-exp(-(m0-m3)/m4...
Value
Error
m1
-12.436
0.73199
m2
39.834
1.6425
m3
5.7487
0.29714
m4
4.739
0.68302
Chisq
11.252
NA
R
0.99782
NA

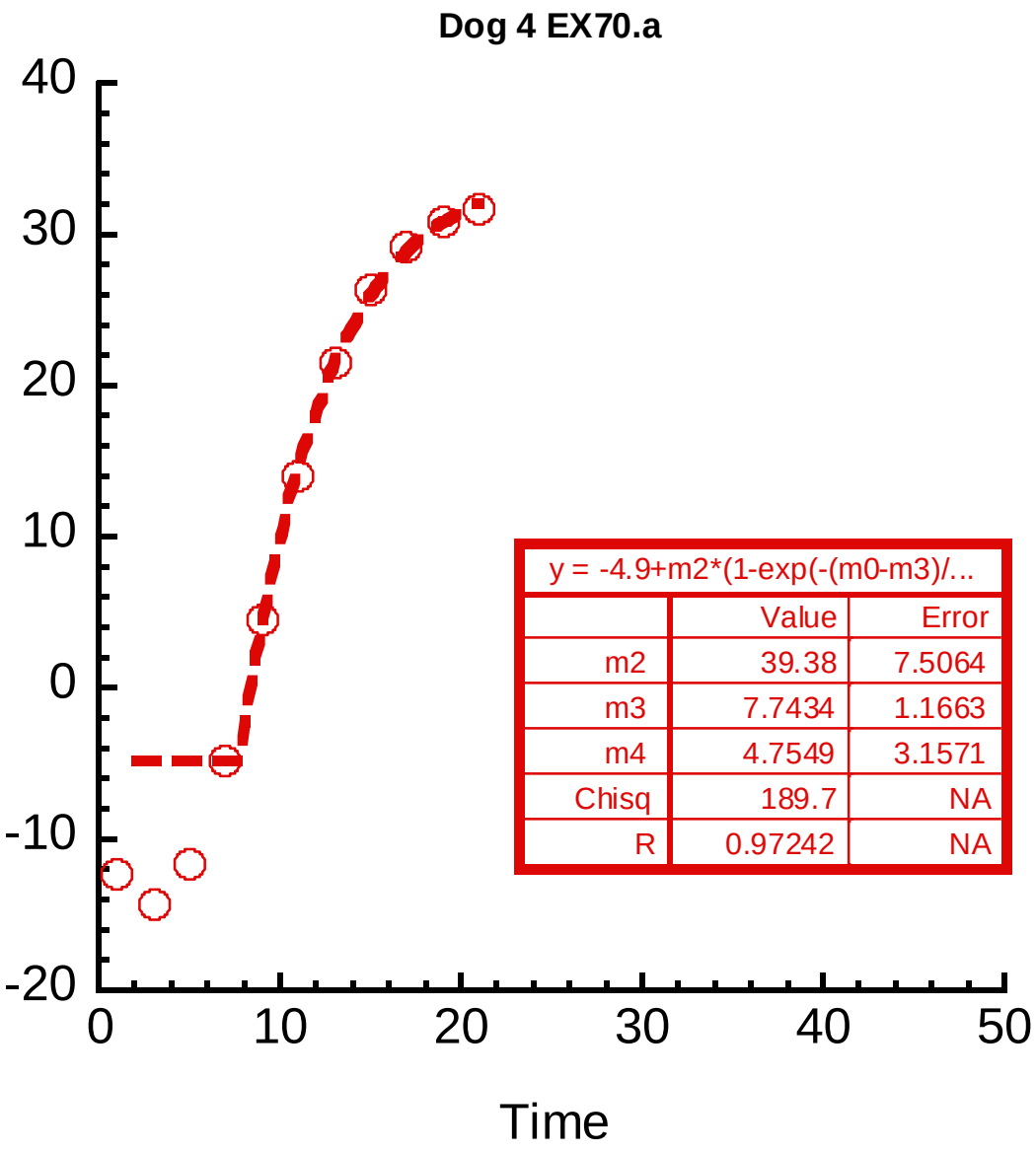
Dog 4 EX70.a
40
30
20
10
0
-10
-20
0
10
20
30
40
50
Time
y = -4.9+m2*(1-exp(-(m0-m3)/...
Value
Error
m2
39.38
7.5064
m3
7.7434
1.1663
m4
4.7549
3.1571
Chisq
189.7
NA
R
0.97242
NA

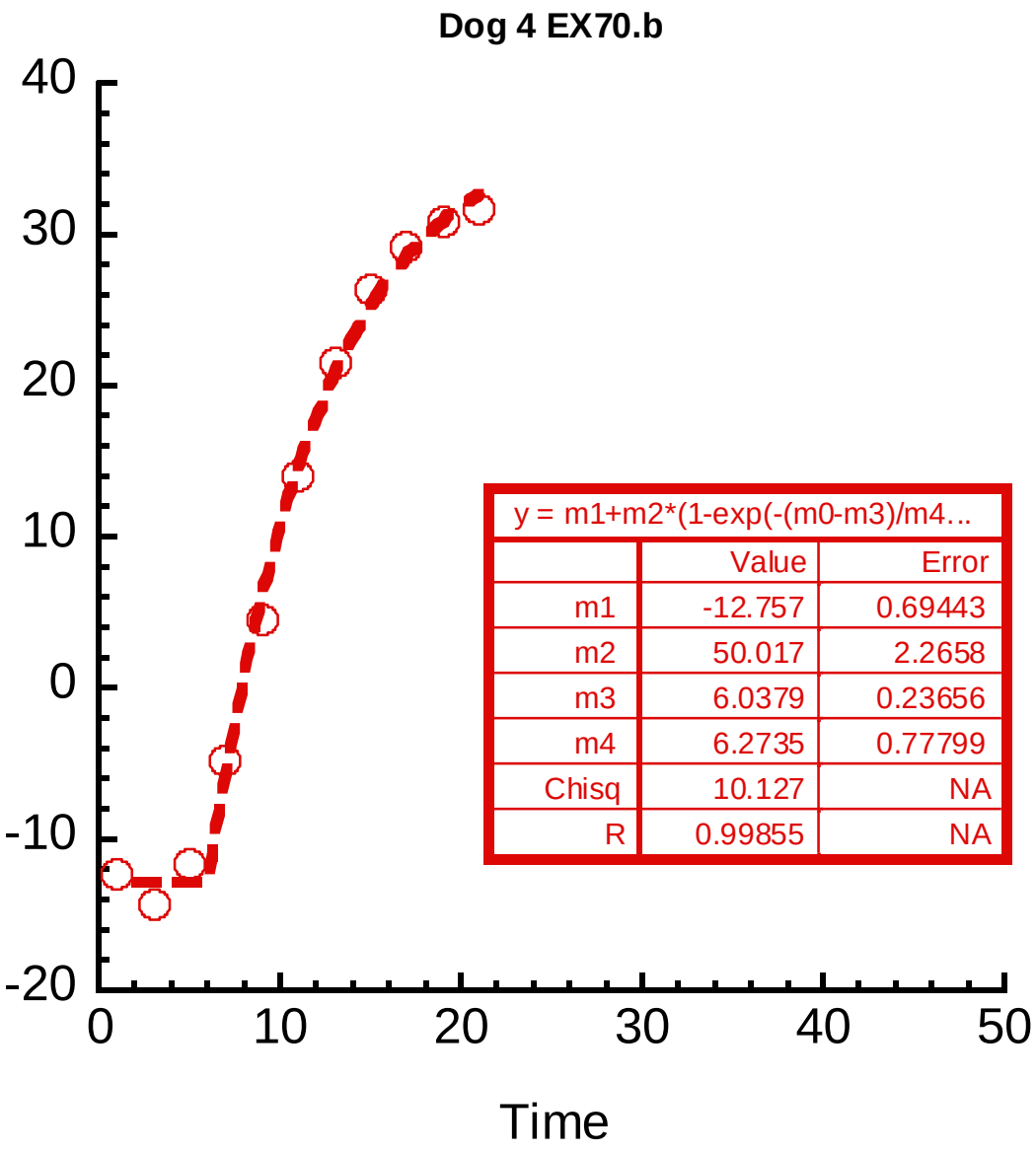
Dog 4 EX70.b
40
30
20
10
0
-10
-20
0
10
20
30
40
50
Time
y = m1+m2*(1-exp(-(m0-m3)/m4...
Value
Error
m1
-12.757
0.69443
m2
50.017
2.2658
m3
6.0379
0.23656
m4
6.2735
0.77799
Chisq
10.127
NA
R
0.99855
NA

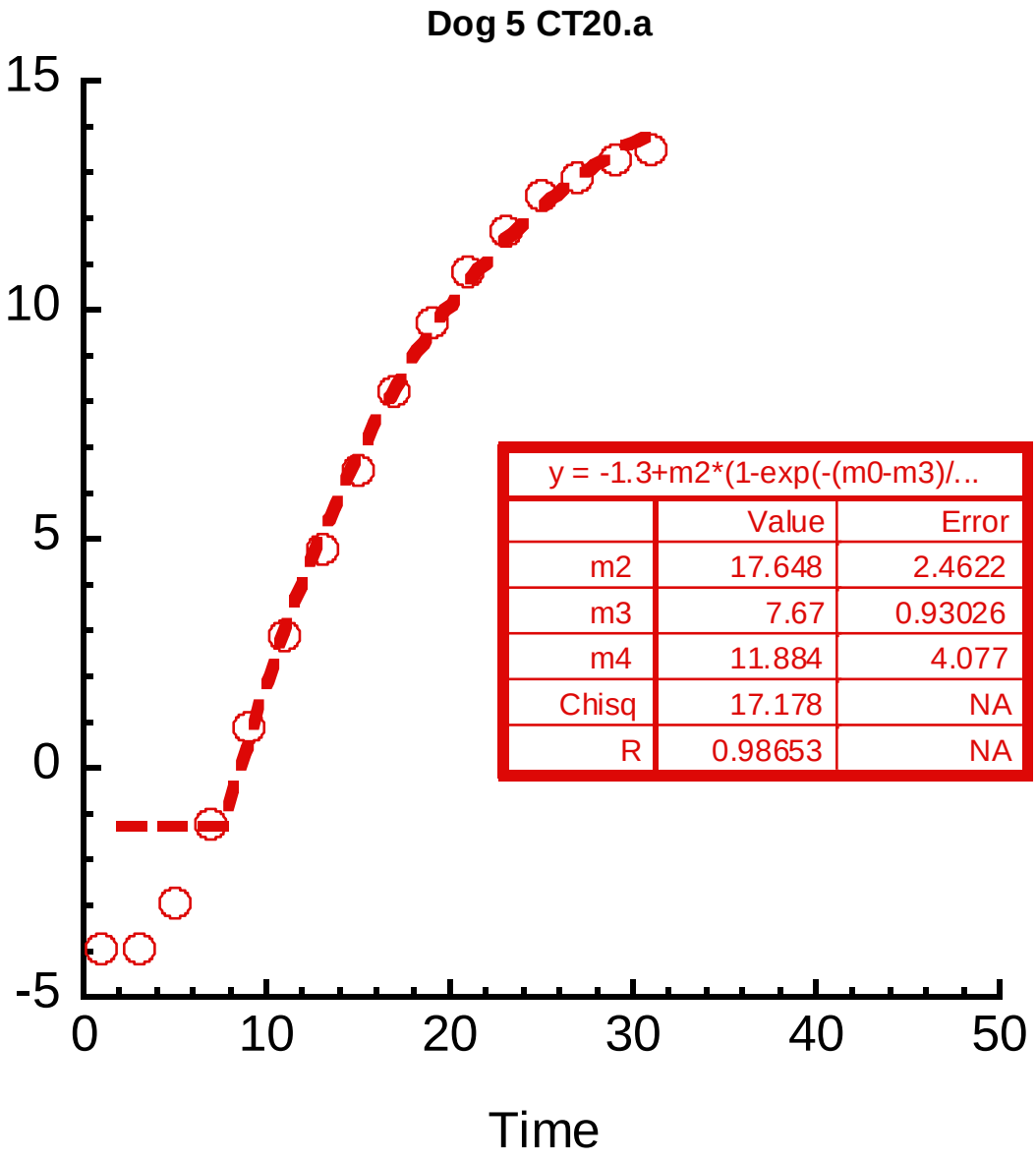
Dog 5 CT20.a
15
10
5
0
-5
0
10
20
30
40
50
Time
y = -1.3+m2*(1-exp(-(m0-m3)/...
Value
Error
m2
17.648
2.4622
m3
7.67
0.93026
m4
11.884
4.077
Chisq
17.178
NA
R
0.98653
NA

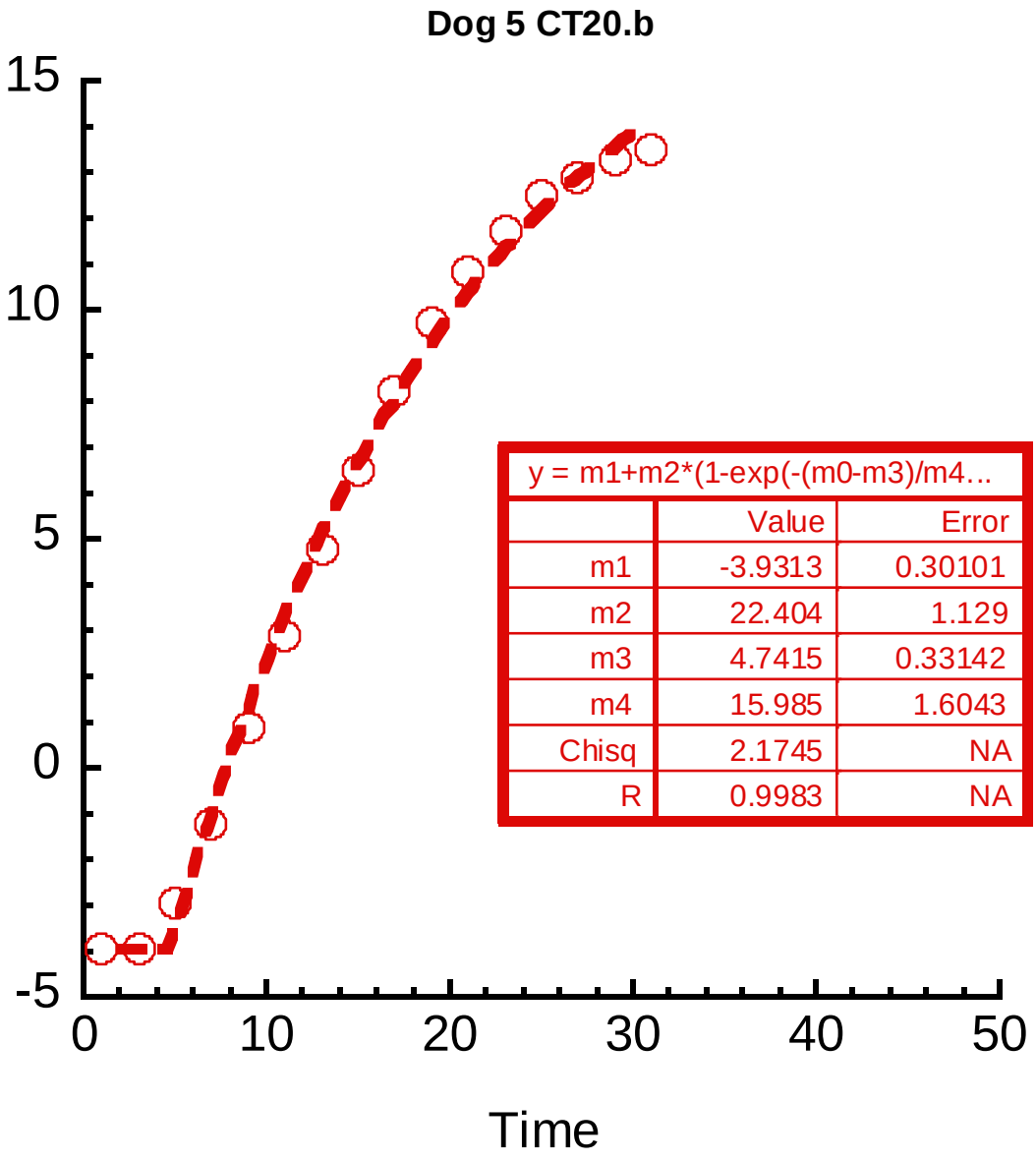
Dog 5 CT20.b
15
10
5
0
-5
0
10
20
30
40
50
Time
y = m1+m2*(1-exp(-(m0-m3)/m4...
Value
Error
m1
-3.9313
0.30101
m2
22.404
1.129
m3
4.7415
0.33142
m4
15.985
1.6043
Chisq
2.1745
NA
R
0.9983
NA

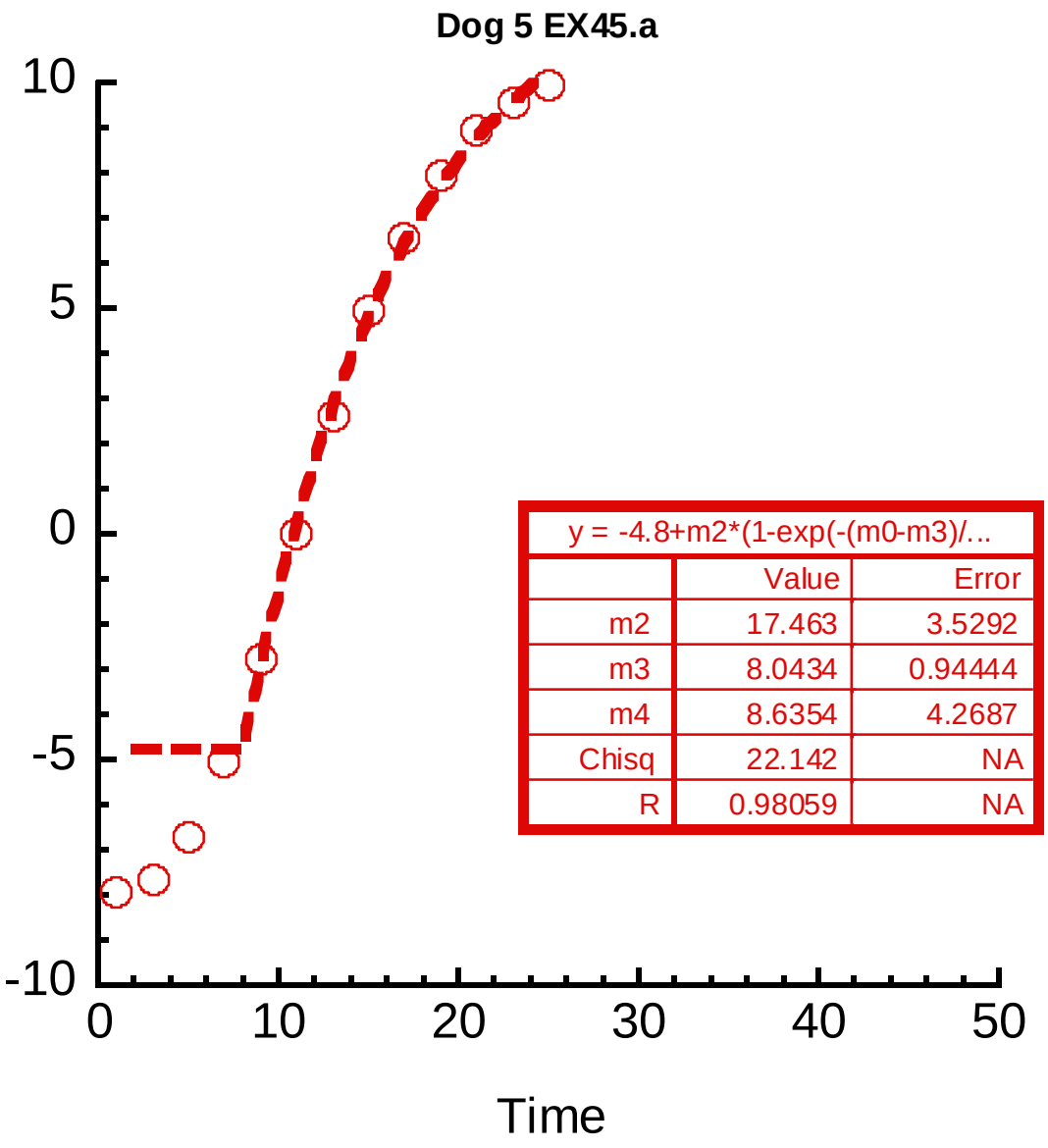
Dog 5 EX45.a
10
5
0
-5
-10
0
10
20
30
40
50
Time
y = -4.8+m2*(1-exp(-(m0-m3)/...
Value
Error
m2
17.463
3.5292
m3
8.0434
0.94444
m4
8.6354
4.2687
Chisq
22.142
NA
R
0.98059
NA

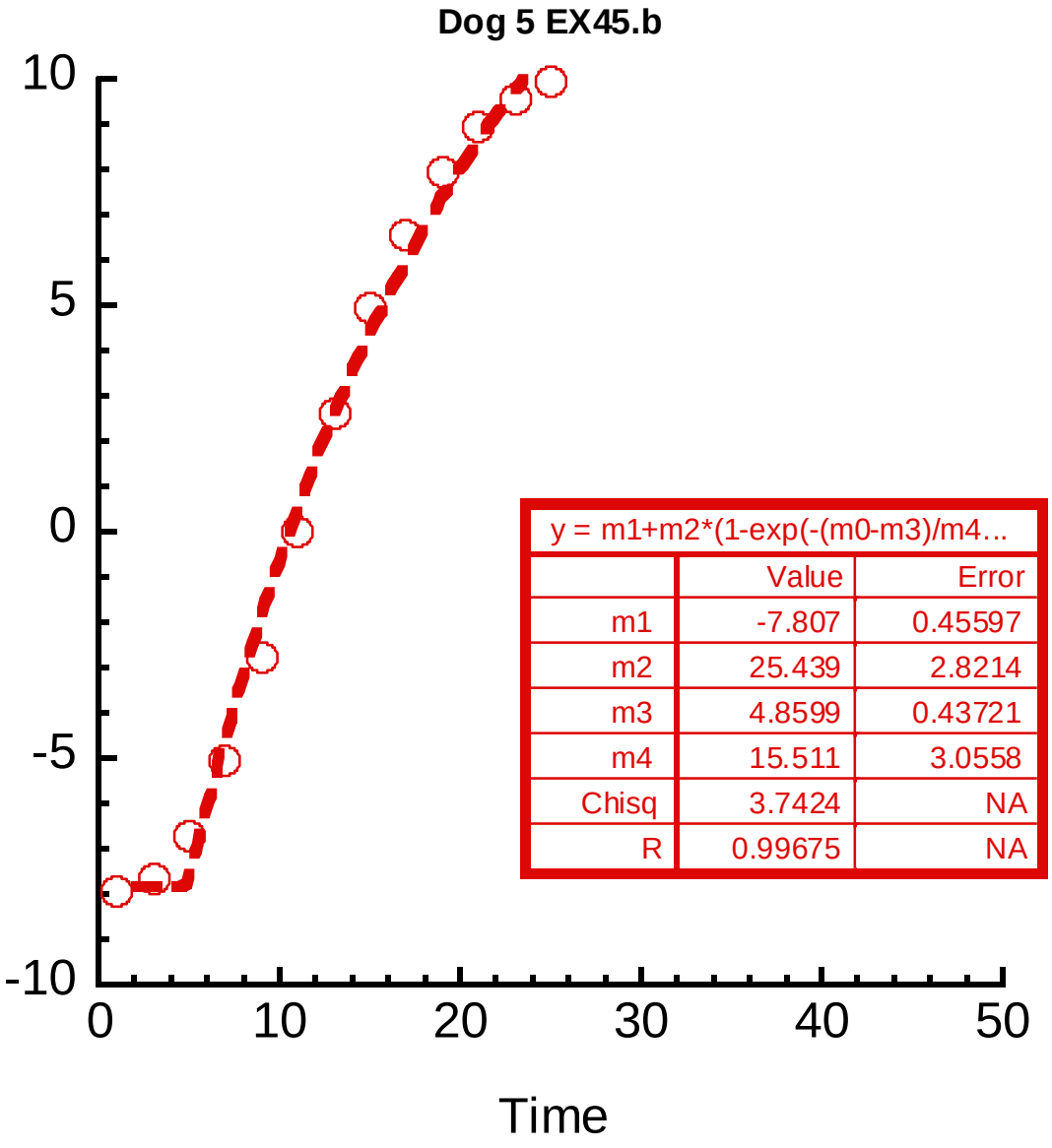
Dog 5 EX45.b
10
5
0
-5
-10
0
10
20
30
40
50
Time
y = m1+m2*(1-exp(-(m0-m3)/m4...
Value
Error
m1
-7.807
0.45597
m2
25.439
2.8214
m3
4.8599
0.43721
m4
15.511
3.0558
Chisq
3.7424
NA
R
0.99675
NA

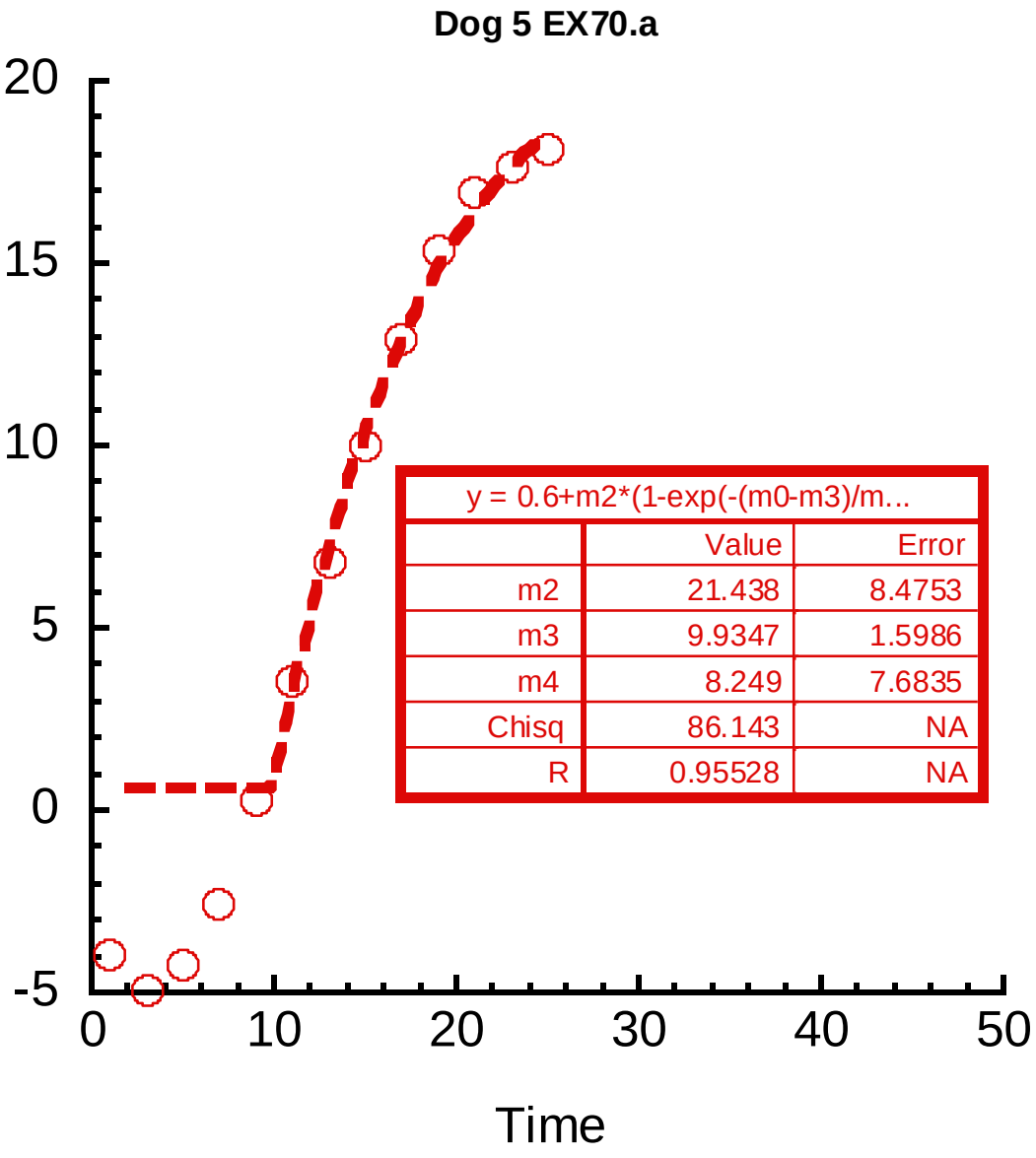
Dog 5 EX70.a
20
15
10
5
0
-5
0
10
20
30
40
50
Time
y = 0.6+m2*(1-exp(-(m0-m3)/m...
Value
Error
m2
21.438
8.4753
m3
9.9347
1.5986
m4
8.249
7.6835
Chisq
86.143
NA
R
0.95528
NA

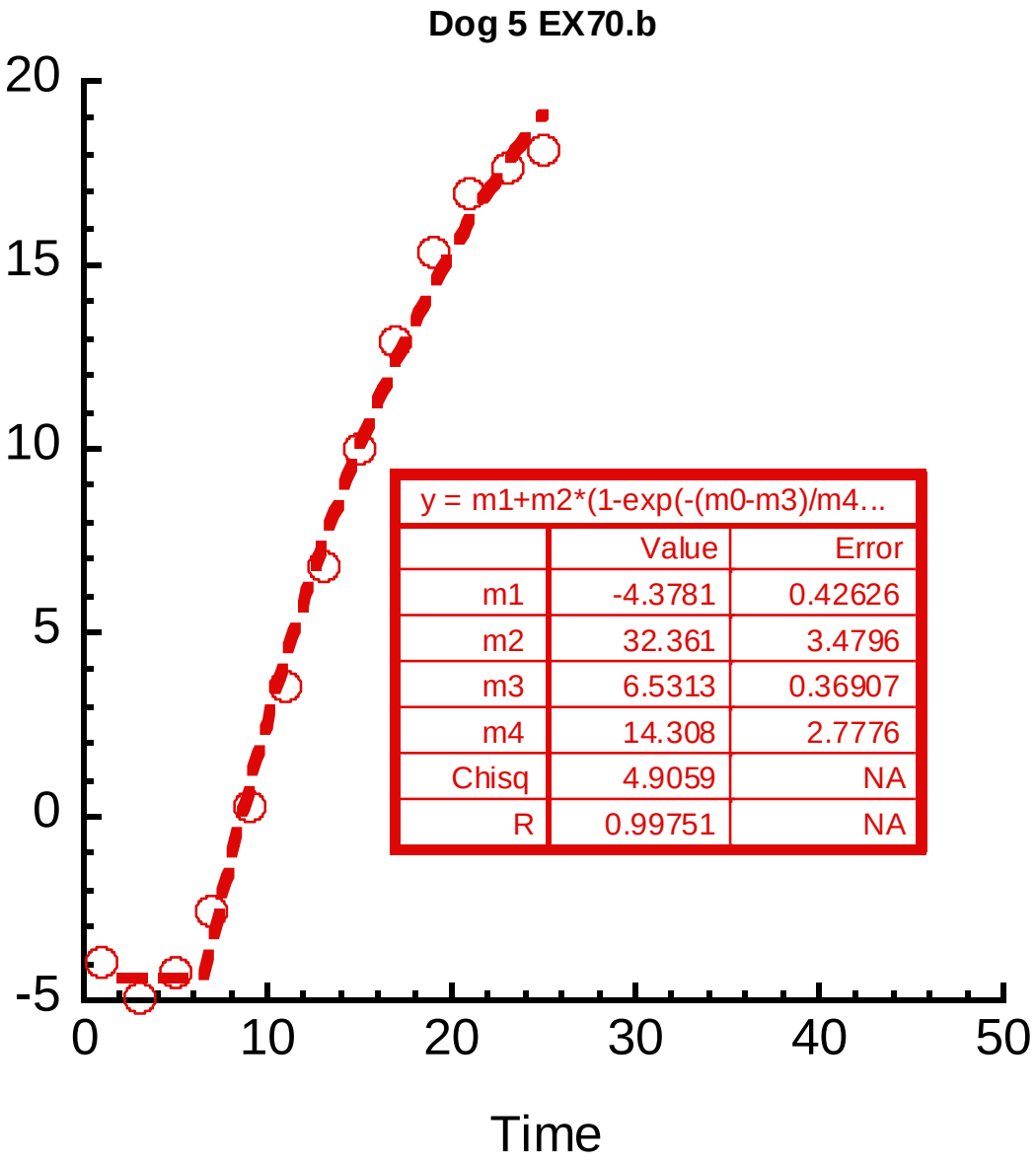
Dog 5 EX70.b
20
15
10
5
0
-5
0
10
20
30
40
50
Time
y = m1+m2*(1-exp(-(m0-m3)/m4...
Value
Error
m1
-4.3781
0.42626
m2
32.361
3.4796
m3
6.5313
0.36907
m4
14.308
2.7776
Chisq
4.9059
NA
R
0.99751
NA

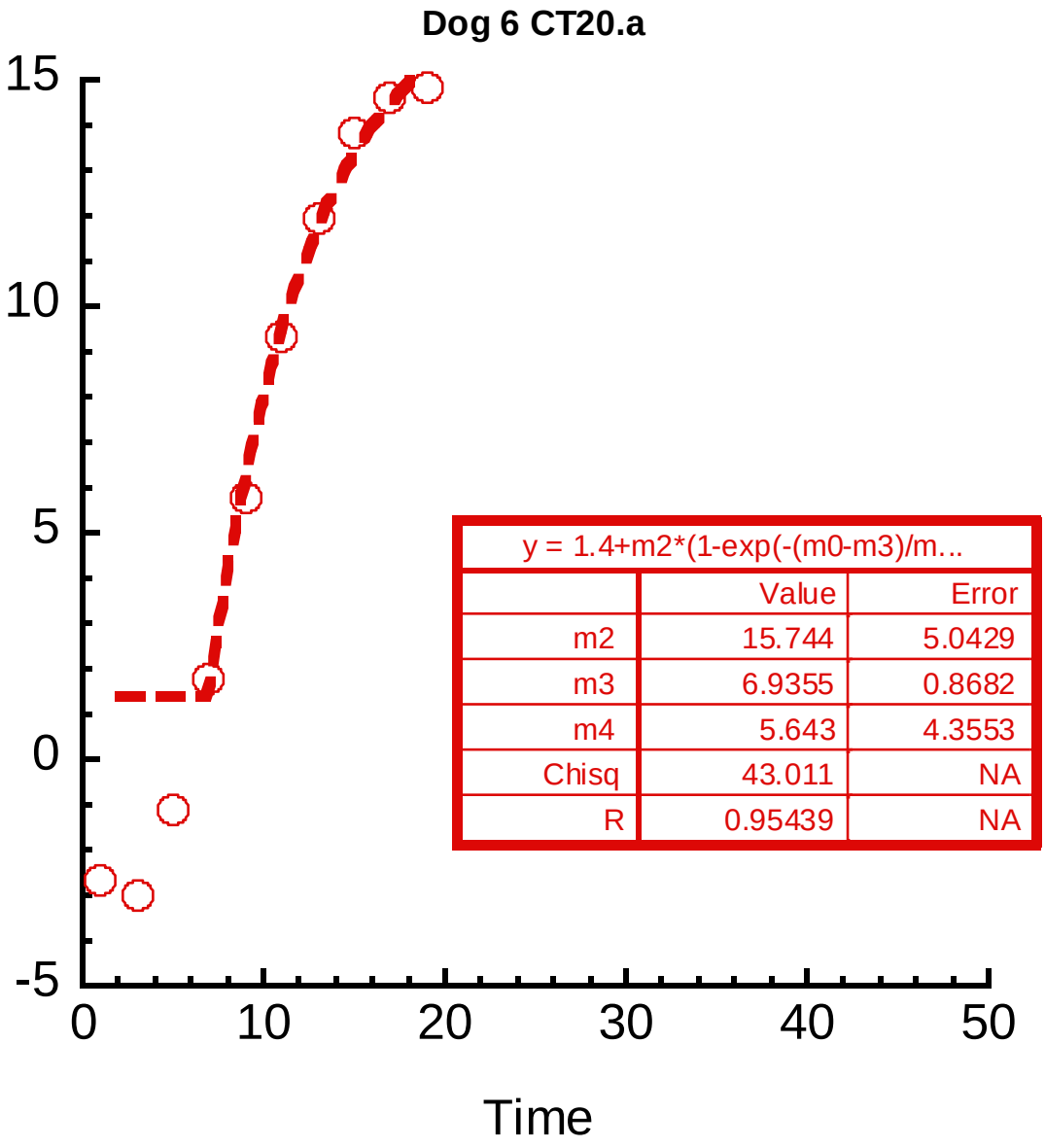
Dog 6 CT20.a
15
10
5
0
-5
0
10
20
30
40
50
Time
y = 1.4+m2*(1-exp(-(m0-m3)/m...
Value
Error
m2
15.744
5.0429
m3
6.9355
0.8682
m4
5.643
4.3553
Chisq
43.011
NA
R
0.95439
NA

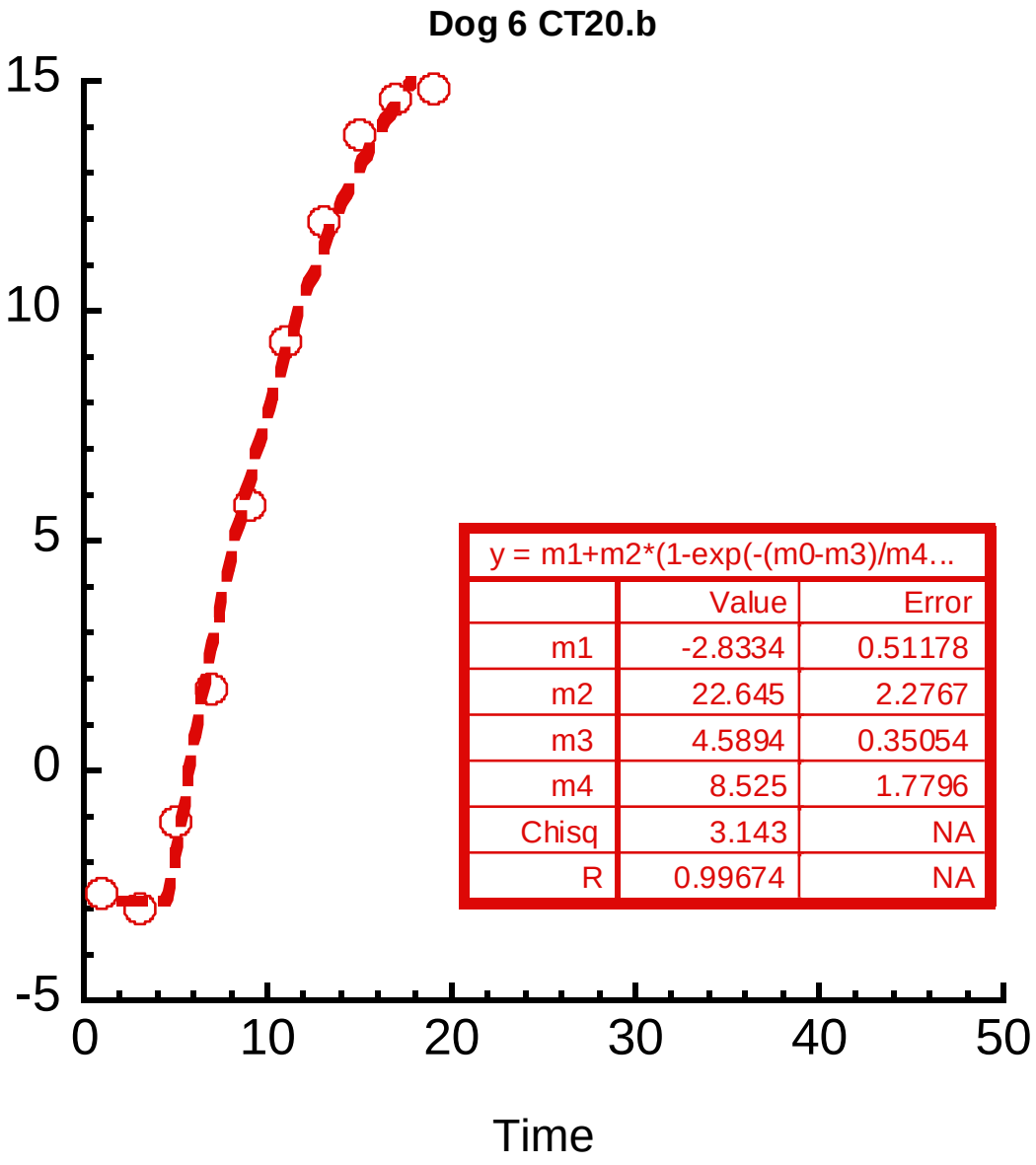
Dog 6 CT20.b
15
10
5
0
-5
0
10
20
30
40
50
Time
y = m1+m2*(1-exp(-(m0-m3)/m4...
Value
Error
m1
-2.8334
0.51178
m2
22.645
2.2767
m3
4.5894
0.35054
m4
8.525
1.7796
Chisq
3.143
NA
R
0.99674
NA

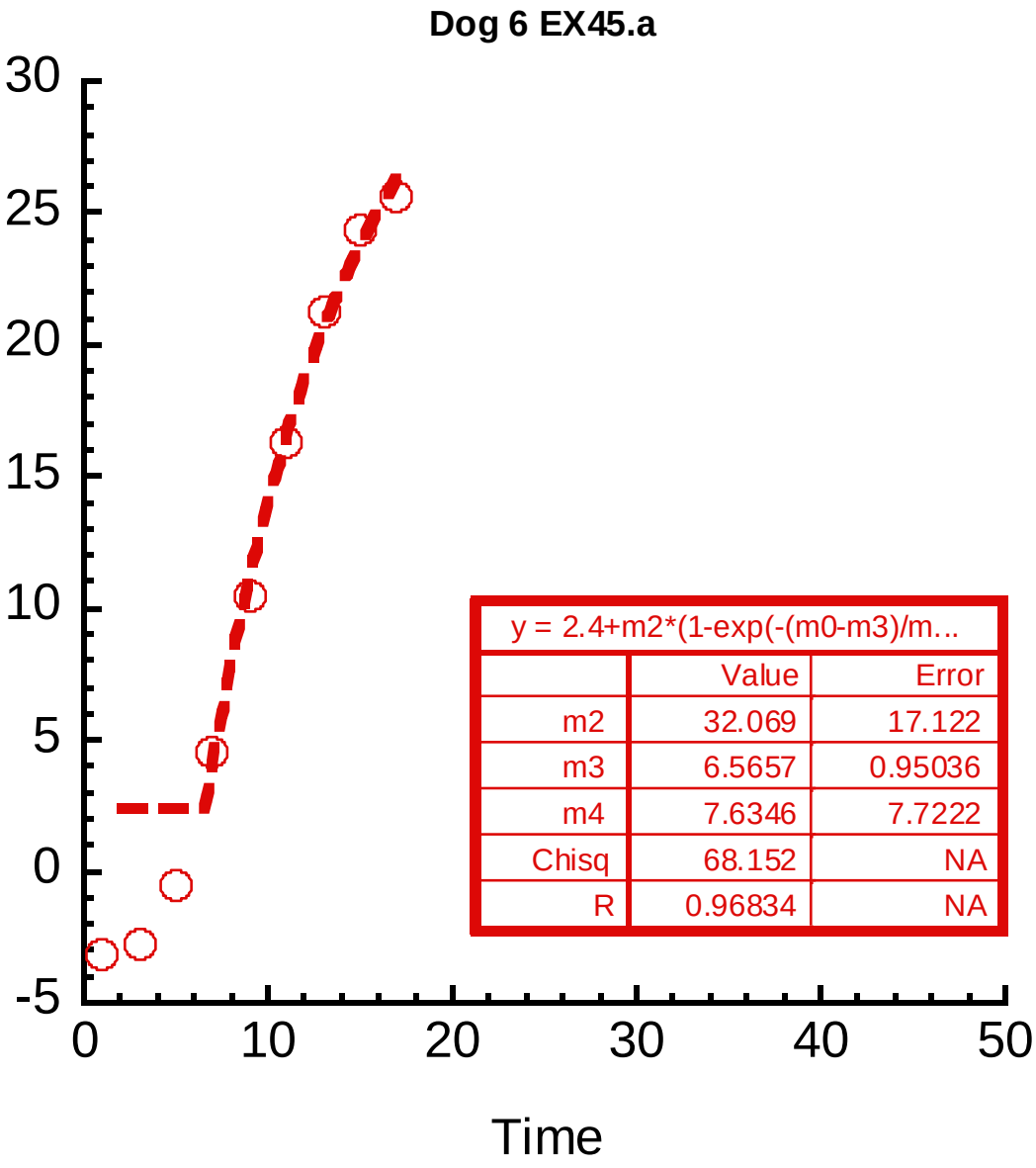
Dog 6 EX45.a
30
25
20
15
10
5
0
-5
0
10
20
30
40
50
Time
y = 2.4+m2*(1-exp(-(m0-m3)/m...
Value
Error
m2
32.069
17.122
m3
6.5657
0.95036
m4
7.6346
7.7222
Chisq
68.152
NA
R
0.96834
NA

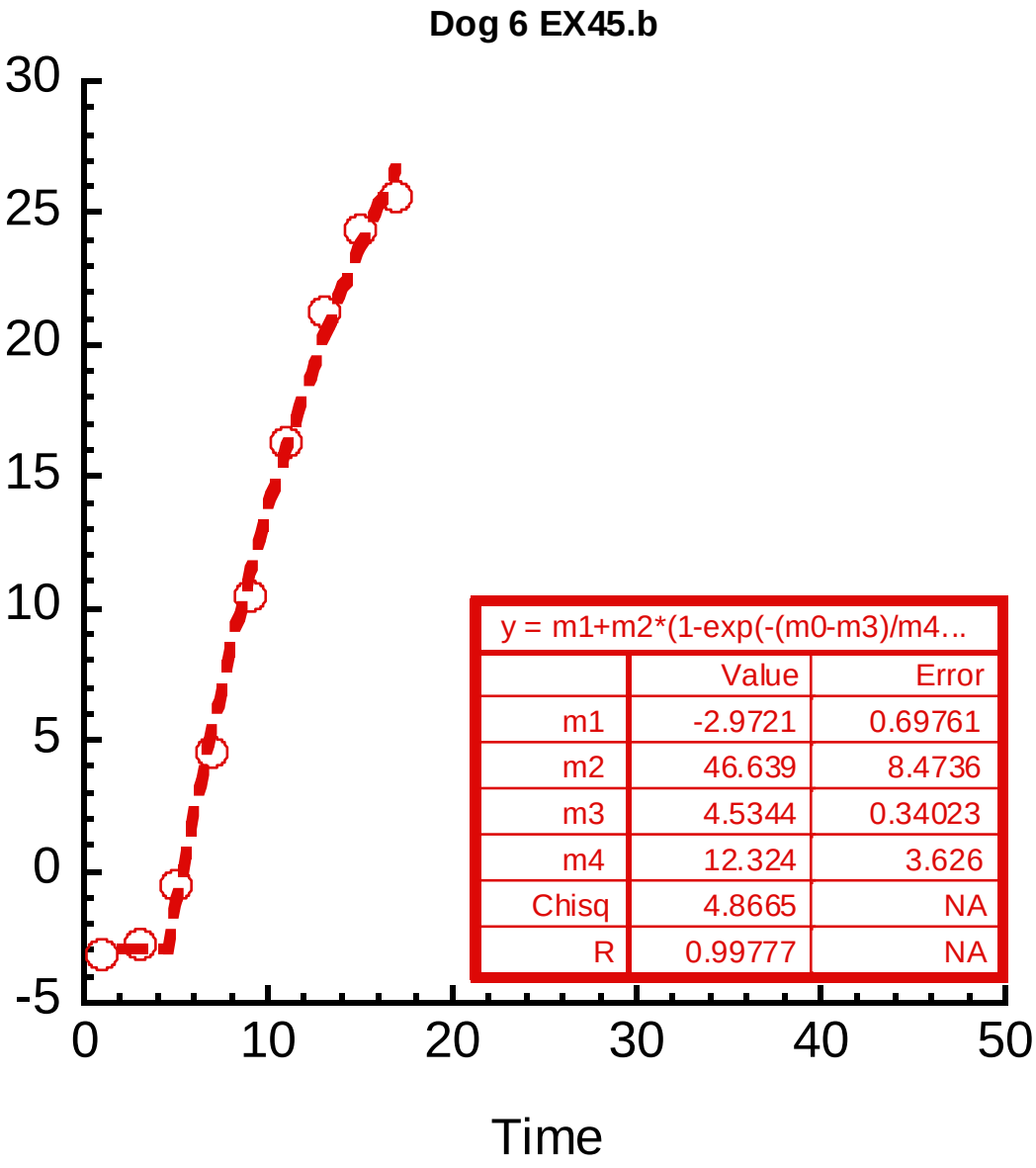
Dog 6 EX45.b
30
25
20
15
10
5
0
-5
0
10
20
30
40
50
Time
y = m1+m2*(1-exp(-(m0-m3)/m4...
Value
Error
m1
-2.9721
0.69761
m2
46.639
8.4736
m3
4.5344
0.34023
m4
12.324
3.626
Chisq
4.8665
NA
R
0.99777
NA

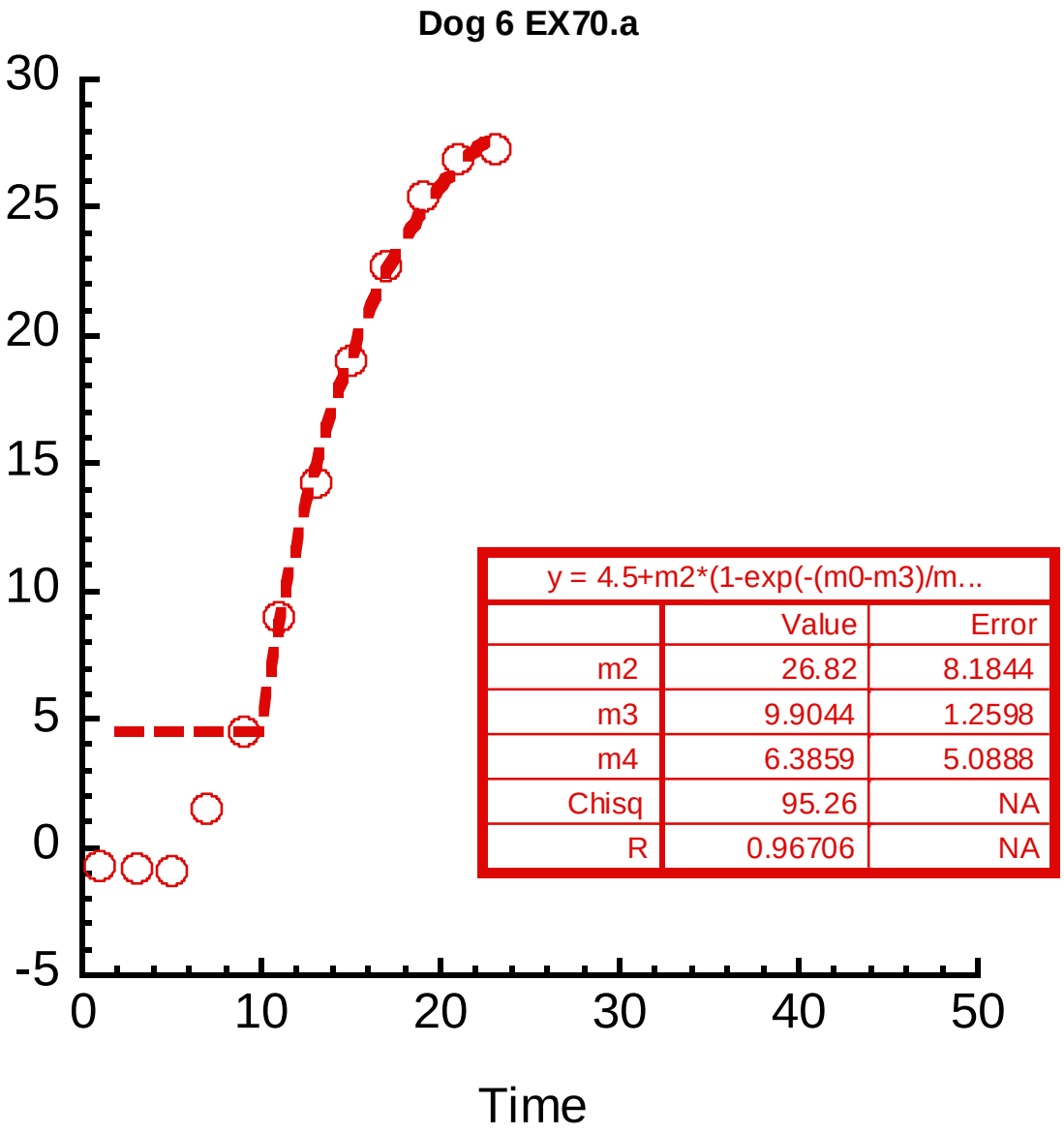
Dog 6 EX70.a
30
25
20
15
10
5
0
-5
0
10
20
30
40
50
Time
y = 4.5+m2*(1-exp(-(m0-m3)/m...
Value
Error
m2
26.82
8.1844
m3
9.9044
1.2598
m4
6.3859
5.0888
Chisq
95.26
NA
R
0.96706
NA

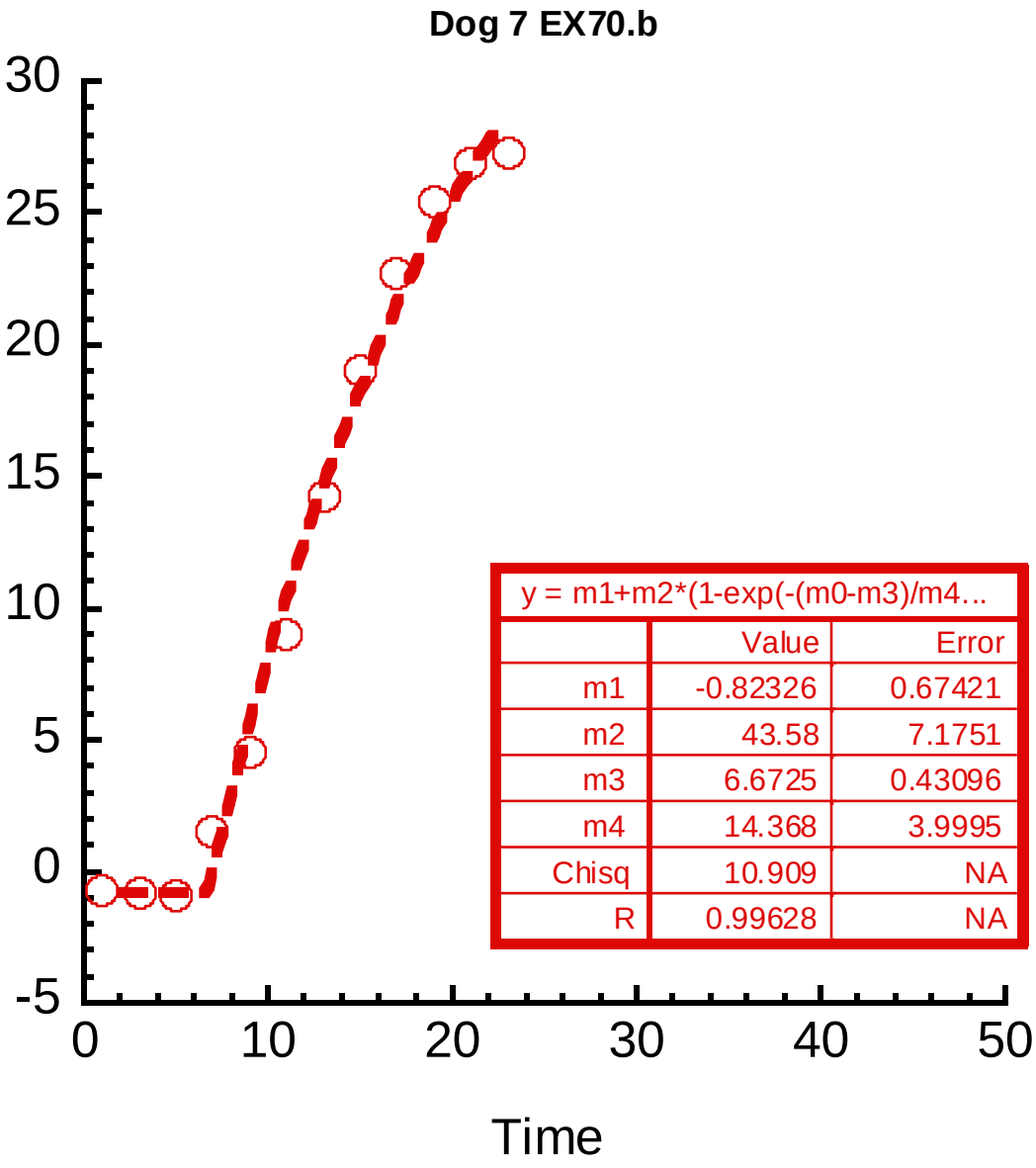
Dog 7 EX70.b
30
25
20
15
10
5
0
-5
0
10
20
30
40
50
Time
y = m1+m2*(1-exp(-(m0-m3)/m4...
Value
Error
m1
-0.82326
0.67421
m2
43.58
7.1751
m3
6.6725
0.43096
m4
14.368
3.9995
Chisq
10.909
NA
R
0.99628
NA

FORCE GRAPHS

DATA WERE AVERAGED OVER EACH CONTRACTION

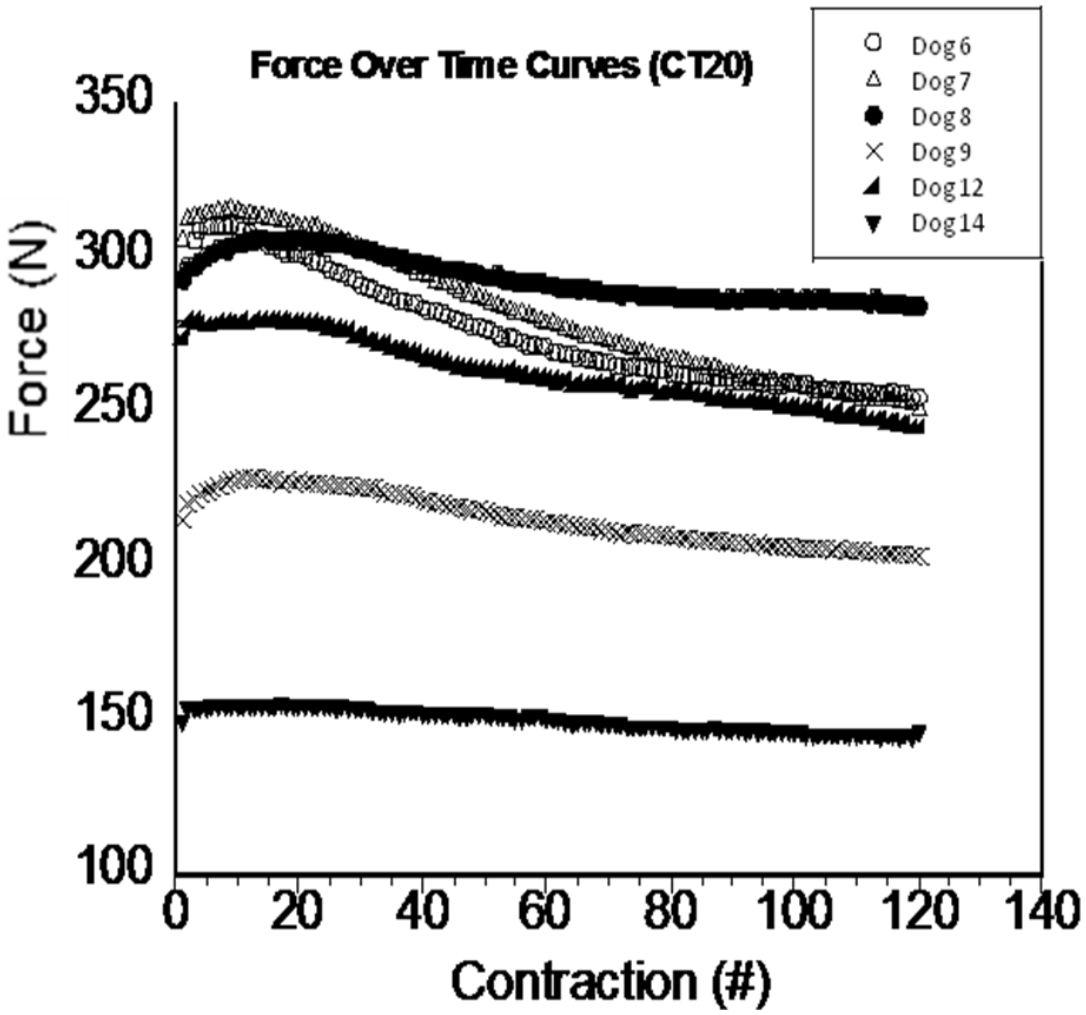
Force Over Time Curves (CT20)
Dog 6
Dog 7
Dog 8
Dog 9
Dog 12
Dog 14
Force (N)
350
300
250
200
150
100
0
20
40
60
80
100
120
140
Contraction (#)

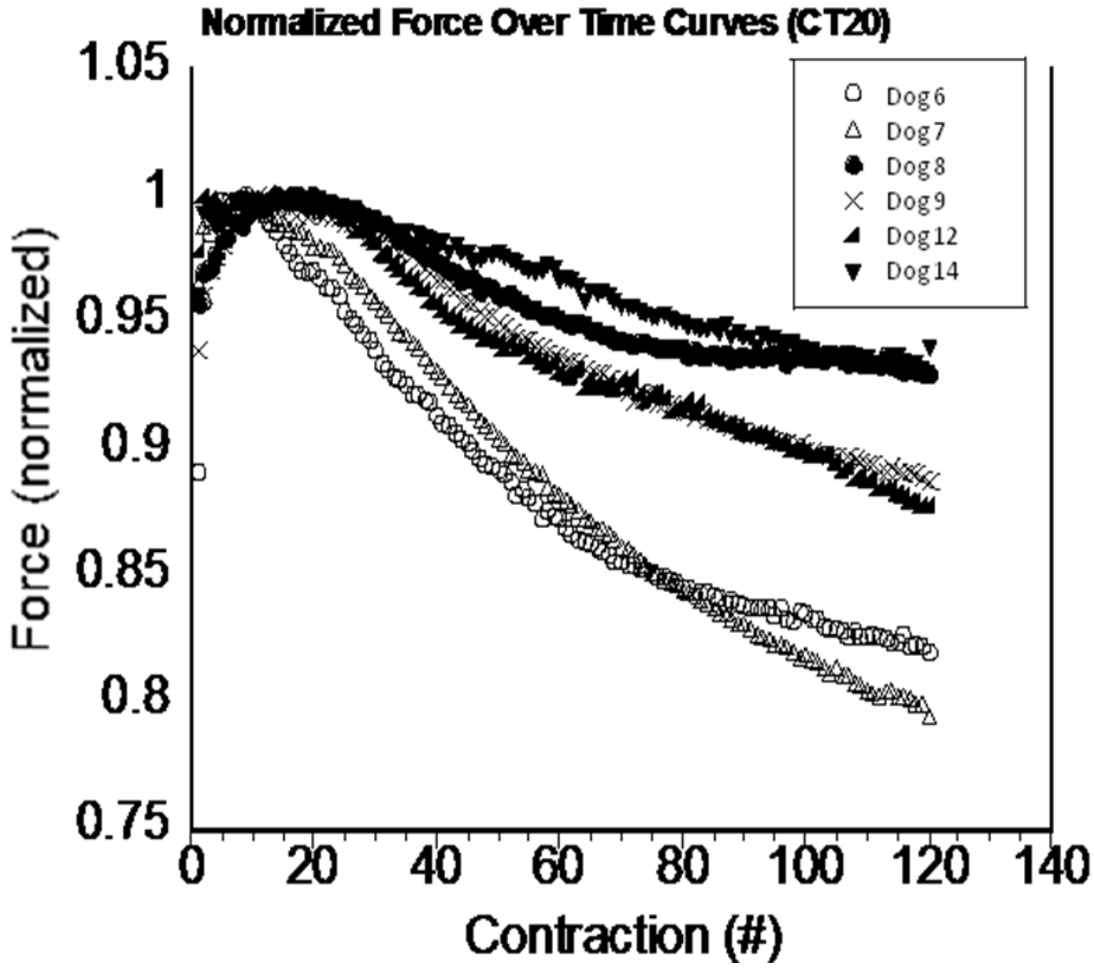
Normalized Force Over Time Curves (CT20)
Force (normalized)
1.05
1
0.95
0.9
0.85
0.8
0.75
0
20
40
60
80
100
120
140
Contraction (#)
Dog 6
Dog 7
Dog 8
Dog 9
Dog 12
Dog 14

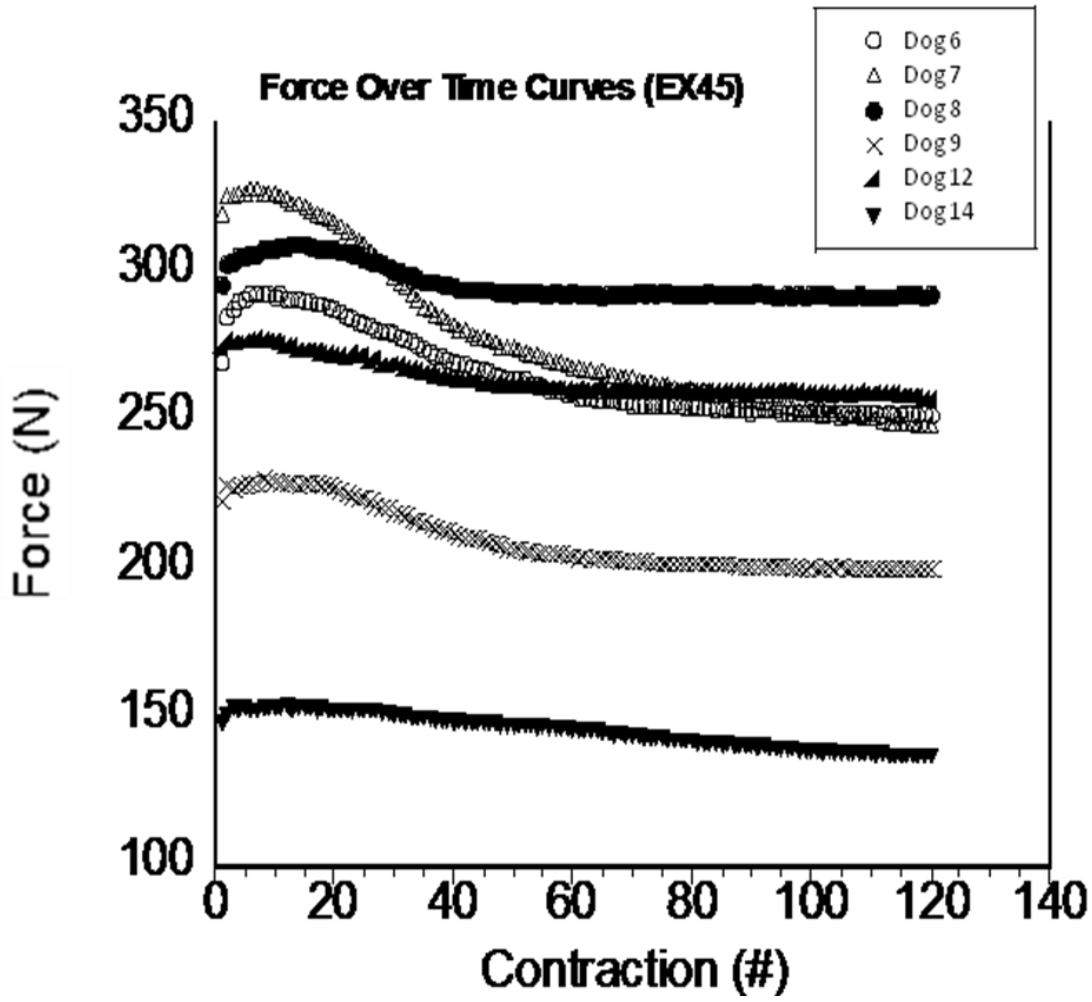
Force Over Time Curves (EX45)
Dog 6
Dog 7
Dog 8
Dog 9
Dog 12
Dog 14
Force (N)
350
300
250
200
150
100
0
20
40
60
80
100
120
140
Contraction (#)

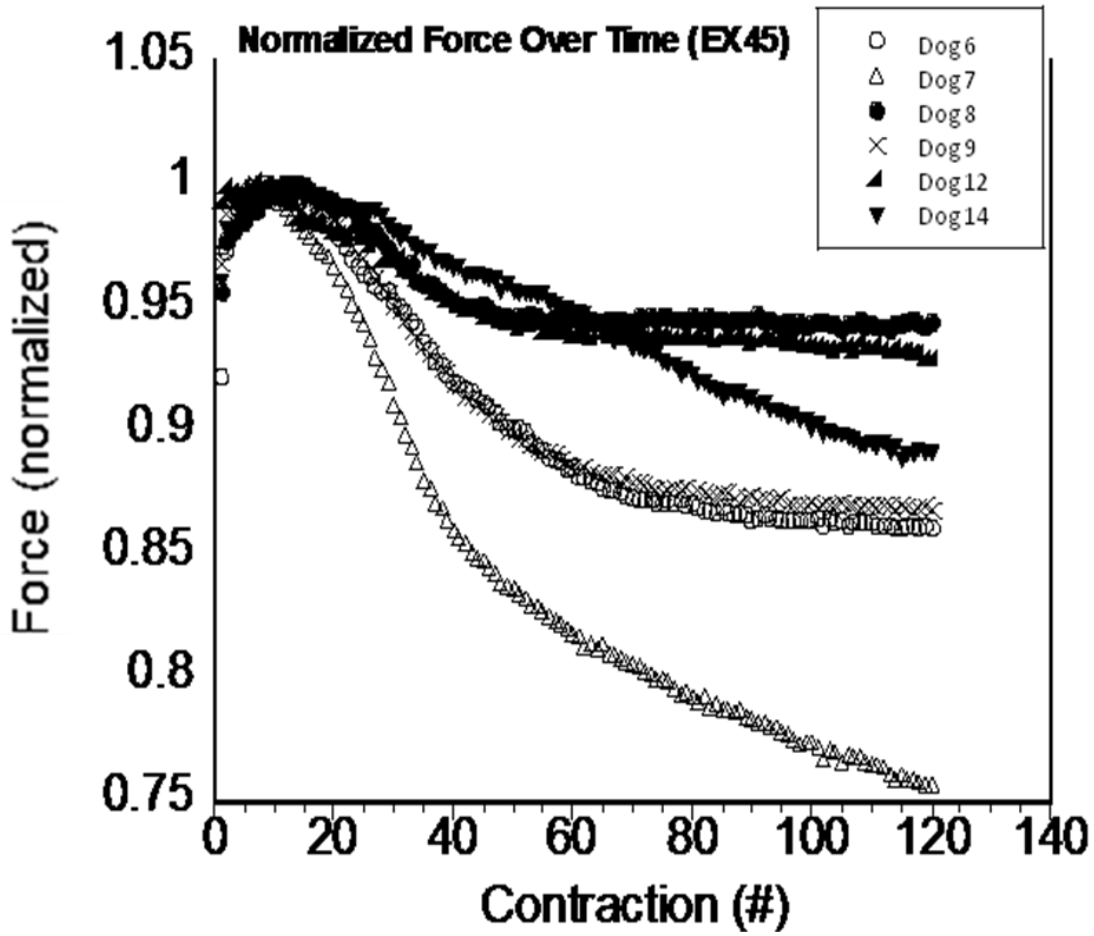
Normalized Force Over Time (EX45)
Dog 6
Dog 7
Dog 8
Dog 9
Dog 12
Dog 14
Force (normalized)
1.05
1
0.95
0.9
0.85
0.8
0.75
0
20
40
60
80
100
120
140
Contraction (#)

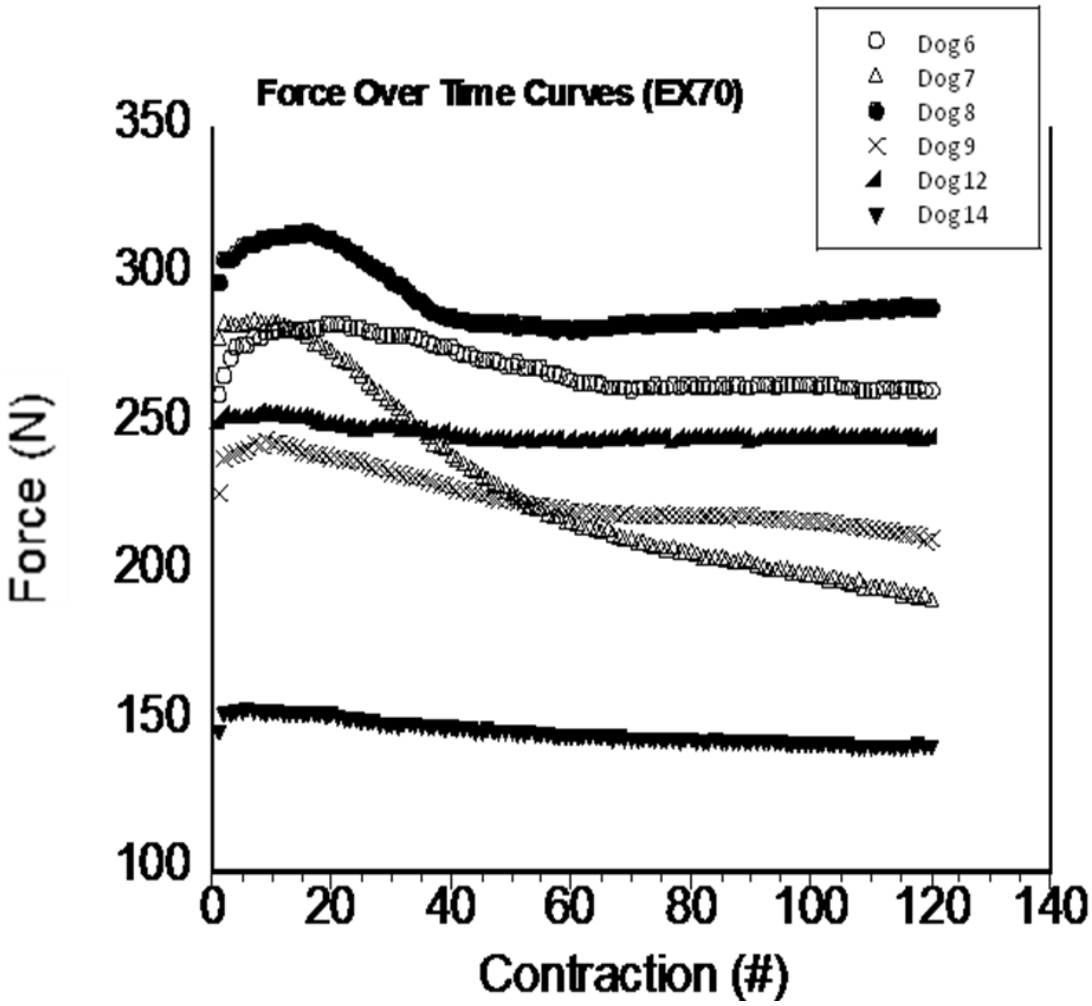
Force Over Time Curves (EX70)
Dog 6
Dog 7
Dog 8
Dog 9
Dog 12
Dog 14
350
300
250
200
150
100
Force (N)
0
20
40
60
80
100
120
140
Contraction (#)

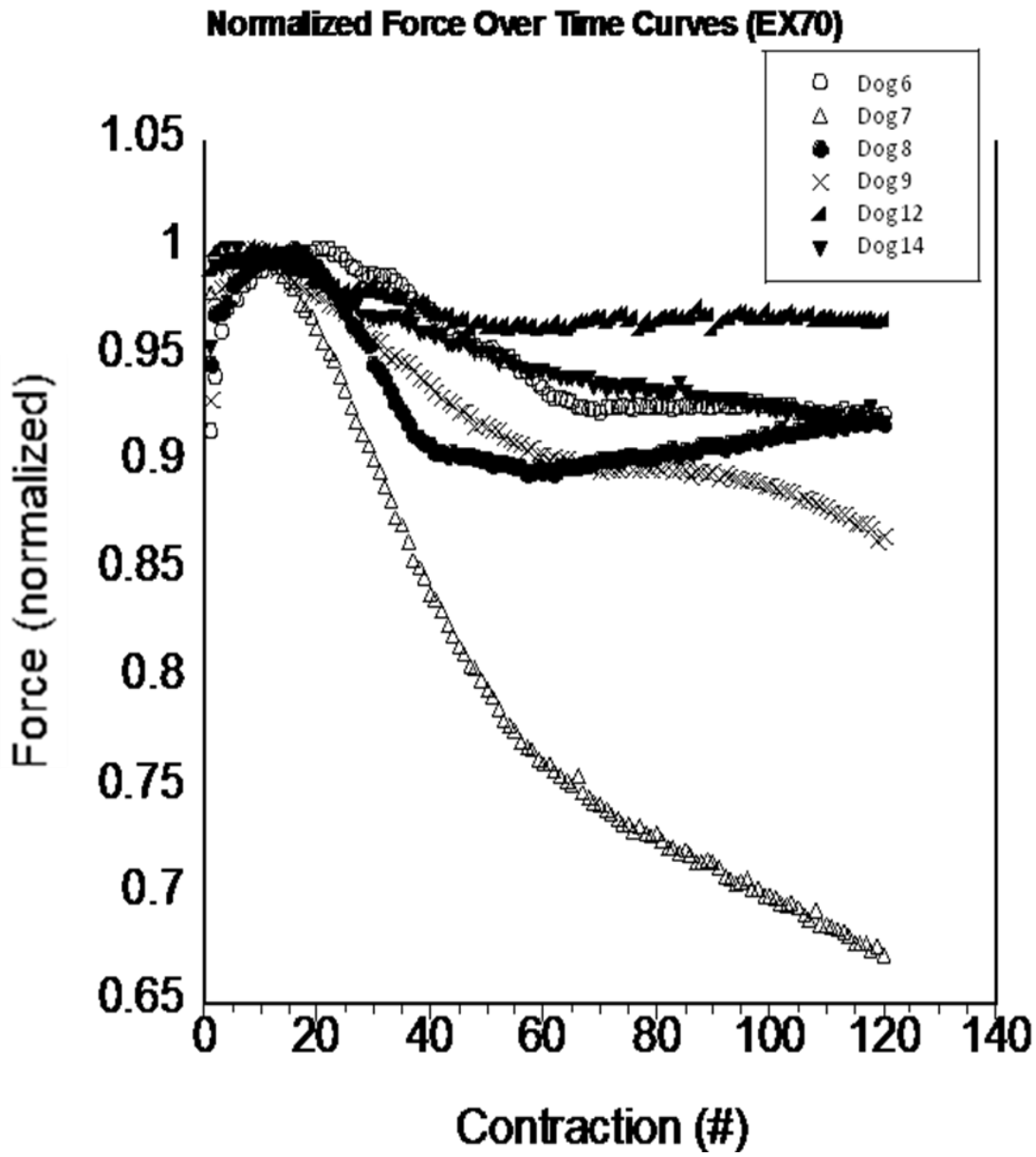
Normalized Force Over Time Curves (EX70)
Dog 6
Dog 7
Dog 8
Dog 9
Dog 12
Dog 14
1.05
1
0.95
0.9
0.85
0.8
0.75
0.7
0.65
Force (normalized)
0
20
40
60
80
100
120
140
Contraction (#)

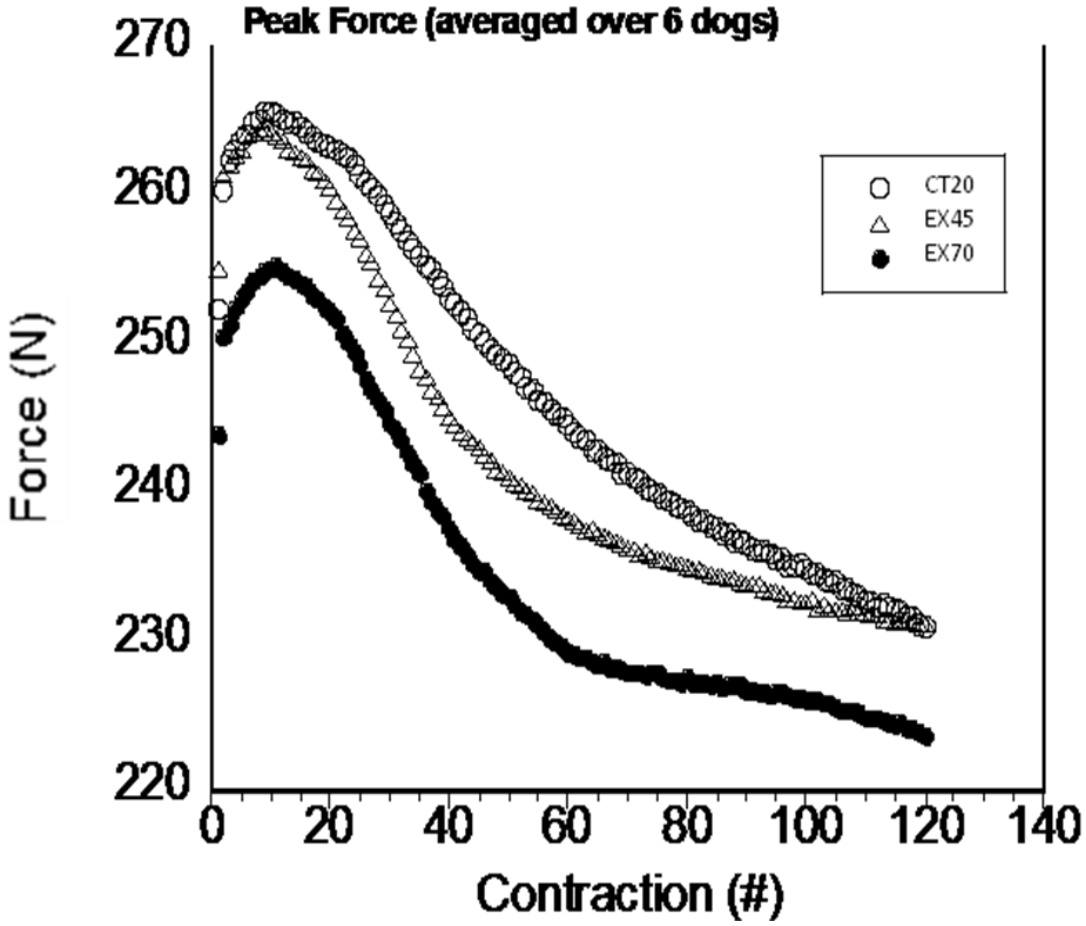
Peak Force (averaged over 6 dogs)
270
260
250
240
230
220
Force (N)
0
20
40
60
80
100
120
140
Contraction (#)
CT20
EX45
EX70

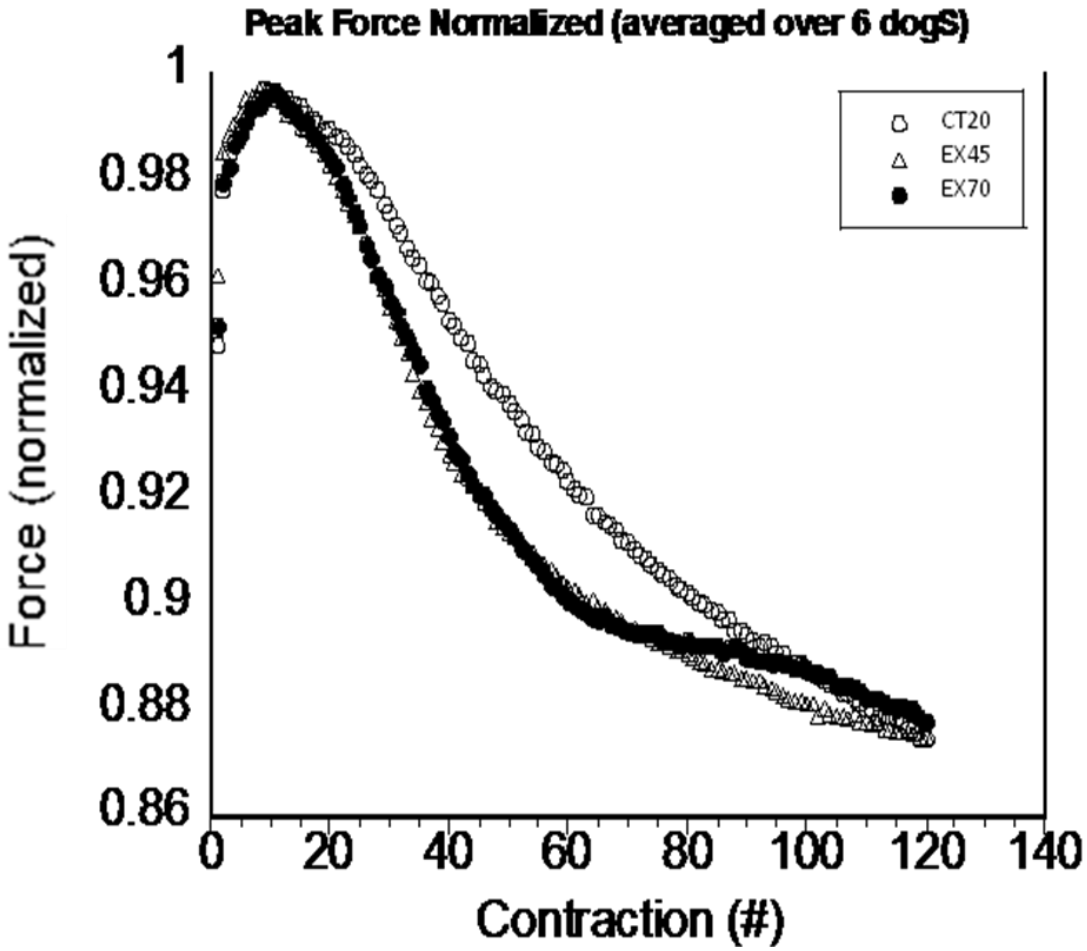
Peak Force Normalized (averaged over 6 dogS)
Force (normalized)
1
0.98
0.96
0.94
0.92
0.9
0.88
0.86
0
20
40
60
80
100
120
140
Contraction (#)
CT20
EX45
EX70

APPENDIX C

Selected Lab Manual Notes

In all lab notebooks the trials are listed as CT1, CT2, EX25, and EX50. We subsequently have named these CT (when mentioned), CT20, EX45, and EX70 for clarity. Also, 14 dogs were used in these experiments. Dogs 1-5 served as pilot animals, and dogs 6-14 were experimental animals. As you will see, dogs 6, 7, 8, 9, 12, and 14 ended up being the animals used for final analysis. These animals were subsequently renumbered as 1, 2, 3, 4, 5, and 6. Finally, we had some difficulty in regulating blood gases and blood pH throughout the experiments, usually having to administer bicarbonate and O_2 throughout, as well as altering the breathing rate. As can be seen, keeping these animals alive throughout the day of experiments also proved to be a substantial challenge. Toward the end of the experiments we began to worry that perhaps the tubes were not getting clean enough and we replaced all tubing.

Dog 1 (6/19/08) – Difficult day. During the first trial (CT1 in log book), the indwelling oximeter shut off because it went too low (below 0). From here forward we played the game of setting the oximeter as high as possible (95-100) before a trial to be sure it doesn't bottom out (all trials are calibrated based on the Co-Ox Machine and blood samples, so it doesn't matter what the oximeter tells use during the trial so long as we get data). During CT2 I set the steady state flow to the wrong number and thus we had to abort trial. Toward the end of the day we tried to do some additional "flow steps" to help in future determining of metabolic turn-on time and noticed that the muscle had become edematous (and perhaps it was already a bit like this during EX70?). Today we experienced our first trouble "calculating blood flow tau" after CT1 and having it ready for the next trial. Also, we had some trouble with resting blood flow pressure before and after contractions (after contractions, it seems to take a higher blood flow to maintain a decent perfusion pressure of muscle).

Dog 2 (6/20/08) – More difficulties of fitting blood flow response from CT1 to determine tau for further trials. Despite the usual difficulties of resting flow and perfusion pressure, the rest of the day's trails were unremarkable.

Dog 3 (6/24/08) – Usual difficulty of calculating from CT1 and the resting flow. Other than that, trials went fine. On the last trial of this day (EX25), the O_2 sat dropped as force and pressure both bottomed out; the dog died on us during the trial.

Dog 4 (6/26/08) – Besides usual concerns, unremarkable day. Made it through all trials fine.

Dog 5 (6/27/08) – Besides usual concerns, unremarkable day. Made it through all trials fine.

**Had discussion about what to do with problems with resting perfusion pressure and flow and fitting CT1 correctly in a short enough time to get through rest of trials without dog/muscle failing. Ultimately we decided that a blood flow tau of 20 sec would be used as a control, and we would slow blood flow delivery by ~25 and ~50 sec (so tau values of 45 and 70). After the analysis of dogs 1-5 we realized that we may need larger slowing of flow rates than previously used.

Dog 6 (9/9/08) – Very good day of experiments. Unremarkable. (DOG 1)

Dog 7 (9/16/08) – Very good day of experiments. Unremarkable. As we finished the last experimental trial of this study and began flow steps the muscle slipped because a bone nail popped out of the bone. This did not affect data for these experiments. (DOG 2)

Dog 8 (9/18/08) – Trouble with perfusion pumps to begin day. Not sure what went wrong. We think the tubing has been left in and warped and that is affecting flow rates. We switched pumps and that seemed to solve the problem. Otherwise unremarkable, good day of experimentation. (DOG 3)

Dog 9 (9/21/08) – Had some trouble regulating blood gases of animal. Strangely, at one point arterial pH was low, arterial PCO_2 high, and arterial PO_2 high. Despite the fact that the ventilator was up to a fairly high breathing rate. Turns out the inflation device in the trachea had deflated. Upon re-inflation blood gases stabilized. Also, at the end of this experimental day we began experimenting with determining how much blood flow (measured by a probe on the venous side of the muscle) is from blood being pumped out of the rested muscle. At both high flow and low flows, we clamped the arterial side and began contractions. It appeared that most blood was ejected in the first contraction, with progressively smaller amounts ejected for ~3 to 4 contractions. Animal died before we could complete these pilot experiments. (DOG 4)

Dog 10 (9/23/08) – Some strange results on the day. At one point (after EX50) we stopped contractions and we saw a dropping of venous O_2 sat. Perhaps it was the oximeter acting up again. Then, after EX25, we were discussing adding on a trial of faster blood flow delivery when we realized the dog had died on us sometime during or toward the end of EX25. We had to exclude dog 10 from the study because of this and subsequently ordered 4 more beagles.

Dog 11 (10/7/08) – As we started our first run, our oximeter bottomed out on us again. Then, as we tried to start again later, the leg of the animal (the experimental leg) popped out from where it was being held during the trial. As we did our second trial of the day the results looked extremely strange and we soon realized the animal had died on us. Thus, Dog 11 was also excluded from the study.

Dog 12 (10/9/08) – Unremarkable day through the experimental trials. After those were done we did "flow steps" to determine metabolic response time. During these experiments everything went goofy. There appeared to possibly be a clot somewhere and we simply had to stop the flow steps. Data for slow flow experiments were good though. (DOG 5)

Dog 13 (10/12/08) – We made it through 2 trials on this day before the animal died on us. We are not quite sure what happened. We believe we may have removed too much blood from the animal at one point before giving it back (speeding up the pump and not emptying that blood into the jugular reservoir immediately) and thus sent the animal into cardiac shock. Thus, Dog 13 was also excluded from the study.

Dog 14 (10/14/08) – Unremarkable, good experimentation day. The animal died on us, but only after all experimental trials for this study + flow steps + clamping of arterial side to analyze amount of blood per contraction for both high and low flows. All data for this dog were fine to use. (DOG 6)